

FEATURES OF TERNARY PHASE DIAGRAMS

Most often presented: Triangular Coordinate System

- the base of three dimensional depiction (Fig. 4.10)
- Temperature is the vertical axis.
(Constant Pressure for Condensed Ph)
- Three independent variable : Temperature
- Concentration of two Ph. (Third being the difference)
- Fig. 4.10 is cumbersome to present graphically
- So typically T-axis is not shown
- Instead, a view along T-axis is used.
- Composition axes given as a equilateral triangle.
- Three dimensionality shown as constant-T contours.
- Equivalent to constant-elevation contours.
- Liquidus is a surface (which is a line in Binary PD)

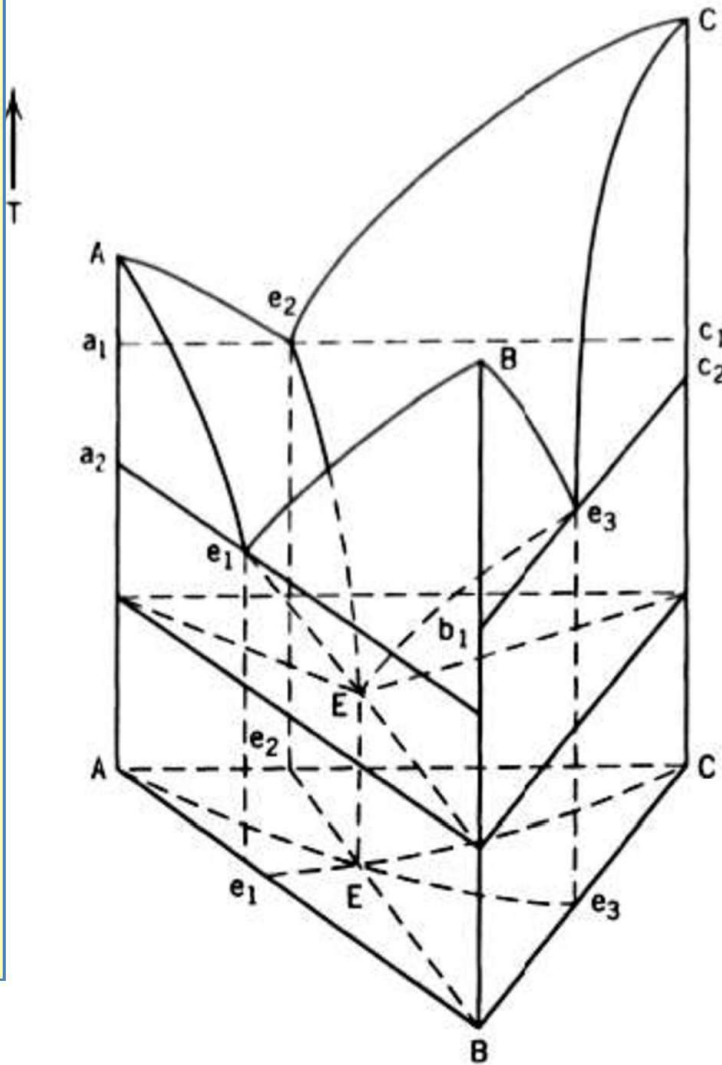


Fig. 4.10 Ternary eutectic phase diagram with limited solid solution for all three endmembers and no intermediate compounds.

Reading Composition

Construct lines parallel to each side through the point.

Compo: 27% A, 46% B and 27% C

Conc. A is ZERO on line CB,

C = 0 on AB and B=0 on AC

At point A, B, C, they are 100% resp.

Line A presents Conc. of A, = 27%

Line B = Conc. B = 46%,

and Line C = 27% C

Alternatively; C= 100- (A+B)

Composition can also be:

from any one side

As shown in side AB:

a = fraction of A

b = fraction of B and c = frac. C

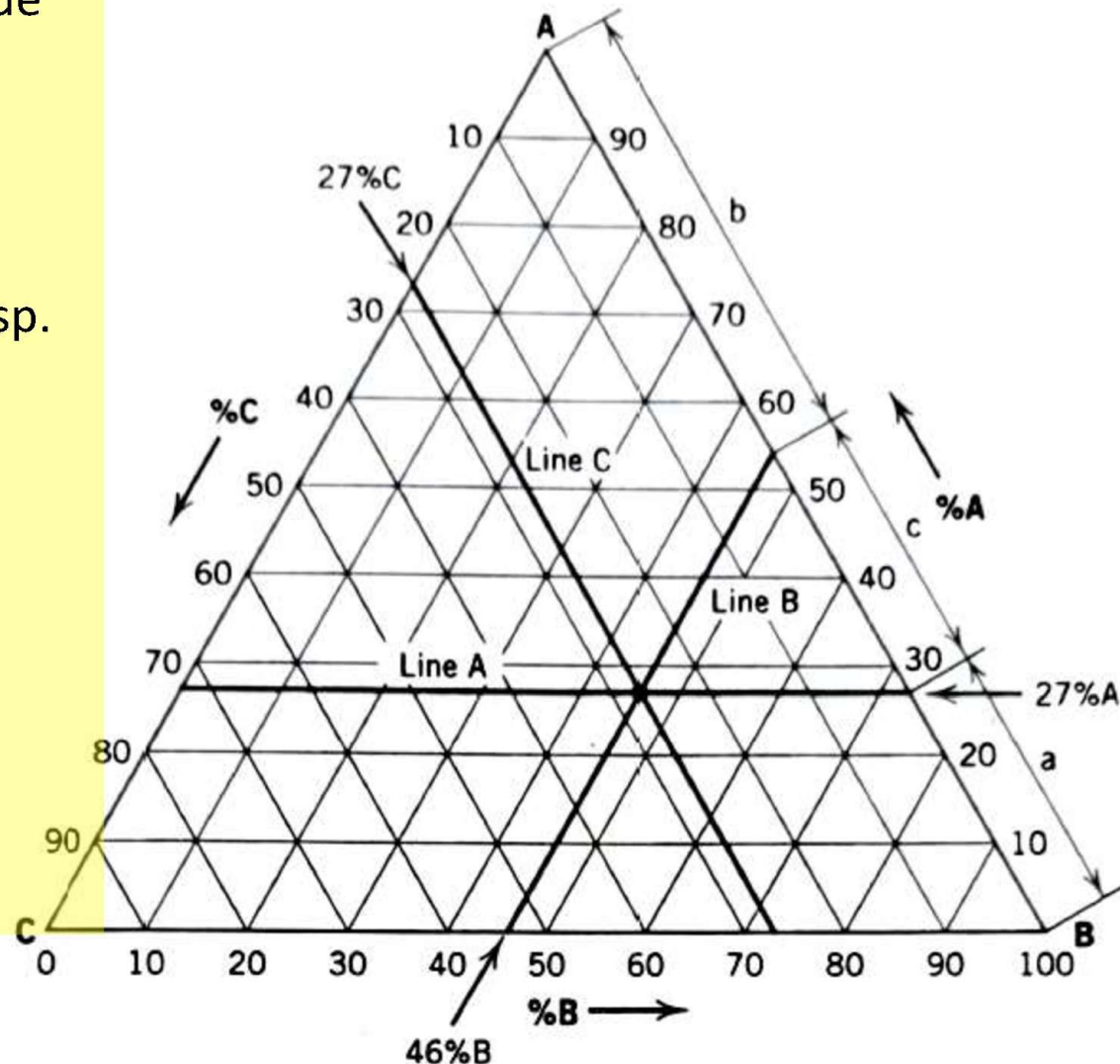


Fig. 4.11 Reading composition from a ternary diagram. The lines parallel to the three sides show concentration at 10% intervals. The composition of the point is read from the intersection of lines parallel to the three sides.

Identification of compounds (Solid Phases): Small open dot "o"

Three pure end member compounds:

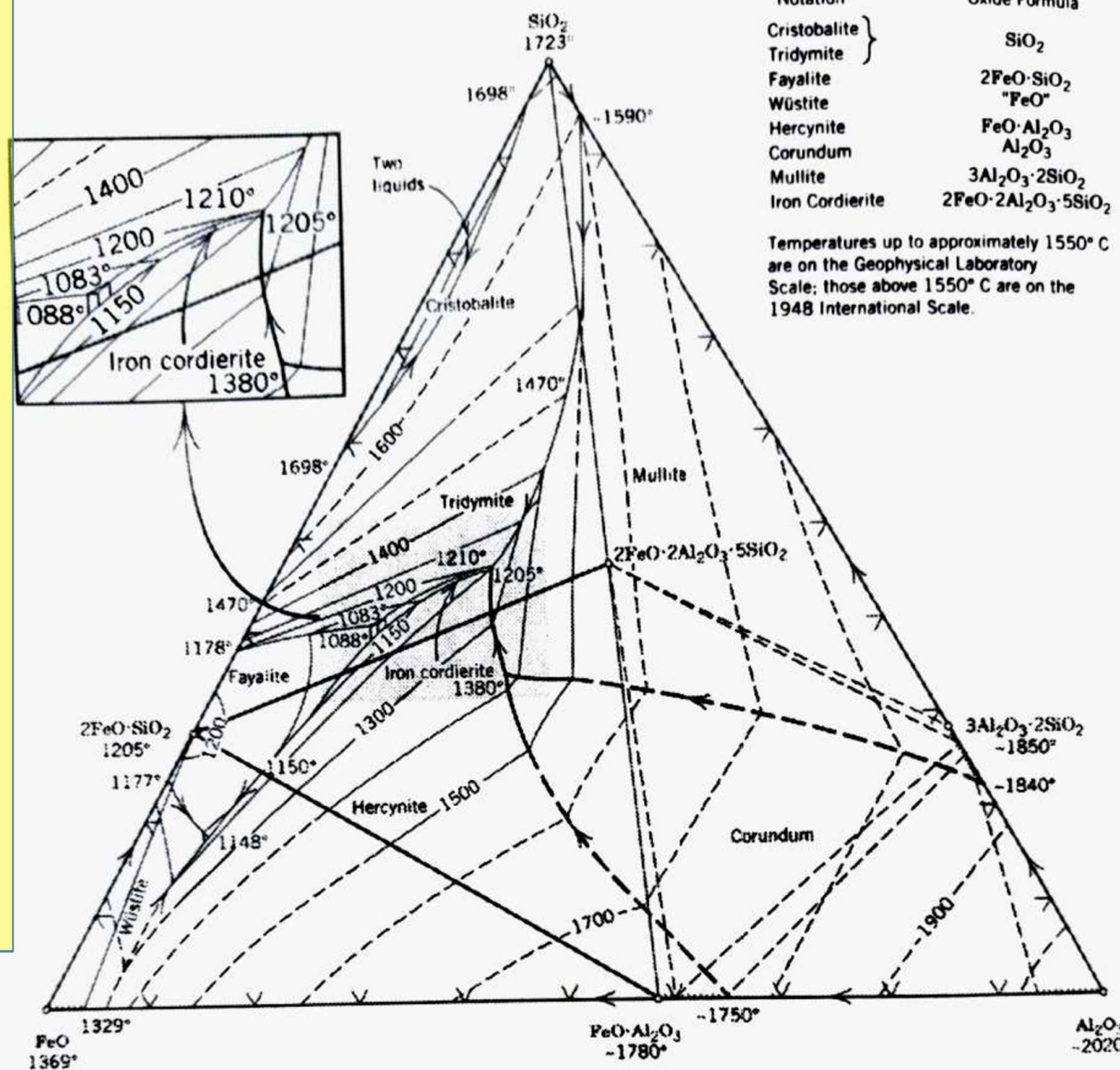
FeO, Al₂O₃, SiO₂

Any side represents:

Binary Diagram,

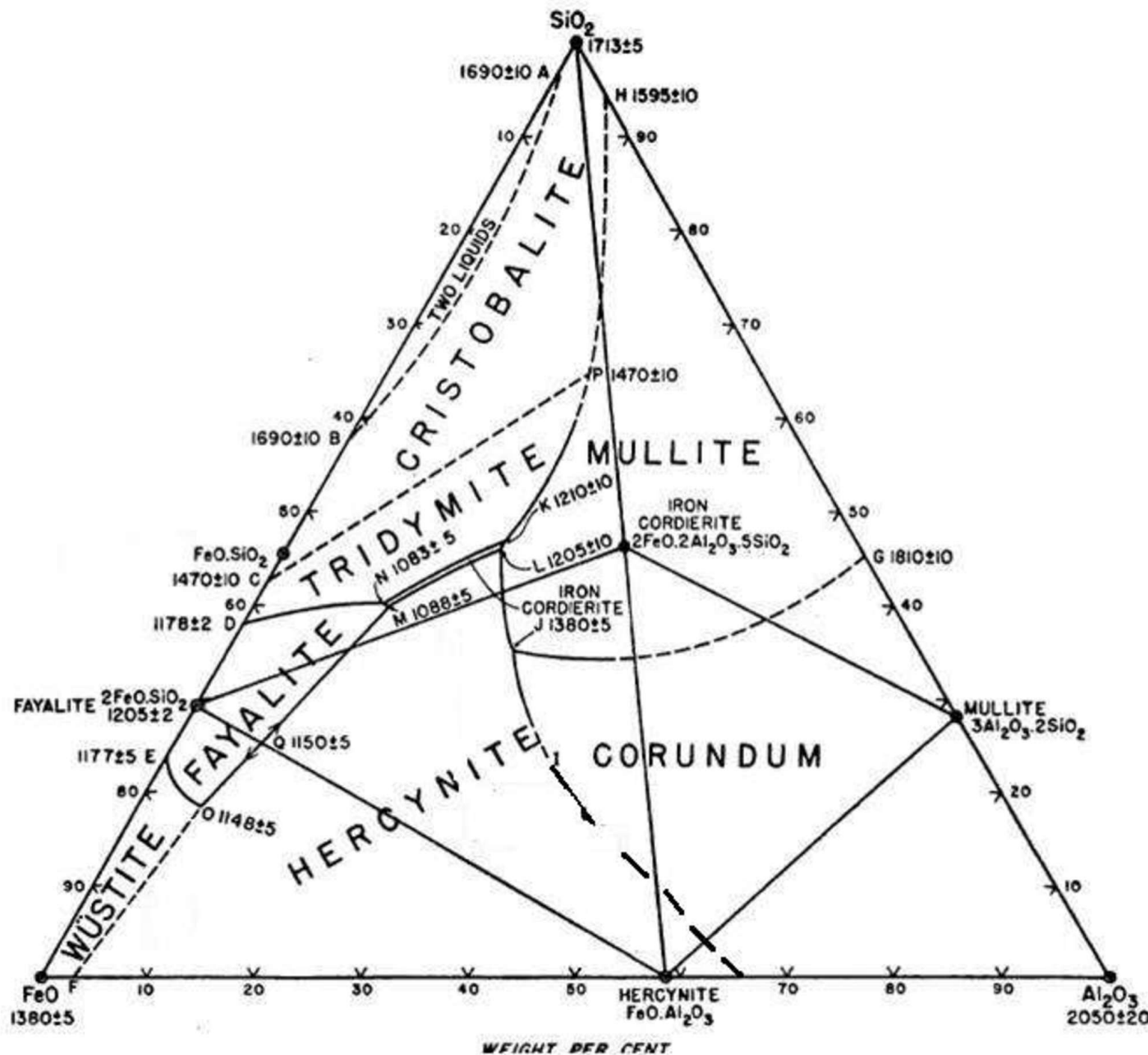
Binary Intermediate compounds: Fayalite, Hercyanite, Mullite

Ternary Compound: Iron Cordierite inside the triangle. MP of some compounds shown near "o". Hatch marks near the compounds : range of Solid Solubility



Notation	Oxide Formula
Cristobalite	SiO ₂
Tridymite	$2\text{FeO}\cdot\text{SiO}_2$
Fayalite	"FeO"
Wüstite	$\text{FeO}\cdot\text{Al}_2\text{O}_3$
Hercyanite	Al_2O_3
Corundum	$3\text{Al}_2\text{O}_3\cdot 2\text{SiO}_2$
Mullite	$2\text{FeO}\cdot 2\text{Al}_2\text{O}_3\cdot 5\text{SiO}_2$
Iron Cordierite	

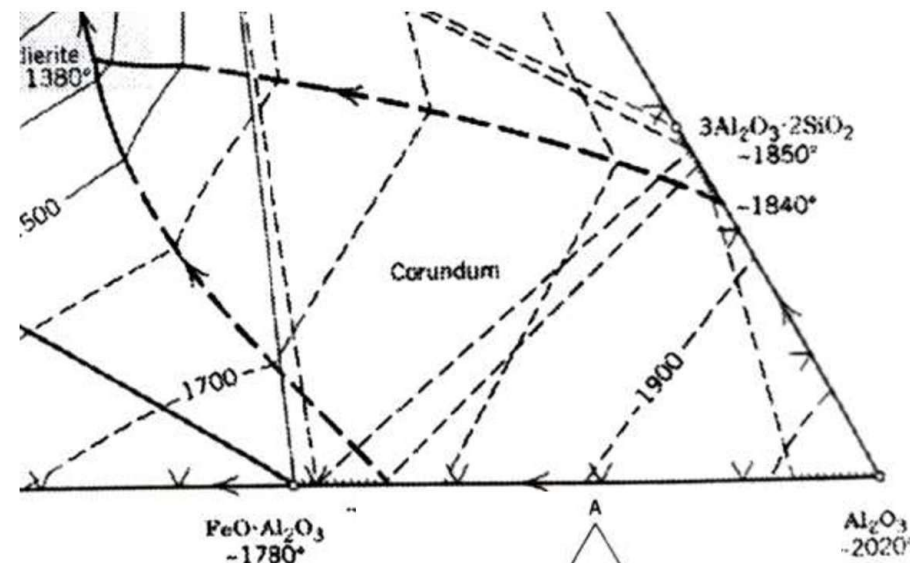
Temperatures up to approximately 1550° C are on the Geophysical Laboratory Scale; those above 1550° C are on the 1948 International Scale.



Primary Phase Fields (PPF)

Of a Compound: The region over which it is **the first solid** to crystallize from any liquid of that region upon cooling.
: The portion of liquidus surface.

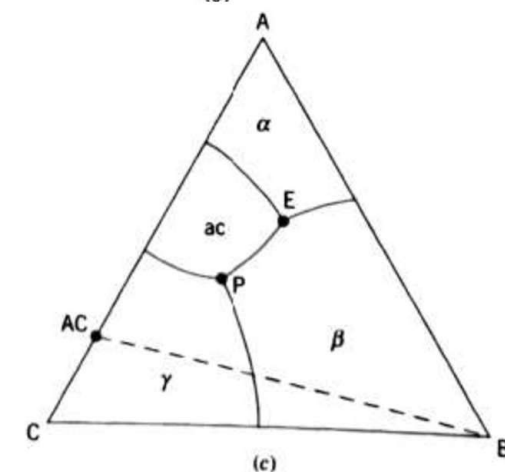
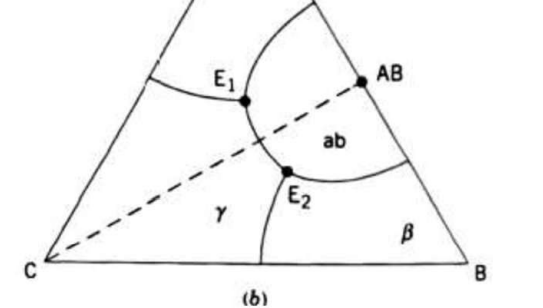
PPF: Bounded by heavy solid lines (some cases dashed: low level of confidence)

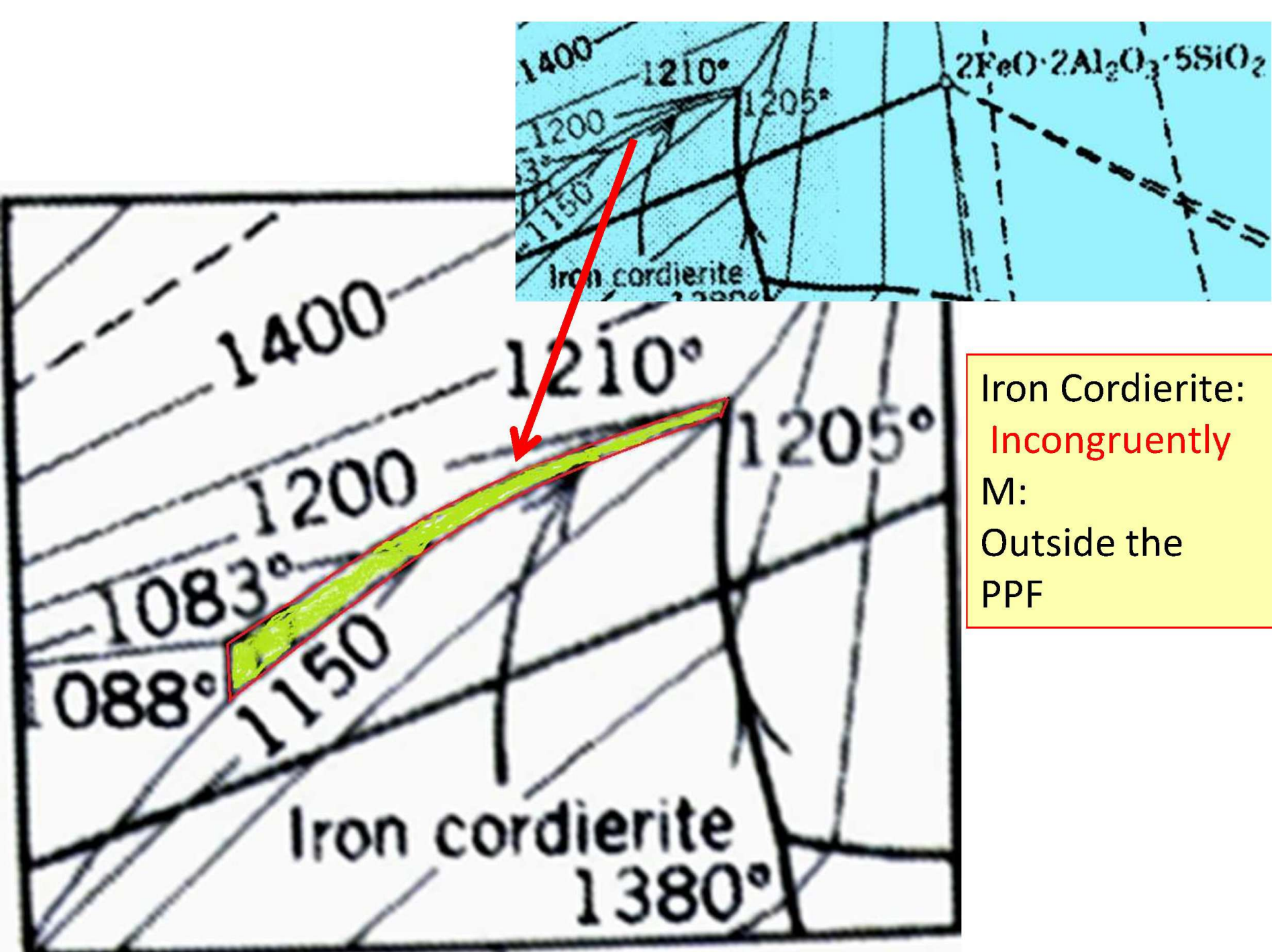


Congruently and Incongruently Melting Compounds

Congruently M: The composition lies within its own PPF/ or on the boundary.

Incongruently M: Outside the PPF





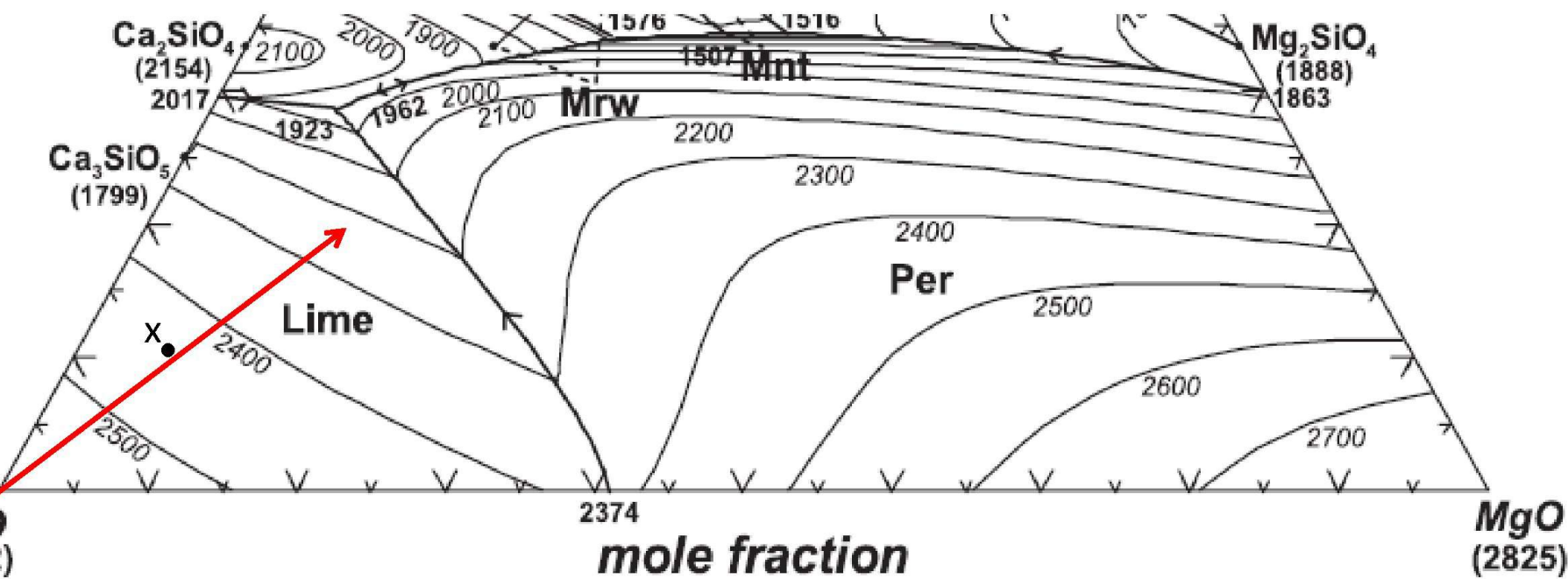
Iron Cordierite:
Incongruently
M:
Outside the
PPF

Boundary Curves (BCs) and Temperature Contours (TC)

BCs are the lines those separates PPF: Along which one liquid is in equilibrium with two solid phases. ($F=1$). ($F=C-P+1 = 3-3+1$)

The point at which BC intersects the side of triangle = system becomes two components (Solids). T of that point usually labeled.

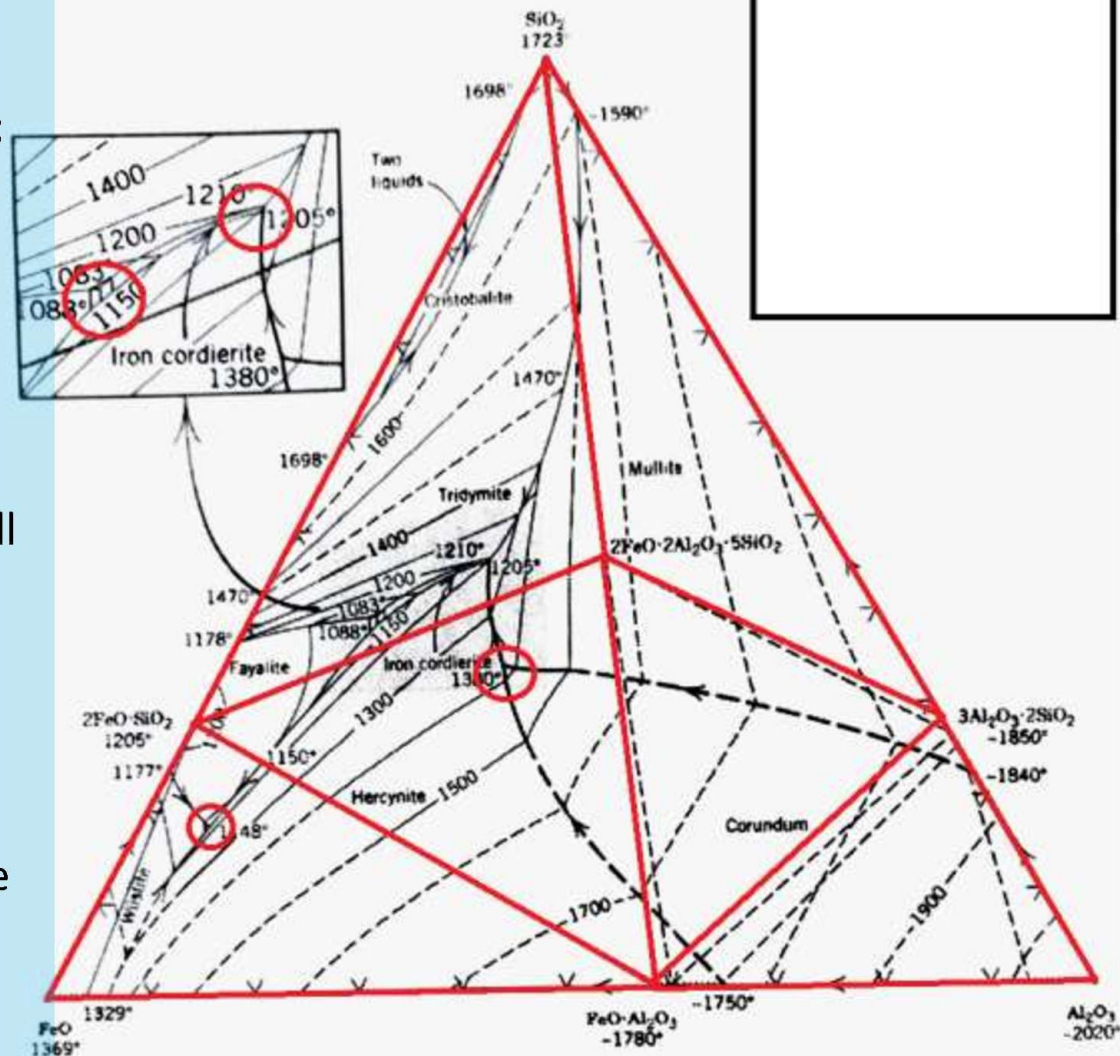
Temperature Contours (TC): Line of constant temperature showing the shape of liquidus surfaces, the topographical map. At BCs TCs must join, representing sharp valley between two PPFs. BCs are often labeled with arrows to indicate decreasing T direction. (Important for determination of crystallization path).



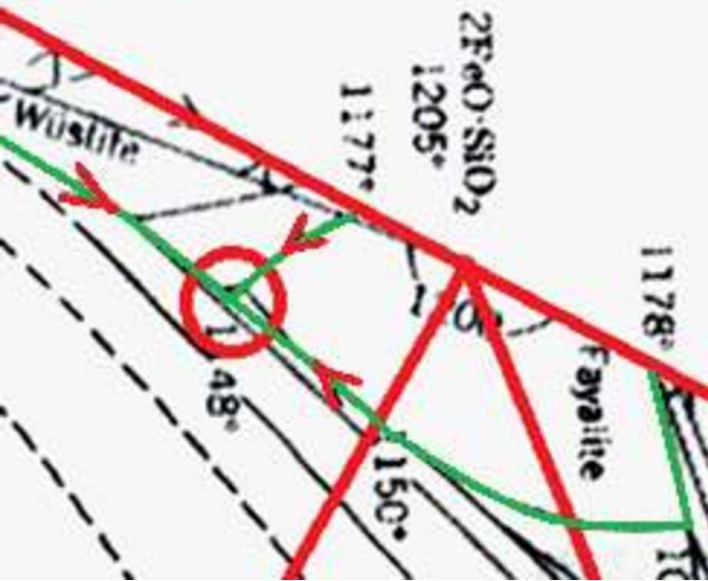
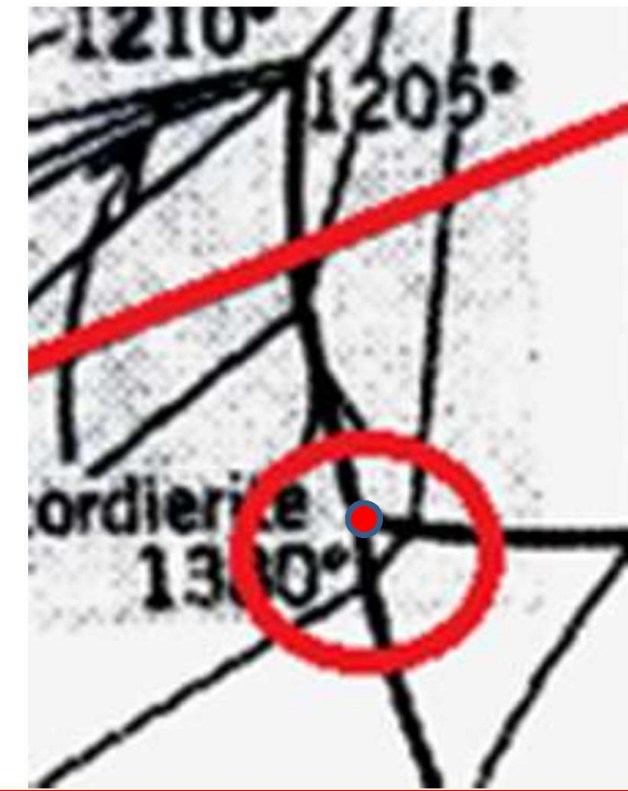
Ternary Invariant Points (IP) and Compatibility Triangles (CT)

Intersection of three (3) boundary curves in a TPD defines a **INVARIENT** point (**Critical Pt.**).

- also the intersection of three (s) PPF : Three PP + one Liquid are in equilibrium
- $F=0$ ($F=3-4+1$), (Condensed P Rule): Neither, **T**, nor **Composition** can be varied.
- T of IP ; usually labeled. IP can be; **Eutectics** or **Peritectics**
- If decreasing **T arrows** of three BCs all point towards CP => **Ternary Eutectics**.
- If one or more arrows point away=> **Ternary Peritectics**.
- More reliable second method: **Compatibility Triangles** methods
- **Compatibility Triangle:** That join three solid phases in equilibrium at a CP
- If CP lies inside CT=> **Eutectics**
- Outside this CT => **Peritectics**



1148°C => FeO:2FeO.SiO₂ : FeO.Al₂O₃ => Inside => **Eutectic**, 1083°C => **Eu**
1380°C => Outside => **TP**, 1210°C=> **TP**, 1205°C=> **TP**, 1088°C=> **TP**

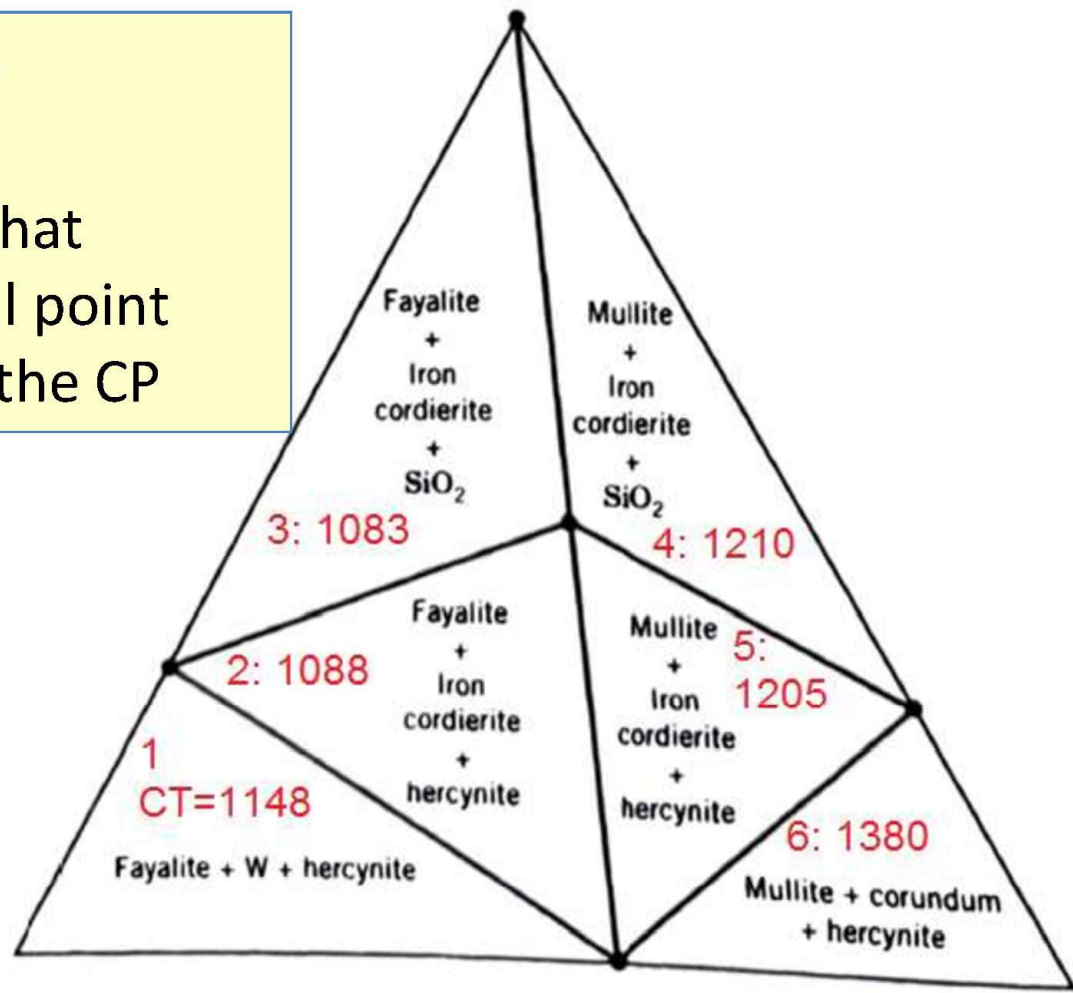
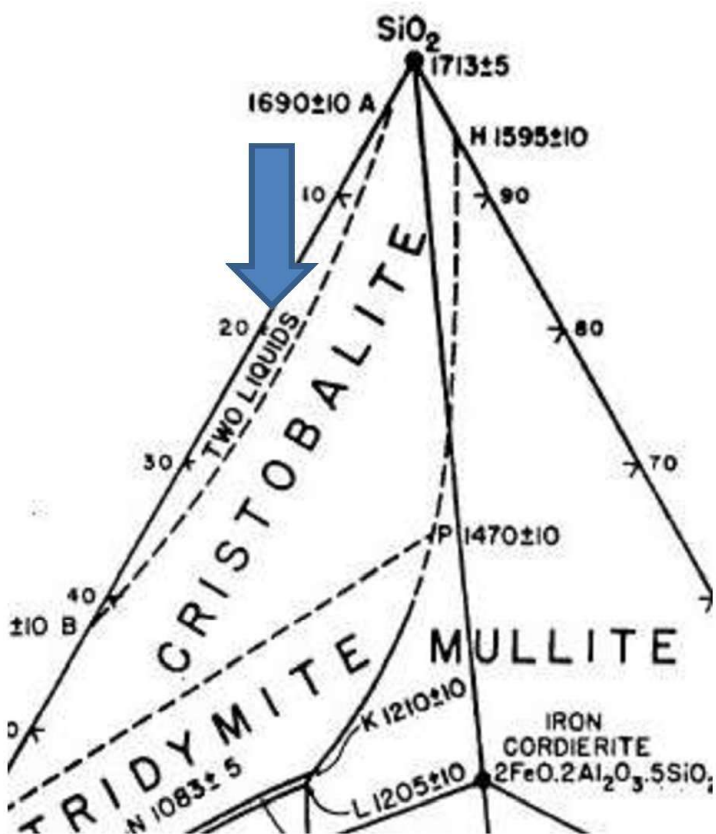


$1148^{\circ}\text{C} \Rightarrow \text{FeO}:2\text{FeO}.\text{SiO}_2 :$
 $\text{FeO}.\text{Al}_2\text{O}_3 \Rightarrow \text{Inside} \Rightarrow \text{Eutectic},$
 $1083^{\circ}\text{C} \Rightarrow \text{Eutectic}$
 $1380^{\circ}\text{C} \Rightarrow \text{Outside} \Rightarrow \text{TP},$
 $1210^{\circ}\text{C} \Rightarrow \text{TP},$
 $1205^{\circ}\text{C} \Rightarrow \text{TP},$
 $1088^{\circ}\text{C} \Rightarrow \text{TP}$

Solidus Temperatures (ST)

Of a composition:

- (1) Identify the comp. tri. for that composition and its critical point and CP-T, ST is the CP-T of the CP



Liquid-Liquid Immiscibility:

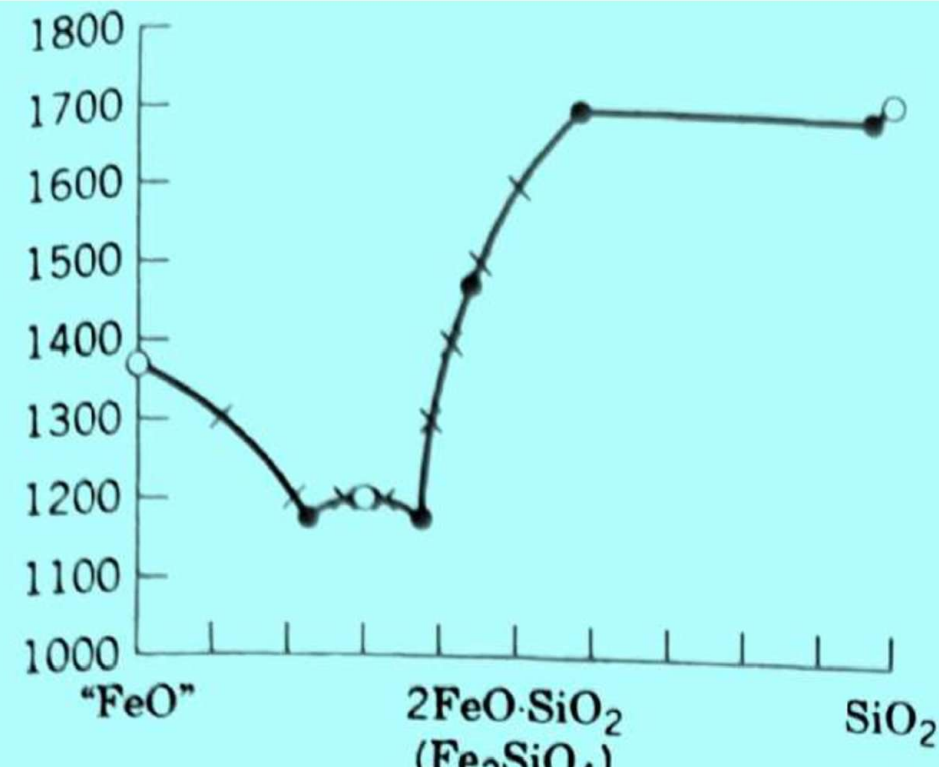
Range of compositions over which two liquids coexist

OPERATIONS USING TERNARY DIAGRAMS

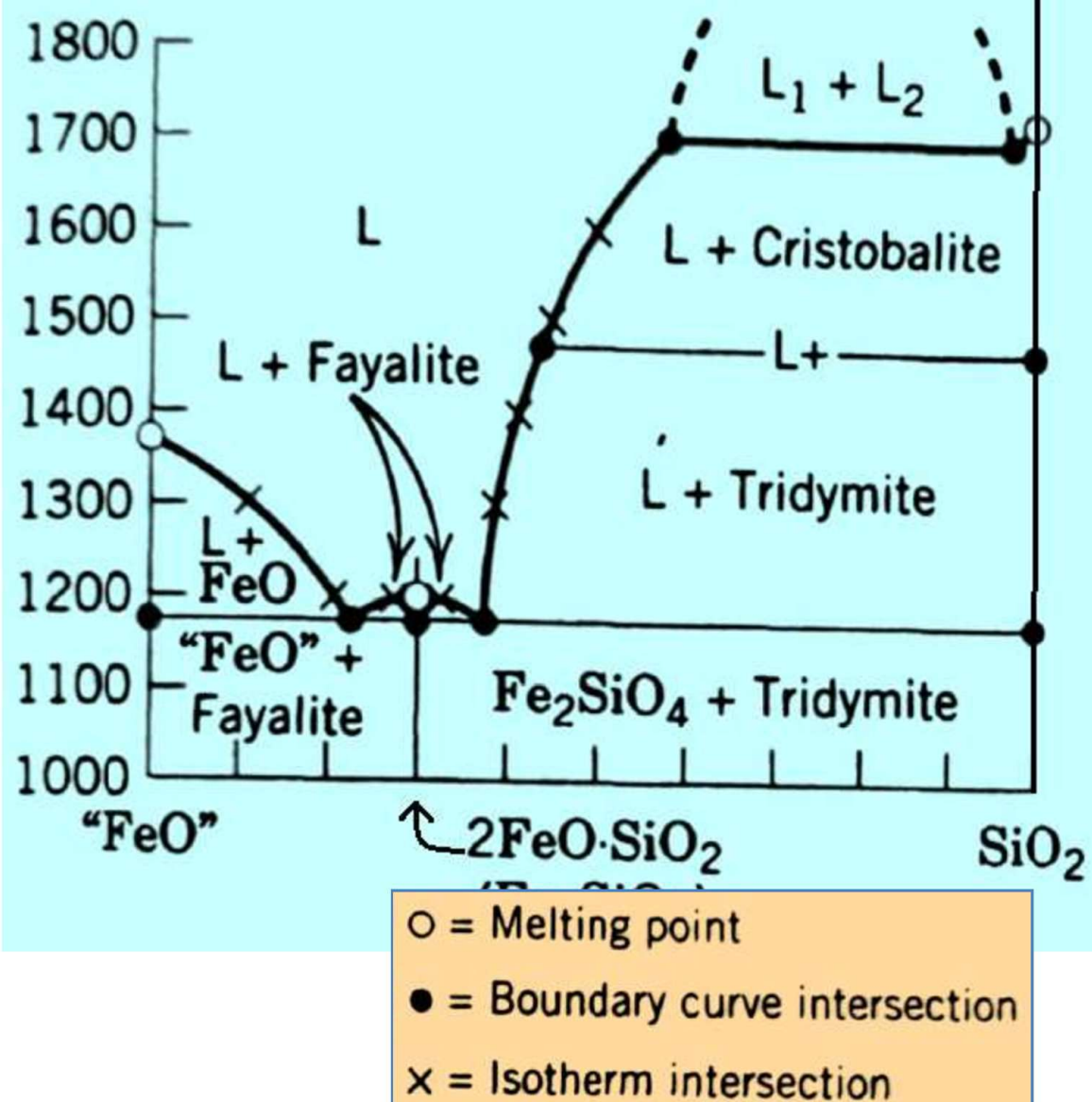
Constructing Binary Diagrams from Ternary Diagrams

- Read MP of Compounds
- Read Boundary Curve intersect Temp
- Mark those on Binary Diagram
- Connect those to get liquidus

MP Wustite:	1369
Boundary Curve Wustite:Fayalite:	1177
MP Fayalite:	1205
Boundary Curve Fay: Tridy :	1178
Boundary Curve Tridy: Crist :	1470
Boundary Curve Crist : 2L region:	1698
MP Crist:	1723



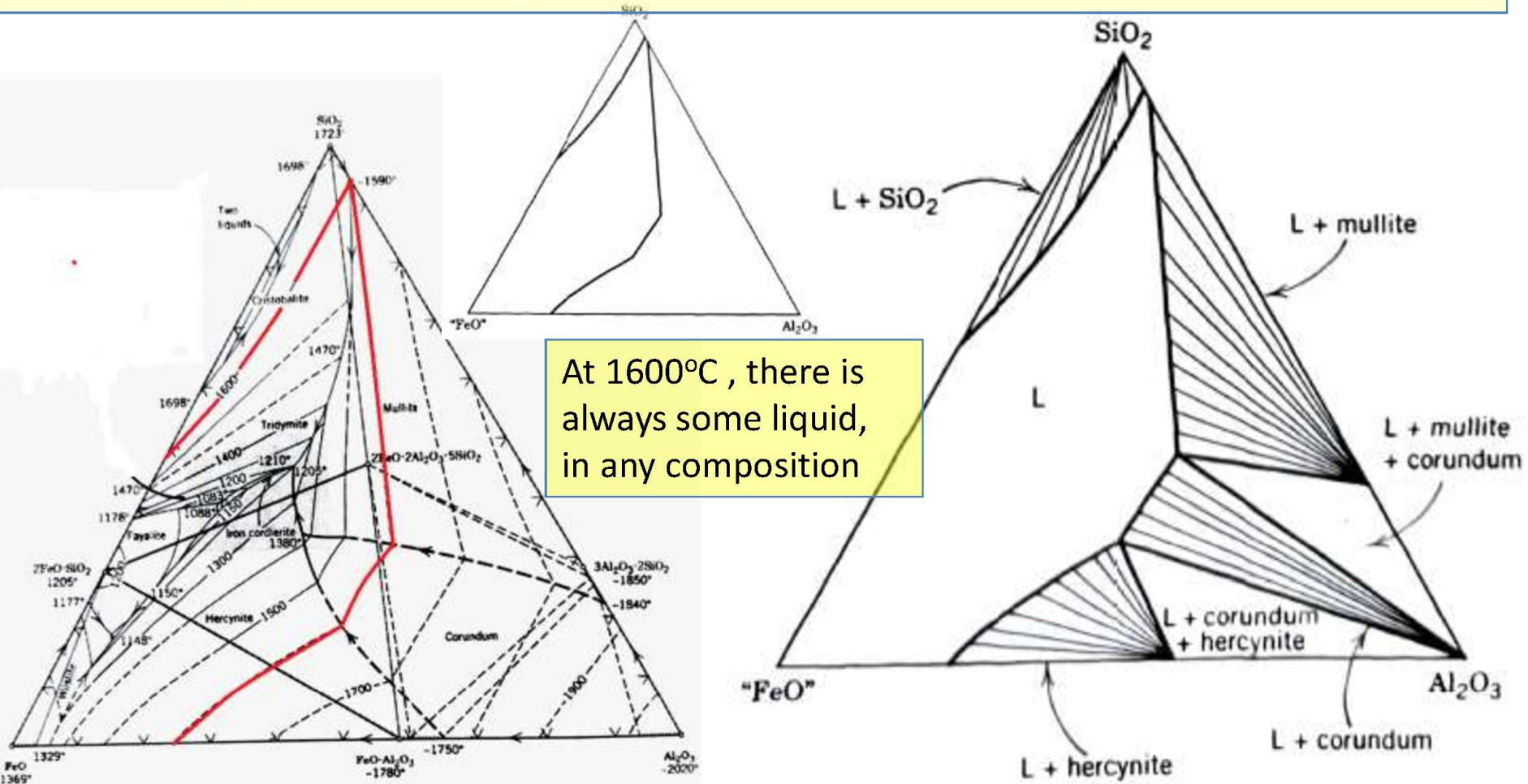
- At BC intersection point; identify two solid phase and one liquid phase in equilibrium: Binary Invariant Point
- Draw the vertical line corresponding to binary compounds
- Connect the two solid phases with horizontal tie line.
- Draw any Liquid-Liquid Immiscibility
- Label the phase fields.



Constructing Isothermal Sections

At 1600°C in SiO₂-Al₂O₃-FeO PD

- 1st : To locate and draw in the 1600°C isothermal contours where it appear in PPF.
- * 4 arcs: represents liquid in equilibrium with four solids (1) Crystobalite (2) Mullite, (3) Corundum and (4) Hercynite. * Each Segment: two phases are in equilibrium: (a) Liquid of composition at isotherm and (b) primary solid phase. * Tie lines join two phases. # One, Two and Three phase fields are labeled.



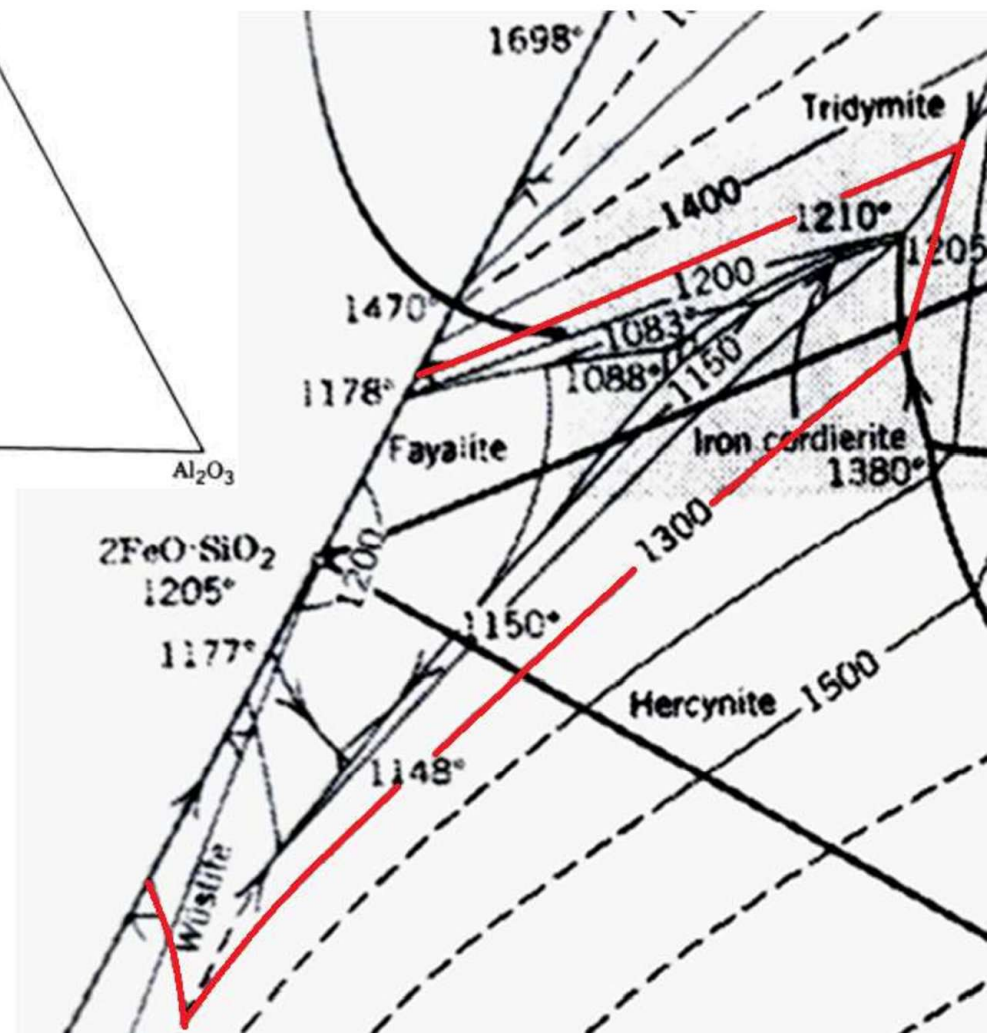
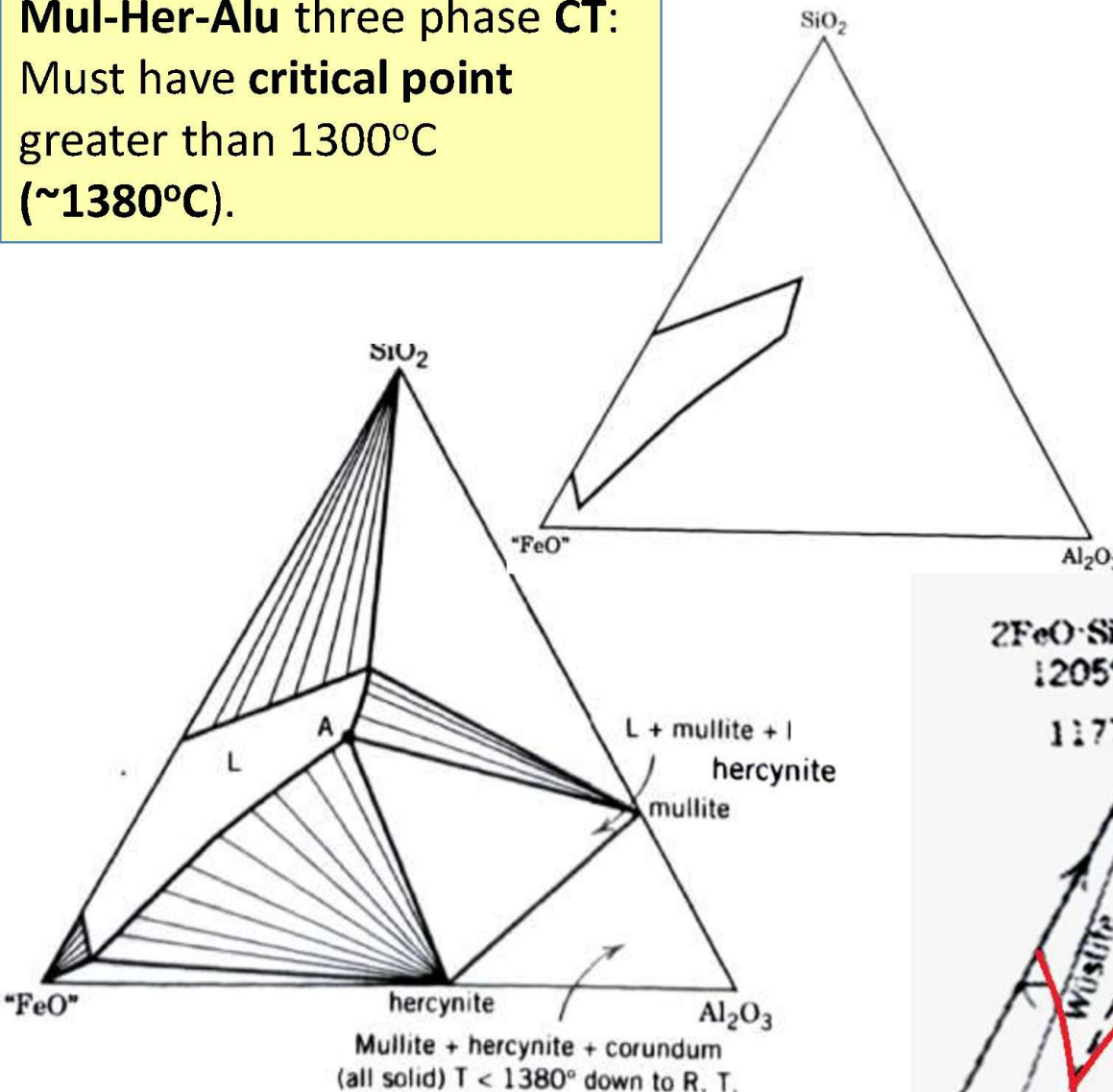
Isothermal section for subsolidus region: 1300°C isotherm, lower-right-hand corner contains subsolidus information; **point A** is in equilibrium with **mullite** and **hercynite**: so M & H must be in equili. And a tie line between two must be drawn:

Mul-Her-Alu three phase CT:

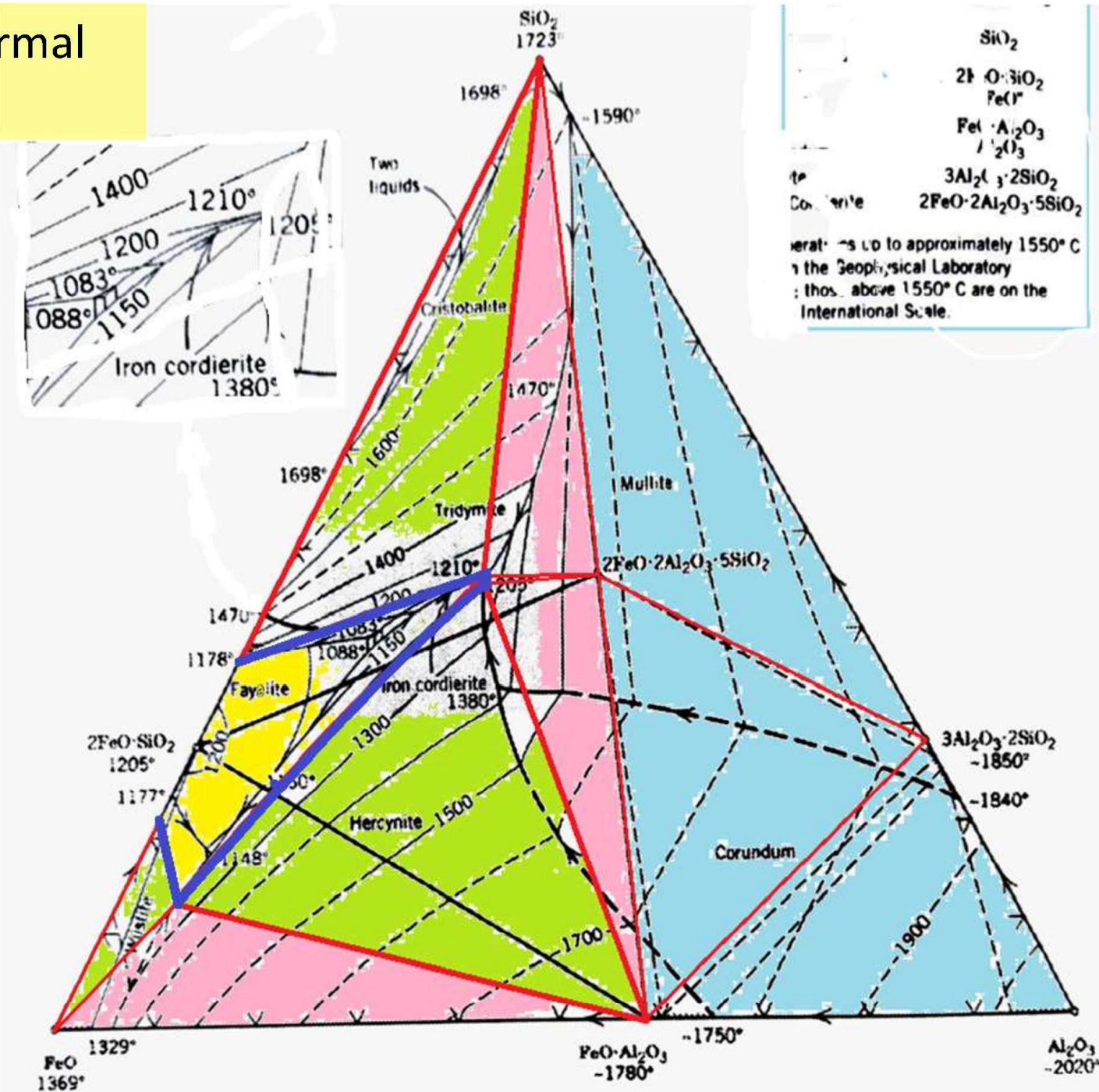
Must have **critical point**

greater than 1300°C

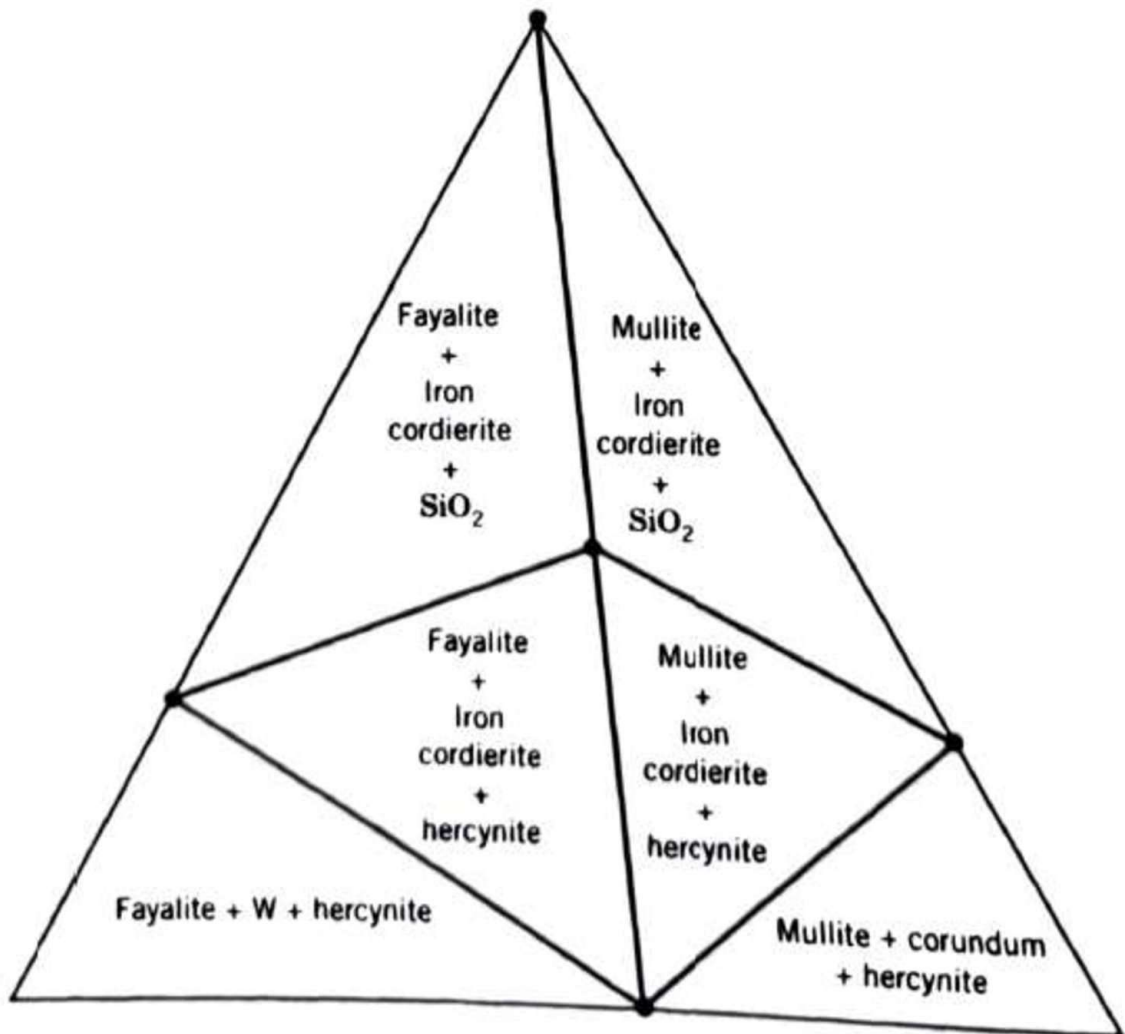
(~1380°C).



1200 °C Isothermal Section



Isothermal Section at Temperature below all Critical Temperature



Ternary Lever Rule (LR)

Two Phase Region: Apply binary LR

Three Phase Region:

Ternary LR (for: A,B, and C three phase in equilibrium and overall composition X),

Fraction

$$B = x/(x+y+z)$$

$$C = z/(x+y+z)$$

$$A = y/(x+y+z)$$

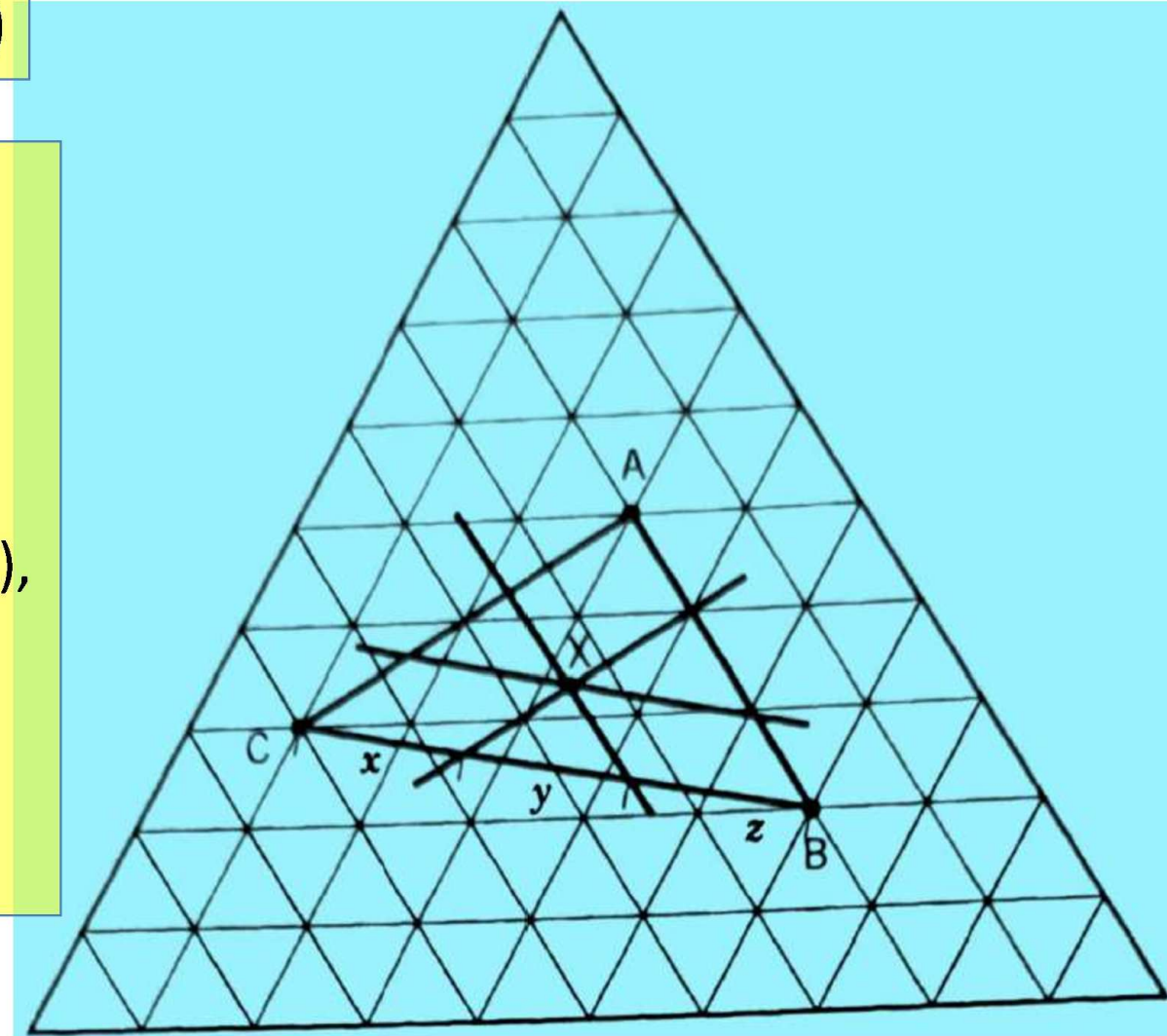


Fig. 4.19 Application of ternary lever rule to a scalene triangle representing a three-phase equilibrium between A, B and C. Lines drawn through the overall composition at X and parallel to the sides of the triangle are used to determine the relative amounts of A, B and C (see text).

For One phase fraction

Determination:

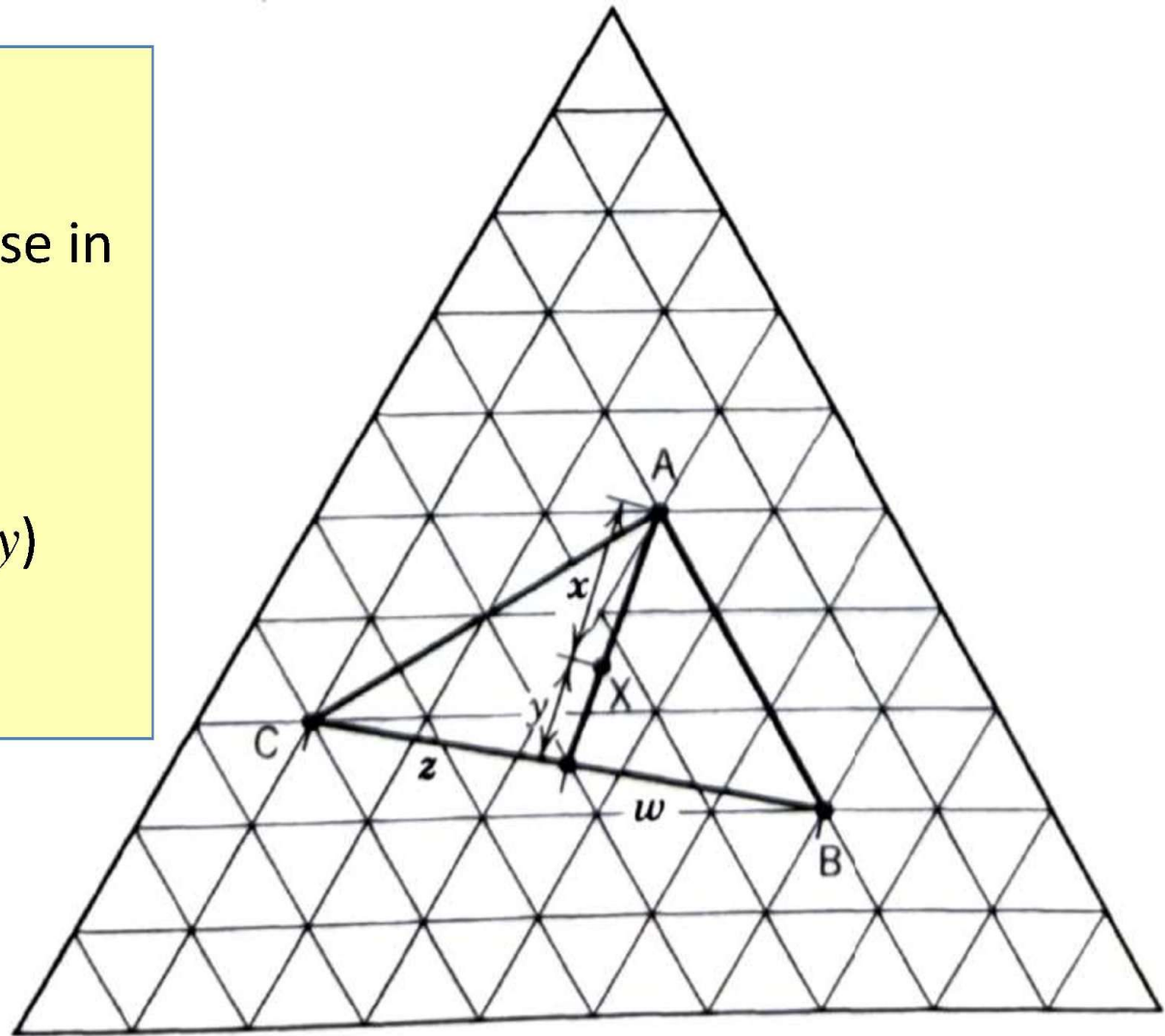
for: A,B, and C three phase in equilibrium and overall composition X),

$$\text{Fraction of A} = y/(x+y)$$

$$\text{Fraction of (B+C)} = x/(x+y)$$

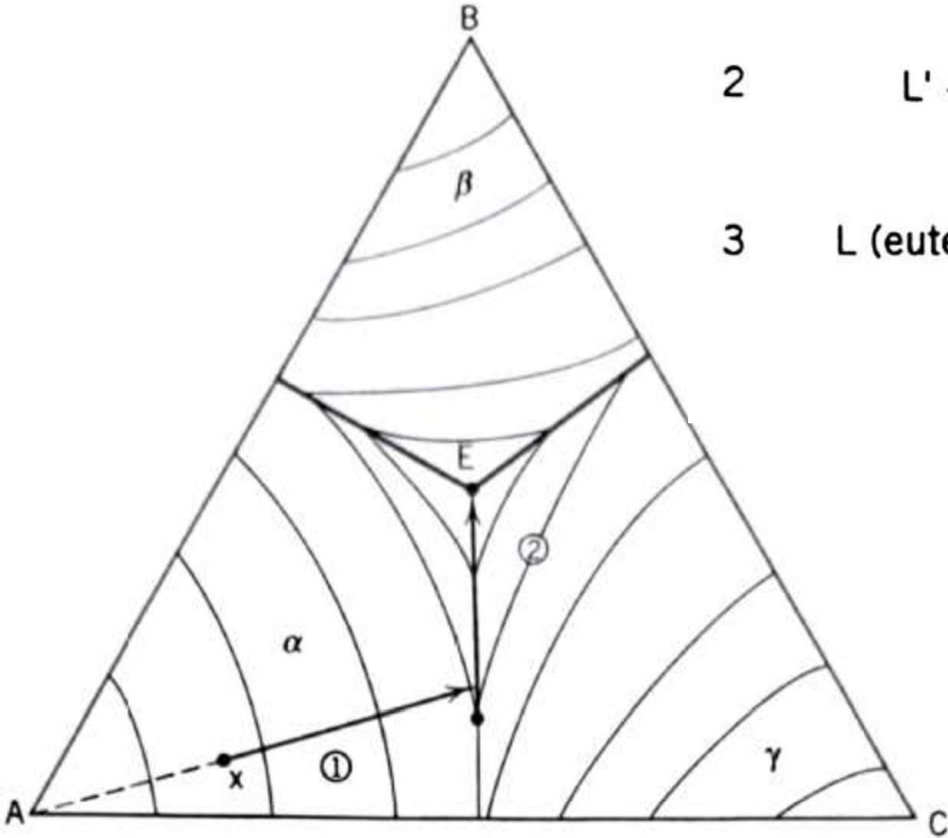
$$\text{Fraction of B} = z/(z+w)$$

$$\text{Fraction of C} = w/(z+w)$$



Alternative geometry for applying ternary lever rule

Reactions upon Heating and Cooling



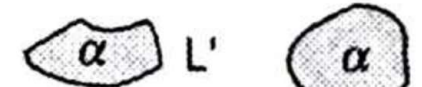
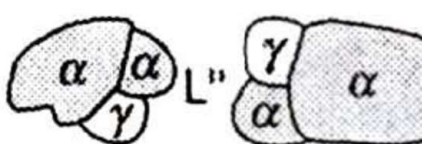
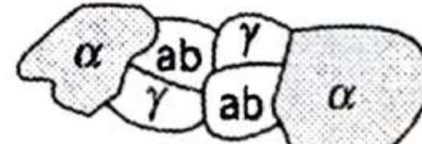
<u>Path</u>	<u>Reaction</u>	<u>Schematic microstructure</u>
1	$L \rightarrow \alpha + L'$	
2	$L' \rightarrow \alpha + \gamma + L''$	
3	$L \text{ (eutectic)} \rightarrow \alpha + \beta + \gamma$	 Eutectic mixture of α, β, γ .

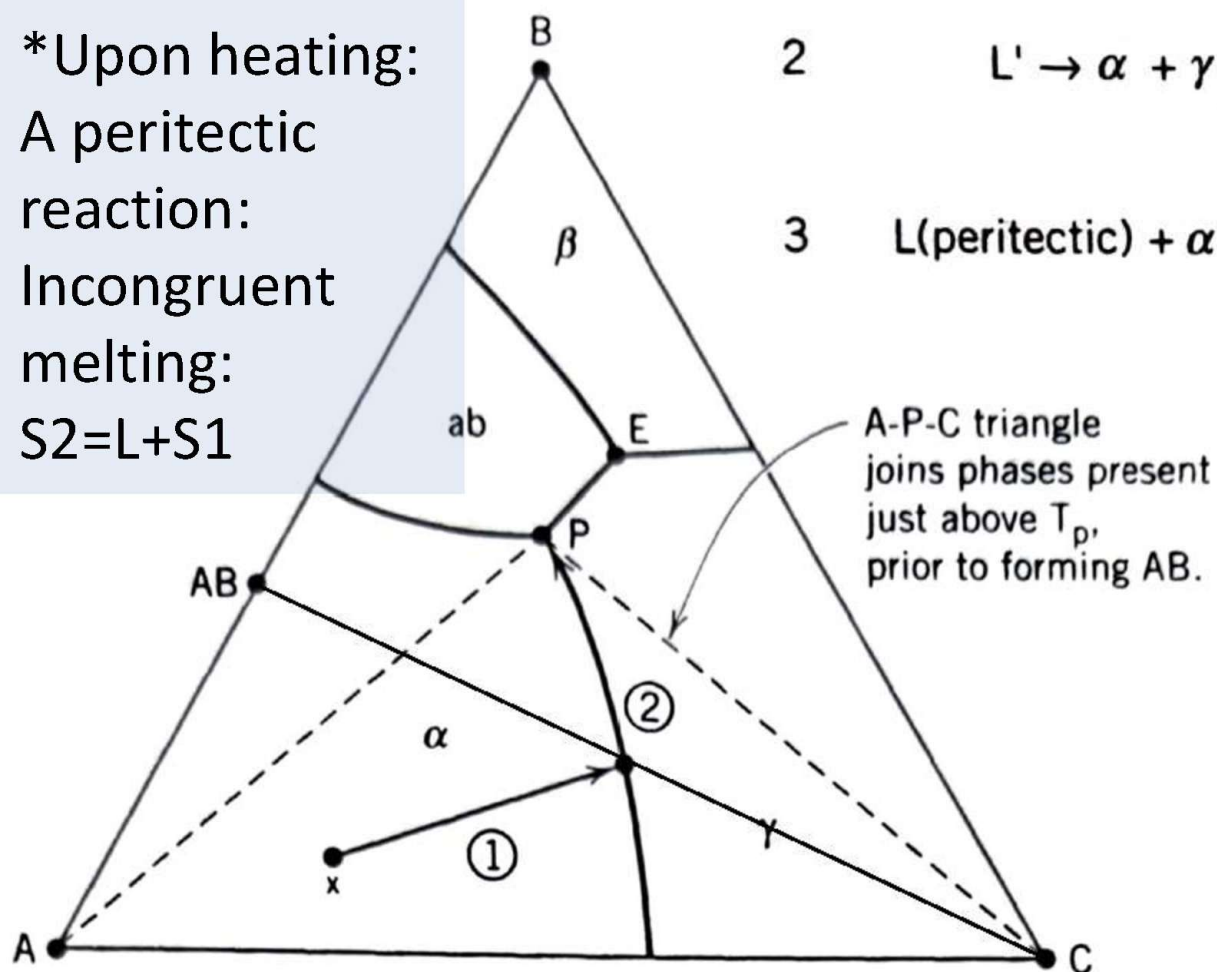
Ternary Eutectic Reaction:
 Eutectic solidification: Single liquid \rightarrow three solid phases \rightarrow Finely divided or lamellar Microstructure
 $L \text{ (eu)} \rightarrow \text{Solid A} + \text{Solid B} + \text{Solid C}$

Crystallization path in a simple ternary eutectic.

Ternary
 Peritectic
 solidification:
 $L+S_1=S_2+S_3$: so
 pre-existing
 solid resorbed.
 *Upon heating:
 A peritectic
 reaction:
 Incongruent
 melting:
 $S_2=L+S_1$

Crystallization in a ternary peritectic.

<u>Path</u>	<u>Reaction</u>	<u>Schematic Microstructure</u>
1	$L \rightarrow \alpha + L'$	
2	$L' \rightarrow \alpha + \gamma + L''$	
3	$L(\text{peritectic}) + \alpha \rightarrow ab + \gamma$	

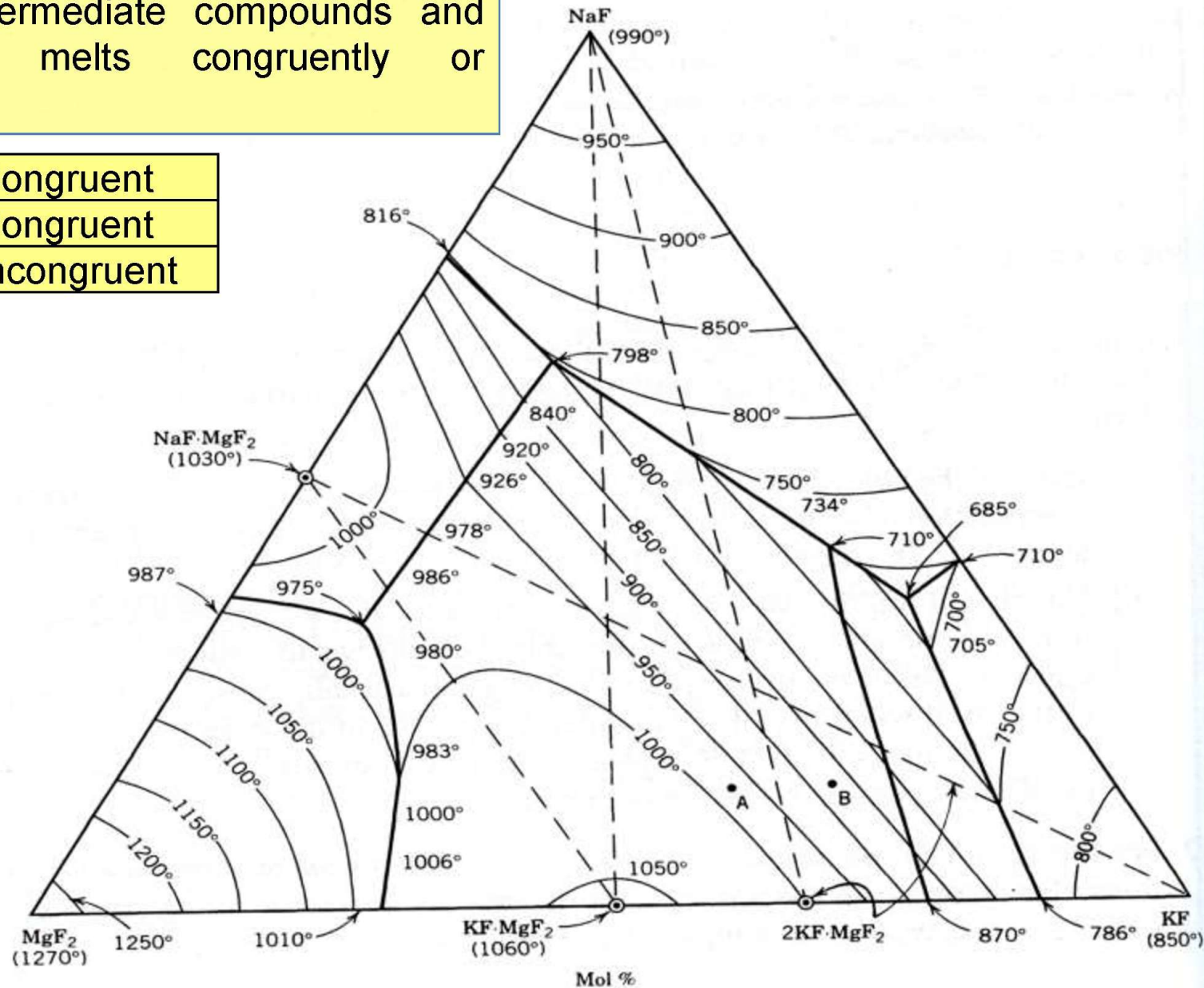


The KF-NaF-MgF₂ ternary diagram shown below. Do the following:

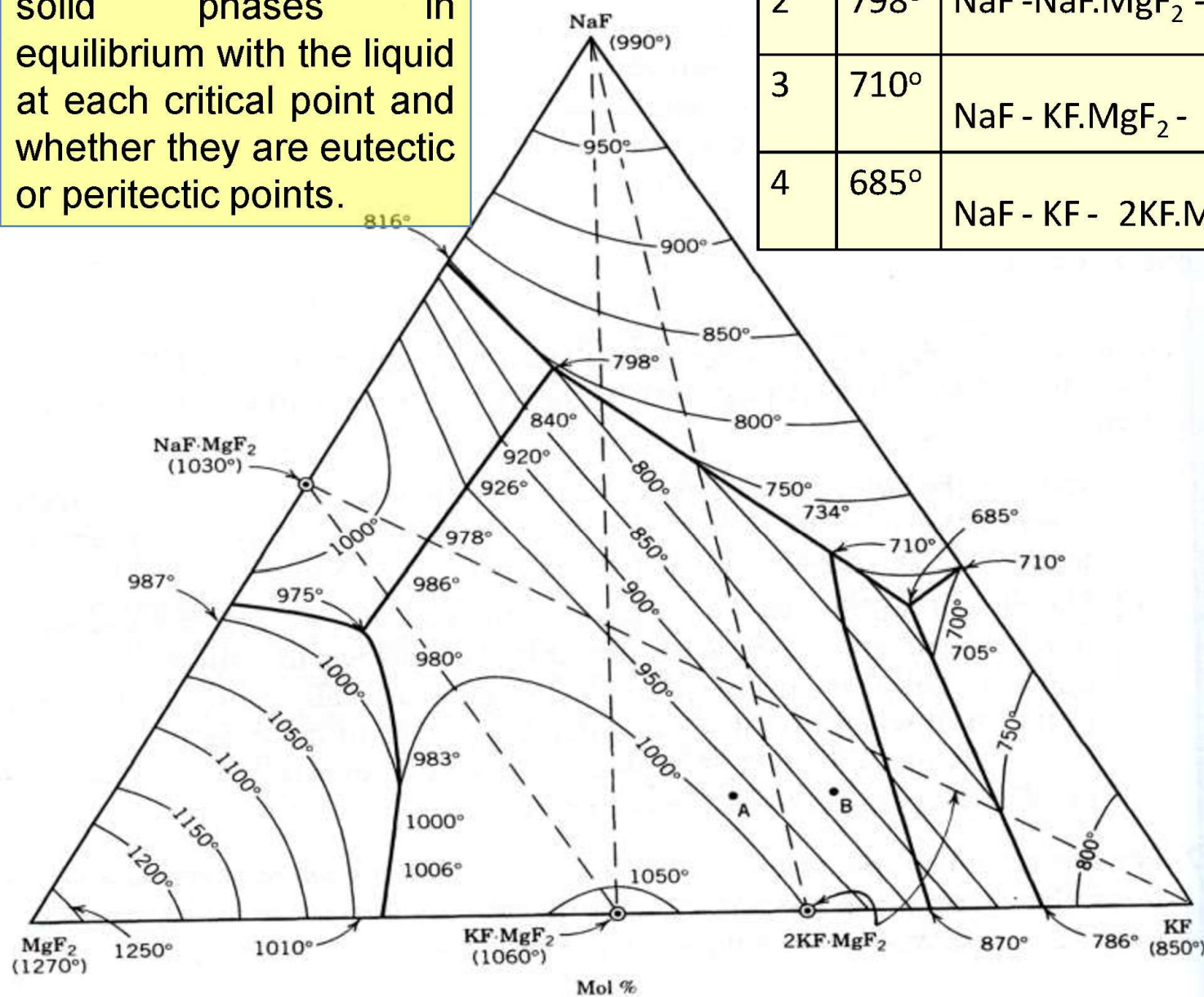
Problem Solving

- Identify the intermediate compounds and whether they melts congruently or incongruently.

$\text{NaF} \cdot \text{MgF}_2$	Congruent
$\text{KF} \cdot \text{MgF}_2$	Congruent
$2\text{KF} \cdot \text{MgF}_2$	Incongruent

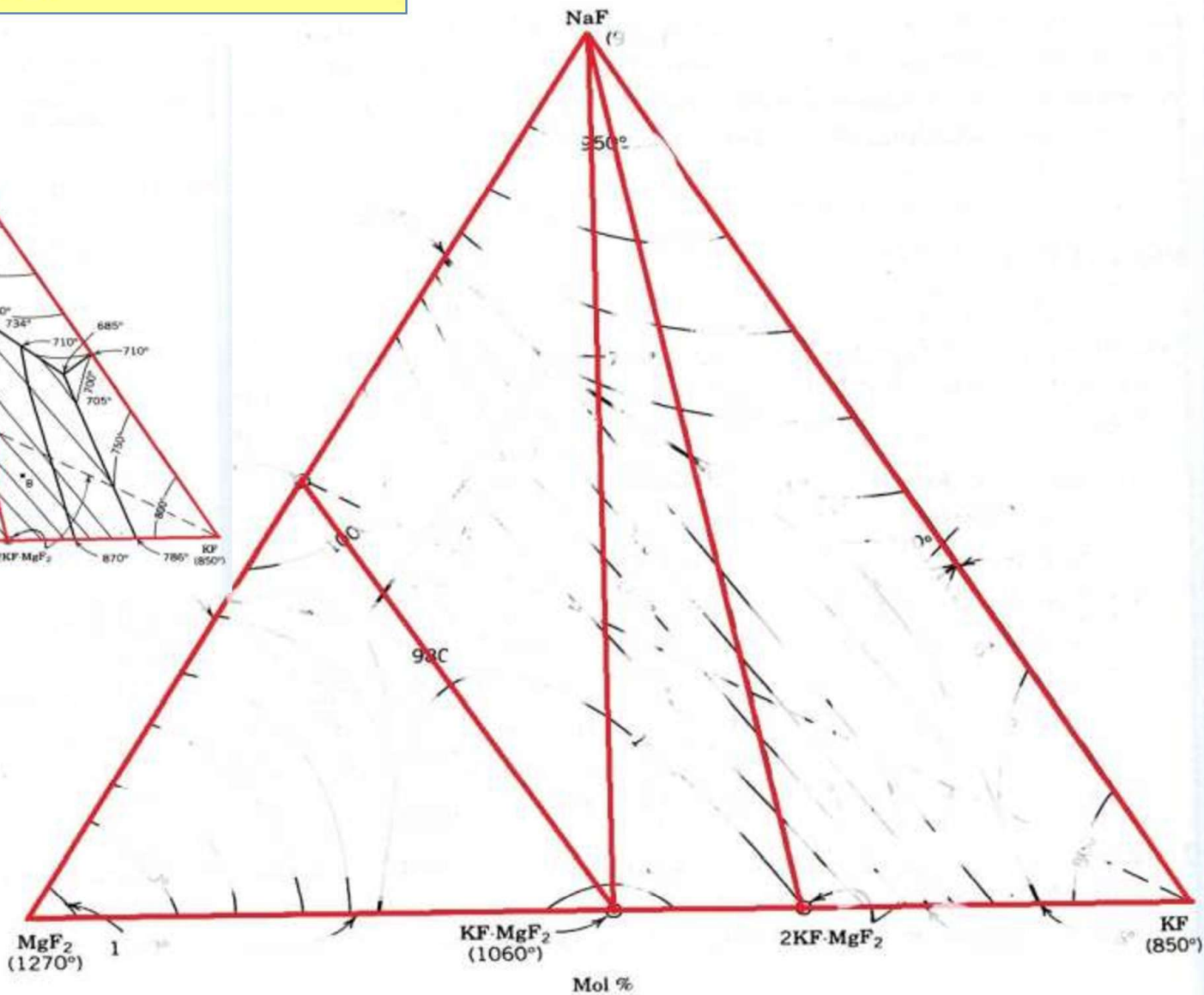
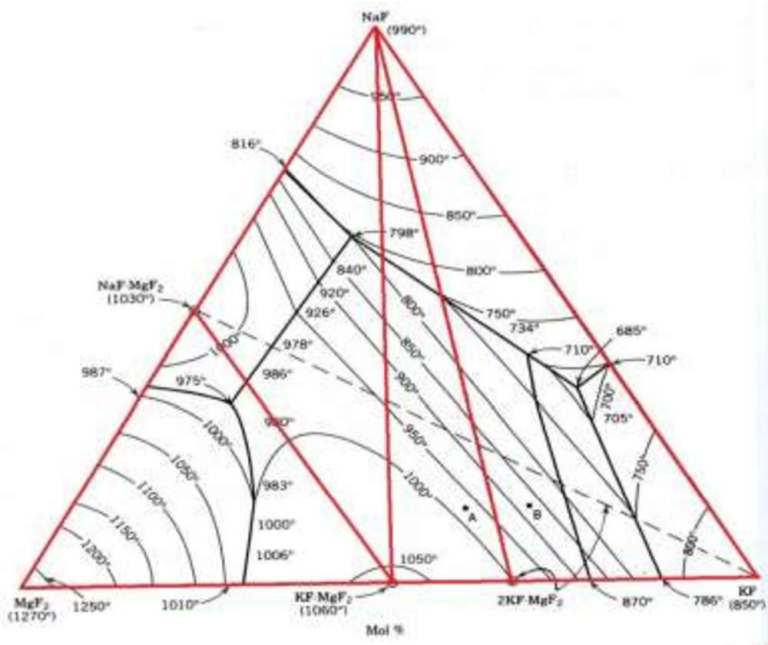


- Identify the ternary critical points, making a table showing the three solid phases in equilibrium with the liquid at each critical point and whether they are eutectic or peritectic points.



1	975°	$\text{MgF}_2 - \text{NaF} \cdot \text{MgF}_2 - \text{KF} \cdot \text{MgF}_2$	Eutectic
2	798°	$\text{NaF} - \text{NaF} \cdot \text{MgF}_2 - \text{KF} \cdot \text{MgF}_2$	Eutectic
3	710°	$\text{NaF} - \text{KF} \cdot \text{MgF}_2 - 2\text{KF} \cdot \text{MgF}_2$	Peritectic
4	685°	$\text{NaF} - \text{KF} - 2\text{KF} \cdot \text{MgF}_2$	Eutectic

- Show the compatibility triangles for this system, in a separate diagram.

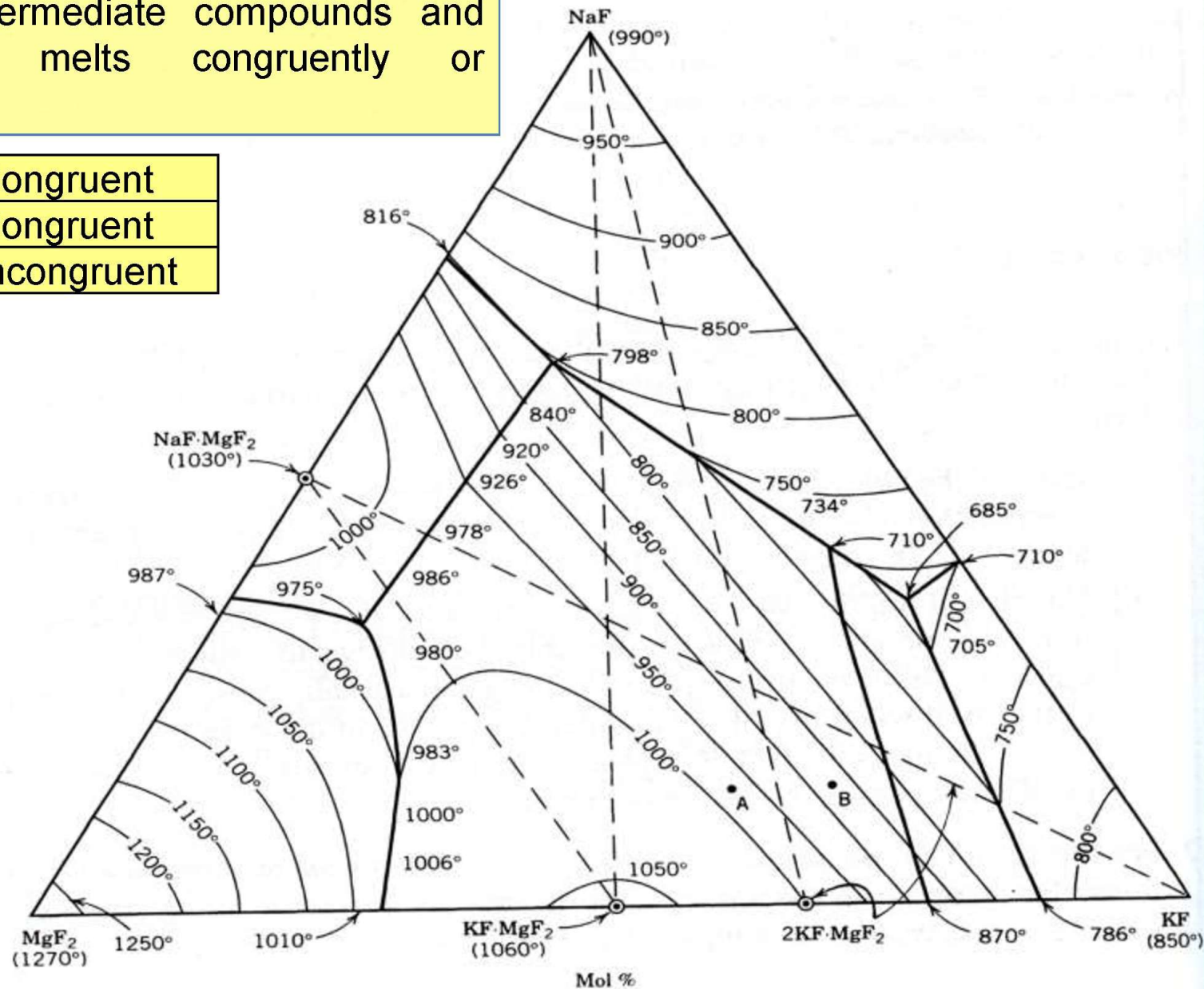


The KF-NaF-MgF₂ ternary diagram shown below. Do the following:

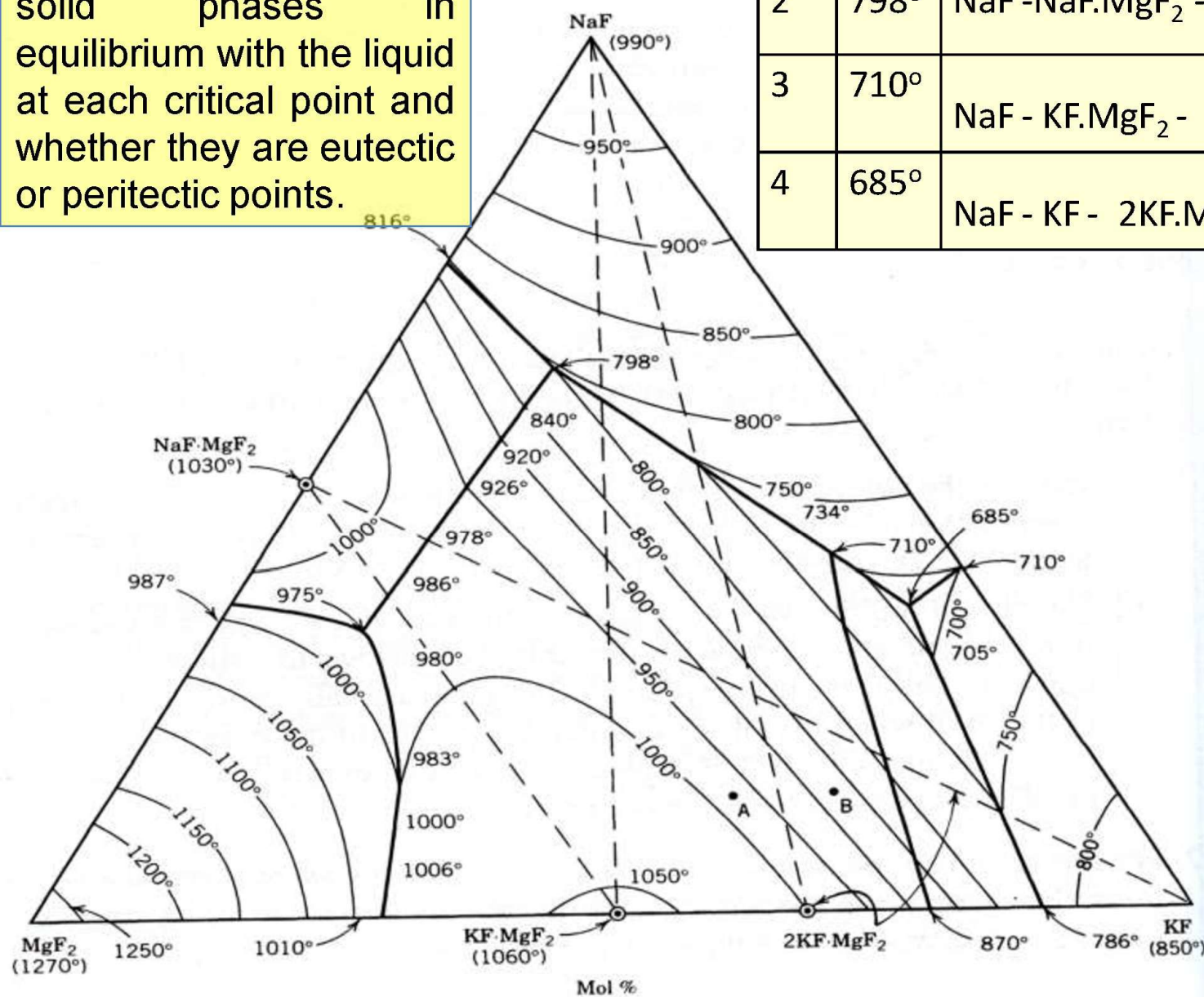
- Identify the intermediate compounds and whether they melt congruently or incongruently.

Problem Solving

NaF.MgF ₂	Congruent
KF.MgF ₂	Congruent
2KF.MgF ₂	Incongruent

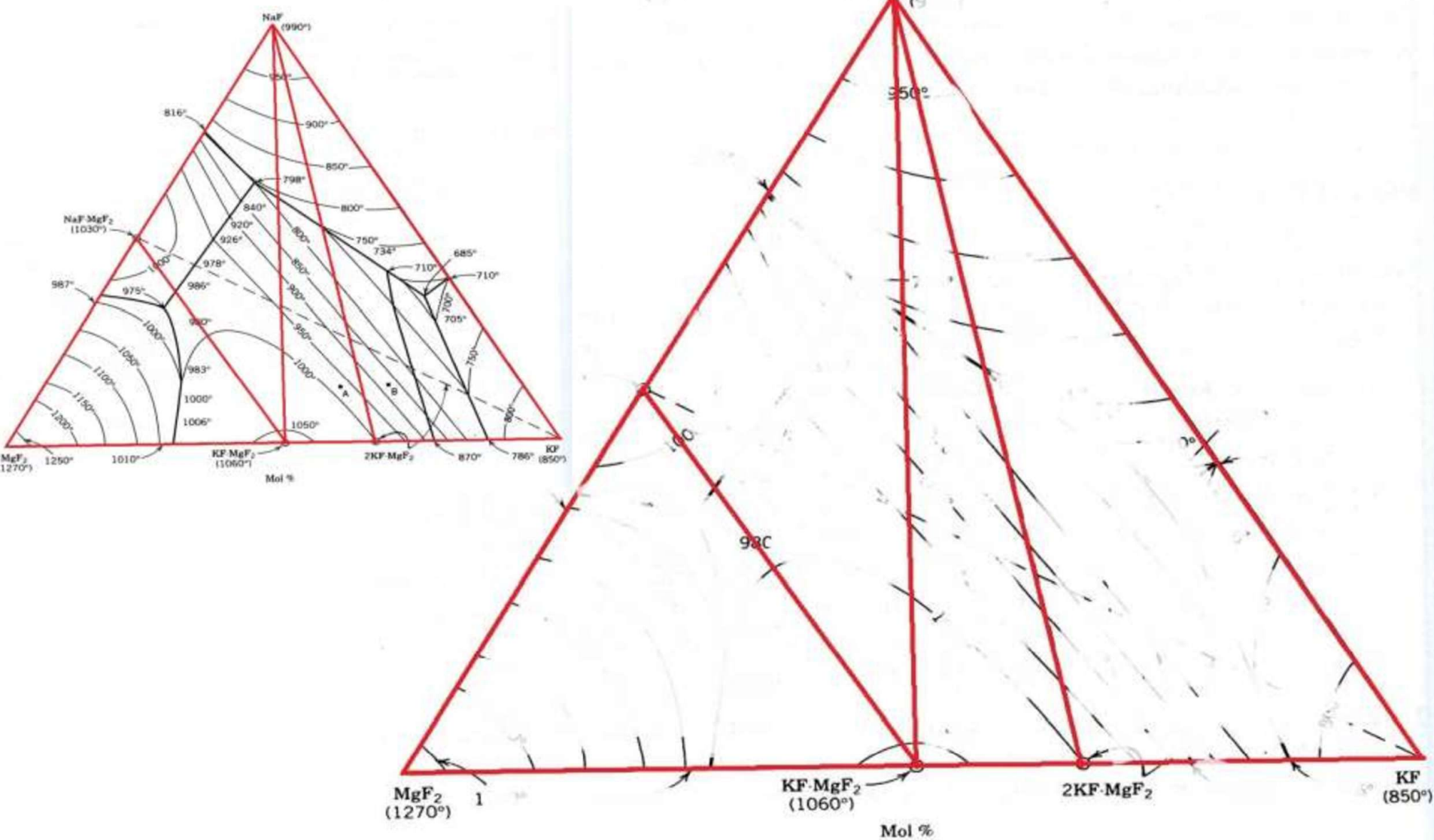


- Identify the ternary critical points, making a table showing the three solid phases in equilibrium with the liquid at each critical point and whether they are eutectic or peritectic points.



1	975°	MgF ₂ - NaF.MgF ₂ - KF.MgF ₂	Eutectic
2	798°	NaF - NaF.MgF ₂ - KF.MgF ₂	Eutectic
3	710°	NaF - KF.MgF ₂ - 2KF.MgF ₂	Peritectic
4	685°	NaF - KF - 2KF.MgF ₂	Eutectic

- Show the compatibility triangles for this system, in a separate diagram.

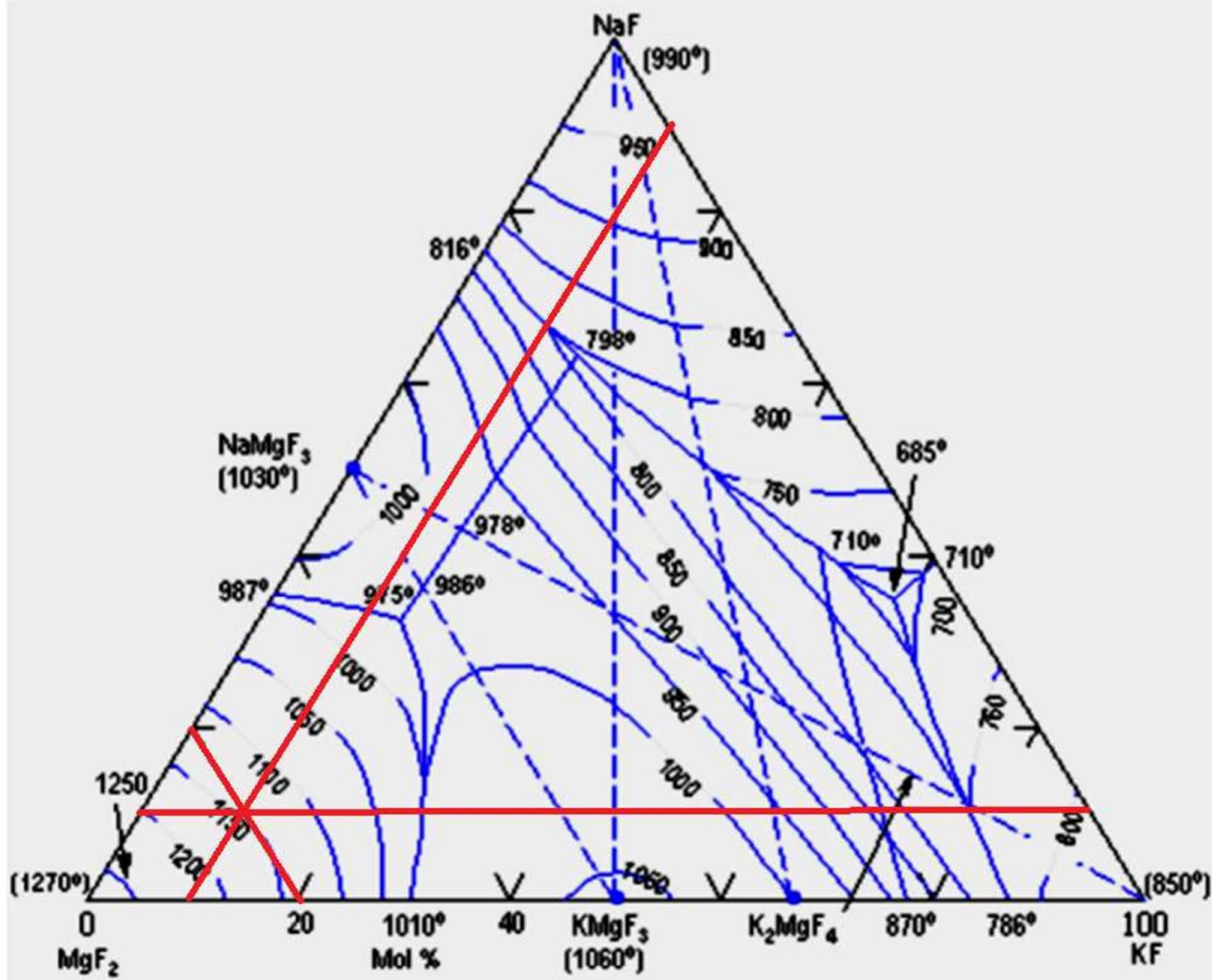


- If a composition of 10:10:80 mole% KF:NaF:MgF₂ is heated, at what temperature does it form a single phase liquid?

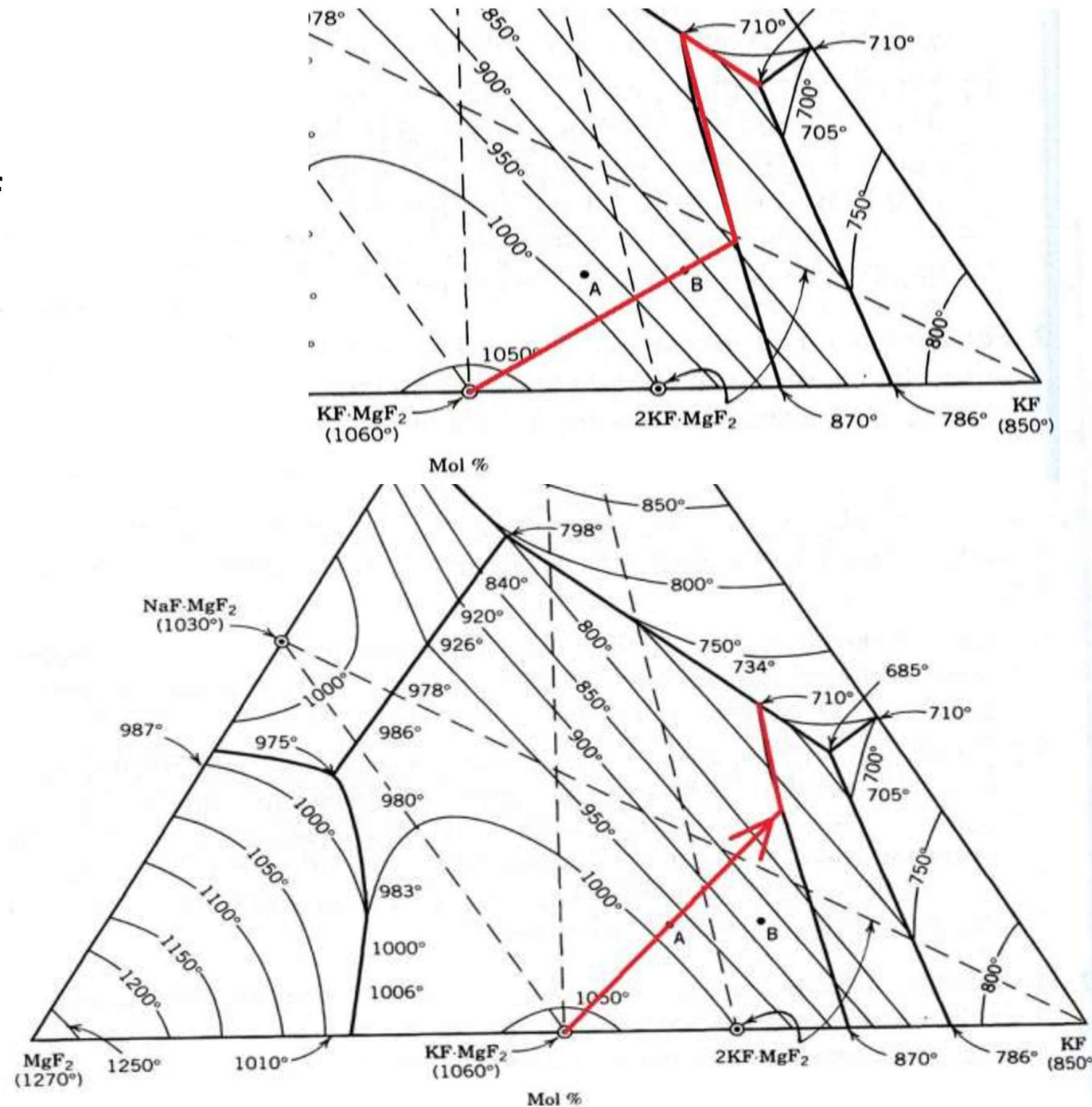
• Ans: 1145 °C

- If a powder mixture of the pure end members is heated, what is the minimum temperature at which a liquid will form?

• Ans: 685°C



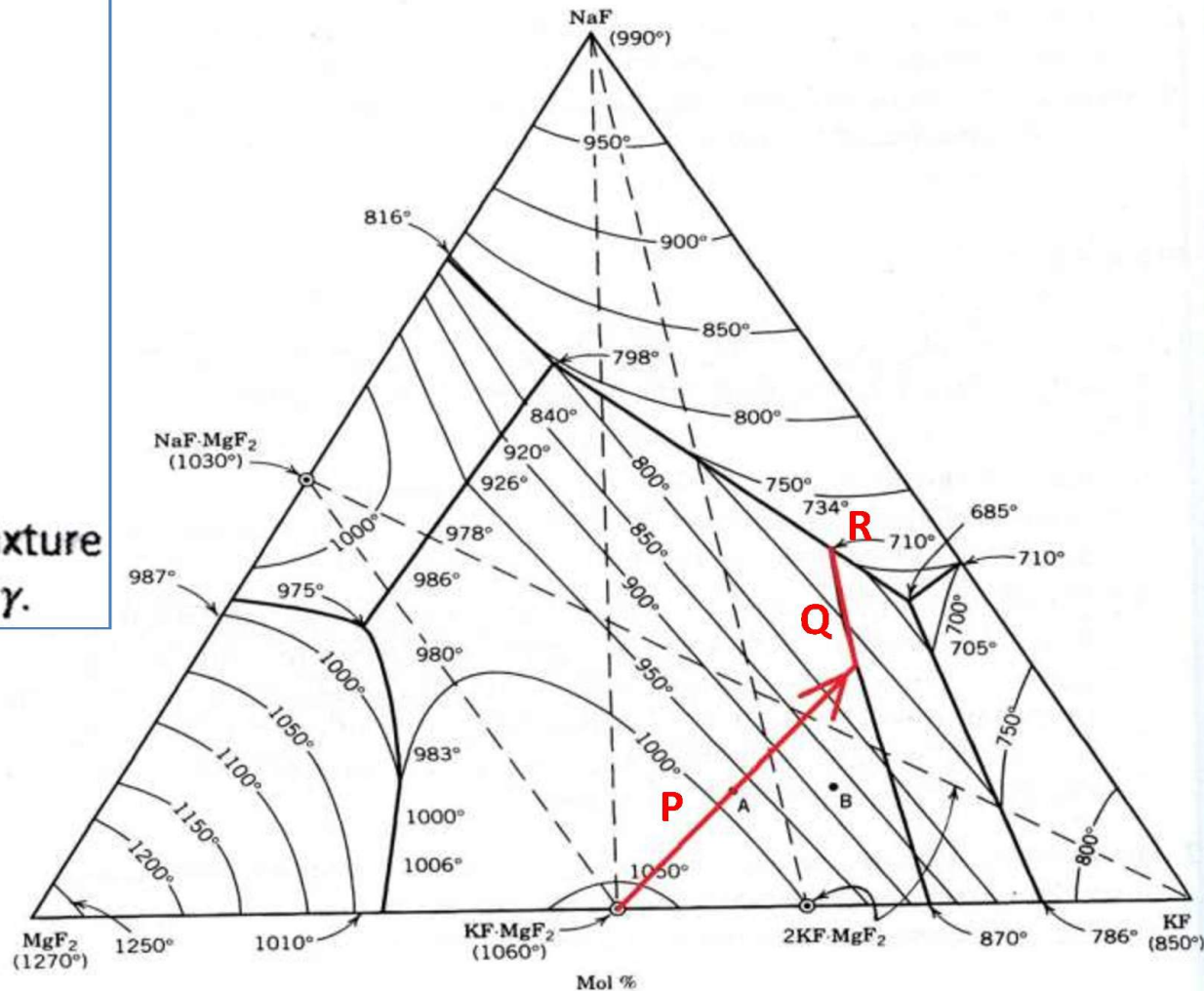
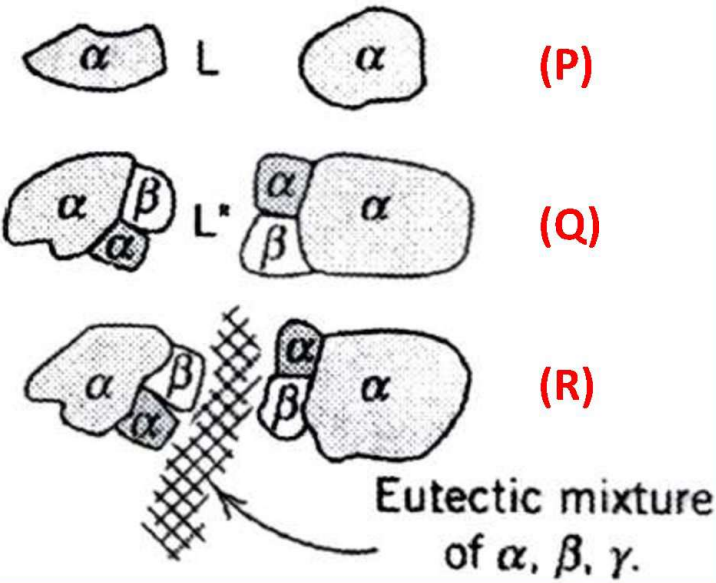
• Explain the crystallization path for single phase liquid of the composition marked A. How does it differ from that marked B?



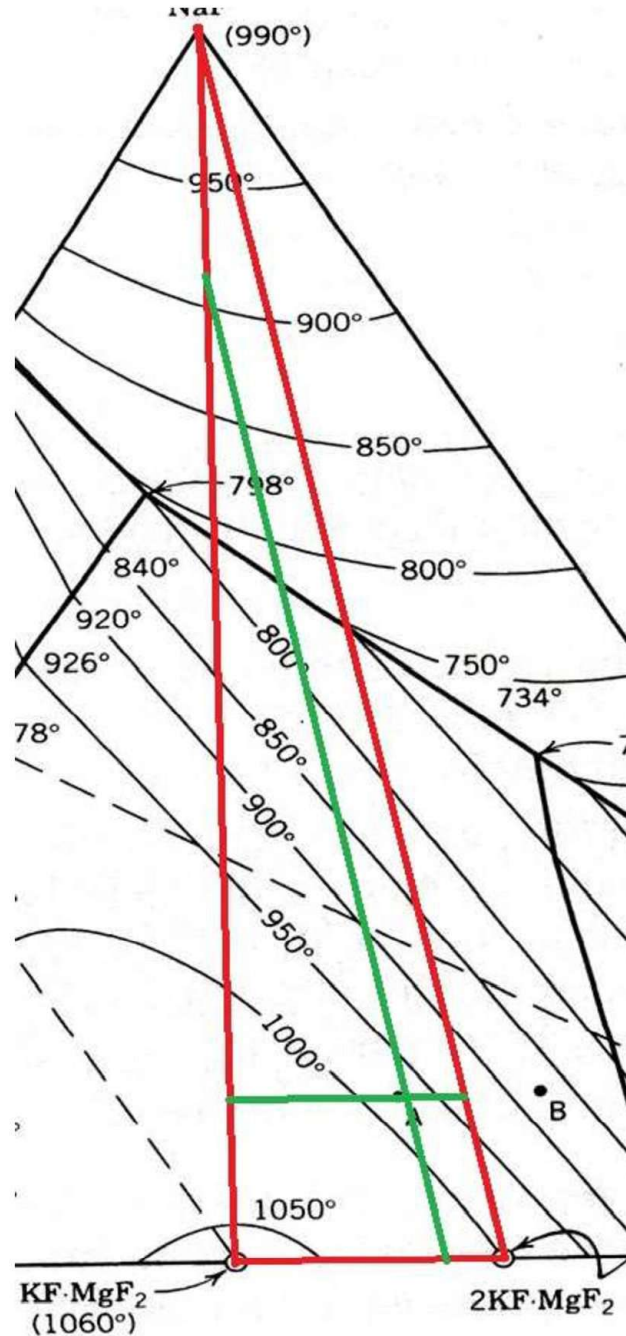
- Also sketch what the microstructure might look like after reaching room temperature.

$$KF.MgF_2 = \alpha, 2KF.MgF_2 = \beta, NaF = \gamma$$

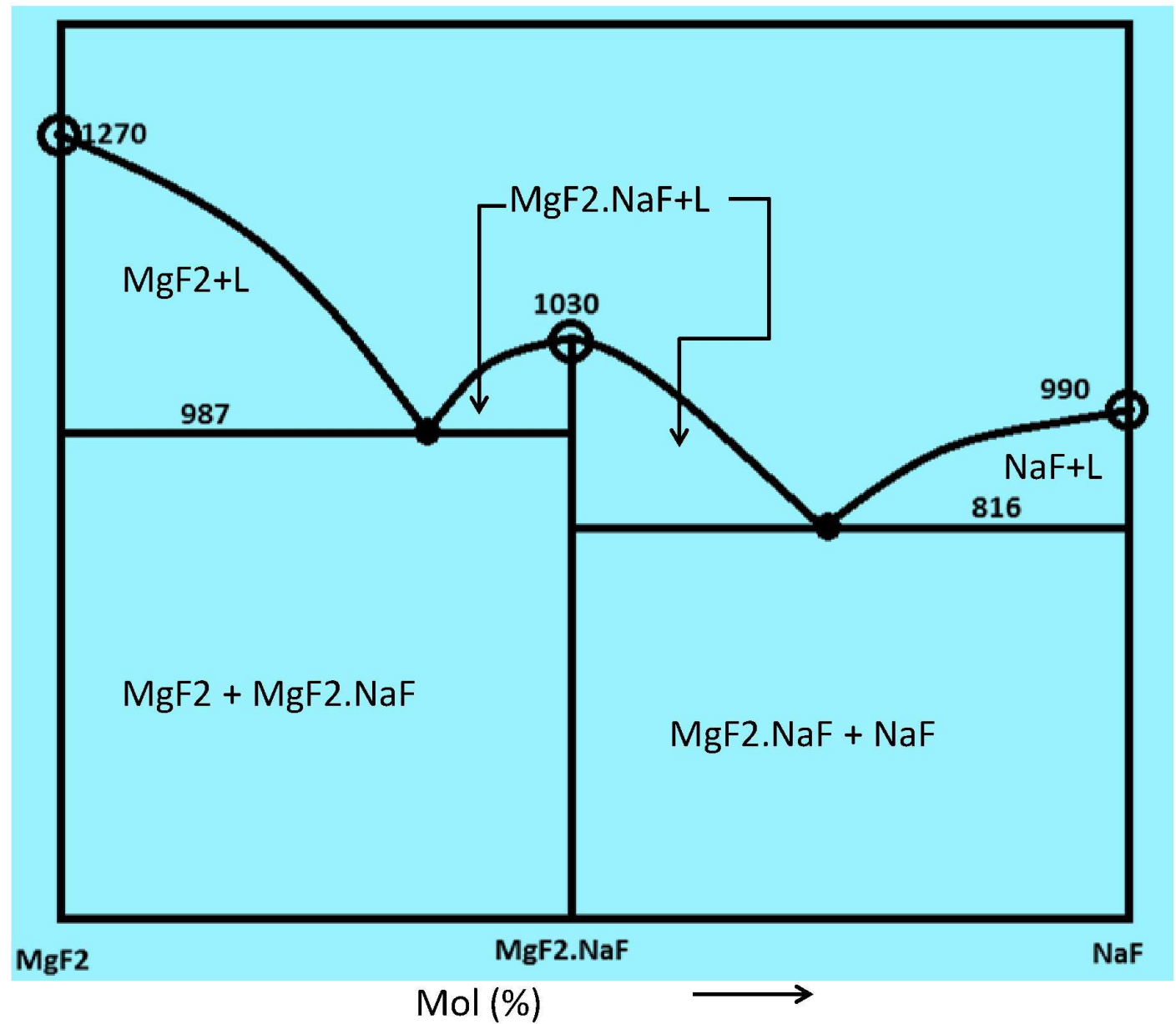
Schematic microstructure



- For the composition A, determine the phases present and fraction of each phase at room temperature.



- From the data available draw the binary phase diagram between NaF-MgF₂



- Cements may be defined as adhesive substances capable of uniting fragments or masses of solid matter to a compact whole.
-

Portland Cement

European Pre-standard: Cement is a **hydraulic binder**, i.e. a finely ground inorganic material which, when mixed with water, forms a paste which **sets and hardens** by means of **hydration reactions** and processes and which, after hardening, **retains its strength and stability even under water**.

ASTM Standard C 219-94 defines: Portland cement as 'a hydraulic cement produced by pulverizing **Portland-cement clinker, and usually containing calcium sulfate'**

Portland cement clinker is a hydraulic material; consist of at least **two-thirds** by mass of **calcium silicates** ($(\text{CaO})_3\text{SiO}_2$ and $(\text{CaO})_2\text{SiO}_2$), the remainder containing Al_2O_3 , Fe_2O_3 and other oxides. The ratio by mass (CaO/SiO_2) shall be **not less than 2.0**. The content of magnesium oxide (MgO) shall not exceed 5.0 per cent by mass.

It is necessary for the manufacturer to produce, **as economically as possible**, a material which is **sound** (i.e. it does not expand significantly after hardening) and which, when ground with the appropriate amount and form of calcium sulfate to a **specific surface area** (Blaine) of **300-350 m²/kg**, develops a **28-day strength** (when tested using the method given in EN 196-1) of **50-65 N/mm²**.

SiO_2 (%)	22.2
Al_2O_3 (%)	4.2
Fe_2O_3 (%)	2.4
Mn_2O_3 (%)	0.08
P_2O_5 (%)	0.15
TiO_2 (%)	0.27
CaO (%)	63.9
MgO (%)	1.0
SO_3 (%)	2.7
CO_2 (%)	0.79
K_2O (%)	0.74
Na_2O (%)	0.14
Free lime (%)	1.5
Loss on ignition (%)	1.7
Insoluble residue (%)	1.7
Na_2O equivalent (%)	0.63
$\text{C}_3\text{S}^{\text{a}}$ (%)	46
$\text{C}_2\text{S}^{\text{b}}$ (%)	29
$\text{C}_3\text{A}^{\text{c}}$ (%)	7.1
$\text{C}_4\text{AF}^{\text{d}}$ (%)	7.3
Density (kg/m^3)	3130
Surface area (m^2/kg)	383
Coarser than 45 μm (%)	13.4

PYRO-PROCESSING

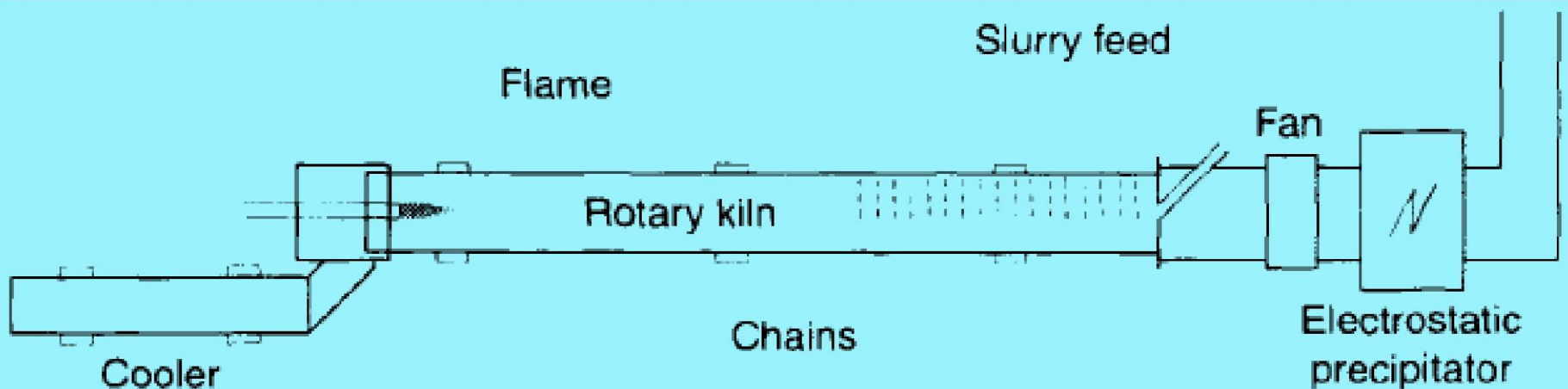


Fig. 2.3 Wet process (shown here with a rotary cooler).

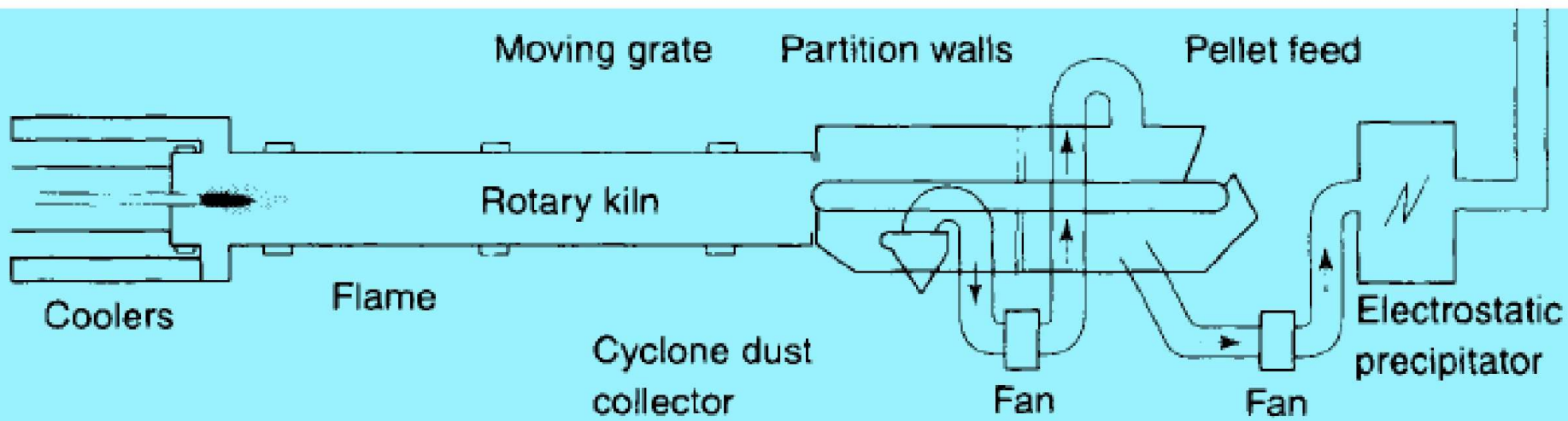
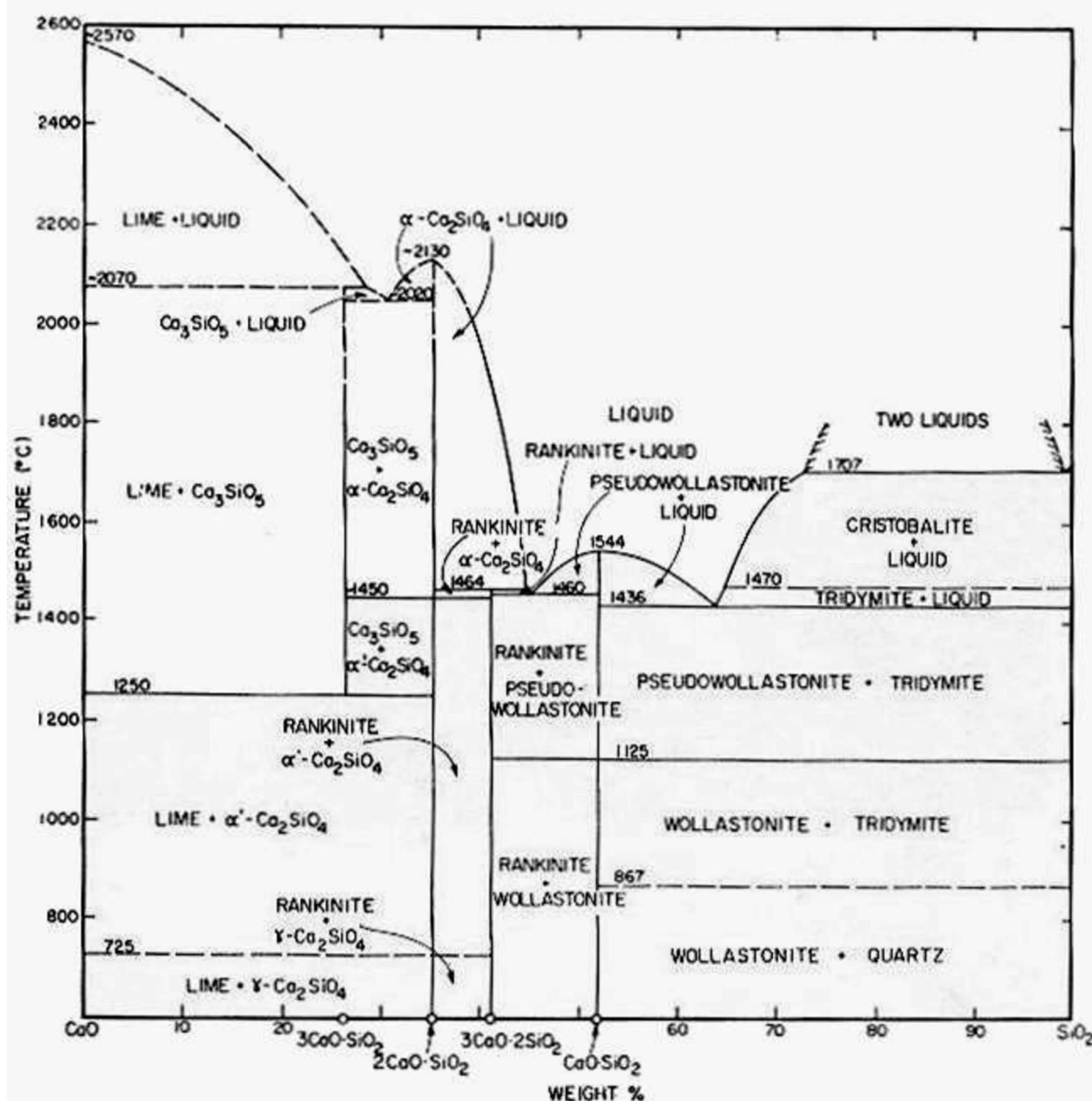


Fig. 2.4 Semi-wet/dry process (shown here with a planetary cooler).

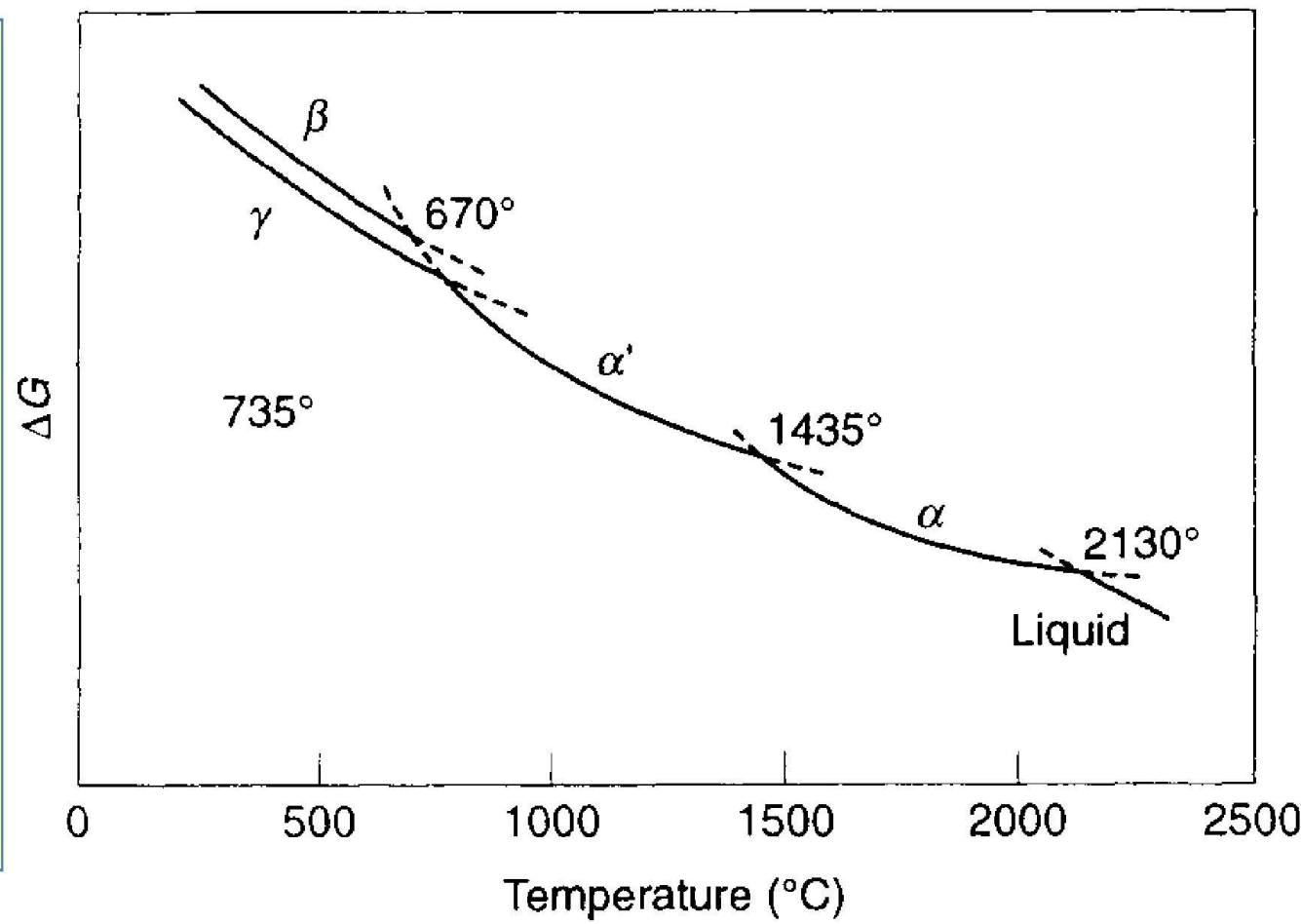
The system CaO-SiO₂

The phase diagram contains four binary compounds, CS, C₃S₂, C₂S and C₃S. Neither the calcium metasilicates (CS) nor rankinite (C₃S₂) are appreciably hydraulic and are not found in Portland cement clinkers.

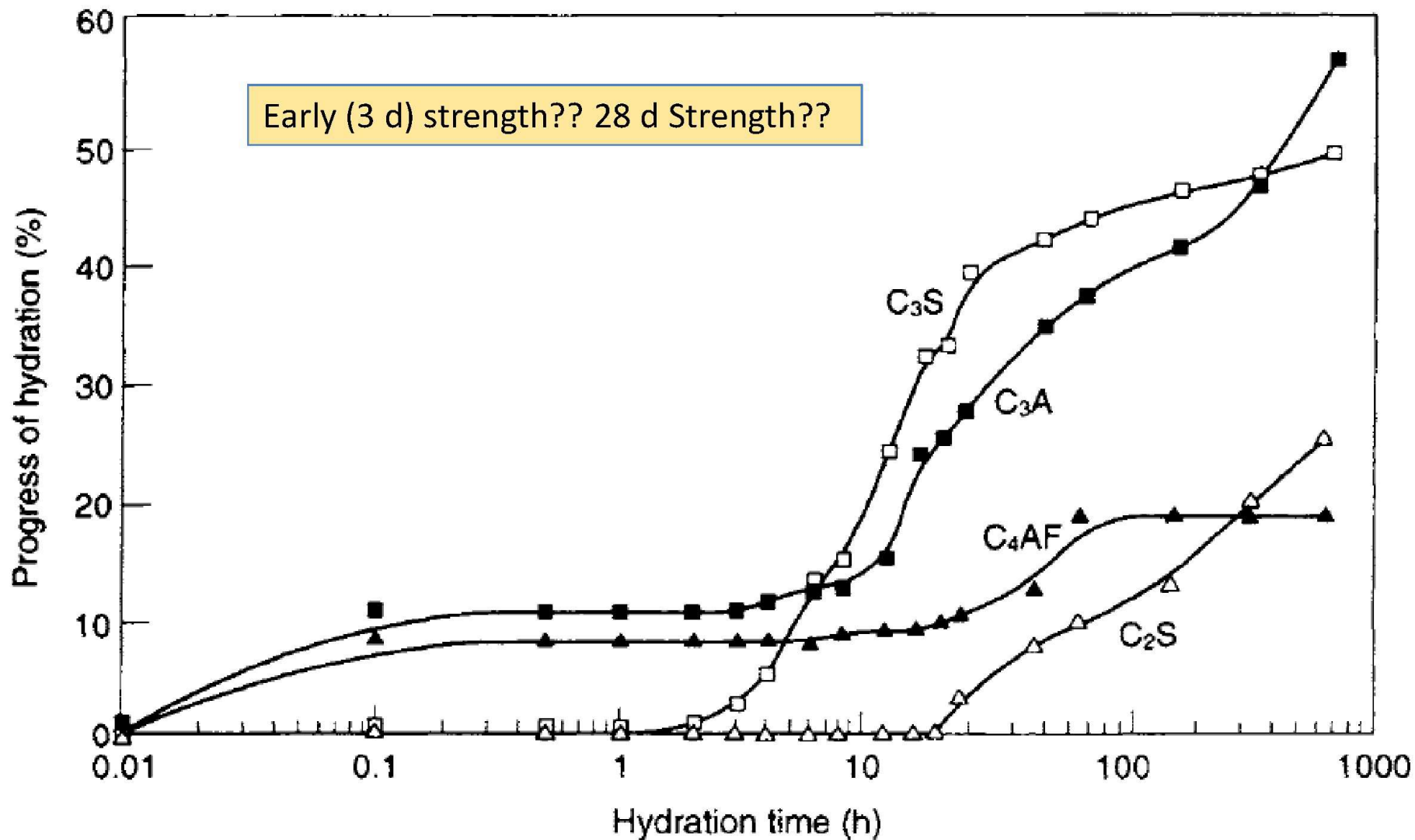


Dicalcium silicate (C₂S) is an important constituent of Portland cement clinker (comprising **20-40 per cent** by weight). It exhibits a number of polymorphs, the hydraulically important polymorph in Portland cement being ***beta-C2S***.

On cooling from elevated temperatures, alpha-C₂S passes through a number of closely related polymorphs before transforming to the beta-C₂S form at 670°C.

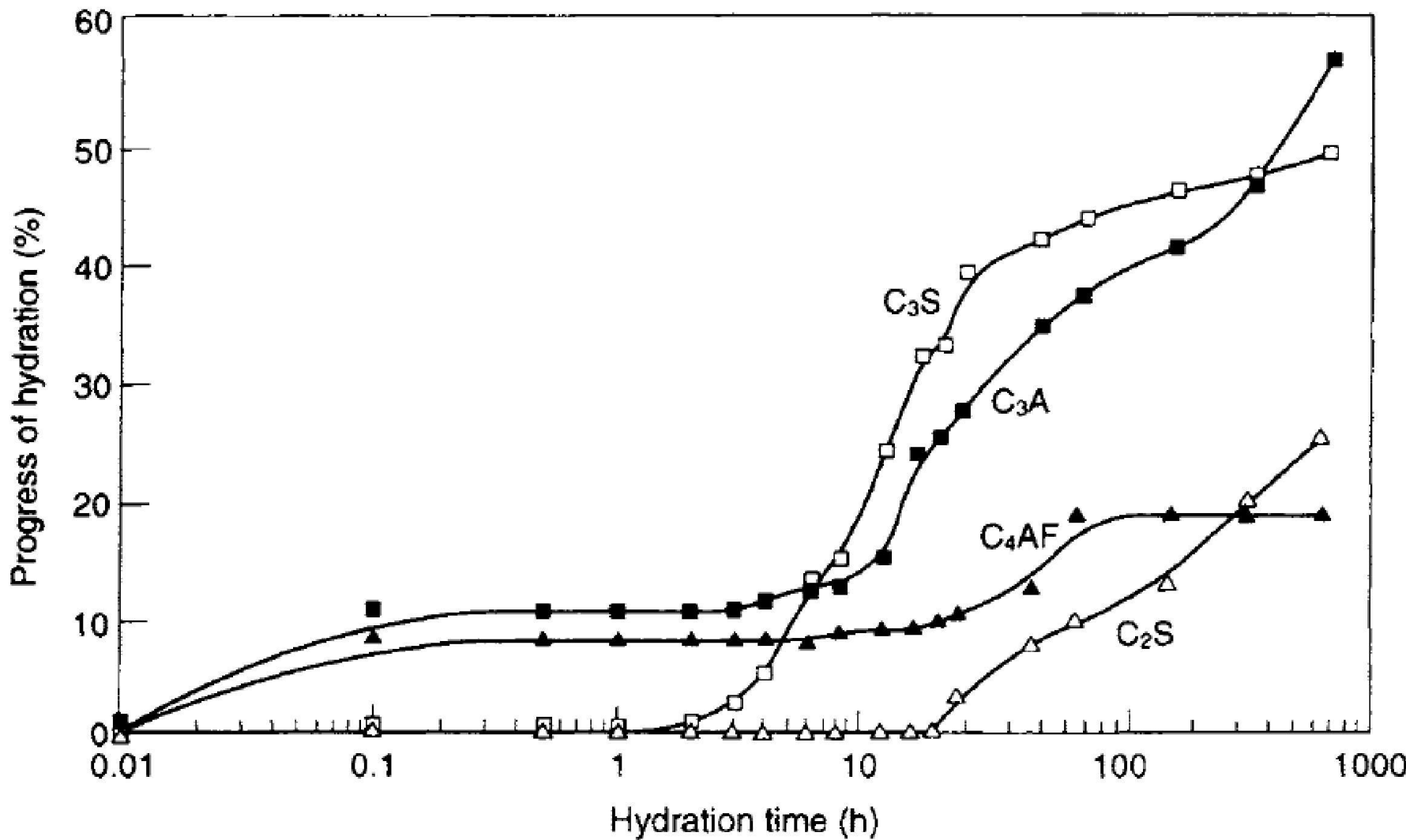


The transformation at lower temperature to the **gama-modification** is accompanied by a **volume increase** responsible for the well-known phenomenon of 'dusting'. Gama-C₂S is **non-hydraulic**, but fortunately **beta-C₂S** can be stabilised to low temperature by **quenching** or by formation of **solid solution** with a large number of **oxide impurities** which dissolve at high temperature alpha phase. Examples of impurities include **boric oxide, phosphorus pentoxide and magnesia**. **Impure form** of beta-C₂S is **belite**, the, which is present in cement clinker. Pure beta-C₂S is not an equilibrium phase under normal atmospheric conditions, and therefore its existence is not reflected in the equilibrium CaO-SiO₂ diagram.



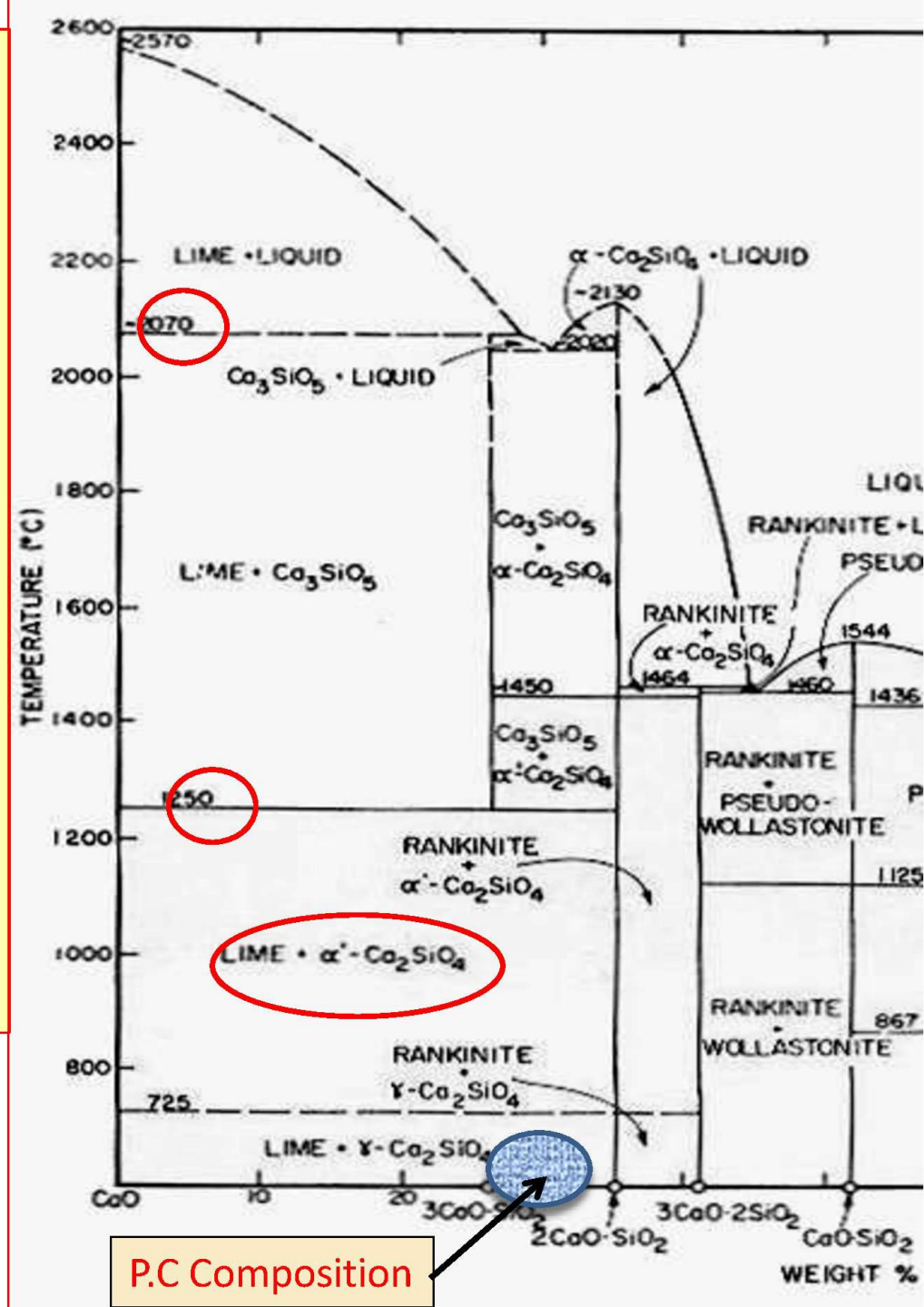
The most abundant phase of Portland cement clinker is **Alite (55-65%)**, an impure form of tricalcium silicate (C₃S). Majority Hydration by **28 d**.
 $2\text{C}_3\text{S} + 6\text{H} > \text{C}_3\text{S}_2\text{H}_3$ (CSH) + 3 CH. CSH: **Main binder**.

Early (3 d) strength?? 28 d Strength??



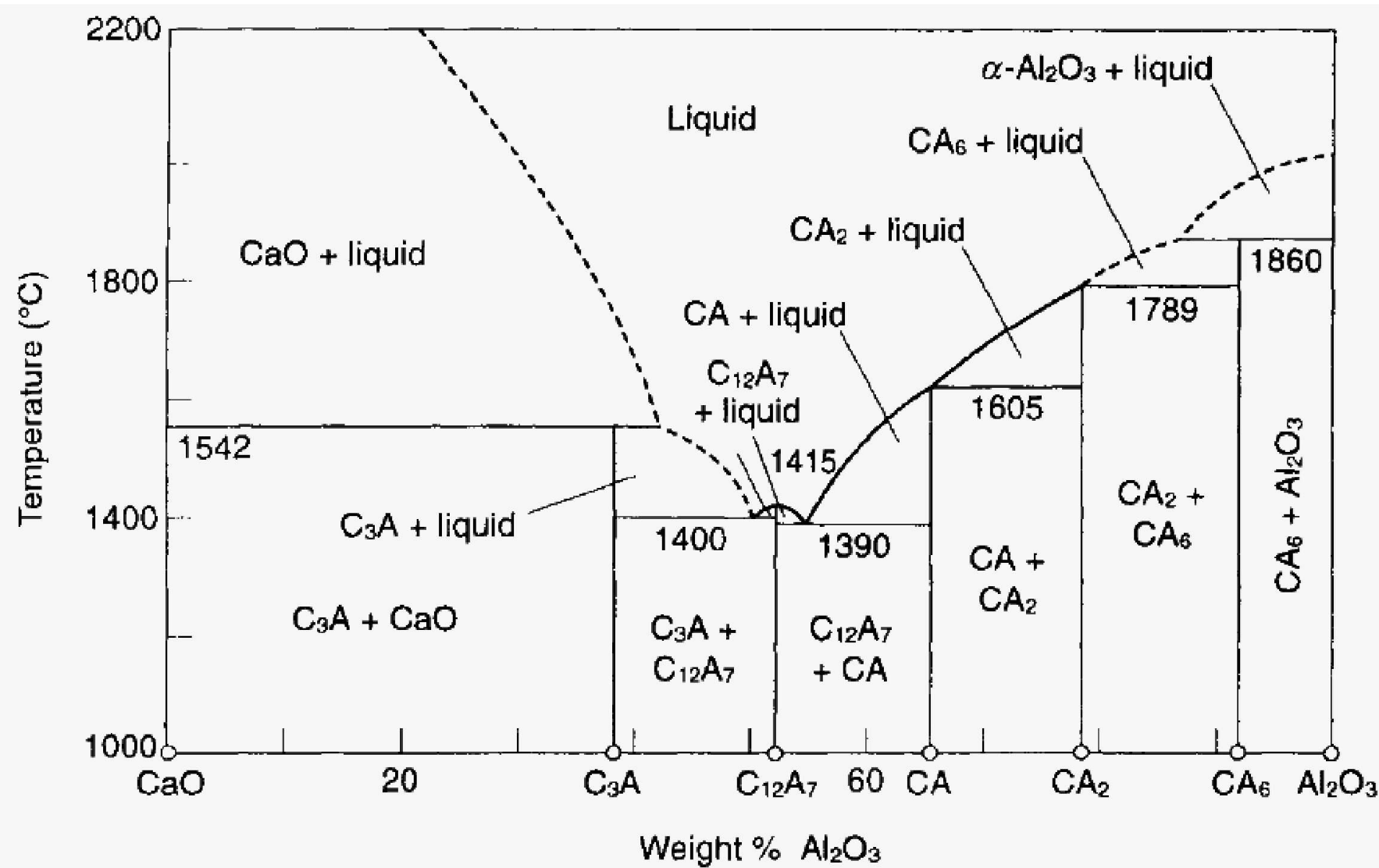
C3S is stable from its incongruent melting at 2070°C to approximately 1250°C.

- **Unusual feature**, products of dissociation are **CaO** and **C2S**: Rate of dissociation is comparatively slow: moderately rapid cooling is sufficient to prevent dissociation: thus **thermodynamically metastable**. Slow Cooling > Decomposition.
- **Rapid Cooling** (18-20 C/min): Increased: 28 d strength, Soundness, SO₄-Resistivity



The system CaO-Al₂O₃: * rapid decrease in liquidus by the addition of Al₂O₃.

*Significant in reducing the burning temperatures. > economic levels. This system contains the stable phases **C3A**, **CA**, **C12A₇**, **CA₂** and **CA₆**. C3A melts incongruently at 1542°C. **C3A: Rapid Hydration and flash setting.**



The minimum melting compositions are the **eutectics** between 12 CaO-7 Al₂O₃ and either 3 CaO-Al₂O₃ or CaO*Al₂O₃; these are located at **1400°** and **1390°C**, respectively. Beyond the C12A7 eutectic with CA, liquidus temperatures begin to rise rapidly with increasing alumina content. CA melts **incongruently** to CA₂ at **1605°C**; CA₂ melts incongruently to CA₆ at \sim **1789°C**, and CA₆ melts **incongruently** to Al₂O₃ and liquid at \sim **1860°C**. It can be seen that normal aluminous cements having CaO/Al₂O₃ **ratios between 0.9 and 1.2**, will have **lower solidus and liquidus temperatures** than the high-alumina cements, which have CaO/Al₂O₃ ratios between **1.8 and 2.5**. The **high-alumina cements** are, consequently, **more valuable** as a refractory material; however, their **higher raw-materials cost** and the **higher melting temperatures** required add to the **expense** of their production.

C12A7 is an **undesirable** constituent of aluminous cements: it hydrates very rapidly and causes "**flash setting**." This results in **partial hardening** of the wet concrete before it can be placed. The CA, on the other hand, has very **desirable** hydraulic properties. The **high-alumina cements**, depending on their CaO/Al₂O₃ ratio, **contain** mainly CA plus CA2, or with increasing Al₂O₃ content, CA2 plus CA6. Both CA2 and CA6 are relatively **inert to hydration** in neutral solutions (pH = 7) but CA2 will hydrate readily in **alkaline solution**. High-alumina cements containing CA2 can be **mixed with** alkaline solutions (**pH > 12**) and poured or cast in the same manner as portland cements. Thus, **CA and CA2 are the most desirable phases** in the anhydrous clinker.

III. PORTLAND CEMENTS

A. Preparation of the Cement

The chemical and phase compositions of anhydrous portland cements are somewhat more complex than those of the aluminous cements described in the previous section. Portland cements contain CaO , Al_2O_3 , SiO_2 , and Fe_2O_3 as major chemical components: i.e., those components that are present to the extent of 5 mole % or more. In addition, substantial quantities of Na_2O , K_2O , MgO , SO_4^{2-} , and PO_4^{3-} may be present. Before proceeding to examine the relevant phase diagrams, it would be appropriate to review briefly the production of portland cements in order to see what type of information might usefully be obtained from the phase diagrams.

The first stage in the manufacturing process is the selection of raw materials to give the correct bulk composition. Often, no single deposit or

quarry will yield materials having the desired composition, and several types of rock, such as limestone and argillaceous shale, must be ground and intimately mixed. Next, the feed is introduced into the cool end of a gently inclined shaft kiln. The entire kiln is rotated slowly so that the feed moves on down the incline toward the hot end, or "burning zone," of the kiln. As the feed heats up, a complex series of reactions occurs. Those that take place at comparatively low temperatures, such as the loss of CO_2 from the carbonates, loss of H_2O from the clay minerals, etc., will not be discussed further. In the hot zone, a temperature of $1350^{\circ}\text{--}1500^{\circ}\text{C}$ is maintained. This temperature is always kept sufficiently high to allow a liquid phase to develop. The liquid phase hastens reaction, because material transport proceeds more rapidly through a liquid phase than would be the case in an all-solid-state reaction. Therefore, rather thorough reaction and recrystallization of the starting materials takes place in the burning zone. The temperature of this zone and the duration of the "burn" are chosen carefully. On the one hand, the temperature must not be allowed to rise to the point where the cement becomes fluid, or the resulting melt will attack the refractory lining of the kiln. On the other hand, the time and temperature conditions must permit a reasonably close approach to the equilibrium distribution of phases, and this state must be achieved rapidly enough to permit reasonable fuel economy. A usual compromise is thus to keep the proportion of liquid relatively low, and the physical texture of the resulting fired product is aptly described as "clinker." The clinker is a thoroughly indurated mass of crystalline phases that are held together by a ceramic bond between adjacent crystals as well as by an interstitial liquid phase.

The clinker is discharged continuously from the hot zone of the kiln and is chilled in an air blast. Finally, the cooled clinker is ground to produce cement powder. It is this cement powder that, when mixed with water and appropriate aggregates, hydrates to form cement or concrete. Thus the process is conveniently divided into two stages: first, manufacture of the anhydrous cement clinker and second, the hydration stage. Phase diagrams appropriate to each stage will now be considered, starting with the anhydrous clinker.

B. Phase Composition of the Clinker

The simplest phase assemblage found in normal clinkers usually comprises at least five or six phases: tricalcium silicate (C_3S); tricalcium aluminate (C_3A); an iron-containing "ferrite" phase, having the approximate

composition C_4AF ($F = Fe_2O_3$), a silicate glass of variable composition; and possibly, free lime, CaO . In many low-iron-oxide cements, the sum of only three of the chemical components ($CaO + Al_2O_3 + SiO_2$) is equal to or greater than 90 wt % of the total. Therefore, it would be appropriate to consider the $CaO-Al_2O_3-SiO_2$ system first. One of the limiting binary systems, $CaO-Al_2O_3$, has already been discussed: to account for the quantitatively most important phases, we need also to examine the $CaO-SiO_2$ system.

C. The $CaO-SiO_2$ System

A phase diagram of the $CaO-CaSiO_3$ portion of the $CaO-SiO_2$ system is shown in Fig. 5. In the high-lime compositions, which are of interest to cement chemistry, two binary phases— Ca_3SiO_5 and Ca_2SiO_4 —are encountered. The polymorphism of these compounds will be described in detail. At the liquidus, Ca_3SiO_5 melts incongruently to CaO and liquid at $2070^{\circ}C$;

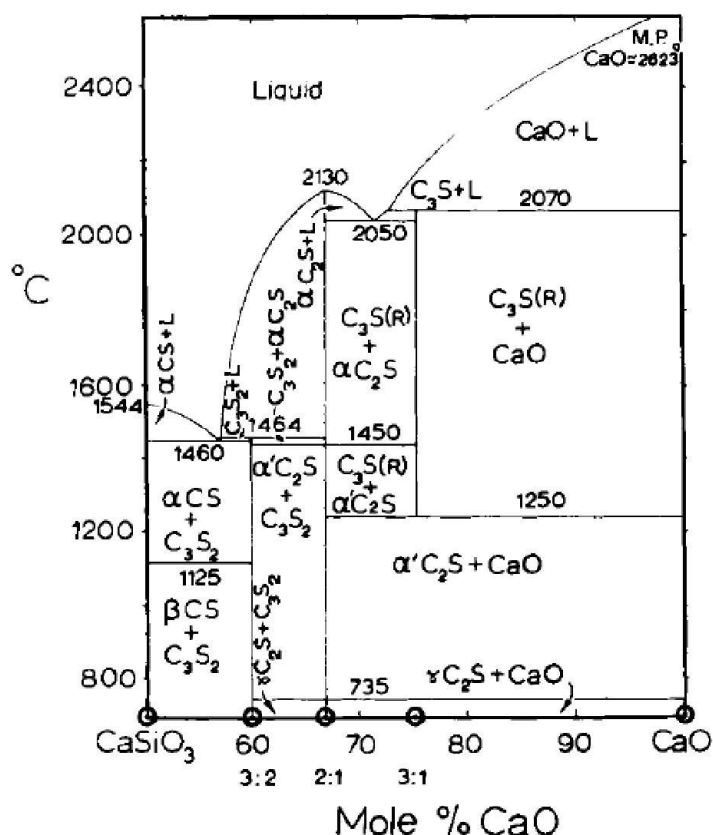


Fig. 5. Phase diagram for a portion of the system $CaO-SiO_2$. See text for a discussion of the polymorphism of C_3S (tricalcium silicate): $C_3S(R)$ indicates the rhombohedral phase.

Ca_2SiO_4 melts congruently at 2130°C. In more acid compositions two additional phases are encountered, $\text{Ca}_3\text{Si}_2\text{O}_7$ (rankinite) and CaSiO_3 (pseudo-wollastonite, or $\alpha\text{-CaSiO}_3$). Rankinite melts incongruently to Ca_2SiO_4 and liquid at 1467°C; CaSiO_3 melts congruently at 1544°C. CaSiO_3 also has another polymorph (wollastonite, $\beta\text{-CaSiO}_3$), which is stable below approximately 1125°C. Rankinite and CaSiO_3 are not ordinarily encountered in portland cements.

1. Ca_2SiO_4

The polymorphism of Ca_2SiO_4 is shown in Fig. 6. Four crystalline phases are known: three of these, α , α' , and $\gamma\text{-Ca}_2\text{SiO}_4$, have a range of thermodynamic stability at 1 bar pressure: the fourth phase, $\beta\text{-Ca}_2\text{SiO}_4$,

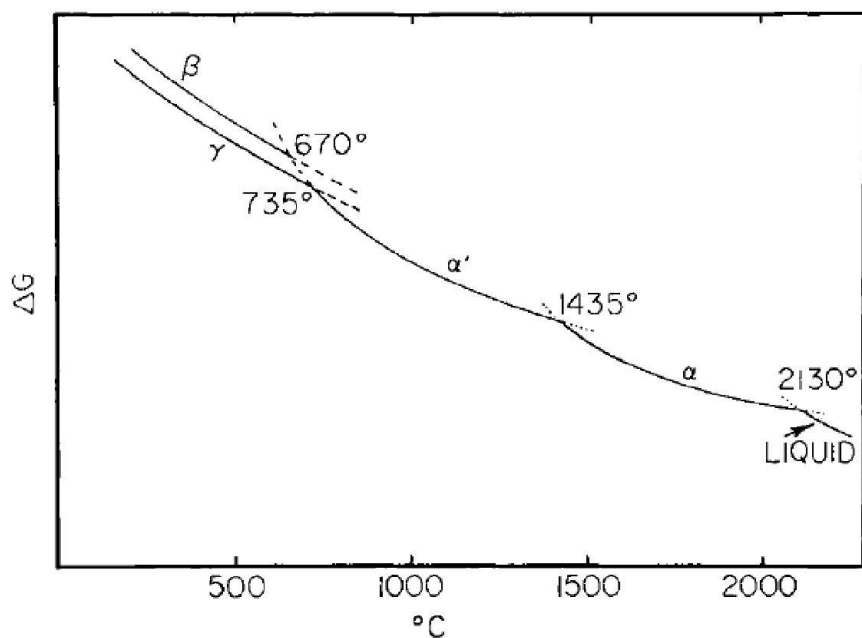


Fig. 6. Relative free energies of the polymorphs of Ca_2SiO_4 as a function of temperature.

is monotropic. The phase stable between 1435°C and the melting point is designated $\alpha\text{-Ca}_2\text{SiO}_4$. This phase has a close structural relationship to the α' phase, which is stable over a range of temperatures below 1435°C. The inversion between the two phases is rapid and normally nonquenchable. With equilibrium cooling, $\alpha'\text{-Ca}_2\text{SiO}_4$ inverts to $\gamma\text{-Ca}_2\text{SiO}_4$ at $\sim 735^\circ\text{C}$. This inversion is, however, not rapid. The solid requires a good deal of structural reorganization to pass from the α' phase to the much more open, olivine-type, $\gamma\text{-Ca}_2\text{SiO}_4$ phase. Therefore, the α' phase tends to persist metastably below the equilibrium temperature: this possibility is shown in Fig. 6 by the metastable prolongation of the free-energy curve for the α' phase to

temperatures below $\sim 735^{\circ}\text{C}$. The metastable persistence of the α' phase does not continue to temperatures much below $\sim 670^{\circ}\text{C}$, for at this temperature, another phase transition occurs, and the $\alpha'\text{-Ca}_2\text{SiO}_4$ inverts to the monotropic $\beta\text{-Ca}_2\text{SiO}_4$. This reaction is characteristically rapid. Once $\beta\text{-Ca}_2\text{SiO}_4$ has formed, its conversion to the more stable γ phase is possible in theory, at any temperature; the use of a free-energy-temperature diagram shows this clearly, because both stable and metastable states can be represented. At any temperature, the stable phase in Fig. 6 is that which has the lowest free energy. However, when another component is added, e.g., CaO or SiO₂, only the lowest-free-energy portion of Fig. 6 would usually be shown: this can be seen by comparing Fig. 6 with the relevant portion of Fig. 4.

In practice, the kinetics of the $\beta \rightarrow \gamma$ reaction are rather sluggish, especially at ambient temperatures. Once initiated, however, the conversion of β - to $\gamma\text{-Ca}_2\text{SiO}_4$ tends to be autocatalytic. All polymorphic transitions must, in theory, be accompanied by changes attending the transformation of one phase to another. The volume change of the $\beta \rightarrow \gamma$ reaction is especially large. If the $\beta \rightarrow \gamma$ reaction occurs after the cement is partially hydrated, the resulting volume increase cannot be accommodated and the strength of the set cement is much reduced, often with spectacular results. Several solutions have been proposed for this serious technological problem. First, modern portland cements are often proportioned so as to contain a high ratio of C₃S/C₂S. One solution is thus to reduce greatly the quantity of Ca₂SiO₄ that is present, or even eliminate it. Its complete elimination is often economically not feasible or necessary. It might seem that, if Ca₂SiO₄ must be present, it would be more desirable to have it present as the γ phase. This is not the case, as the β phase is more hydraulic (e.g., hydrates more readily to form a strong bond with the aggregate) than is the γ phase. Provided that ways can be found to dependably prevent or inhibit the $\beta \rightarrow \gamma$ inversion, $\beta\text{-Ca}_2\text{SiO}_4$ may be a relatively desirable constituent. A number of factors that cannot be represented on a phase diagram are important in influencing the kinetics of the $\beta \rightarrow \gamma$ reaction. For example, the previous thermal and mechanical history of the Ca₂SiO₄ has an important bearing on the low-temperature sequence of inversions. Crystals that have passed through the $\alpha \rightarrow \alpha'$ inversion tend to convert more readily to $\gamma\text{-Ca}_2\text{SiO}_4$ upon cooling than those that have never been taken above the $\alpha\text{-}\alpha'$ inversion temperature. Slow clinker cooling rates, particularly in the 600°–750°C range, favor the attainment of equilibrium, and hence formation of $\gamma\text{-Ca}_2\text{SiO}_4$.

The discussion has thus far been confined to pure Ca₂SiO₄. However, impurities also play a major role in shaping the sequence of low temperature inversions. A wide range of oxides are capable of forming at least a limited range of solid solutions with Ca₂SiO₄ at clinkering temperatures. Oxides

whose solubility in the α or α' phases is equal to, or exceeds 0.5 mole %, include Na_2O , K_2O , MgO , FeO , Fe_2O_3 , Al_2O_3 , Mn_2O_3 , Cr_2O_3 , CrO_4^{3-} , VO_4^{3-} , and PO_4^{3-} . The temperature of the $\alpha-\alpha'$ inversion is very sensitive to the presence of these oxides; in fact, Newman and Wells (1946) have used the changes in the $\alpha-\alpha'$ inversion temperature with changing bulk composition to measure the equilibrium solubility of each of these oxides in the $\alpha\text{-Ca}_2\text{SiO}_4$ phases. The effects of various substituents may be broadly classified as follows. First, there are substituents that form only a very limited range of solid solutions with both the α and α' phases. This case is shown schematically in Fig. 7a. Substituents in this class include Al^{3+} , Fe^{3+} , and Mn^{3+} .

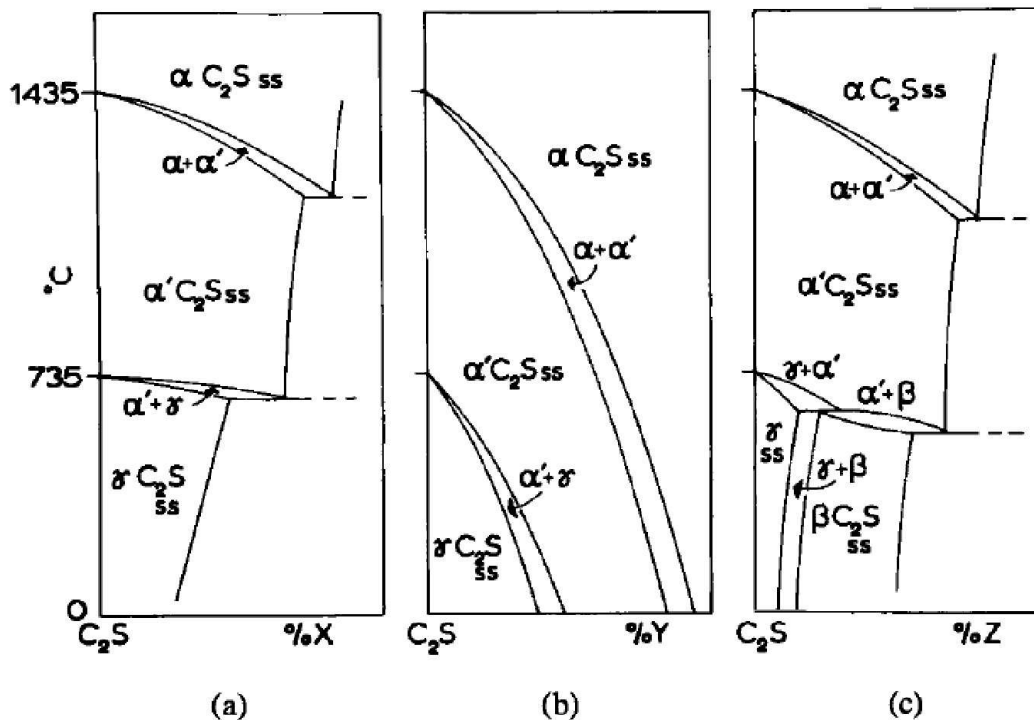


Fig. 7. Schematic phase diagrams showing the effect of additives on the polymorphism of Ca_2SiO_4 . These additives, and the nature of their effects, are discussed in the text.

These ions do not have a major influence either on the stability of the β and γ phases at lower temperatures, or on the sequence of metastable changes that are encountered in the low-temperature range. The $\alpha \rightarrow \alpha'$ inversion temperature is lowered, but only slightly, by these substituents: the quantitative extent of solid solution is, at most, 1–2 mole % in the temperature range of interest, about 1430°C . Second, there are those substituents that form extensive solid solutions with either, or both, α - and $\alpha'\text{-Ca}_2\text{SiO}_4$. The phosphorous-substituted Ca_2SiO_4 solid solutions are an example. The effect of this type of solubility is shown schematically in Fig. 7b: in all cases that have been studied, the solubility of the added ion is greater in the high form than in the low. This causes the inversion temperature to fall with increasing solid solution. The two phase region: ($\alpha + \alpha'$ solid solutions) sweeps downwards, and the $\alpha' \rightarrow \gamma$

inversion temperature (which likewise becomes a two phase region) is lowered below room temperature. This means that the metastable $\alpha' \rightarrow \beta$ inversion temperature is probably depressed as well, and that only α or α' , or a mixture of α and α' phases are likely to be encountered, provided that a sufficient quantity of substituent has been used. In practice the necessary quantity is only a few mole percent P_2O_5 . Last are those substituents whose effects are not fully understood. B_2O_3 is an example of such a substituent. Ca_2SiO_4 solid solutions containing B^{3+} , even in amounts as small as 0.2–0.5 mole %, always give β - Ca_2SiO_4 upon either rapid quenching or slow cooling to room temperature. It is not certain if the B^{3+} merely prevents the β phases from converting to the γ phase, or if the relative order of stability of the β and γ phases are reversed by B^{3+} substitution. In the former case, γ - Ca_2SiO_4 would still be the thermodynamically stable phase at low temperatures, and the barriers to actually obtaining it during the cooling stage would be purely kinetic. However, in the latter case, which is shown schematically in Fig. 7c, the relative stabilities of β and γ phases are shown as having been reversed by increasing substitution of B^{3+} . It is not known which of these two possibilities is the correct one.

2. Ca_3SiO_5

Tricalcium silicate is stable from its incongruent melting at 2070°C to approximately 1250°C. The existence of this lower-temperature stability limit is perhaps an unusual feature, but one that is appearing in many oxide systems as the low-temperature phase relations are studied more thoroughly. Figure 5 shows that the products of dissociation of Ca_3SiO_5 are CaO and Ca_3SiO_5 . The rate of the dissociation reaction is comparatively slow, even at these high temperatures, so that even moderately rapid cooling of industrial clinkers is sufficient to prevent dissociation of the Ca_3SiO_5 present. If clinkers are left to cool slowly, the Ca_3SiO_5 may begin to decompose: this trouble has occasionally been encountered in industrial products. Upon cooling below 1250°C, Ca_3SiO_5 is thus thermodynamically metastable. A number of polymorphic transformations are encountered during the cooling: these cannot be represented on the equilibrium diagram, but may be conveniently represented on a free-energy-versus-temperature plot, similar to that which was used to represent the sequence of phase changes in Ca_2SiO_4 (Fig. 5). These data for Ca_3SiO_5 are shown in Fig. 8, which is based largely on the recent study of Bigaré *et al.* (1967). The form stable at high temperatures, designated (R), has rhombohedral symmetry: basically, the polymorphic inversions encountered at lower temperatures are caused by structural distortions of the high-symmetry R phase. With decreasing temperatures, two monoclinic phases, designated M_{II} and M_I , are encountered, and

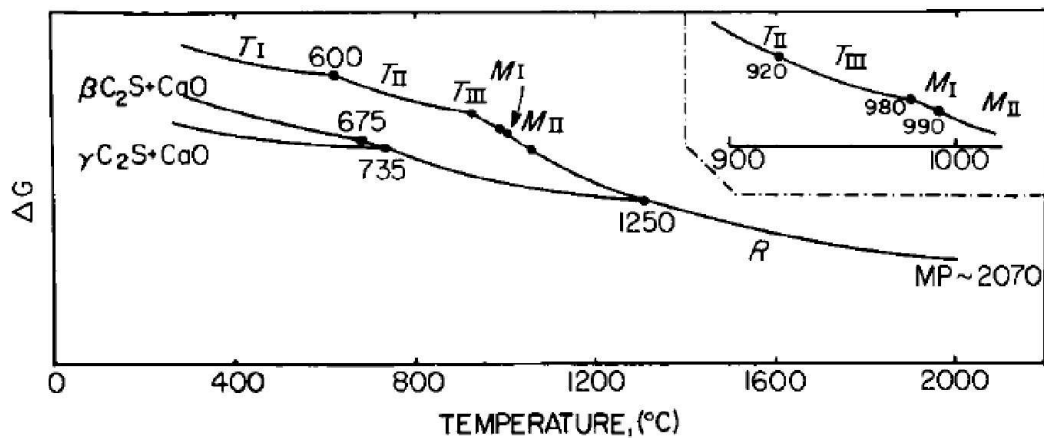
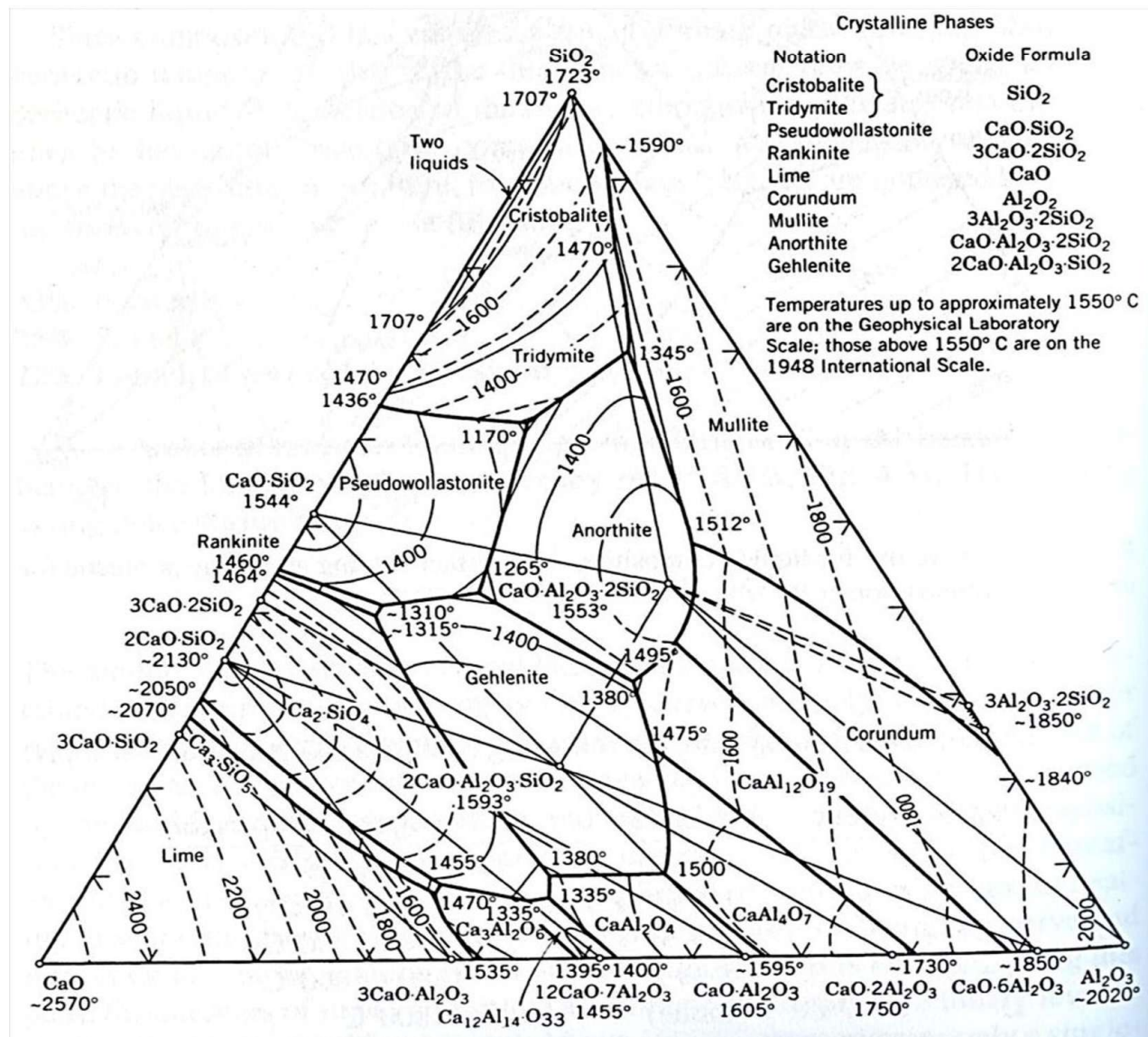


Fig. 8. Relative free energies of the polymorphs of Ca_3SiO_5 as a function of temperature.

then three triclinic phases: T_{III} , T_{II} , and T_I . For pure Ca_3SiO_5 , these inversions are all rapidly reversible both on heating and cooling, and hence cannot be quenched. They must be detected by some direct method: in the study cited above both high-temperature powder x-ray photographs and D.T.A. were used. It is interesting to note that not all the phase transformations were detectable by *both* x-rays and DTA. The enthalpy change accompanying the $M_{II} \rightleftharpoons R$ inversion is too small to be detected by DTA; on the other hand, the $T_{II} \rightleftharpoons T_{III}$ transformation has a reasonably large enthalpy change, but the existence of the transformation could not be detected in high-temperature powder photographs. Small amounts, about 1–2% of alkali, MgO and Al_2O_3 , have a marked influence on the sequence of polymorphic inversions; the experimental evidence is reviewed by Bigaré *et al.* (1967).

D. The $\text{CaO}-\text{Al}_2\text{O}_3-\text{SiO}_2$ System

The low-silica regions of the $\text{CaO}-\text{Al}_2\text{O}_3-\text{SiO}_2$ system are shown in Fig. 3. Insets to the diagram show the range of typical anhydrous cement compositions (center) and an isothermal section through the system at 1500°C (bottom). If the disposition of typical portland cement compositions is examined with respect to the subsolidus compatibility triangles, it can be seen that the range of compositions appropriate to portland cement production lies largely within the three-phase triangle that has as apices: C_3S , C_2S , and C_3A . Assuming, therefore, that the clinker is approximately at equilibrium during the cooling stage, the coexistence of the quantitatively most important phases would be accounted for. It is, however, advisable to follow a given composition through a thermal cycle simulating the clinkering process and predict the sequence of phase changes that would be encountered. A composition representative of a portland cement and designated X, is shown on the 1500°C isothermal section. At this temperature, it lies within



the triangle: C_2S-C_3S -liquid. The liquid composition is fixed at L_X , and the liquid is thus enriched in Al_2O_3 relative to the bulk composition. If desired, the relative proportions of the three phases could be found by an appropriate geometrical construction. If the phase assemblage present at 1500°C is cooled sufficiently rapidly to room temperature, the phase distribution present at the higher temperature may be preserved for subsequent examination. The liquid phase will generally be found to have been preserved as a glass. However, these low-silica glasses are not very persistent, and the glass may crystallize readily during the quenching stage. Therefore, another case that may be treated is one where the liquid originally present at the high temperature crystallizes, but where the crystallizing liquid fails to react with the crystals already present. This corresponds to fractional crystallization. A simple analogy in a ternary aqueous salt system would be as follows: first, equilibrate a bulk composition under such conditions that an aqueous phase is in equilibrium with two crystalline phases. Centrifuge off the aqueous solution, and again crystallize the solution phase in part or in whole as, for example, by lowering the temperature. The process is easily visualized in an aqueous system of this sort, where an actual physical separation of the aqueous phase is made, but in the $CaO-Al_2O_3-SiO_2$ systems and indeed, in many other silicate systems, it is not necessary to make a physical separation to have fractionation processes operative. Fractionation processes become important because the rate-limiting step in the attainment of equilibrium is usually the rate at which material transport can occur across a crystal-liquid interface. Because this transport occurs only slowly, the crystalline phases are effectively prevented from reacting either with each other or with the liquid. As an example of this, consider the crystallization of the liquid L_X . This is the liquid composition that was generated in the previous example by partial fusion of a typical clinker. If the liquid crystallizes independently; that is, without reaction with the crystalline phases present at the clinkering temperature, the liquid phase will yield an assemblage containing C_2S , C_3A , and $C_{12}A_7$. This is because the liquid composition, unlike the bulk composition from which it originated, lies in the composition triangle $C_2S-C_3A-C_{12}A_7$. Thus, if we assume that the clinker composition designated X in Fig. 3c is first equilibrated at 1500°C, producing C_3S , C_2S , and liquid, and that in the subsequent cooling cycle the liquid crystallizes independently, we might obtain as many as five phases at room temperature. These phases would be C_3S , C_2S , and some residual glass, as well as the products of partially crystallizing the glass: namely, more C_3S , C_2S , and as the fifth phase, $C_{12}A_7$. Textural studies are often helpful in inferring the order of crystallization of phases and these textures become easier to interpret when the thermal history of the specimen is known and when the appropriate phase-equilibrium data are also known. In following

crystallization paths in clinker compositions, the important role of the thermal history in generating complex phase assemblages, containing as many or indeed, sometimes more than the maximum permitted by the phase rule should not be overlooked.

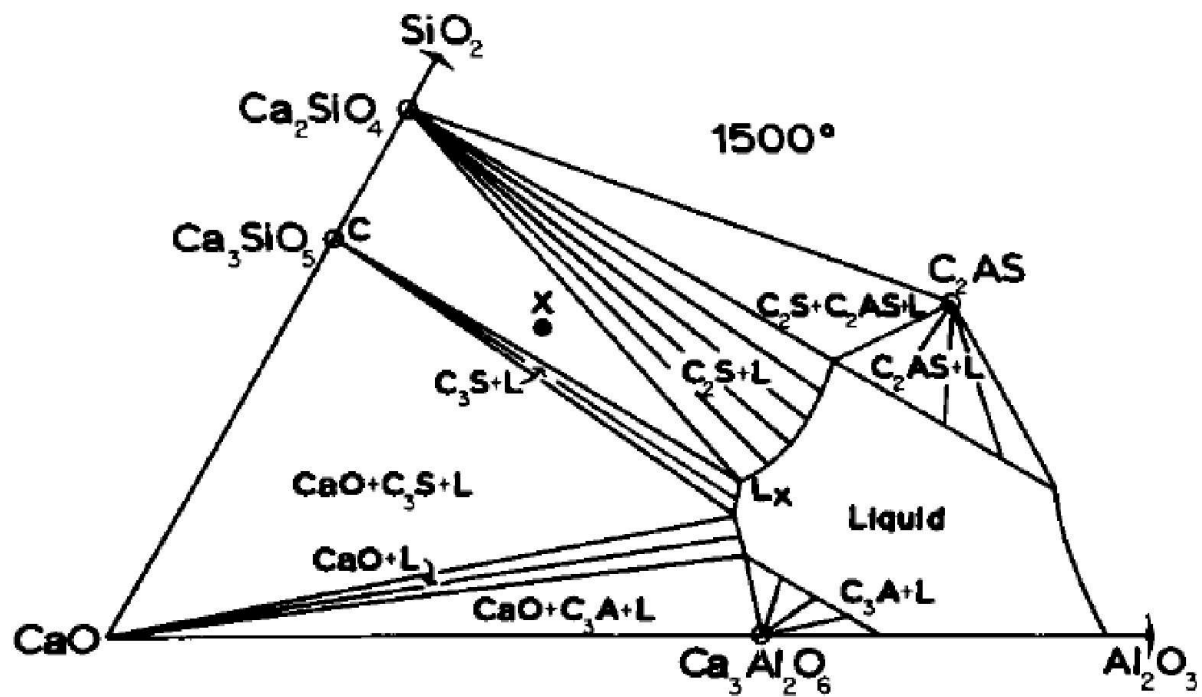
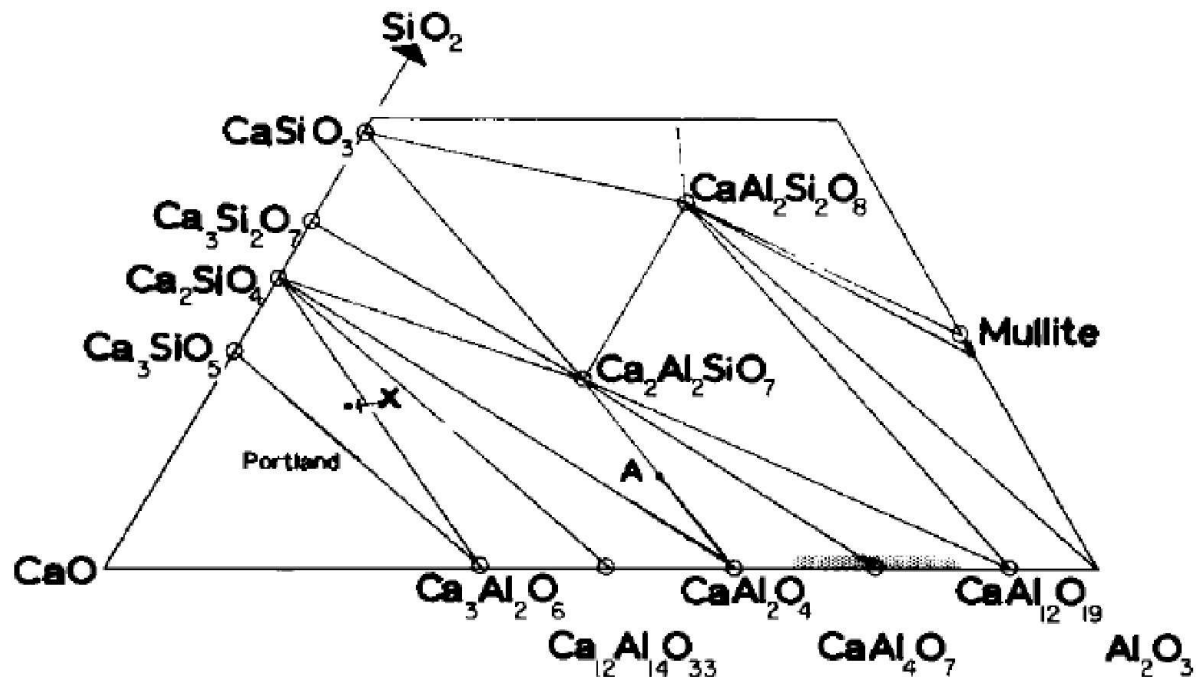
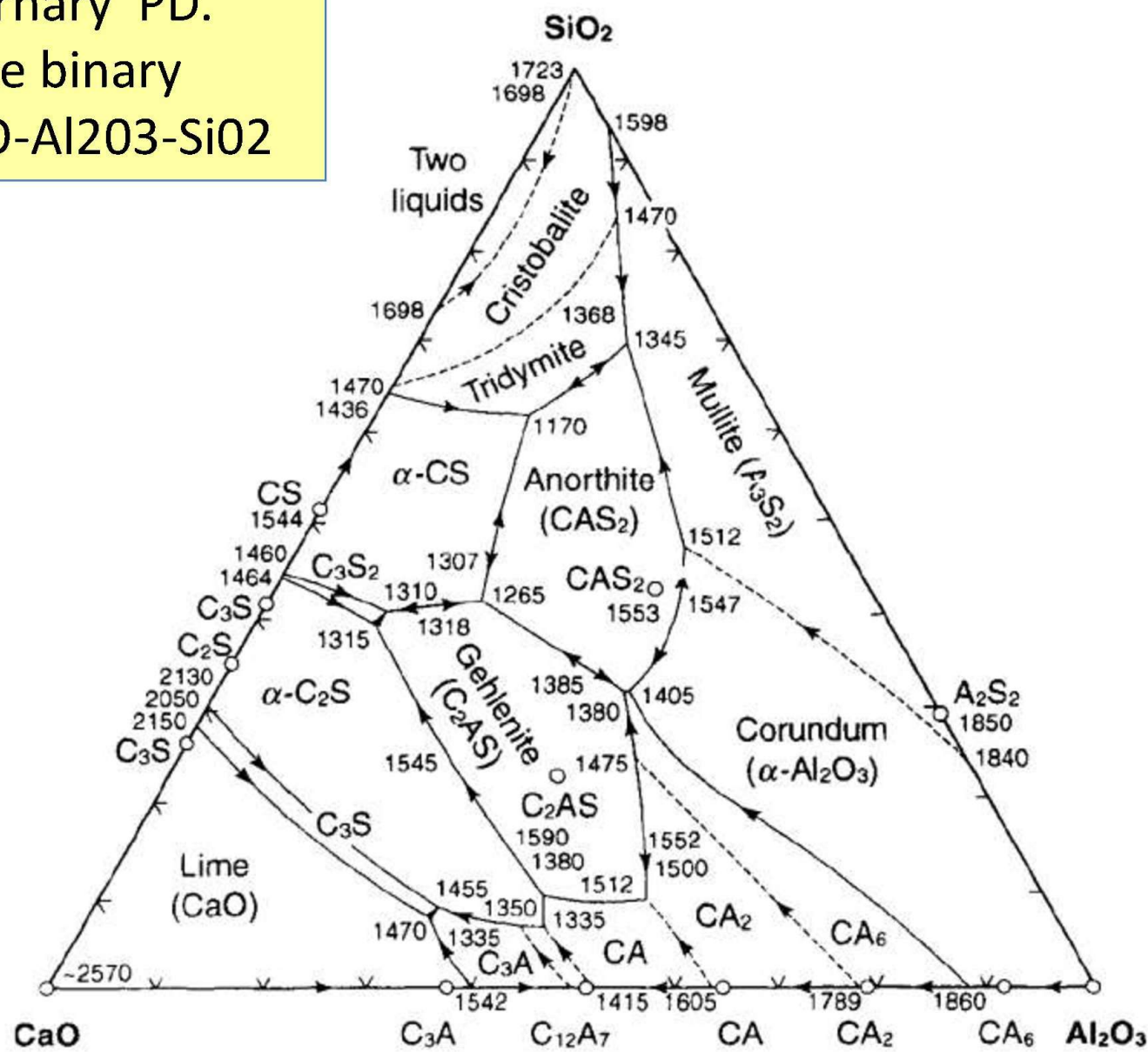


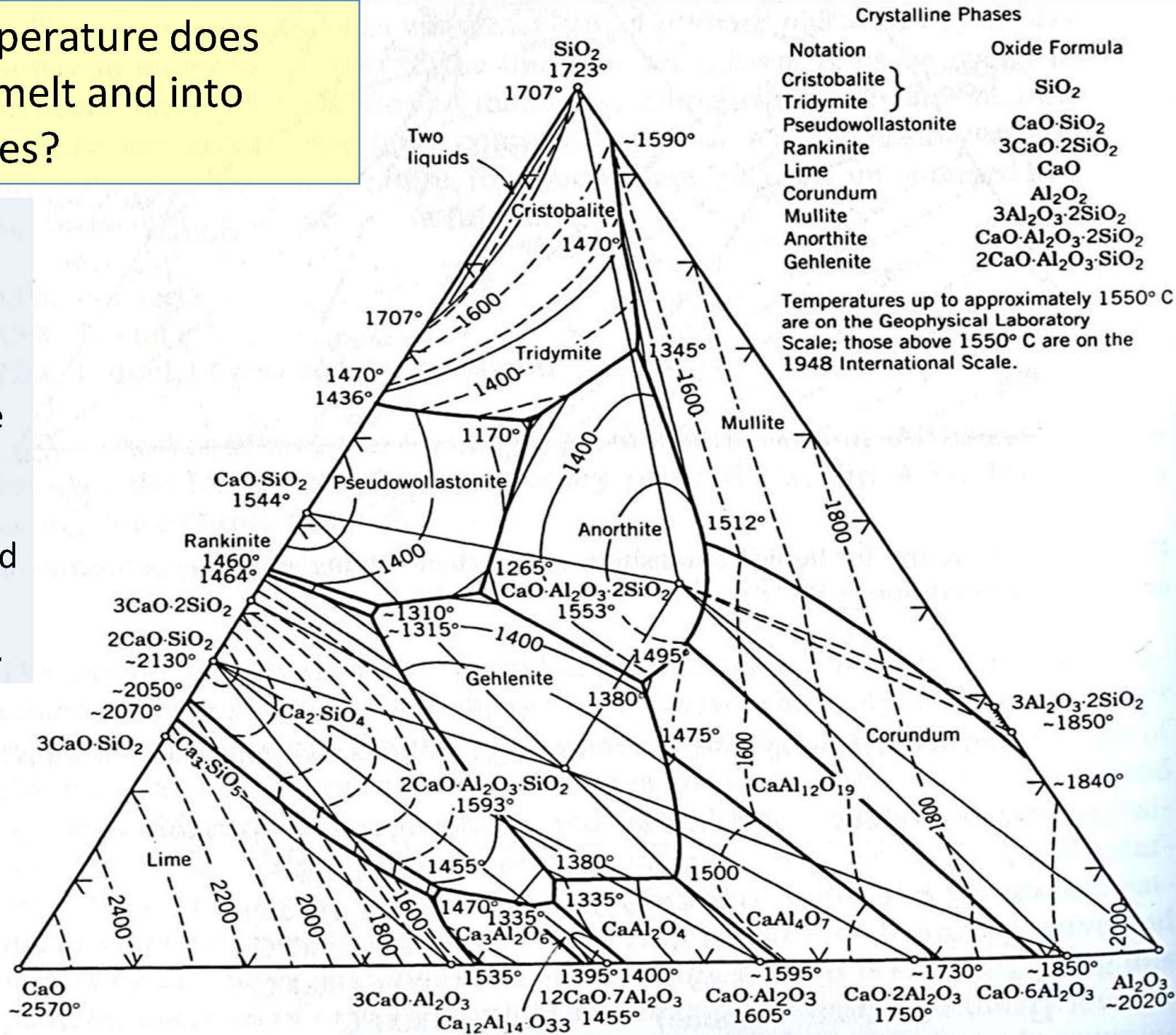
FIG. 3.

The CaO-Al₂O₃-SiO₂ and the CaO-Al₂O₃-Fe₂O₃ are the most relevant ternary PD. (0% PC contains three binary phases shown in CaO-Al₂O₃-SiO₂

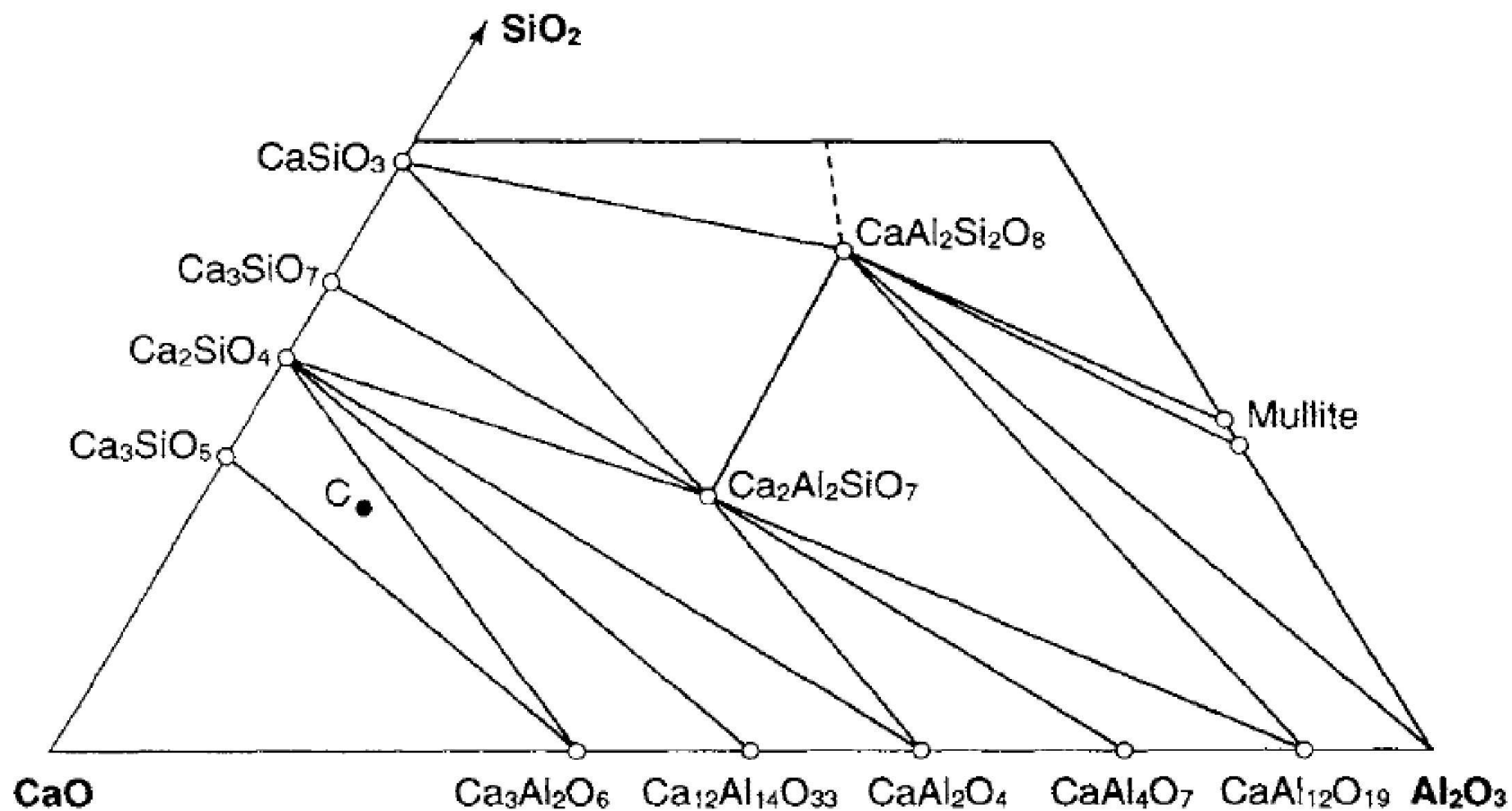


What Temperature does Rankinite melt and into what phases?

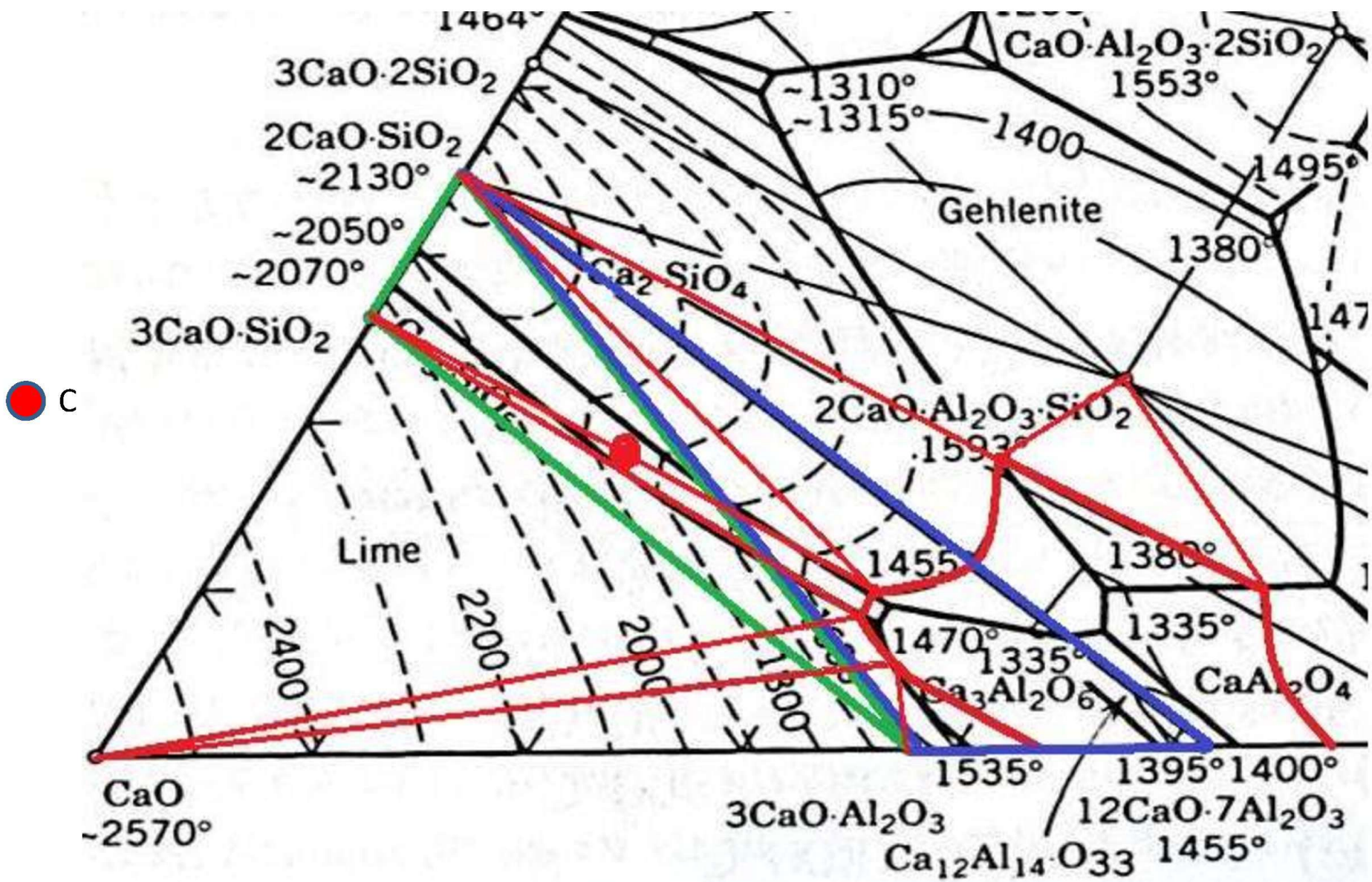
Identify the composition of phases.
Draw The binary phase diagram between anorthite and pseudo-wollastonite.



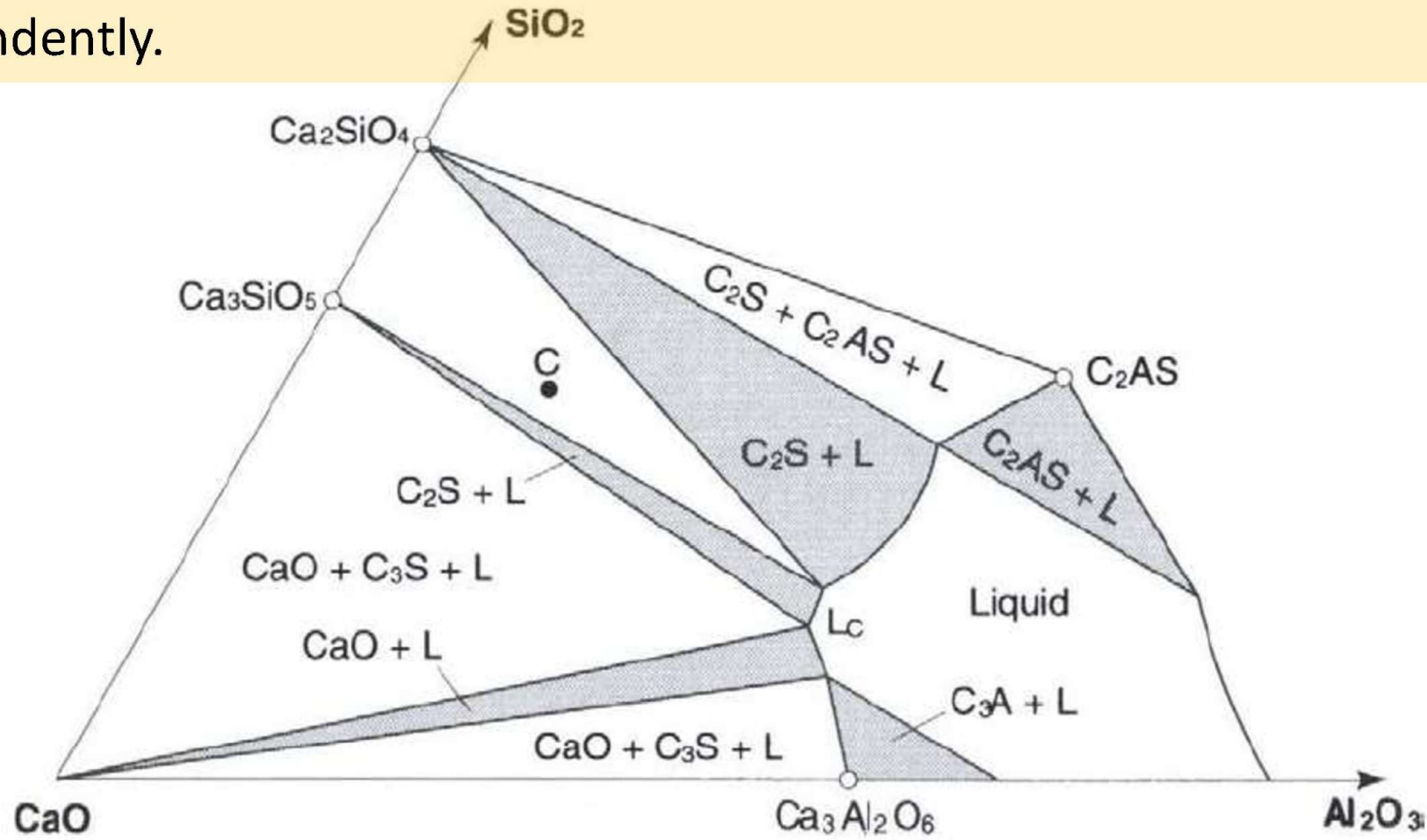
Typical PC composition is: "C",In Sub-solidus section: inside compatibility triangle: **C3S-C2S -C3A**. final phase assemblage obtained on cooling should be these **three phases**. However, practical cooling reactions rather are more complex and some amount of C_{12}A_7 also found. 1500°C may be considered as firing temp; so, 1500°C isothermal section should be consulted.



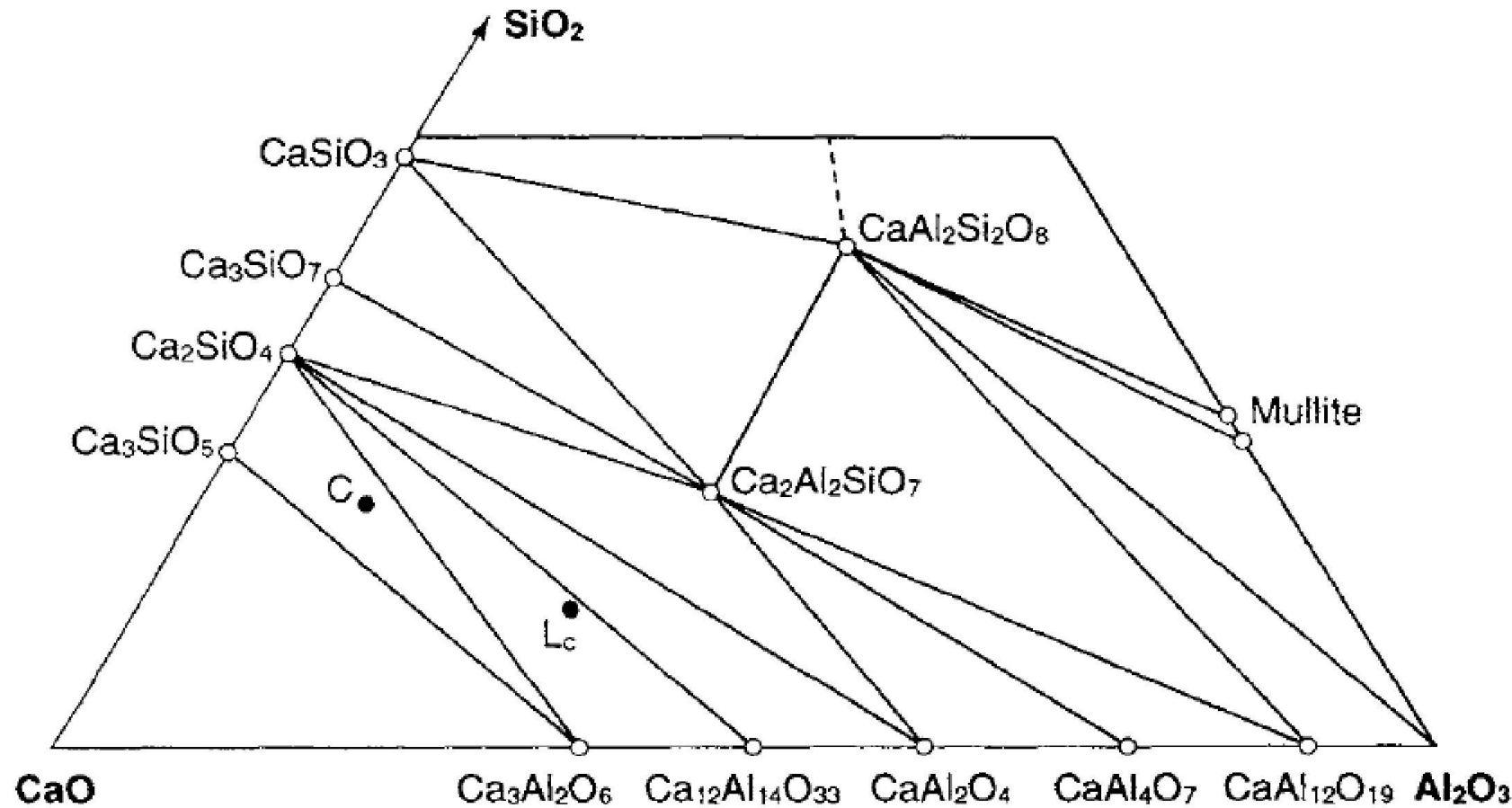
1500°C isotherm is relevant to cement manufacturing: Bulk composition of Portland cement is represented by the **point c**,



"C" is inside; **C₃S, C₂S and a liquid phase of composition Lc**. If clinker is cooled rapidly, liquid, generally \rightarrow glass, But low SiO₂ glass \rightarrow crystallizes, but crystallizing liquids fails to react with solid already present. This is due to fractional crystallization. For which, physical separation; not required. , a condition arising due to the slow rate of reaction between solids and viscous liquid. So Lc crystallizes independently.



Lc., considered in isolation from the solid, would crystallise on cooling to give **C2S**, **C3A** and **C12A7**. In practice all five phases, including **C3S**, **and glass** are observed. The phase rule predicts only three indicating that effectively two metastable equilibrium are observed in this particular case due to fractionation.



- **Normal-aluminous cement**: CaO:36-40; Al₂O₃:40-50; SiO₂:4-9; iron oxide:1-15; TiO₂:1-3; alkali:0-1; and MgO:0-2. Phases: **CA mainly, (C12A7, C2S, C2AS)**
- **High-alumina cement**: 72-82% Al₂O₃, and 15-27% CaO. Iron oxide, silica, and other impurities are kept low and often total only 1-4%. Phases: **CA mainly, plus CA₂, Al₂O₃.**
- Unique properties: (a) **rapid strength** development, even at low temperatures (Majority of strength within 24 h). (b) **high temperature resistance/refractory** performance. (c) **resistance to** a wide range of chemically aggressive conditions (SO₄²⁻, sea water, Acids)
- Basic **raw materials** for CAC: **limestone and bauxite**
- Manufacture: (a) **By fusion**~1600 °C (NAC): reverberatory open-hearth furnaces
- (b) For HAC: **Sintering (Rotary Kiln** for < 4% Fe₂O₃ impurity content).
- **CAC liquid/clinker**: Should be **cooled slowly**: More crystalline phase: more strength.
- **Setting and Hardening**: Both are similar to P.C. rather slow setting.

- **Hydration:** Rapid: Major Heat evolution **within 10 h.** > Development of **high internal temperature (~80°C)** : Should be placed in thin section of max **12 inch lift** at a time and **interval of 24 h.** : Spraying of water after **hardening,**

HYDRATION REACTIONS OF CALCIUM ALUMINATES (CA AND C₁₂A₇)

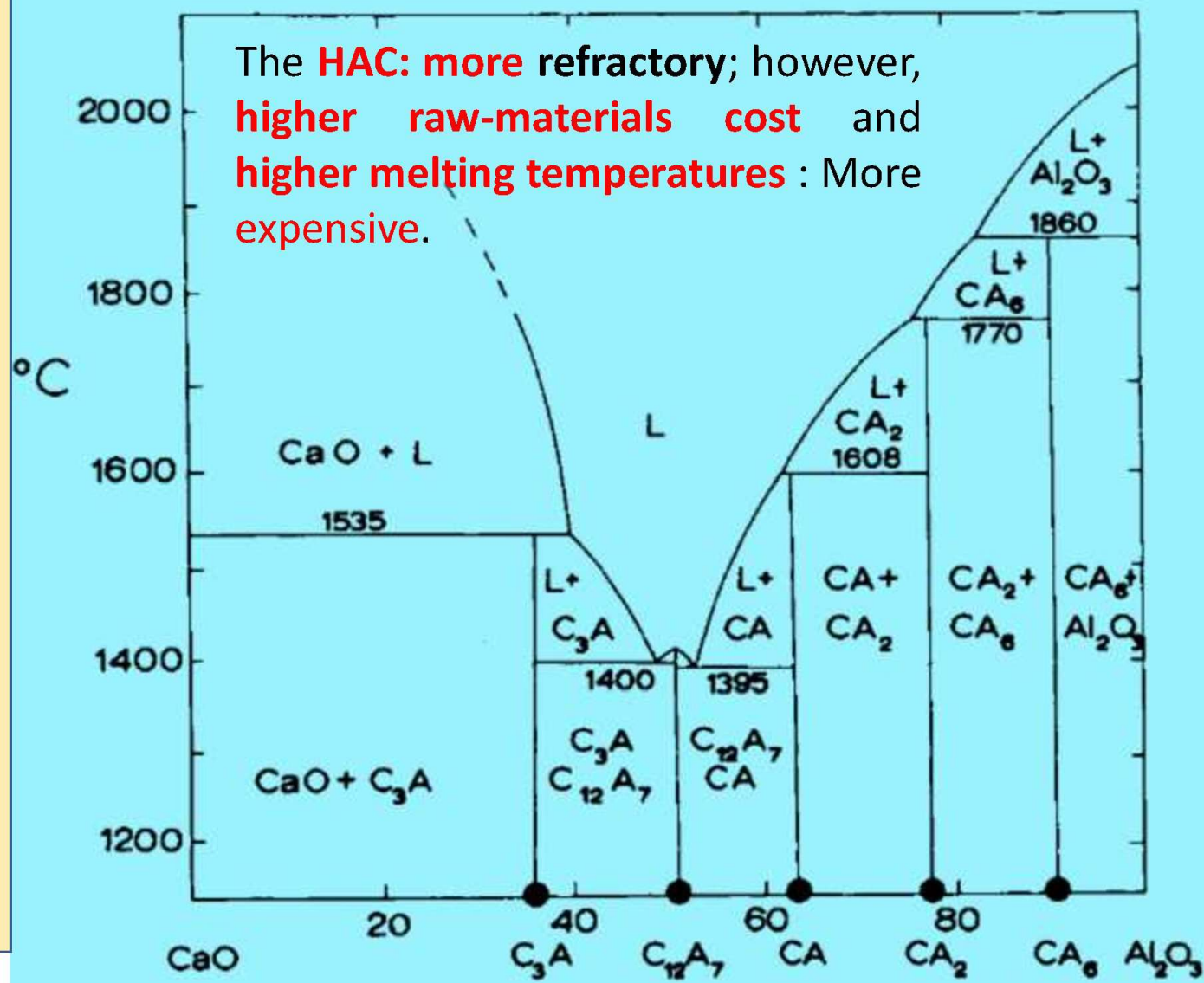


Applications:

- **RAPID HARDENING**: Concrete ferry slipway, Motorway slab repairs, Bridge deck enlargement,
- **ABRASION AND IMPACT RESISTANCE**: (very good resistance to abrasion) industrial floors and dam spillways
- **USE AT LOW TEMPERATURES**: The rapid heat evolution of calcium aluminate cement concrete during hardening is beneficial when concrete is placed at low temperatures. *In Canada* to build foundations in frozen ground. Repairs in industrial cold stores.
- **INDUSTRIAL FLOORS**: impact and abrasion resistance, chemical and acid resistance, Milk, Oil, cold in cryogenic handling facilities, heat in foundries, steel and aluminium mills areas.
- **MINES AND TUNNELS**: Significant quantities: 'mine packing' and rock bolts,
- **HEAT-RESISTANT AND REFRactory CONCRETES** and refractory cast ables

The white CACs essentially lie in the two-component system CaO-Al₂O₃.

For normal aluminous cements having CaO/Al₂O₃ ratios between 0.9 and 1.2, will have lower solidus and liquidus temperatures than the high-alumina cements, which have CaO/Al₂O₃ ratios between 1.8 and 2.5.



C12A7 is an **undesirable** constituent of aluminous cements: it **hydrates very rapidly** and causes "**flash setting.**" This results in **partial hardening** of the wet concrete before it can be placed. The **CA**, on the other hand, has **very desirable hydraulic properties**.

The **high-alumina cements**, depending on their CaO/Al₂O₃ ratio, contain mainly **CA plus CA2**, or with increasing Al₂O₃ content, **CA2 plus CA6**. Both **CA2** and **CA6** are relatively **inert to hydration** in neutral solutions (pH = 7) but CA2 will hydrate readily in **alkaline solution**.

High-alumina cements containing CA2 can be **mixed with** alkaline solutions (**pH > 12**) and poured or cast in the same manner as portland cements. Thus, **CA and CA2 are the most desirable phases** in the anhydrous clinker.

The regions of CACs in the two three component systems $\text{CaO}-\text{Al}_2\text{O}_3-\text{SiO}_2$ (C-A-S) and $\text{CaO}-\text{Al}_2\text{O}_3-\text{Fe}_2\text{O}_3$ (C-A-F)

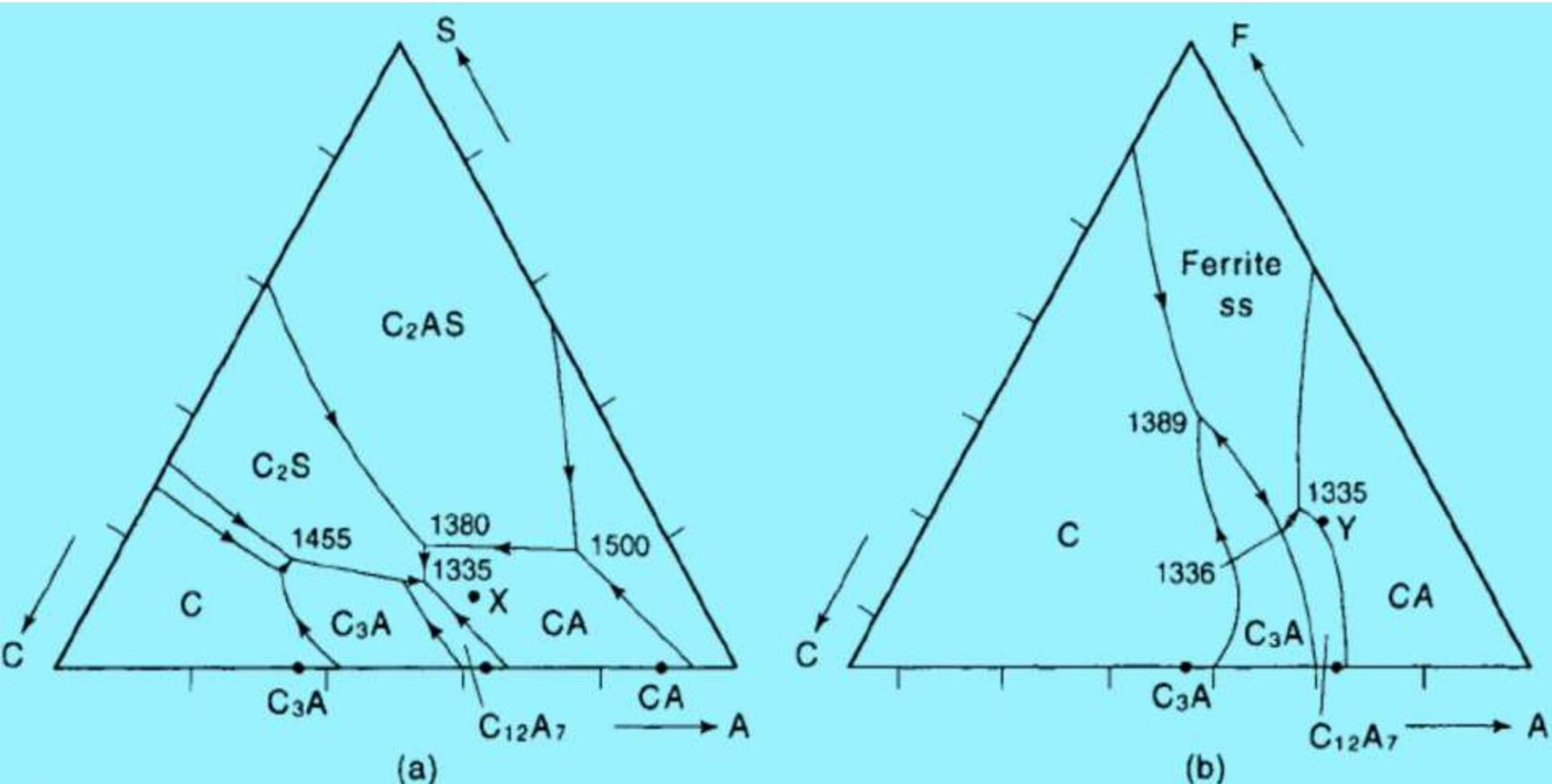
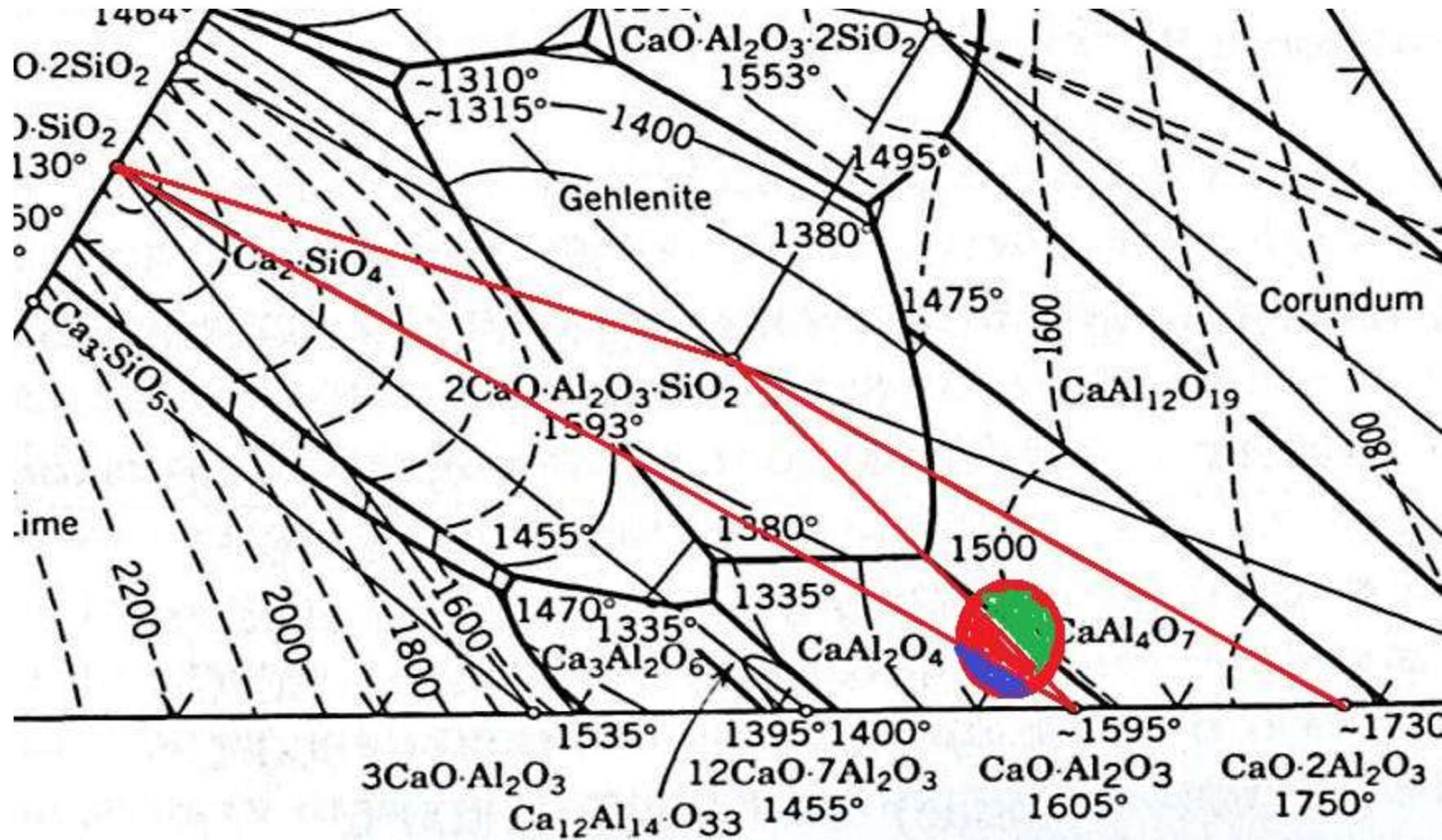
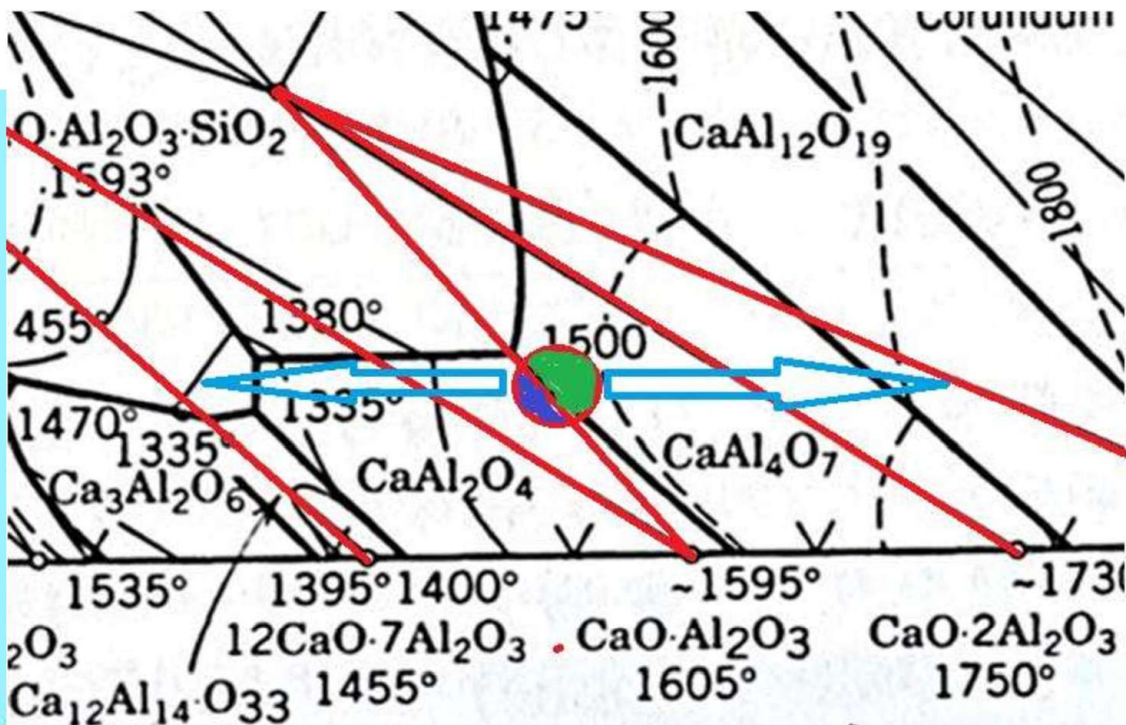
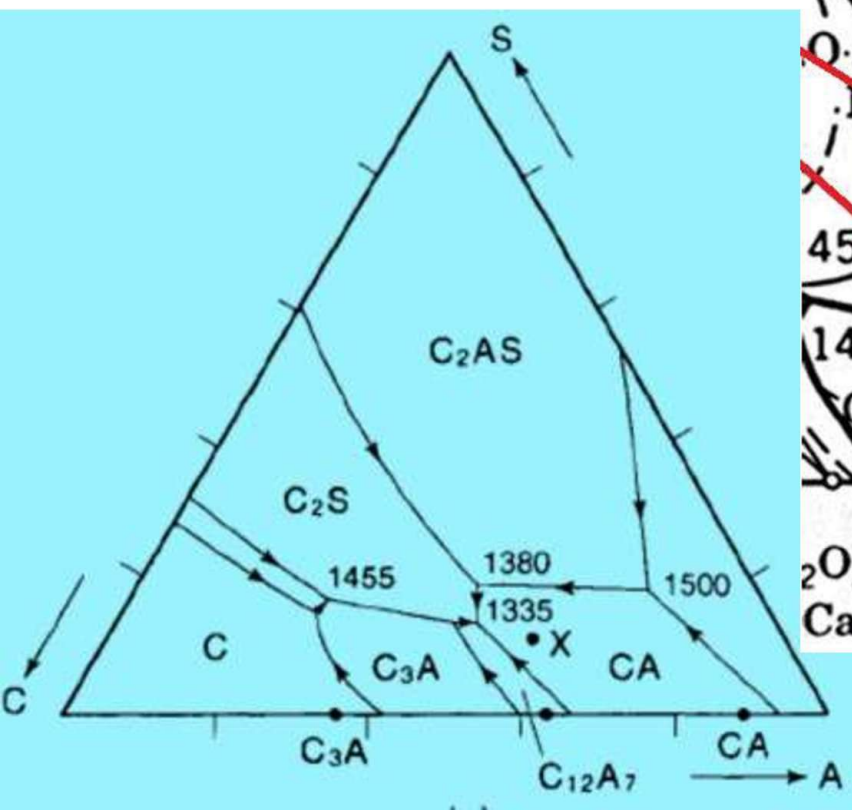


Fig. 13.3 (a) Part of the $\text{CaO}-\text{Al}_2\text{O}_3-\text{SiO}_2$ phase diagram. Point X represents the composition of Cement Fondu excluding iron oxide. (b) Part of the $\text{CaO}-\text{Al}_2\text{O}_3-\text{Fe}_2\text{O}_3$ phase diagram. Point Y represents the composition of Cement Fondu excluding silica.

- C12A7 - CA - C2S * C2S - CA - C2AS * C2AS - CA - CA2
 - Strength primarily on CA, C2AS has very little or no Hydraulic activity
 - So SiO₂ is controlled to get : C2S - CA - C2AS even in C12A7 - CA - C2S

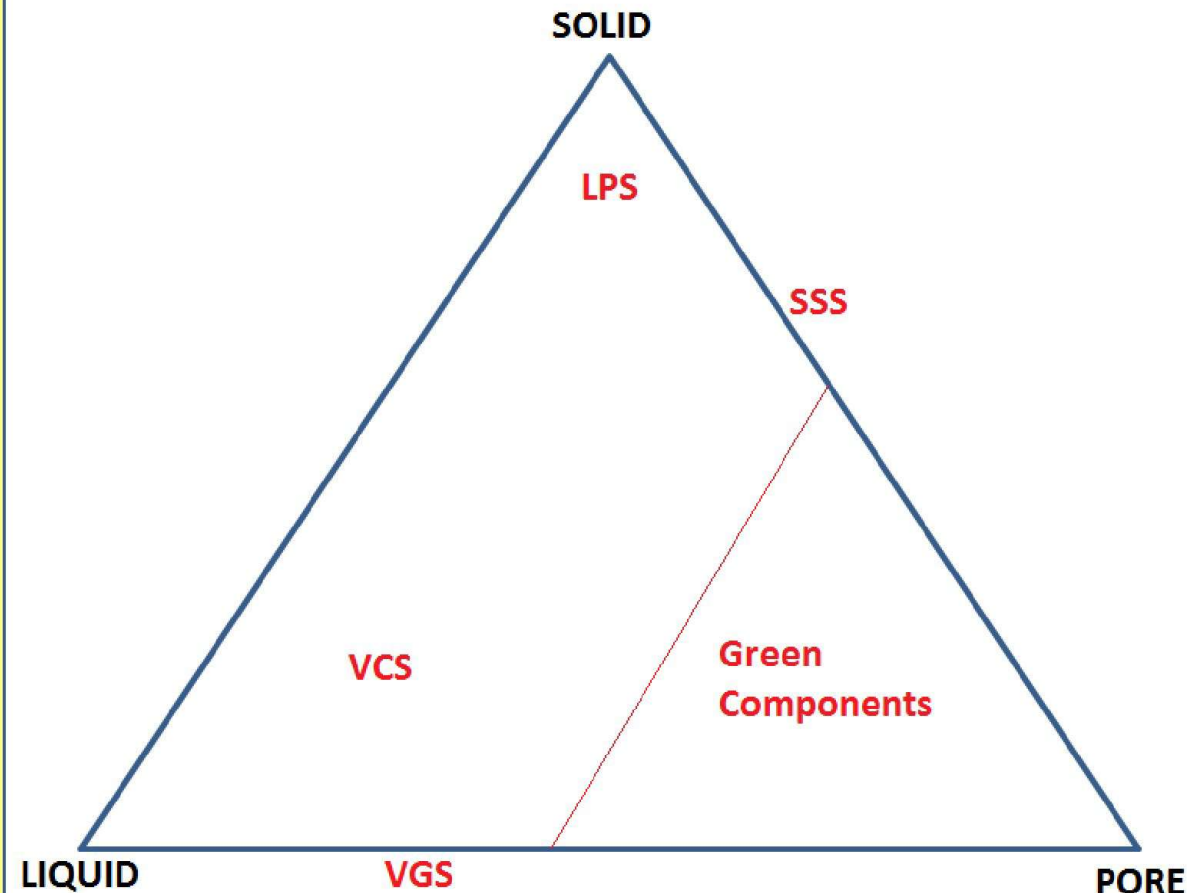


It is necessary to keep the silica contents low. In diagram: a join exists between **CA** and **C₂AS**, **Gehlenite**: one of the principal crystalline silica-containing phases. Composition X, ~ 10 wt % SiO₂ isopleths. equilibrium phase assemblage would contain almost 50% gehlenite. which has **poor hydraulic properties**, produce an **unsatisfactory cement**, therefore to limit the SiO₂ content to much less than 10%; **CaO/Al₂O₃** ratio might be adjusted so that the bulk composition would be shifted along the same isopleth to its intersection with the join **C₂S-CA**. This would avoid gehlenite formation, resulting C₂S, while more hydraulic than C₂AS,



The driving force for sintering is the excess surface energy present in a powder compared with a single crystal of the same composition. As the temperature is increased, the atoms acquire some degree of mobility and a compact of particles undergoes changes of morphology that reduce the overall surface free energy.

- * Solid State Sintering
- * Liquid Phase Sintering (<20% Liquid),
 - Viscous Glass
Sintering: Glass powder densify; Liq and pores: Glaze, Enamel;
 - Viscous Composite
Sintering OR vitrification (>20% Liquid); Whiteware, porcelain



The driving force for sintering:

1. the curvature of the particle surfaces
2. an externally applied pressure, and
3. a chemical reaction.

an externally applied pressure normally provides the major contribution to the driving force when the pressure is applied over a significant part of the heating process as in hot pressing and hot isostatic pressing

A chemical reaction can, in principle, provide a driving force for sintering if it can be used to aid the densification process

the presence of these defects that allow diffusional mass transport.

the major mechanisms of matter transport: lattice diffusion (also referred to as volume or bulk diffusion), grain boundary diffusion, and surface diffusion.; highly defective nature of the grain

boundary, grain boundary diffusion to be more rapid than lattice diffusion, The free surface of a crystalline solid is not perfectly flat,

vacancies, terraces, kinks, edges, and adatoms. migration of vacancies and the movement of adatoms.

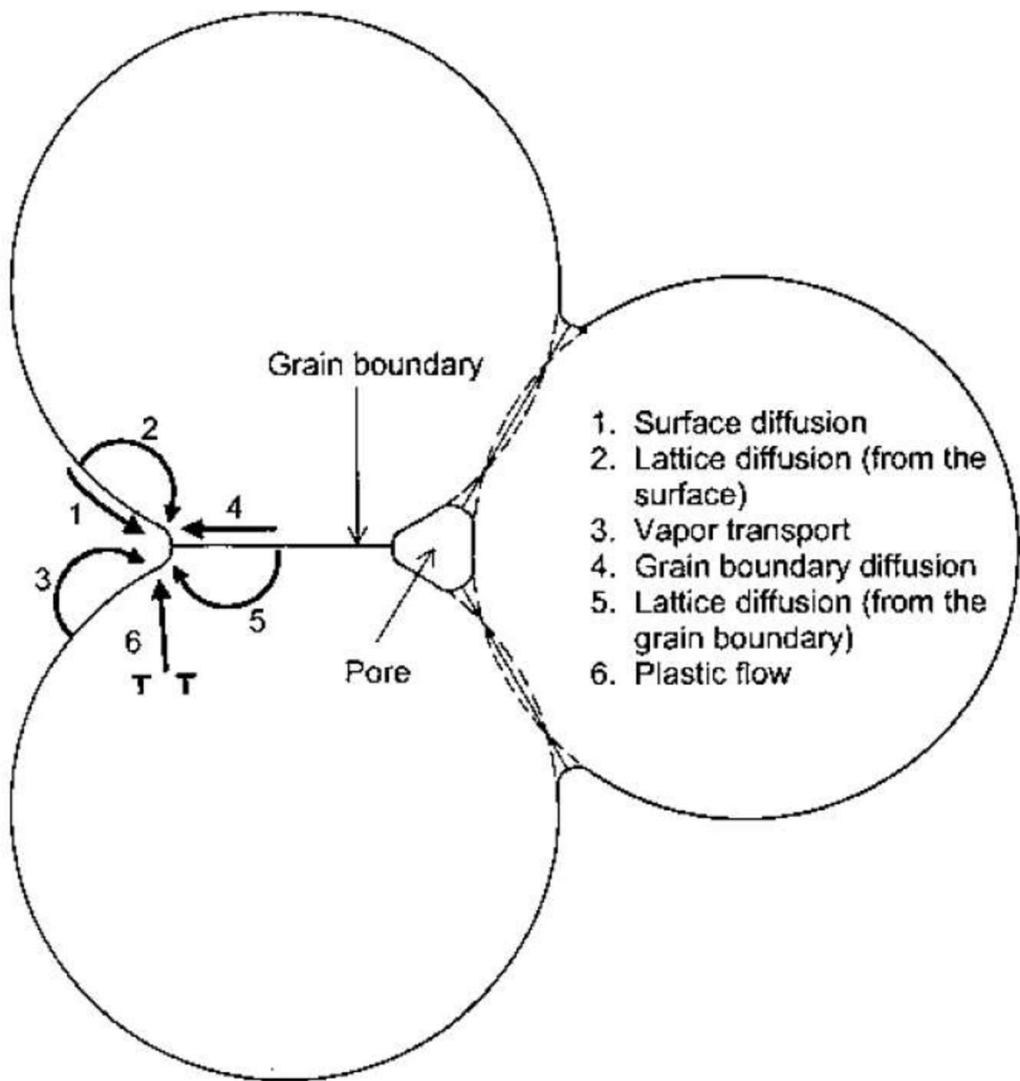
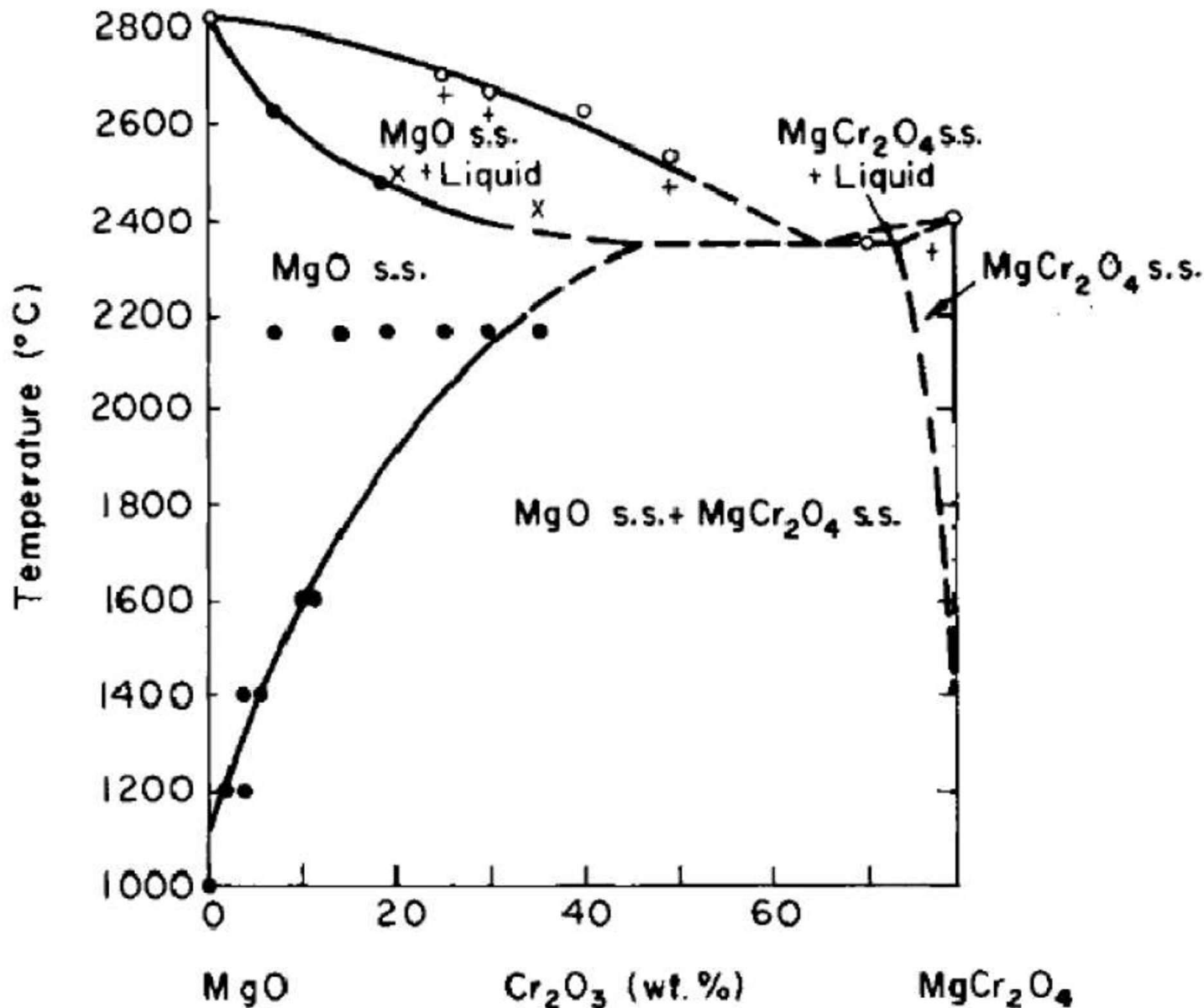


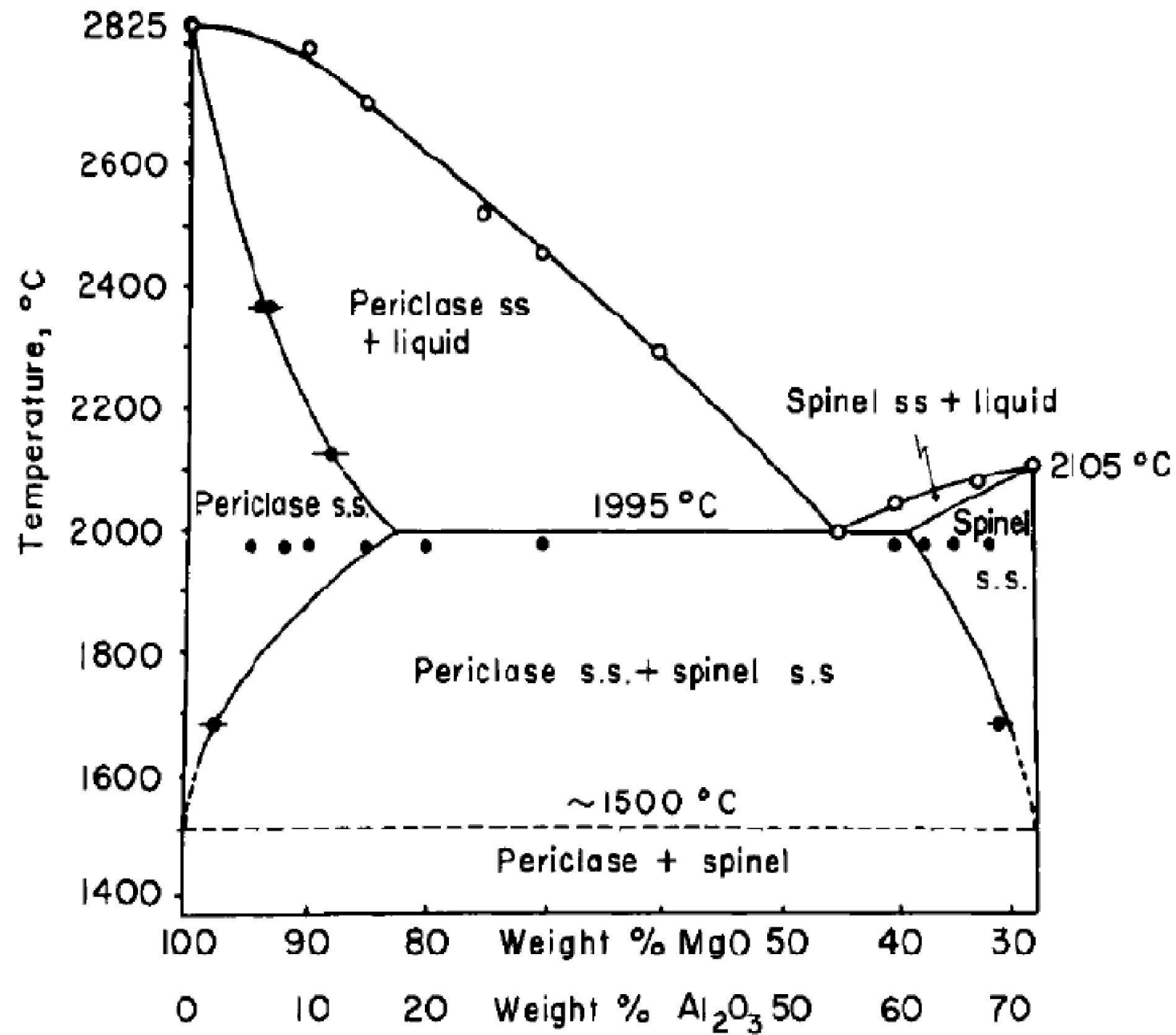
FIGURE 8.1 Six distinct mechanisms can contribute to the sintering of a consolidated mass of crystalline particles:(1) surface diffusion, (2) lattice diffusion from the surface, (3) vapor transport, (4) grain boundary diffusion, (5) lattice diffusion from the grain boundary, and (6) plastic flow. Only mechanisms 1 to 3 lead to densification, but all cause the necks to grow and so influence the rate of densification.

In many ceramic: Solid State sintering (SSS): Phase diagram?? Solid Solution reaction sintering



Figure, show that the formation of solid solution of spinels and periclase is appreciable when samples are fired in the temperature range of normal refractory firing processes, namely, 1400°C to 1600°C.

The contact of the grains of periclase and the spinel permits ion migration and the formation of strong solid solution bonds.



In many ceramic: liquid phase is commonly used to assist in the sintering. Purpose of LPS: (a) **enhance densification rates**, through *enhanced rearrangement of the particulate* and (b) ***enhanced matter transport*** through the liquid. (c) **accelerated grain growth**, (d) produce **specific grain boundary properties**.

Enough liquid; (to coat particles; ~1vol% liquid can coat all 1 micron particles, to fill all pores; ~ 35 vol% liquid. **Liquid must wet solid, Solid must partially soluble in liquid, Particle size, viscosity**

1. Redistribution of the liquid and *rearrangement of the particle* under the influence of capillary stress gradients
2. Densification and grain shape accommodation by *solution-precipitation*
3. *Final-stage sintering driven by the residual porosity in the liquid.*
 - particle rearrangement of the initial network is rapid,
 - major processes that occur by the **solution precipitation** mechanism are **densification and coarsening**.

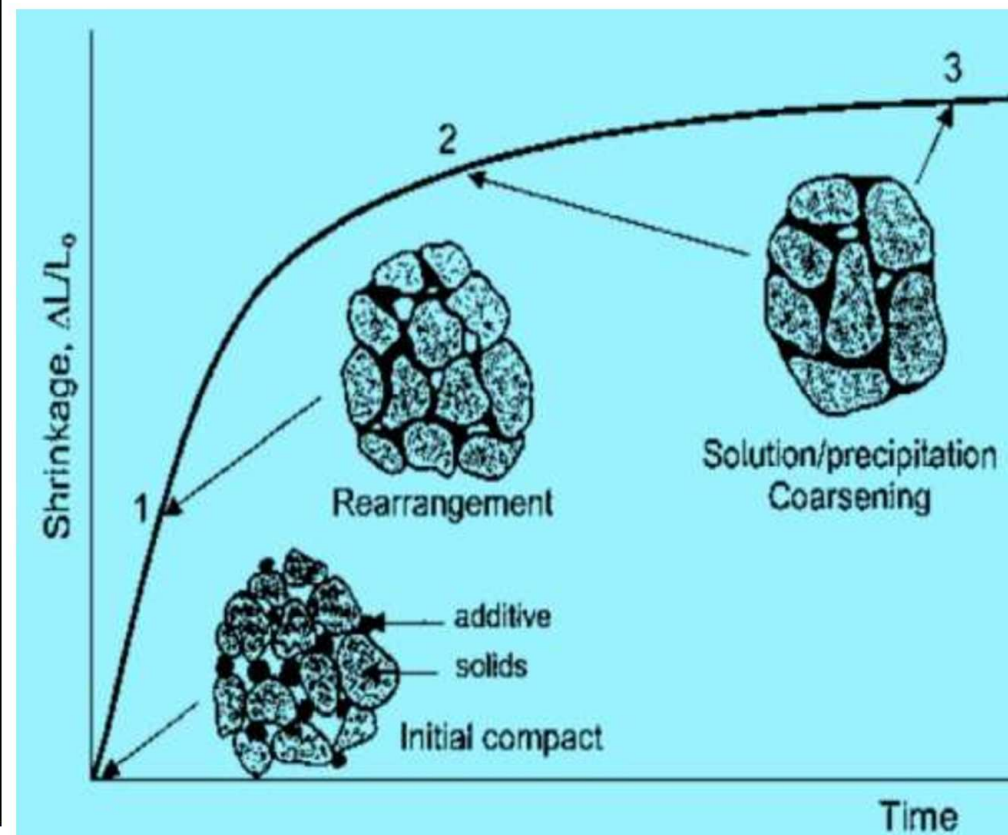


TABLE 10.1 Examples of Common Ceramic Liquid-Phase Sintering Systems

Ceramic system	Additive content (wt %)	Application	Reference
Al_2O_3 (talc)	~5	Electrical insulators	1
MgO (CaO-SiO_2)	<5	Refractories	2
MgO (LiF)	<3	Refractories	3
ZnO (Bi_2O_3)	2–3	Electrical varistors	4,5
BaTiO_3 (TiO_2)	<1	Dielectrics	6
BaTiO_3 (LiF)	<3	Dielectrics	7,8
UO_2 (TiO_2)	~1	Nuclear ceramics	9
ZrO_2 (CaO-SiO_2)	<1	Ionic conductors	10
Si_3N_4 (MgO)	5–10	Structural ceramics	11,12
Si_3N_4 (Y_2O_3 - Al_2O_3)	5–10	Structural ceramics	12,13
SiC (Y_2O_3 - Al_2O_3)	5–10	Structural ceramics	14
WC(Ni)	~10	Cutting tools	51

USE OF PHASE DIAGRAMS IN LIQUIDPHASE SINTERING

Phase diagrams play an important role in the selection of powder compositions and sintering conditions for LPS. Whereas the diagrams give the phases present under *equilibrium* conditions, the reaction kinetics during LPS are often too fast for equilibrium to be achieved, so the PD should therefore serve only as a guide. For a binary system consisting of a major component and a liquid-producing additive, the first task is to determine which additives will form a liquid phase with the major component and under what conditions.

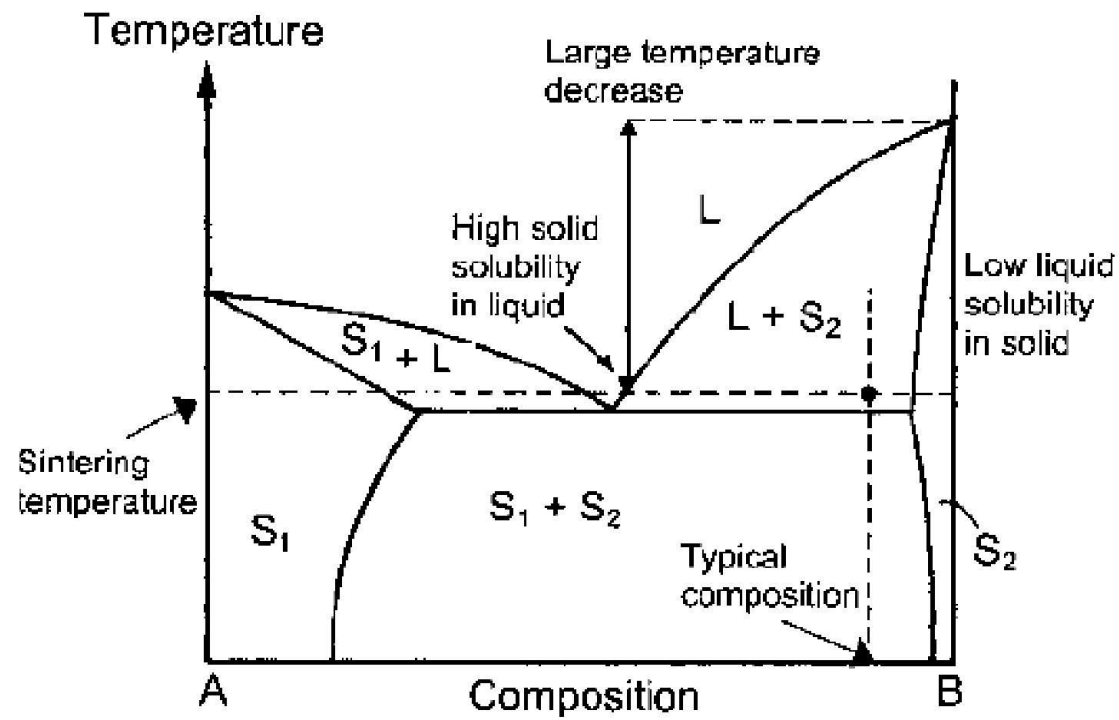


Figure 10.40 shows an idealized binary phase diagram that indicates the desirable composition and temperature characteristics for LPS. In addition to the **solubility requirements**, a desirable feature is a large difference in melting temperature between the eutectic and the base phase. The composition of the system **should also be chosen away from the eutectic composition so that the liquid volume increases slowly** with temperature, thereby **preventing the sudden formation of all of the liquid at or near the eutectic temperature**.

In practice, a typical sintering temperature would be chosen somewhat above the eutectic temperature.

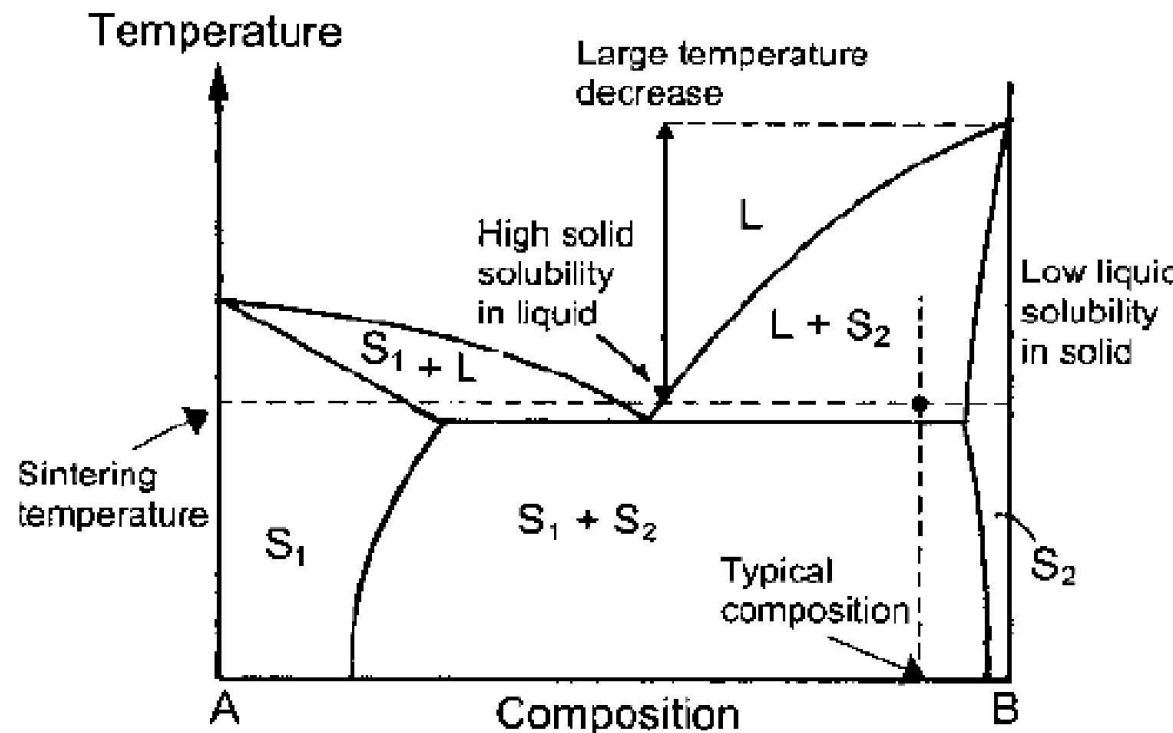


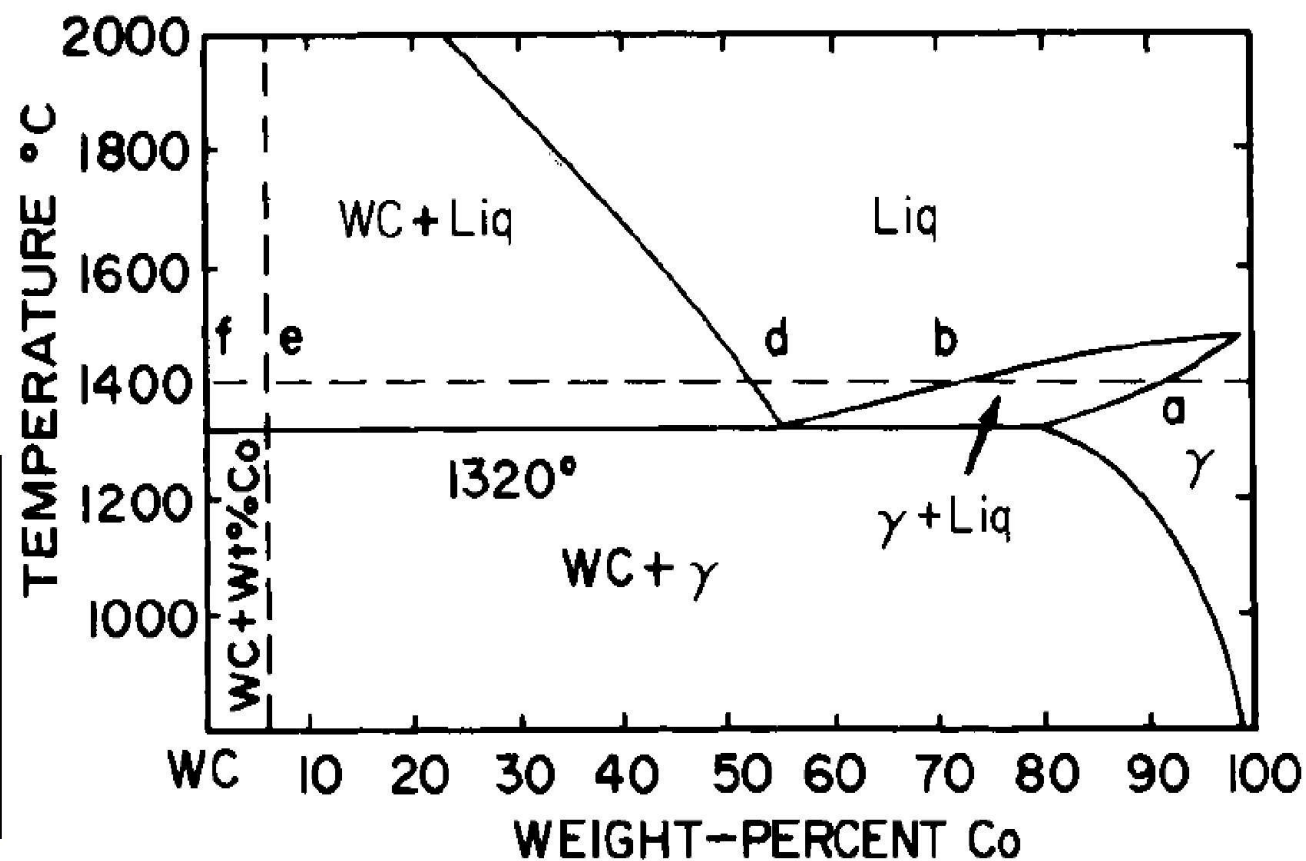
FIGURE 10.40 Model binary phase diagram showing the composition and sintering temperature associated with liquid phase sintering in the $L + S_2$ phase field. The favorable characteristics for liquid-phase sintering include a suppression of the melting temperature, high solid solubility in the liquid, and low liquid solubility in the solid. (From Ref. 16.)

TUNGSTEN CARBIDE-COBALT SYSTEM (cemented carbides):

Tungsten carbide: most commonly and most frequently used tool materials; a brittle solid, ball milled with cobalt (ductile) powder; Many of the physical properties maximises: with a minimum amount of liquid; 94 wt % tungsten carbide with 6 % cobalt is near this optimum composition.; At the sintering temperature, not only does the cobalt react to form a liquid, but tungsten carbide is also dissolved in the cobalt, Co melting point is 1480°C.

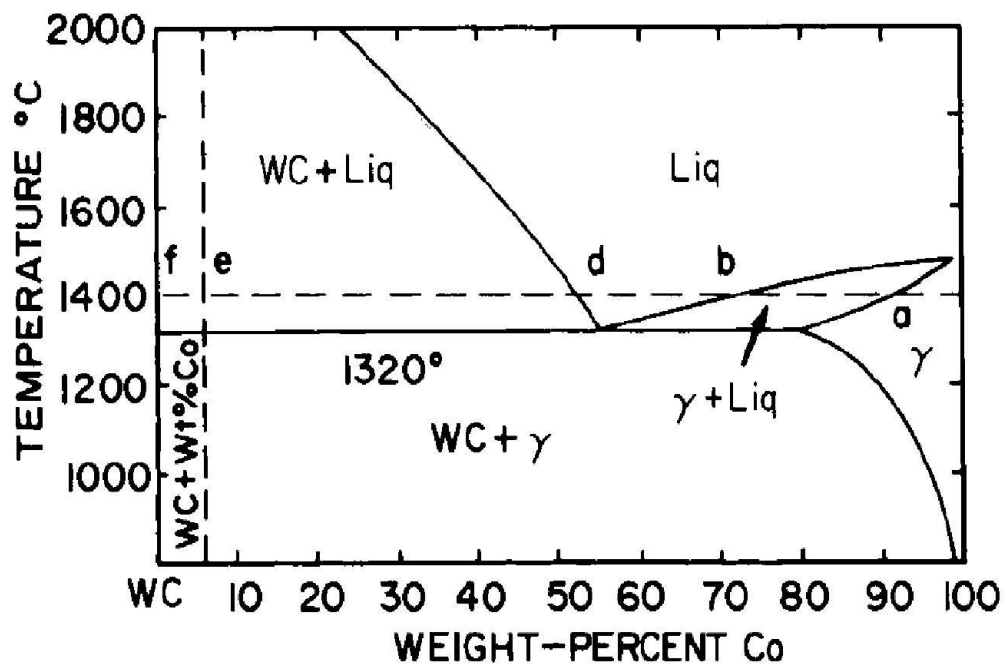
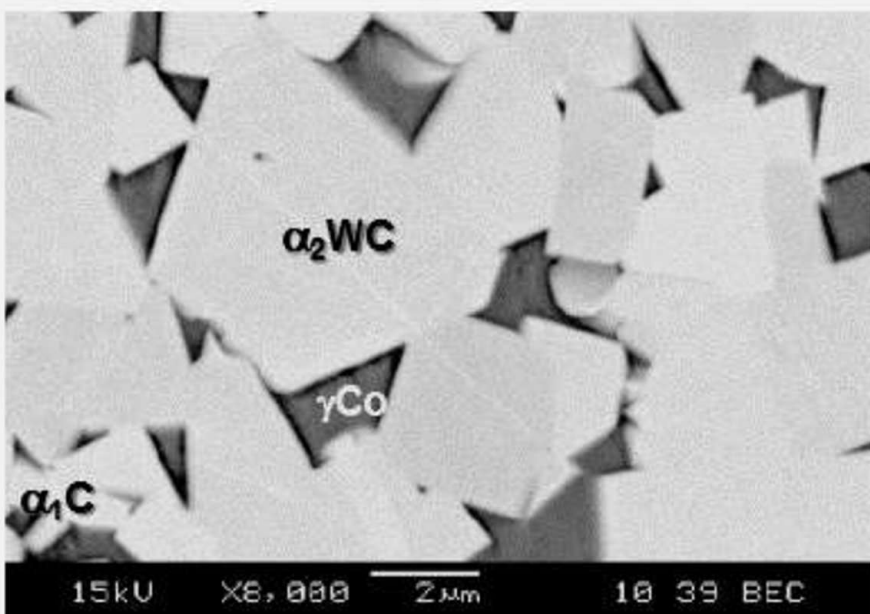
Liquid dissolves all of the cobalt and the cobalt-WC solid solution, 6% cobalt composition forms about 12% by weight (20 vol %) of liquid;

Co as the preferred binder metal: best comminution characteristics in milling, superior wettability for WC, higher solubility of WC in cobalt at sintering temperatures and excellent properties



Surface free energy of the liquid pulls the particles together and the powder compact shrinks until it is near theoretical density. Grain Growth of WC occurs; WC precipitates from eutectic mixture; exsolution of WC: from cobalt solid solution (gamma)

Hard and brittle carbide phase, ductile bonding phase.; contrasting features like: high wear resistance and hardness with high strength and good ductility.



Porcelain: Strong, White, impermeable, Sonorous, Translucent triaxial ceramics with less than 0.5% residual porosity.

Microstructure:
Rounded Quartz
particle, and tiny
mullite crystals
immersed in
viscous silicate
glass. Crack
around the Qtz
grain

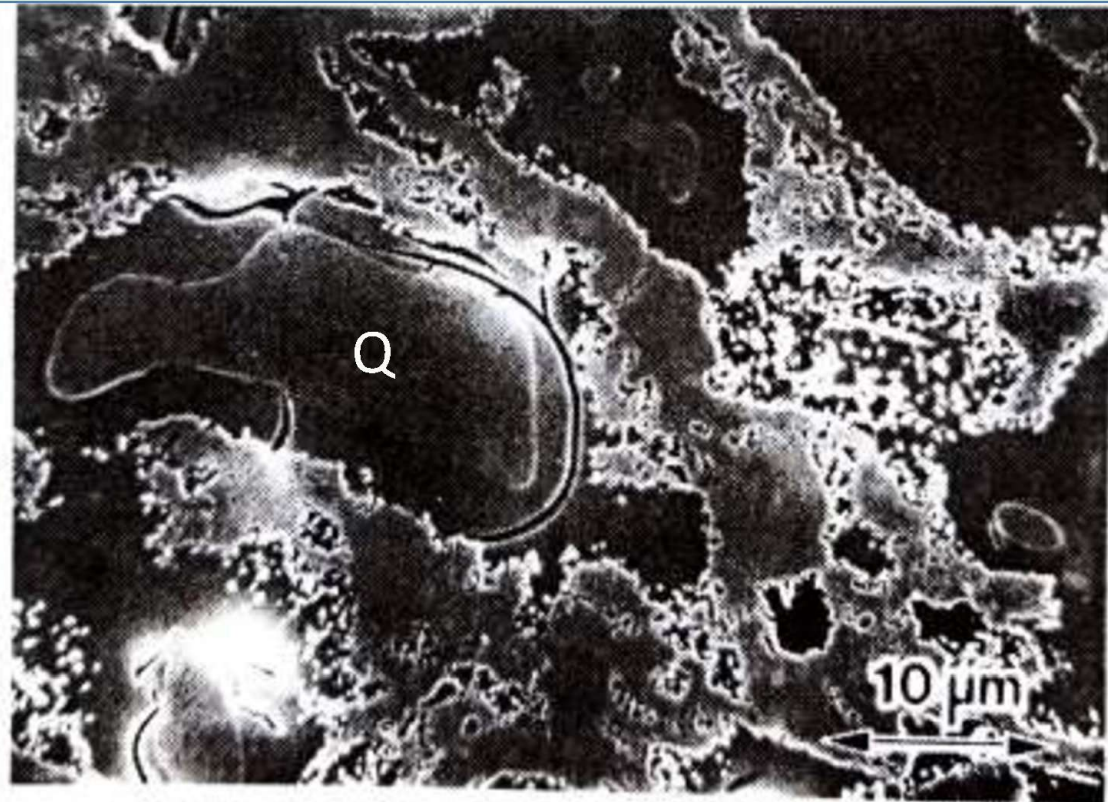


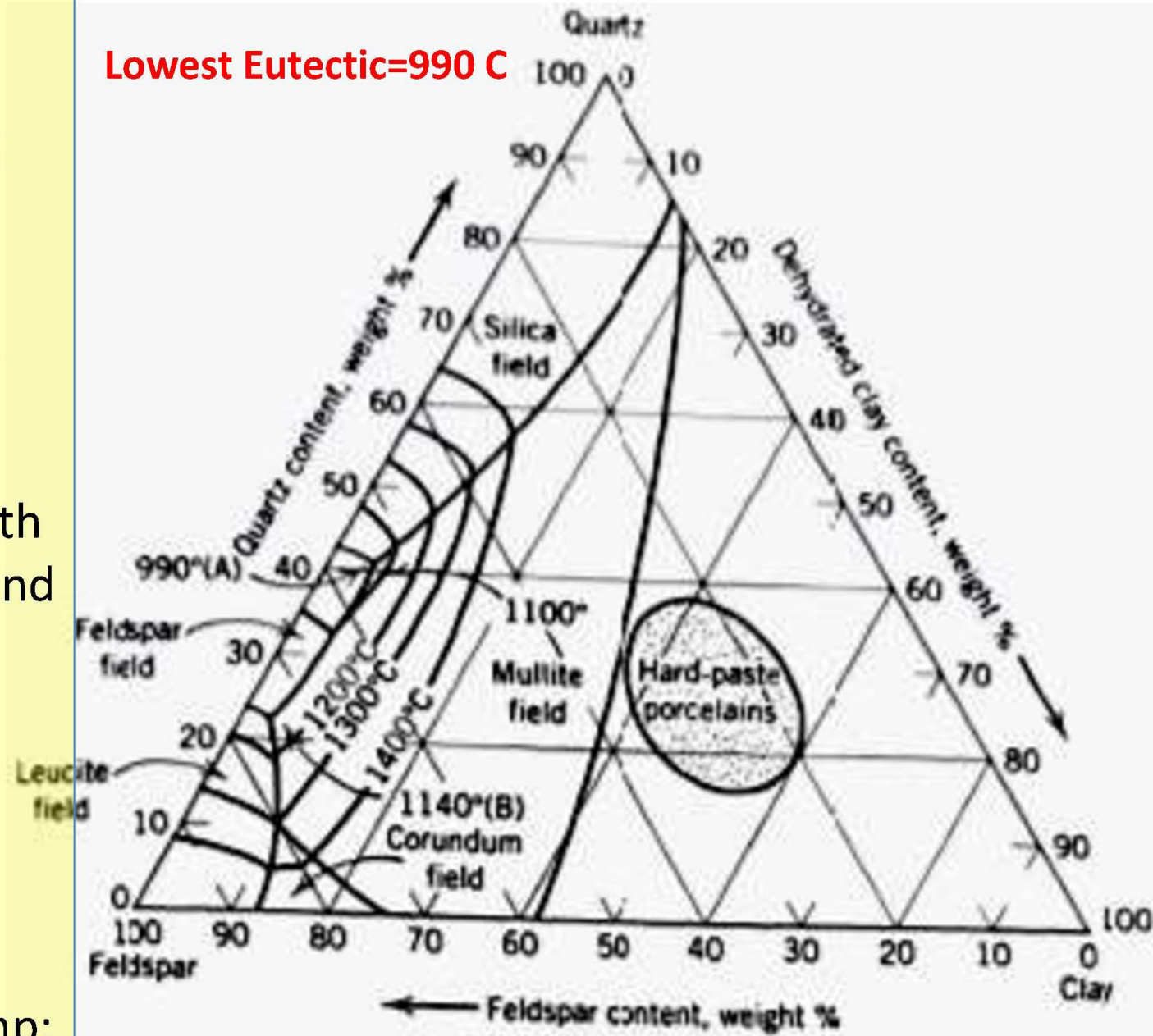
Fig. ST50 K'ang Hsi porcelain made in China at the beginning of the eighteenth century is dense, hard and translucent. The microstructure consists of partly dissolved rounded quartz particles in a matrix of silicate glass which contains fine mullite crystals. The circumferential crack around the quartz grain is enhanced by light etching with 1% hydrofluoric acid.

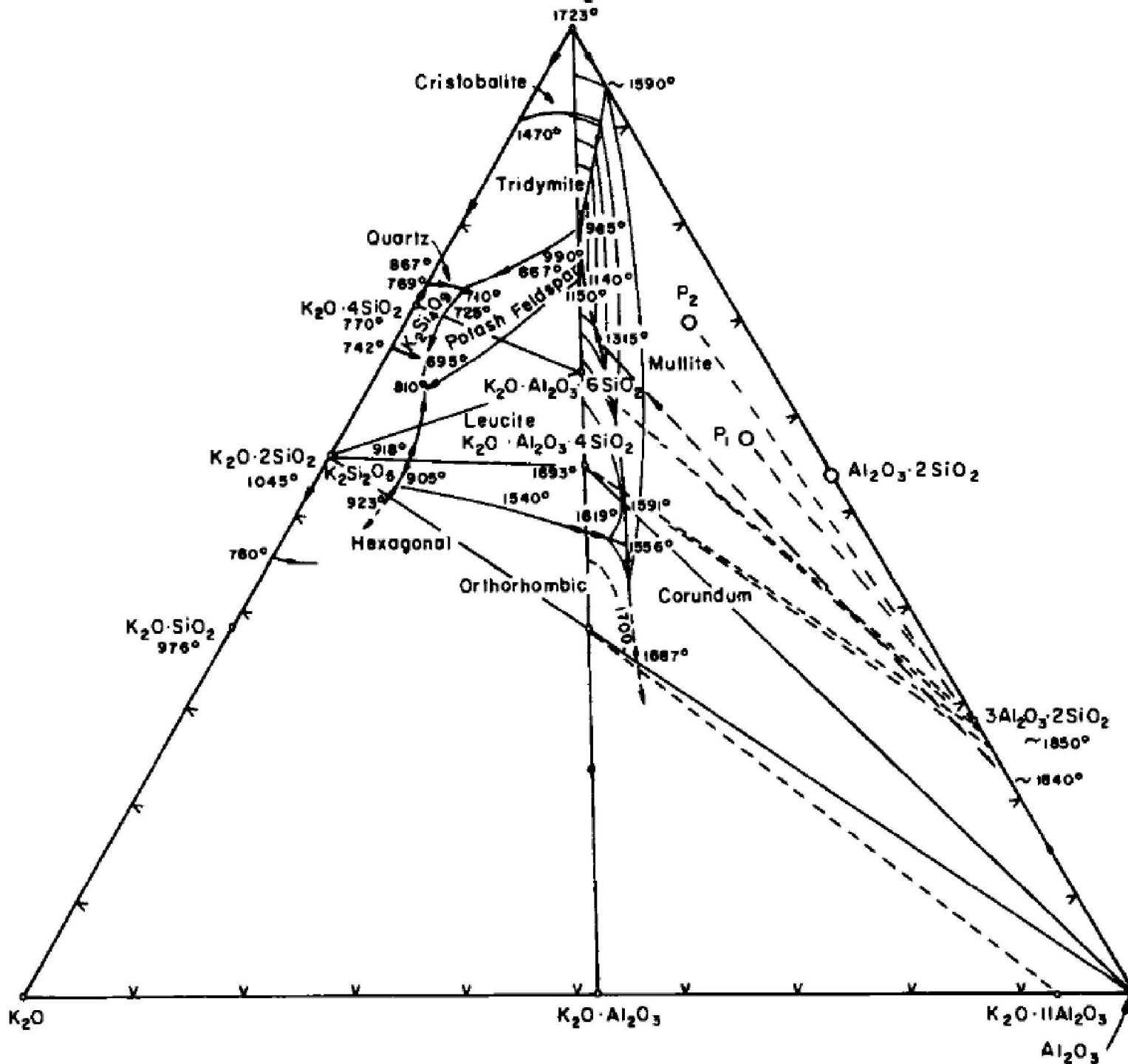
Clay, Quartz and Feldspar Phase

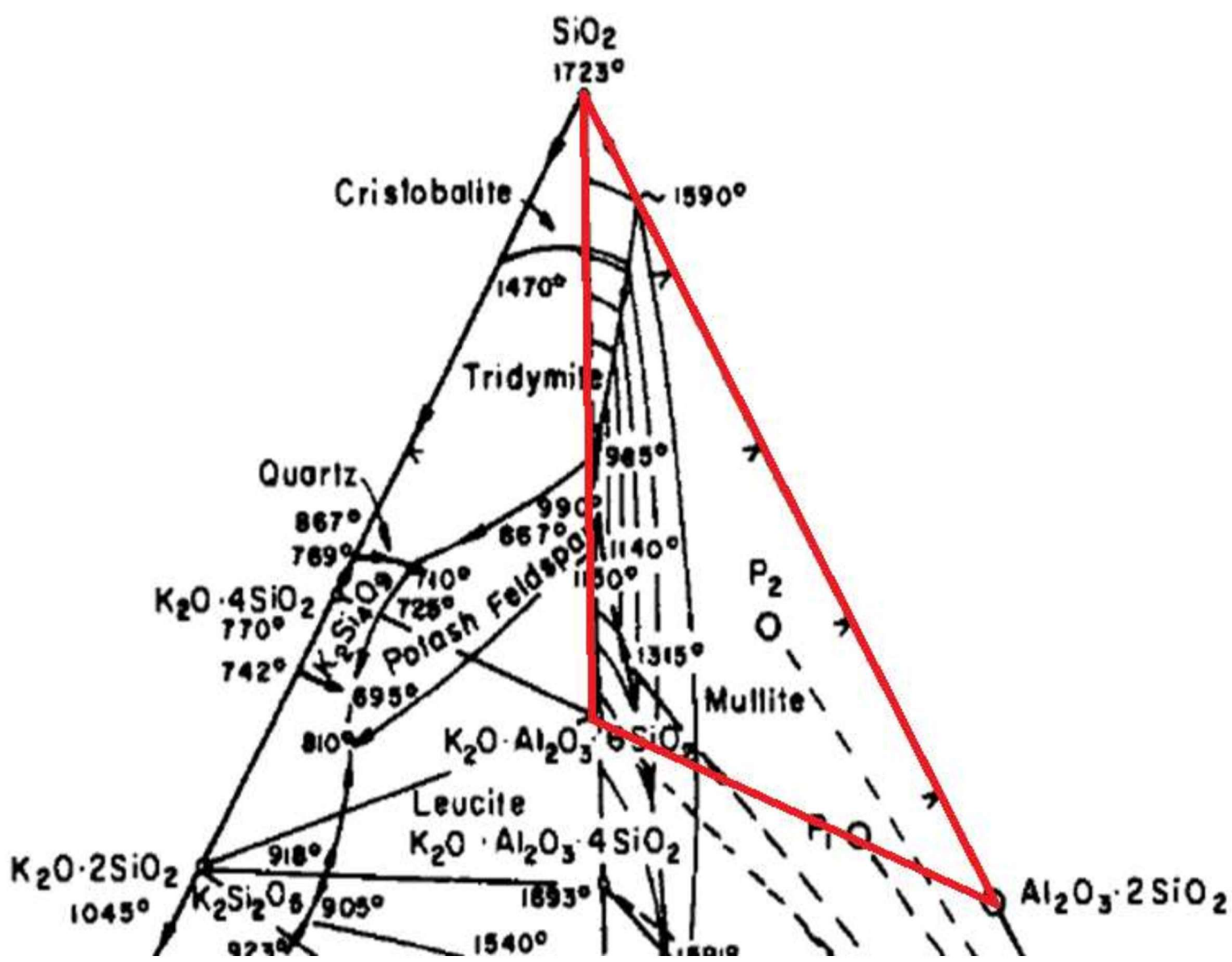
diagram: Porcelain location is shown.
This is the part of $K_2O-Al_2O_3-SiO_2$ PD.

- Kaolinite decomposition
- Feldspar react with amorphous silica and clay.
- Liquid ~ 990 C.
- Mullite crystallization,
- Dissolution of Quartz,
- Typical Firing Temp: 1300 C.

Lowest Eutectic=990 C







At Firing Temp: 1300 C:
 Phases present: Mullite,
 Silica and K-alumino-
 silicate glass liquid

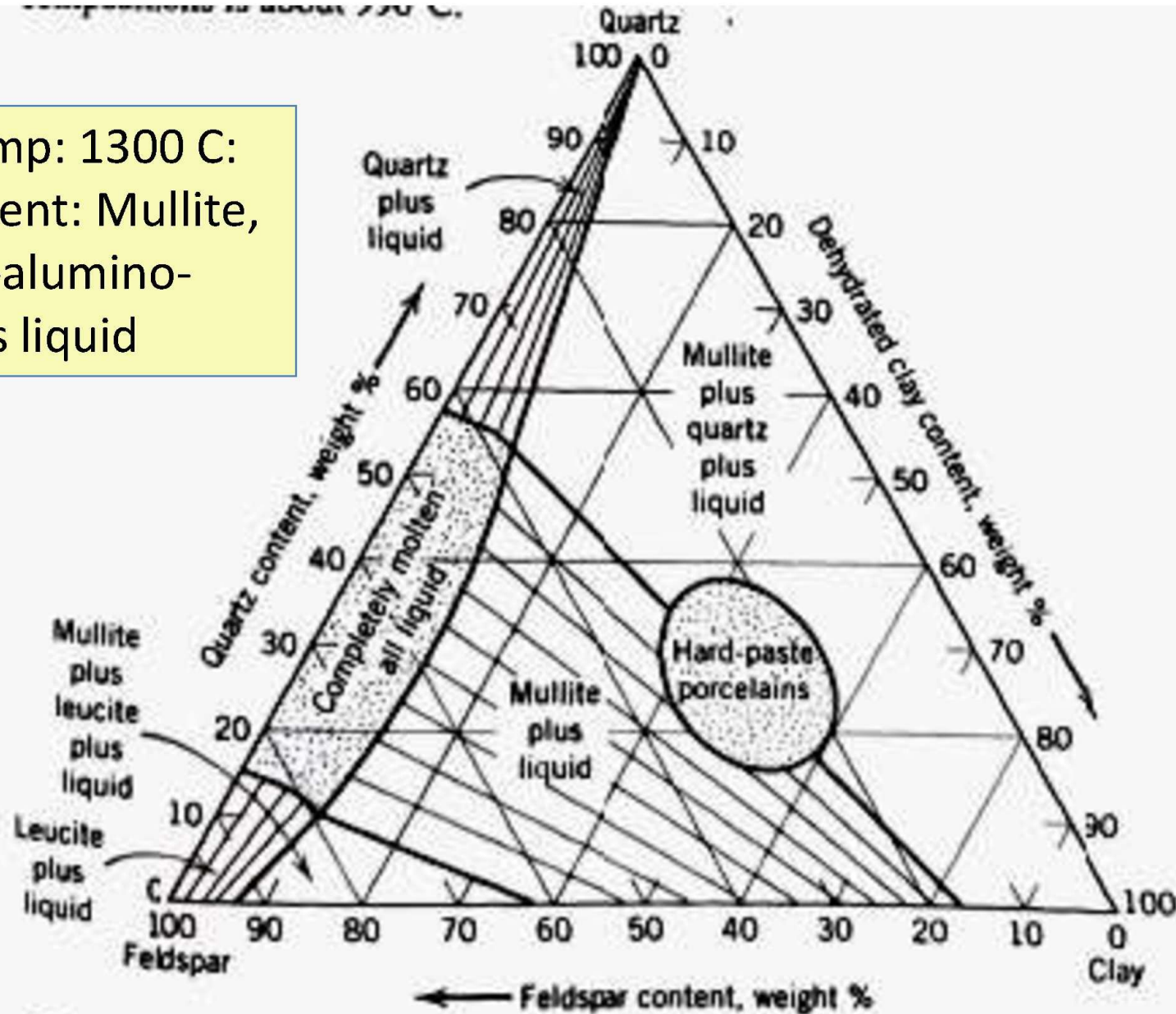
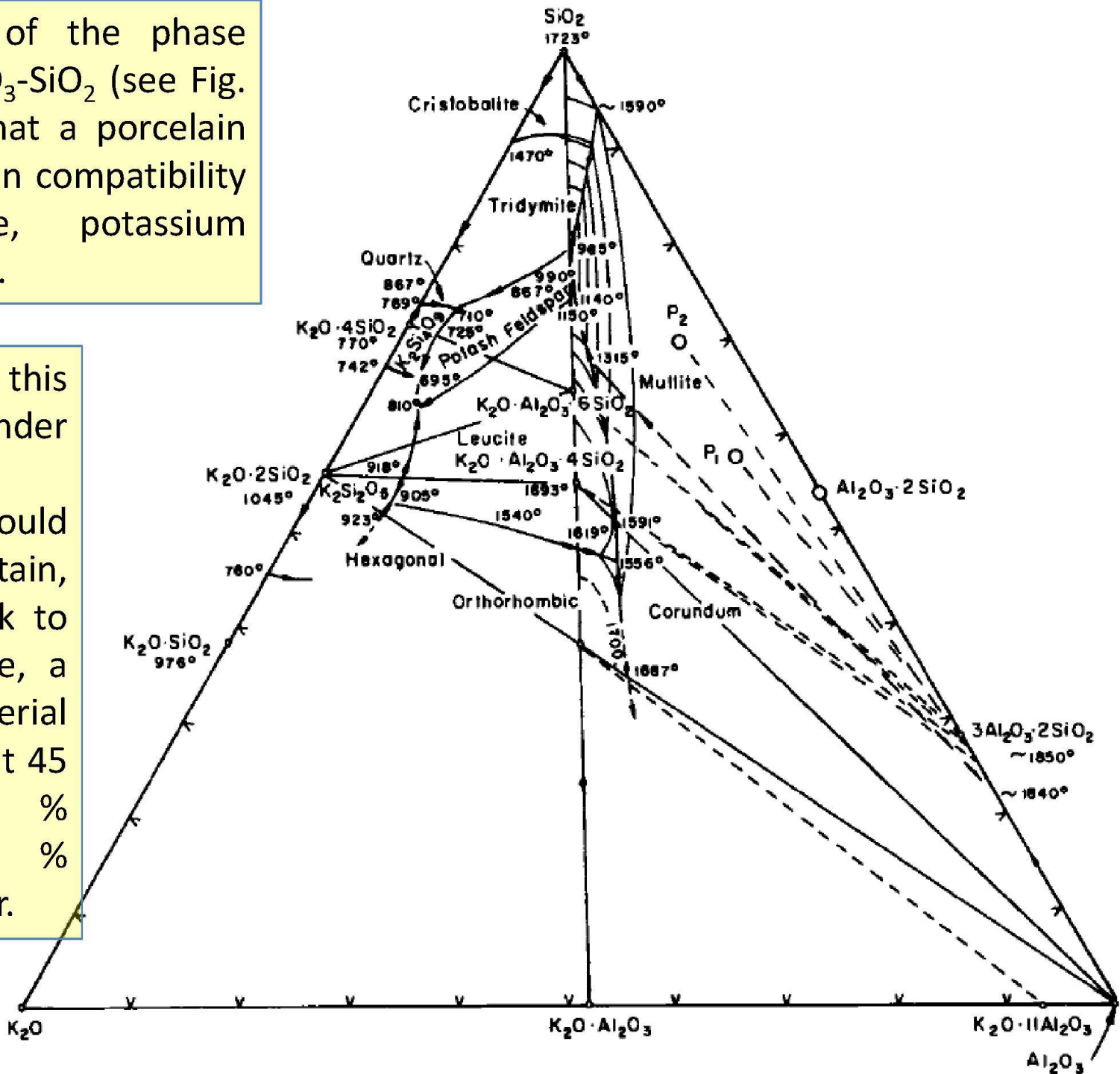


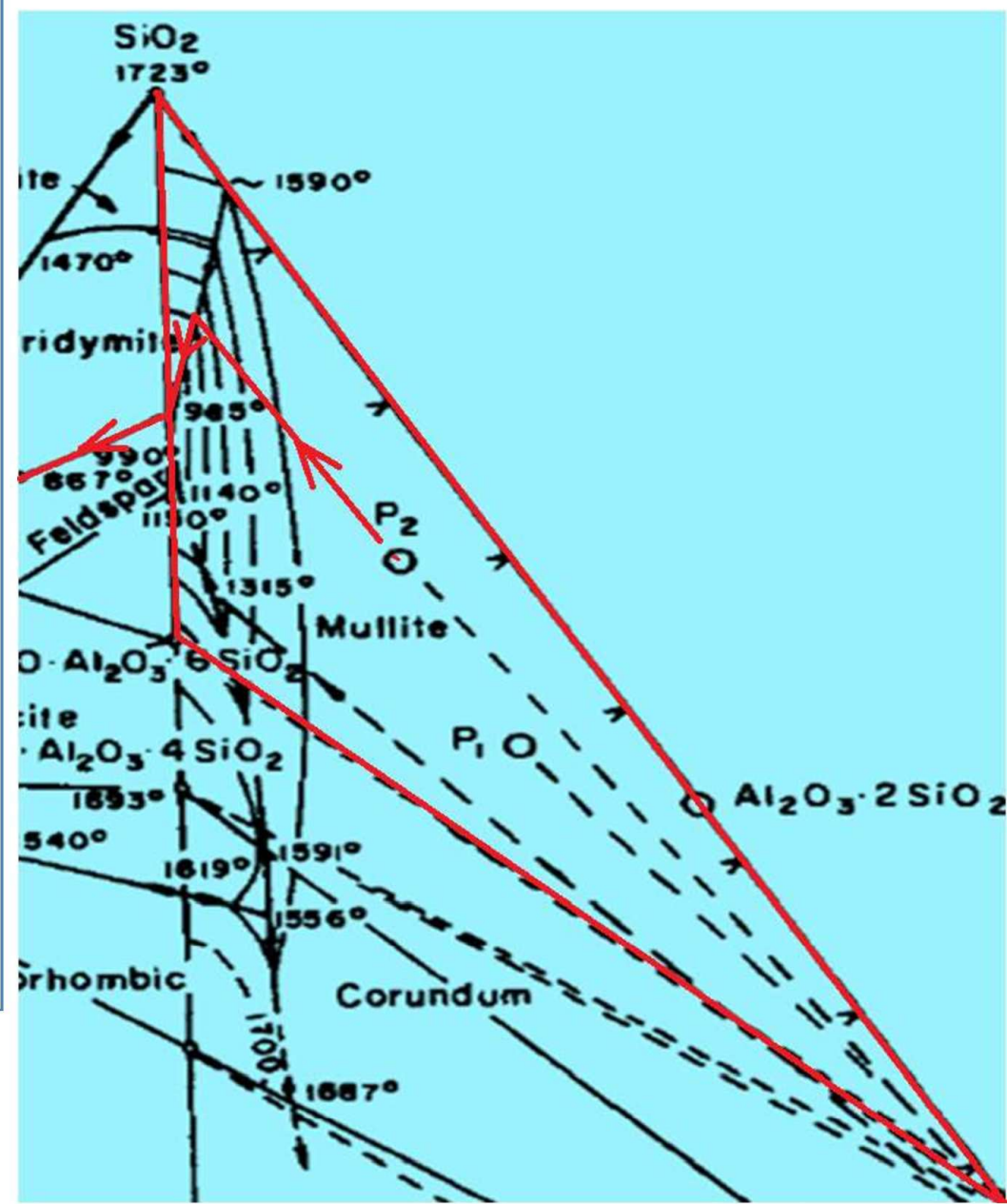
Fig. ST52 An isothermal cut through the phase diagram illustrates the phases present at the firing temperature of hard paste porcelains.

An examination of the phase diagram, K_2O - Al_2O_3 - SiO_2 (see Fig. 6) will indicate that a porcelain composition falls in compatibility triangle: mullite, potassium feldspar, and silica.

Upon firing this composition under equilibrium conditions, one would expect to obtain, upon cooling back to room temperature, a polyphase material consisting of about 45 % quartz, 30 % mullite, and 25 % potassium feldspar.



The composition: in the primary field of crystallization of mullite: mullite will be a stable crystalline phase at the firing temperature of porcelain. Upon cooling from between 1300°-1500°C, tridymite should crystallize as a secondary crystalline phase and, then as the ternary eutectic is obtained, potassium feldspar should crystallize out along with additional tridymite. Upon further cooling, tridymite should transform to quartz.



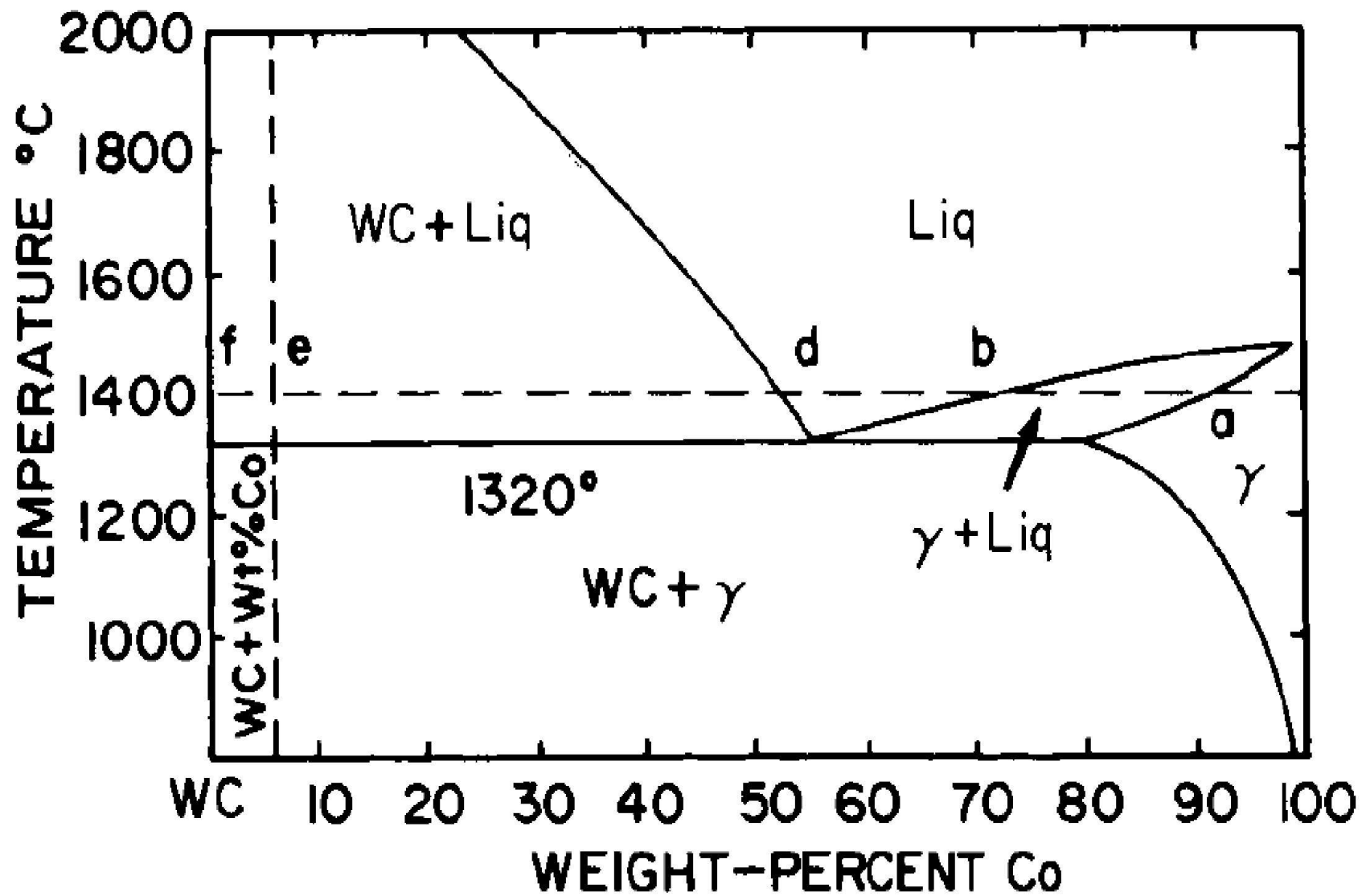
Experience has shown that **equilibrium is never approached** in the sintering of porcelain compositions. It is **true** that **mullite forms** at temperatures above 1000°C in **nearly equilibrium quantities**, but **tridymite and potassium feldspar** have never been observed to crystallize upon the cooling of a porcelain composition. The **quartz** that is **sometimes found** in a fired porcelain body can be traced to **unreacted quartz** crystals only partially dissolved during the firing operation. If the quantity of liquid is insufficient to dissolve all of the quartz, the **quartz may transform** in part or in entirety into **cristobalite** which does not transform to either quartz or tridymite during the cooling of the sintered porcelain.

The firing of porcelain is an excellent example of a multiphase system **governed largely by kinetic processes** rather than equilibrium conditions. The porcelain composition thus at high temperatures will be either **liquid plus mullite** or **liquid, mullite, and cristobalite**. Quartz will be present only if the composition has not been given sufficient time or temperature to reach equilibrium conditions. Upon cooling, **even at reasonably slow rates of cooling, composition will essentially remain fixed** as if it were still at high temperatures. **No transformation from tridymite to quartz or cristobalite to tridymite or cristobalite to quartz occurs.** **No crystallization of the glass to leucite or feldspar** has been observed.

TUNGSTEN CARBIDE-COBALT SYSTEM (cemented carbides): Tungsten carbide: most commonly and most frequently used tool materials; a brittle solid, ball milled with cobalt (ductile) powder; Many of the physical properties maximises: with a minimum amount of liquid; 94 wt % tungsten carbide with 6 % cobalt is near this optimum composition.; At the sintering temperature, not only does the cobalt react to form a liquid, but tungsten carbide is also dissolved in the cobalt, Co melting point is 1480°C.

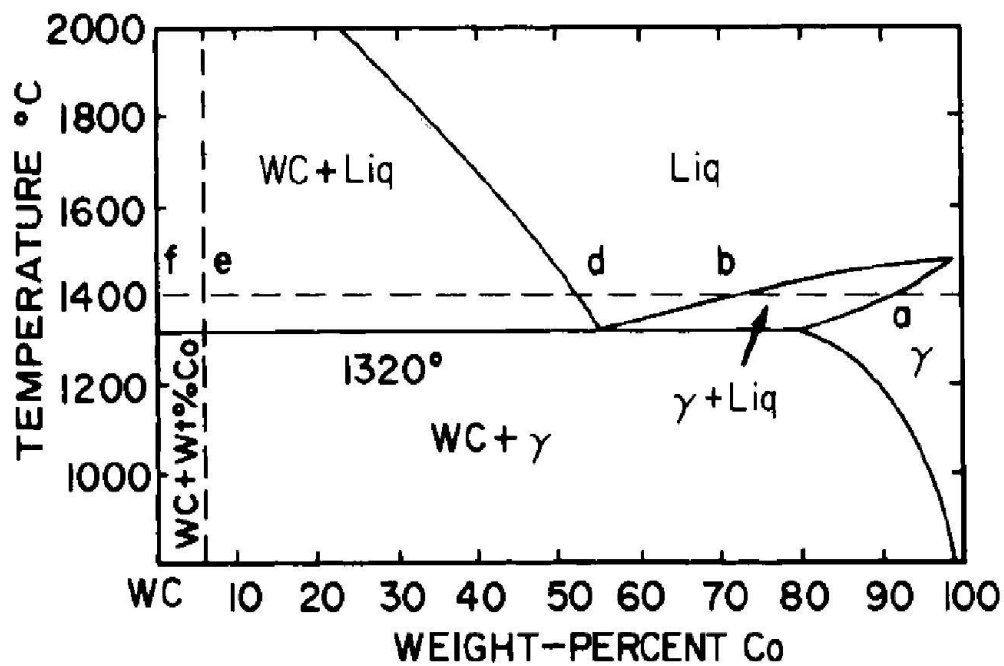
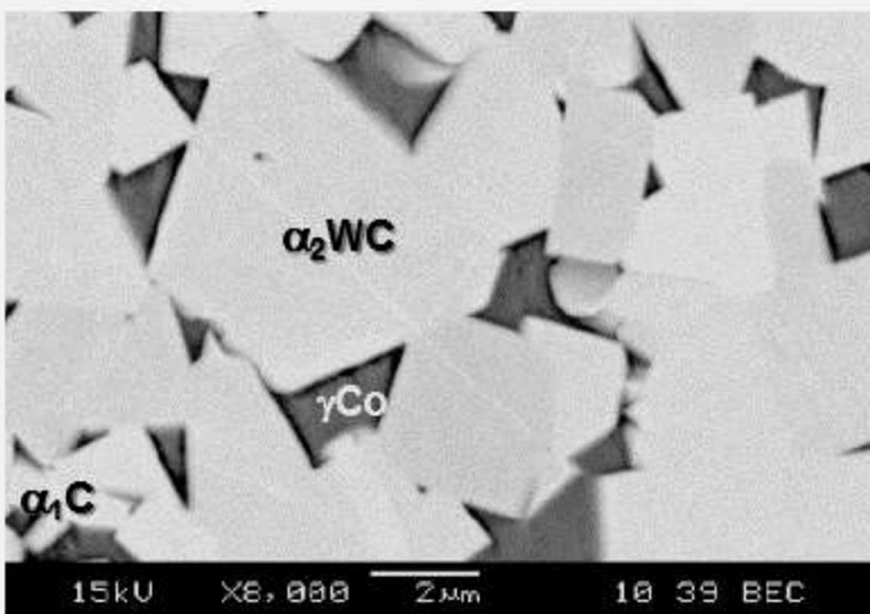
Co as the preferred binder metal: best comminution characteristics in milling, superior wettability for WC, higher solubility of WC in cobalt at sintering temperatures and excellent properties

Liquid dissolves all of the cobalt and the cobalt-WC solid solution, 6% cobalt composition forms about 12% by weight (20 vol %) of liquid;

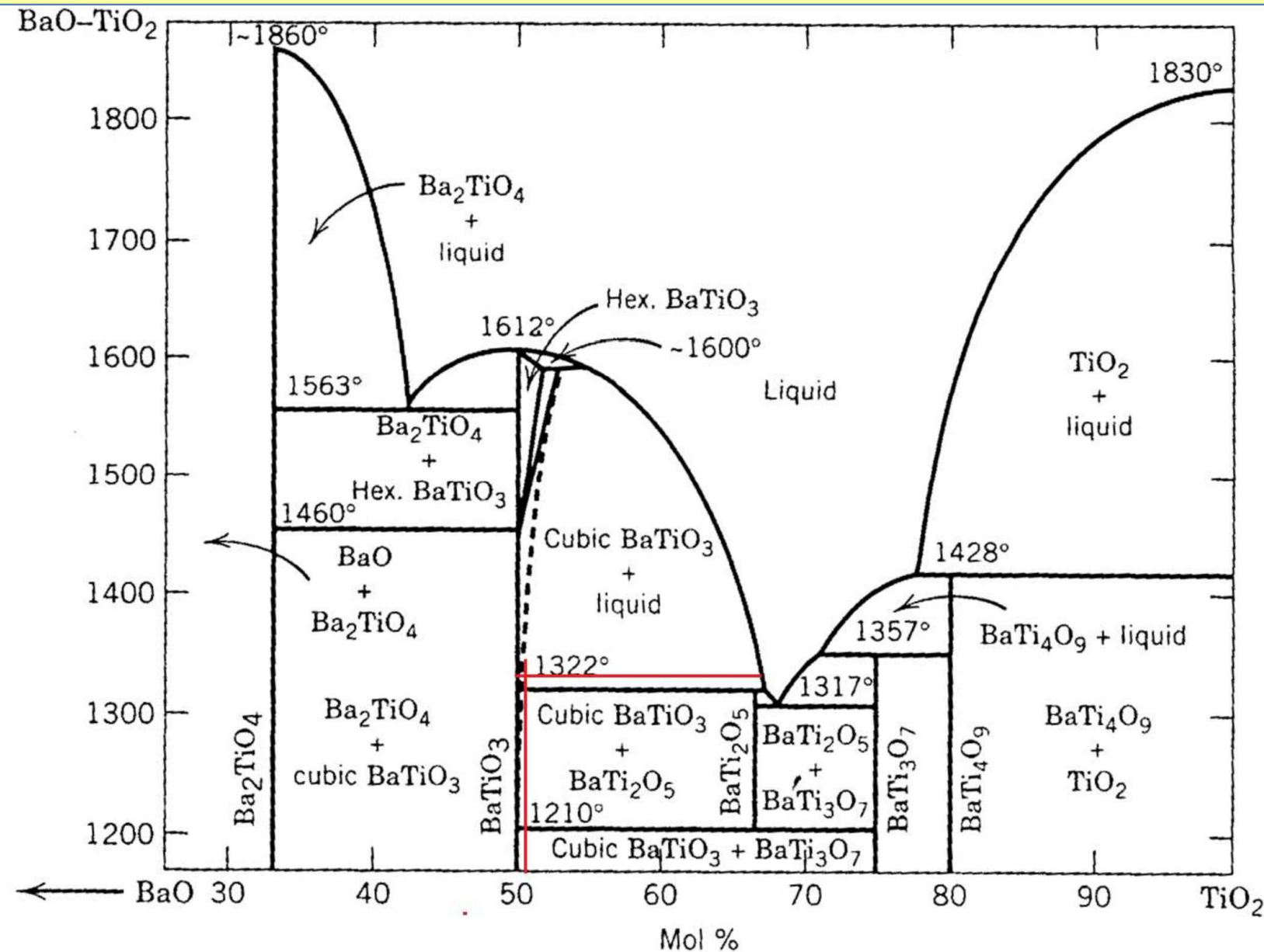


Surface free energy of the liquid pulls the particles together and the powder compact shrinks until it is near theoretical density. Grain Growth of WC occurs; WC precipitates from eutectic mixture; exsolution of WC: from cobalt solid solution (gamma)

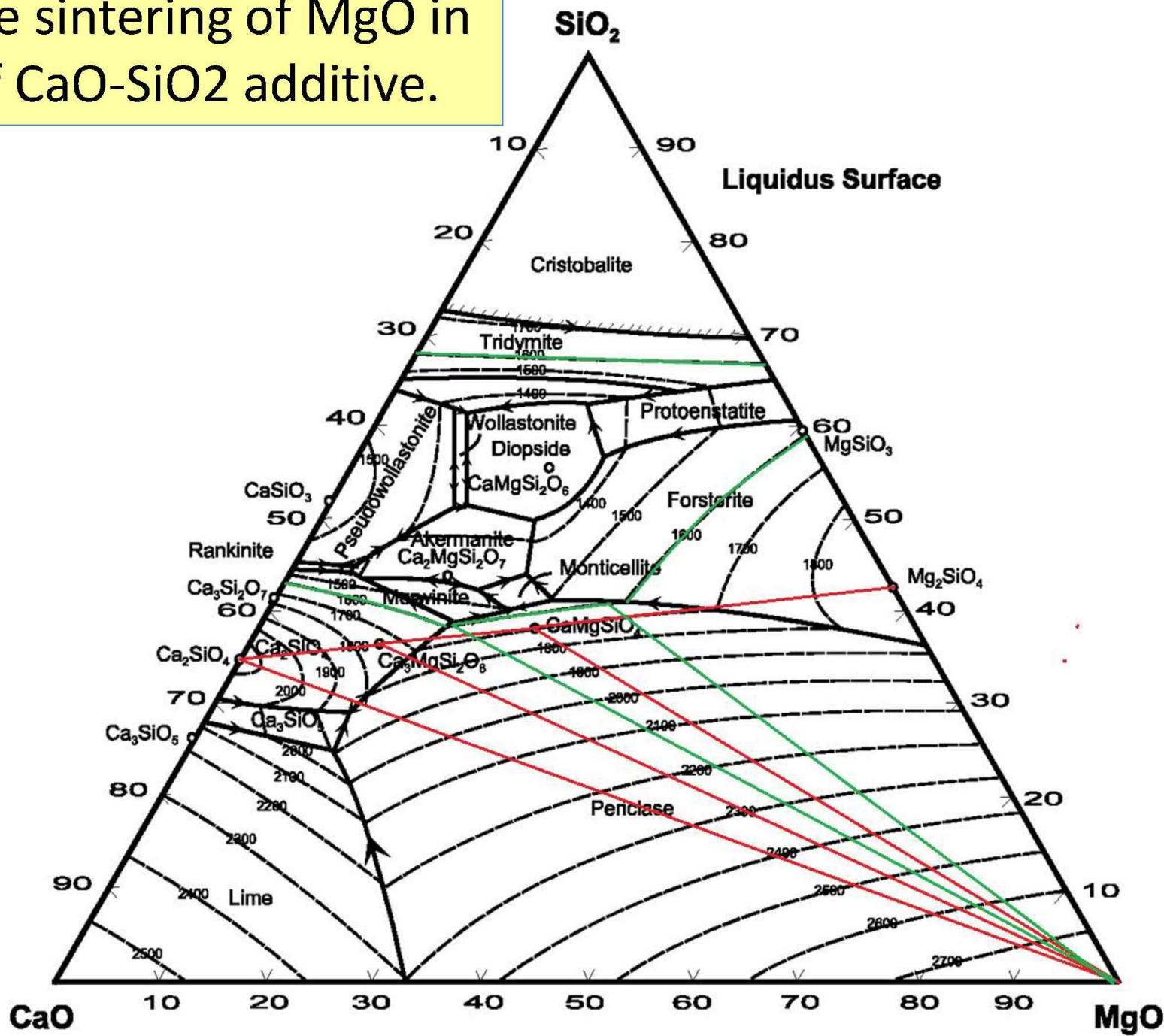
Hard and brittle carbide phase, ductile bonding phase.; contrasting features like: high wear resistance and hardness with high strength and good ductility.



Liquid phase sintering of BaTiO₃ in presence of small amount of excess TiO₂.



Liquid phase sintering of MgO in presence of CaO-SiO₂ additive.



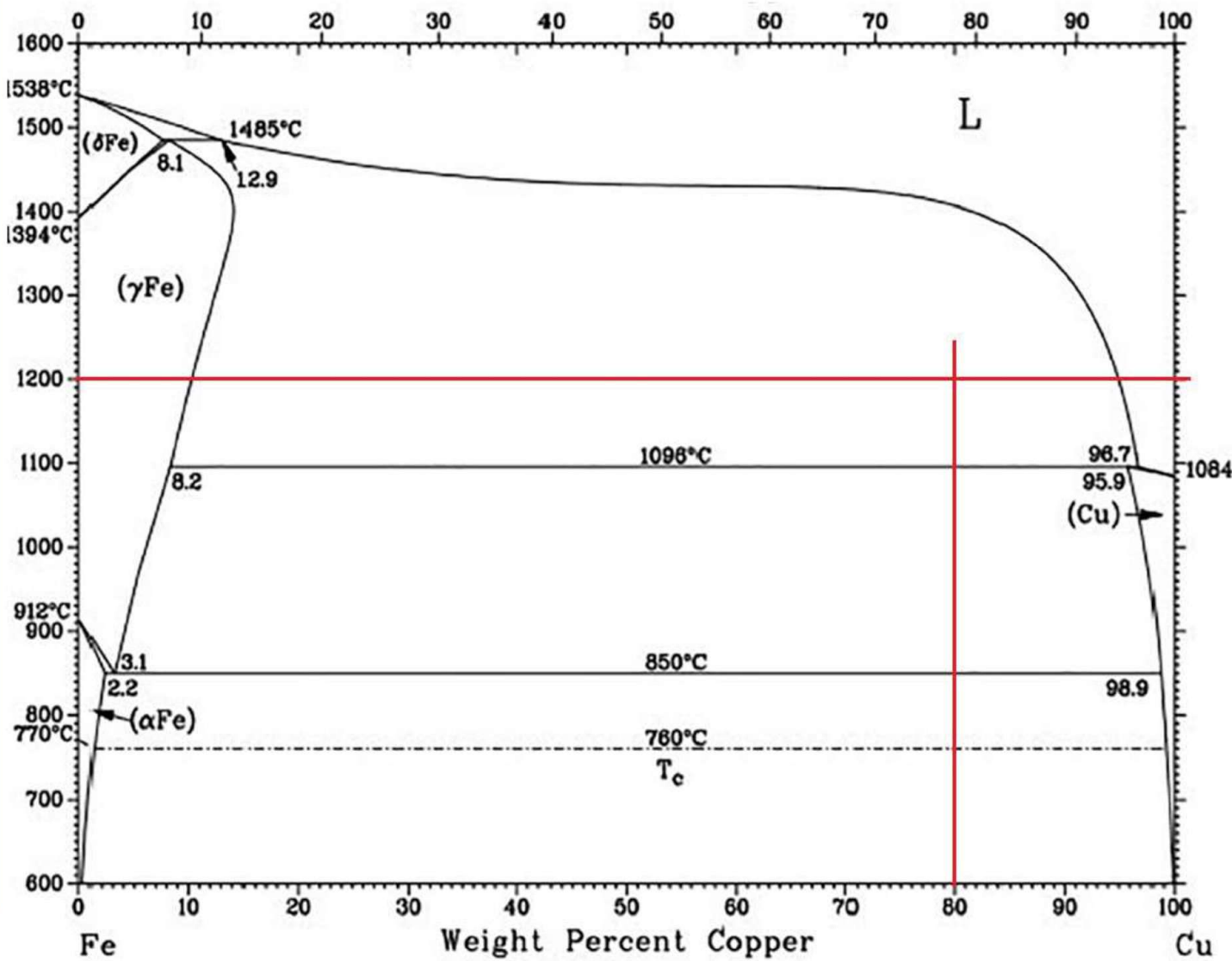
Liquid phase sintering of Fe powder:

Metal bonded diamond tools are suitable for cutting a variety of work-pieces due to its good mechanical and thermal properties. Diamond tools: manufactured: using the **powder metallurgy method**. Co, and Fe are the most frequently used matrices for diamond tools. Co is an important strategic resource, and it has **high prices and toxicity**. Fe-based matrices have gradually replaced the Co-based matrices, Fe and its alloy must be sintered at high temperature; The **risk of graphitization of diamond**, Fe powders are highly active and **easily oxidized** in the air,: Use of Sintering additives: Cu, Sn,

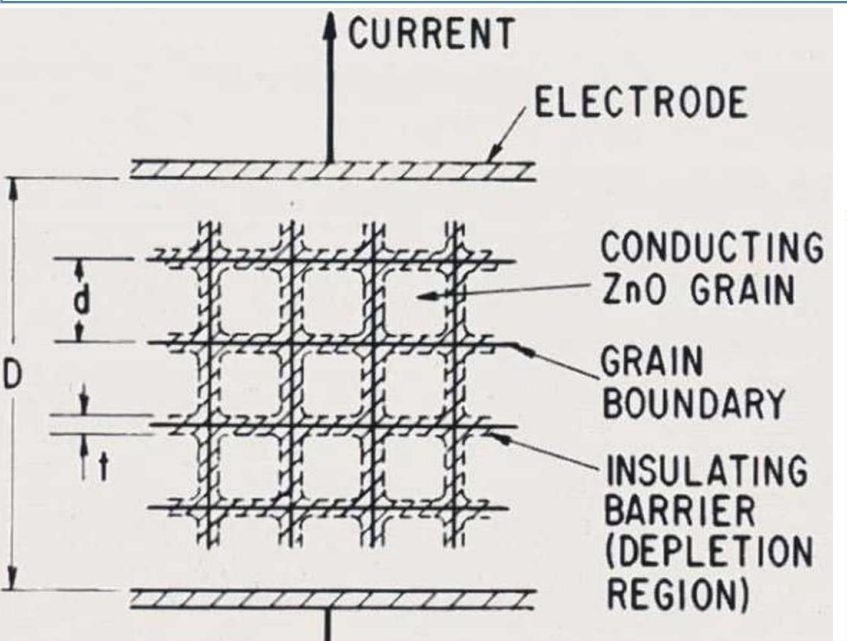
Rapid sintering of iron powder with additions of copper. Approximately **20% by weight of copper**, to near pore free condition below **1200°C**. liquid is formed above the peritectic temperature of **1096°C**. : Inhomogeneous mixture: Cu begin melting at **1084°C**; simultaneous process of the formation of a solid solution of iron and copper.

Rapid sintering takes place, Cu-rich liquid **completely wets** the iron-copper solid solution; as the sintered material cools to room temperature.; **exsolution of iron** from the copper solid solution,

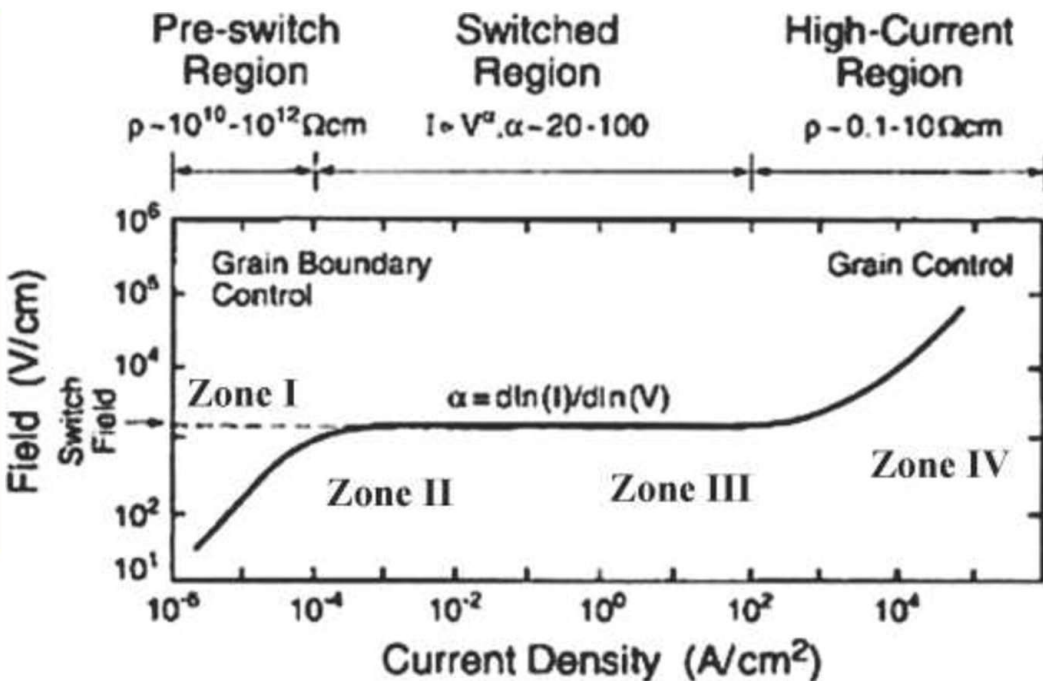
With **20% by weight of copper approximately 12 to 15% liquid will be formed** at a sintering temperature of between **1120° and 1200°C.**



ZnO-based **varistors** are **non-linear** ceramic resistors which are largely used to protect the electric and electronic circuits and components against over-voltages. used in lightning arresters owing to their strongly non-linear I(V) characteristics.



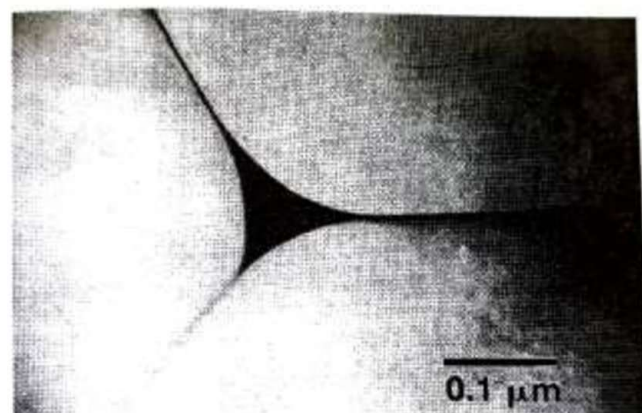
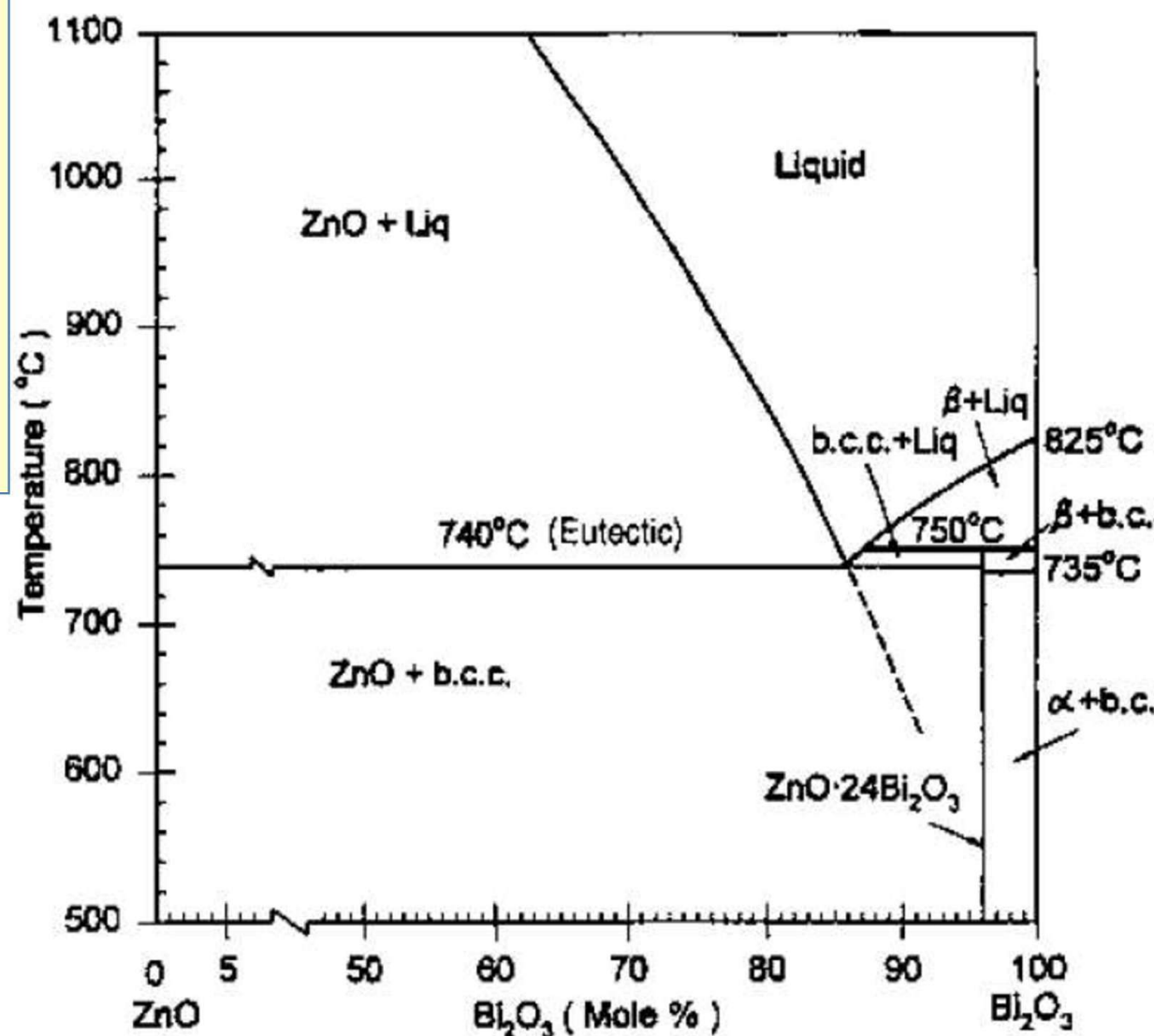
ZnO: liquid-phase sintered with 0.5 mol% of Bi₂O₃ (and small other oxides).



ZnO grains: dimensions in the range of 10 to 100µm. The boundaries between the grains form **double potential barriers** with Schottky junctions having conduction voltages in the range of **3.5V**. The boundary between each grain and its neighbor forms a **Zener-like diode junction**.

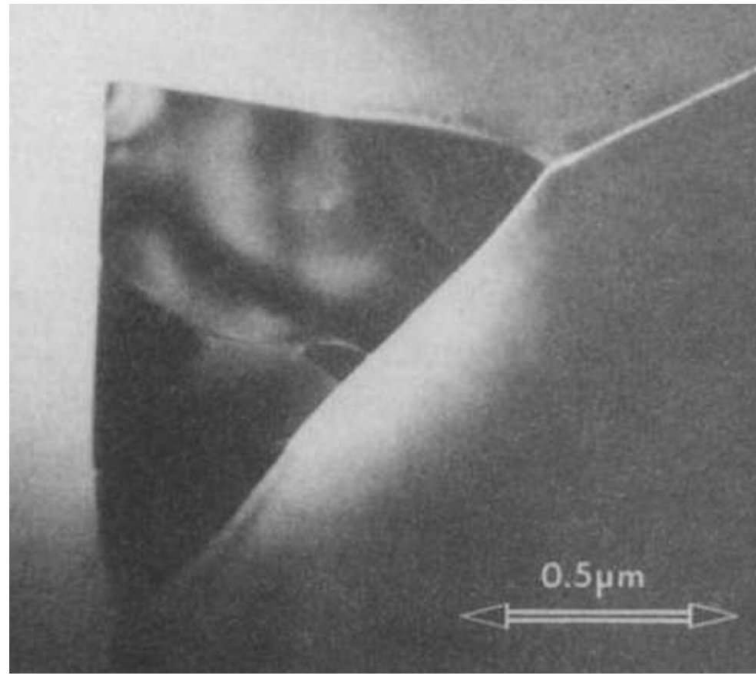
The phase diagram for the **ZnO-Bi₂O₃** system shows the formation of a **Bi-rich liquid phase** above the **eutectic temperature of 740C**.

Samples that have been quenched from the sintering temperature show a **liquid film that completely penetrates the grain boundaries**, indicating a zero dihedral angle.



Bismuth-rich phase at a three-grain junction in zinc oxide exhibits a zero dihedral angle.

However, during slow cooling, the liquid and solid compositions change, with precipitation of the principal phase, leading to a substantial increase in the dihedral angle and to a non-wetting configuration.



ZnO-Bi₂O₃ varistor composition,
annealed for 43.5 h at 610C resulting
in a non-wetting secondary phase.

Silicon nitride is best suited for mechanical engineering applications at high temperatures. The crystal structure of Si_3N_4 has a **high degree of covalent bonding**, so diffusional mass transport by **solid-state diffusion is very slow**.

Si_3N_4 powders: normally liquid phase sintering.

Si_3N_4 powders commonly contain 1–5 wt% SiO_2 as a surface oxidation layer.

oxide additive reacts with the SiO_2 to form a silicate liquid that aids densification.

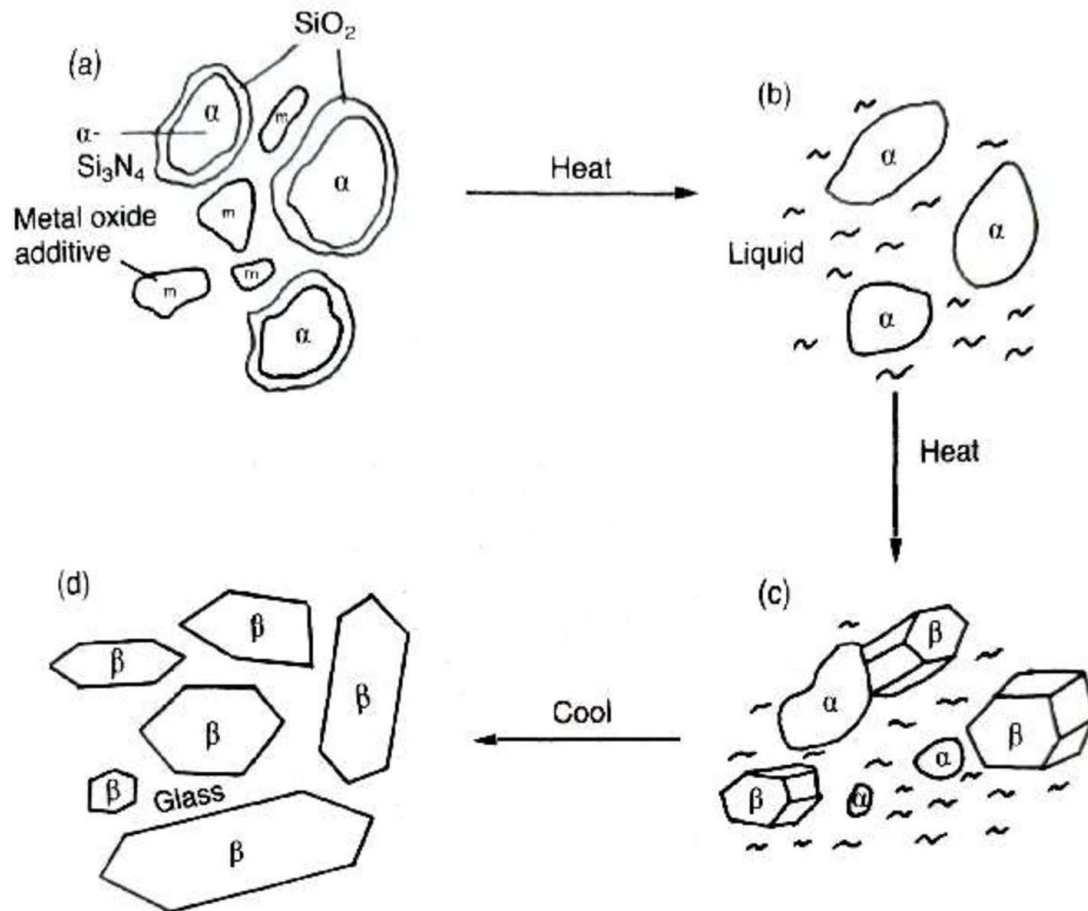
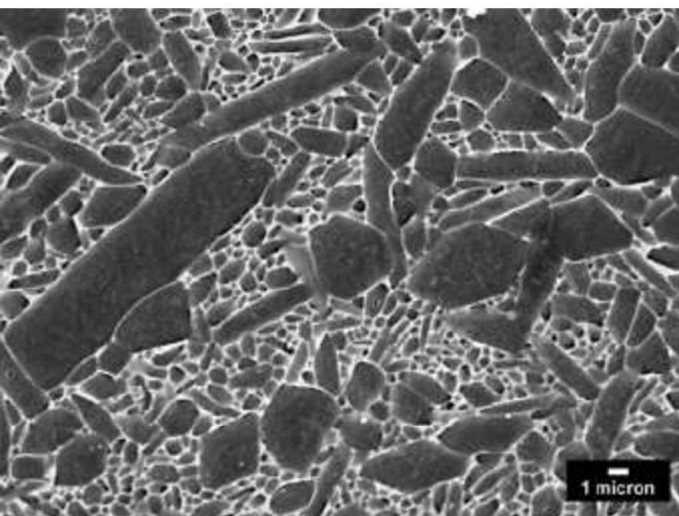


Fig. 7.7 Schematic of solution-precipitation mechanism in HPSN: (a) starting powders; (b) oxynitride/silicate liquid formation and solution of silica and α - Si_3N_4 ; (c) precipitation of β - Si_3N_4 ; (d) final microstructure as viewed in a 2-D section showing hexagonal β - Si_3N_4 grains in a (usually) glassy matrix.

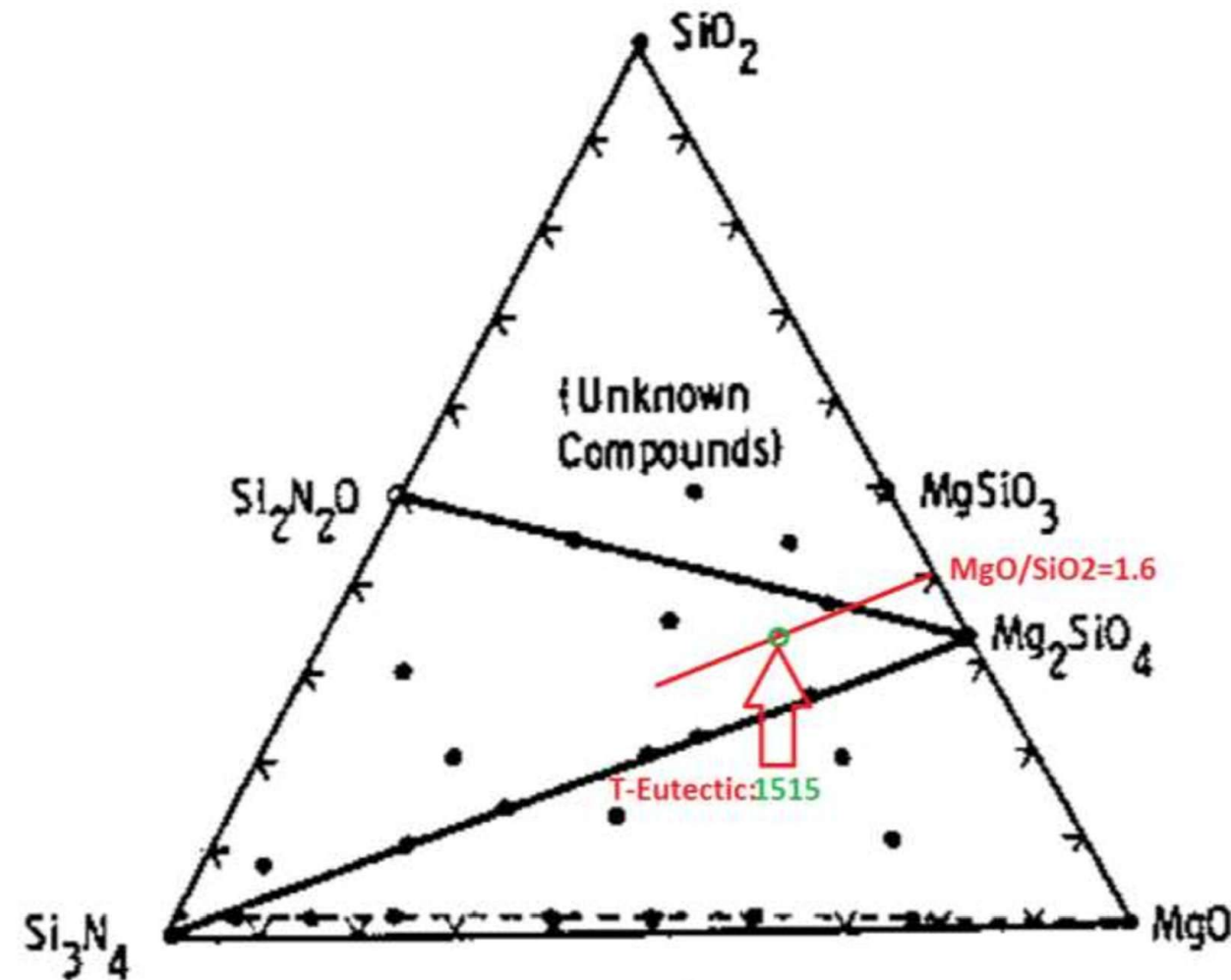
Use of phase diagrams: **MgO** (5–10 wt%): one of the first successful additives. It **forms a eutectic liquid with SiO₂** at 1515 C, but the sintering temperature can be anywhere between 100–300 C higher than the eutectic temperature.

Subsolidus system Si₃N₄-SiO₂-MgO, If equilibrium achieved : materials would contain two phases if the composition lies on the tie lines or three phases if the composition lies within one of the compatibility triangles:

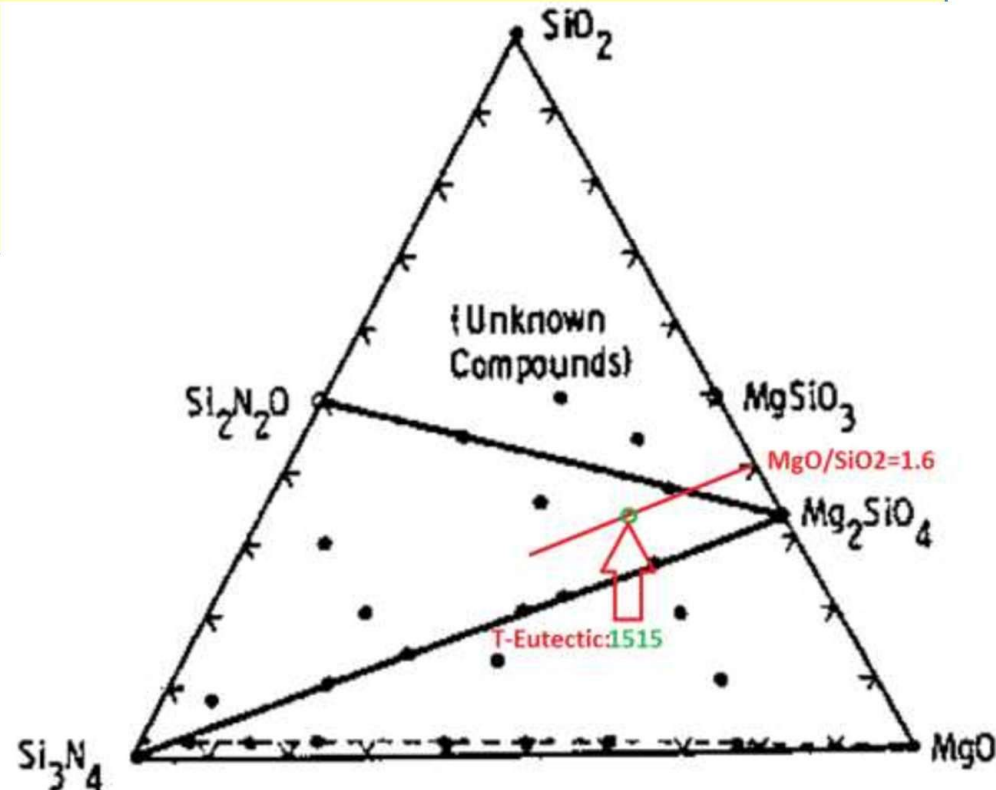
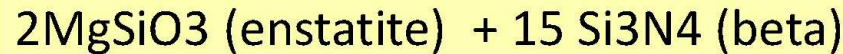
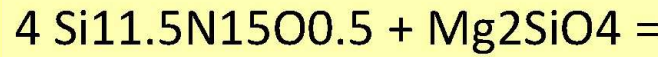
Si₃N₄ MgO Mg₂SiO₄

or

Si₃N₄ Si₂N₂O Mg₂SiO₄.
But, only two phases are observed, Si₃N₄ and glass.



Evaluation of strength at 1400°C as a function of MgO–SiO₂ molar ratio showed a **minimum** in strength at ratios between 1 and 2, ascribed to the composition of the Si₃N₄-ternary eutectic (1515°C) **join with a ratio of 1.6**. The major factor controlling hot strength appeared to be the inter-granular glass derived from the densification aid and which, as indicated above, became the subject of intensive investigation. The importance of inter-granular glass had been shown very early by the complete loss of strength at 1400°C in nitride prepared with 5% MgO. the function of the MgO is to react with oxygen present in the system, either as a coating on the Si₃N₄ particle surfaces, or in the α-Si₃N₄ lattice and, thereby, forming magnesium silicates:



For some applications, ceramics single crystals are required.

Method of Single Crystal Growth in Ceramics: Depends on: Type,, application, and size.

Liquid to Solid
Gas to Solid

Most important is CZ method:

TABLE 29.1 The Uses of Single Crystals

Semiconductor devices

- | | |
|-------------------------------|--|
| 1. Diodes | Si, Ge |
| 2. Photodiodes | Si, GaAs, Cd _x Hg _{1-x} Te |
| 3. Transistors | Si, GaAs, SiC |
| 4. Thyristors | Si |
| 5. Photoconductive devices | Si, Cd _x Hg _{1-x} Te |
| 6. Integrated circuits | Si, GaAs |
| 7. Light-emitting diodes | GaN, SiC |
| 8. Radiation detectors | Si, Ge, CdTe, YAG |
| 9. Strain gauges | Si |
| 10. Hall effect magnetometers | InSb |

Mechanical components

- | | |
|--------------------------------|---|
| 1. Abrasives and cutting tools | SiC, Al ₂ O ₃ |
| 2. Substrates | Diamond, Al ₂ O ₃ |

Magnetic devices

- | | |
|--------------------------|----------|
| 1. Transformer cores | Ferrites |
| 2. Electric motors | Ferrites |
| 3. Tape heads | Ferrites |
| 4. Microwave circulators | Garnets |

Piezoelectric devices

- | | |
|-------------------------------|---|
| 1. Resonant bulk wave devices | SiO ₂ , LiTaO ₃ |
| 2. Surface wave devices | SiO ₂ , LiNbO ₃ , AlN |

Optical devices

- | | |
|----------------------------|---|
| 1. Windows | Al ₂ O ₃ |
| 2. Lenses | CaF ₂ |
| 3. Polarizers | CaCO ₃ |
| 4. Laser hosts | YAG, Al ₂ O ₃ , alexandrite |
| 5. Magneto-optical devices | YIG |
| 6. Electrooptic devices | LiNbO ₃ , ADP, KDP |
| 7. Nonlinear devices | ADP, KDP, LiNbO ₃ |

Jewelry

Diamond, cubic zirconia

Pyroelectric devices

X-ray and particle optical devices

- | | |
|--------------------------------------|------------------|
| 1. Collimators and focusing elements | SiO ₂ |
|--------------------------------------|------------------|

Czochralski technique: (CZ) most important method for the production of bulk single crystals of a wide range of electronic and optical materials. The feed material is put into a cylindrically shaped crucible and melted by resistance or radio-frequency heaters.

After completely molten, a seed crystal with a diameter of typically a few millimeters is dipped from the top into the free melt surface and a melt meniscus is formed. Then, after remelting of a small portion of the dipped seed, the seed is slowly withdrawn from the melt (often under rotation) and the melt crystallizes at the interface of the seed by forming a new crystal portion. During the further growth process, the shape of the crystal, especially the diameter, is controlled by carefully adjusting the heating power, the pulling rate, and the rotation rate of the crystal.

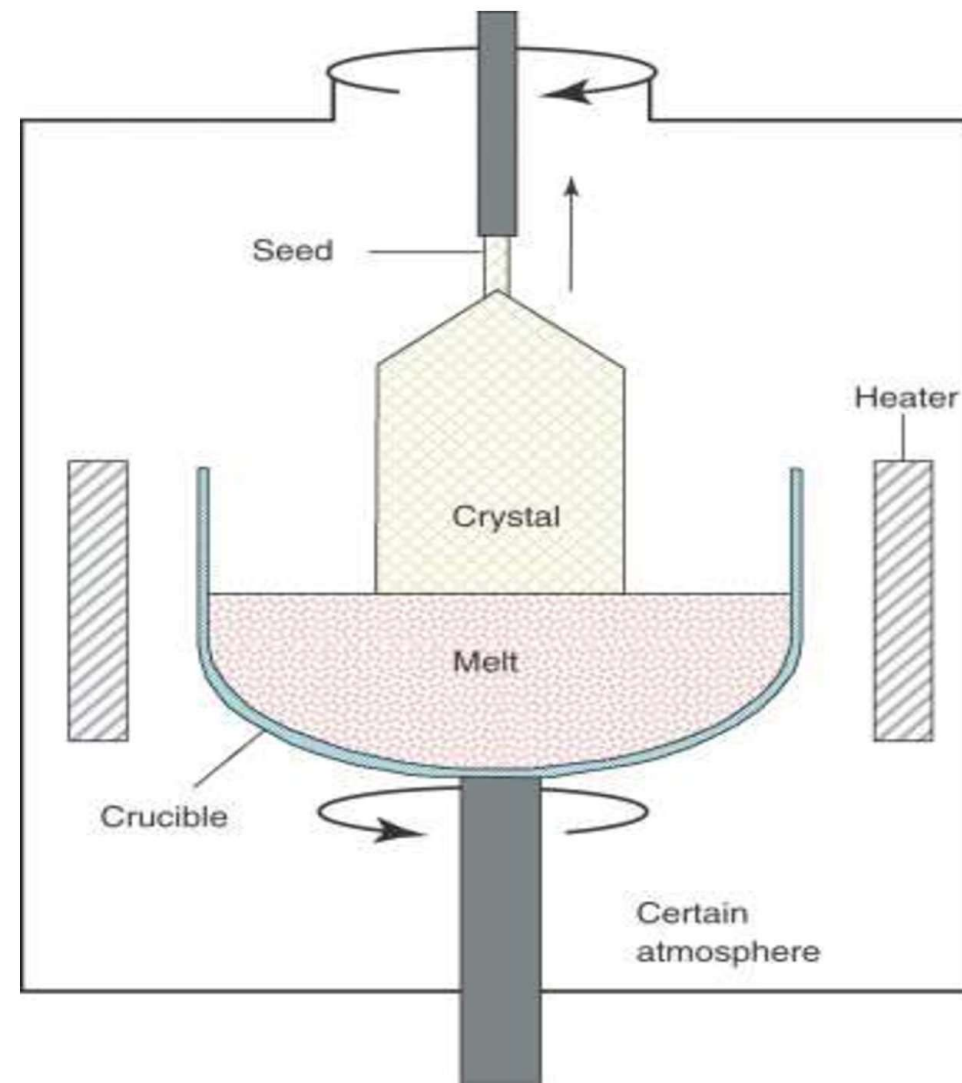


TABLE 29.4 Materials Grown by the Cz Technique (for Crystals ~2cm in Diameter)

Material	T_M (°C)	Crucible	Atmosphere	Pulling rate (mm/h)	Rotation rate (rpm)
Zn	419	Pyrex	Vacuum	400–800	10–30
GaSb	712	Graphite	Hydrogen	50–100	10–30
FeGe ₂	866	Alumina	Vacuum	5–20	20–50
Bi ₁₁ GeO ₂₀	930	Platinum	Oxygen	5–15	10–50
Ge	937	Graphite	H ₂ /N ₂	60–120	20–50
ZnWO ₄	1200	Platinum	Air	8–16	50–100
GaAs	1237	Silica	Arsenic	20–30	10–30
LiNbO ₃	1250	Platinum	Oxygen	3–8	20–30
Sr _x Ba _{1-x} Nb ₂ O ₆	1400	Platinum	Oxygen	3–6	10–20
Si	1420	Silica	Argon	100–200	10–20
MnFe ₂ O ₄	1500	Iridium		3–6	10–20
CaWO ₄	1650	Rhodium	Air	8–16	50–100
LiTaO ₃	1650	Iridium	Nitrogen	8–15	20–40
Y ₃ Al ₅ O ₁₂	1950	Iridium	Nitrogen	1–3	40–60
Al ₂ O ₃	2037	Iridium	Argon	1–3	30–50
MgAl ₂ O ₄	2100	Iridium	Argon	4–8	20–40

The Bridgman–Stockbarger method, The method includes two similar but distinct techniques primarily used for growing boules (single crystal ingots), but which can be used for solidifying polycrystalline ingots as well. The methods involve heating polycrystalline material above its melting point and slowly cooling it from one end of its container, where a seed crystal is located.

A single crystal of the same crystallographic orientation as the seed material is grown on the seed and is progressively formed along the length of the container. The process can be carried out in a horizontal or vertical orientation, and usually involves a rotating crucible/ampoule to stir the melt.

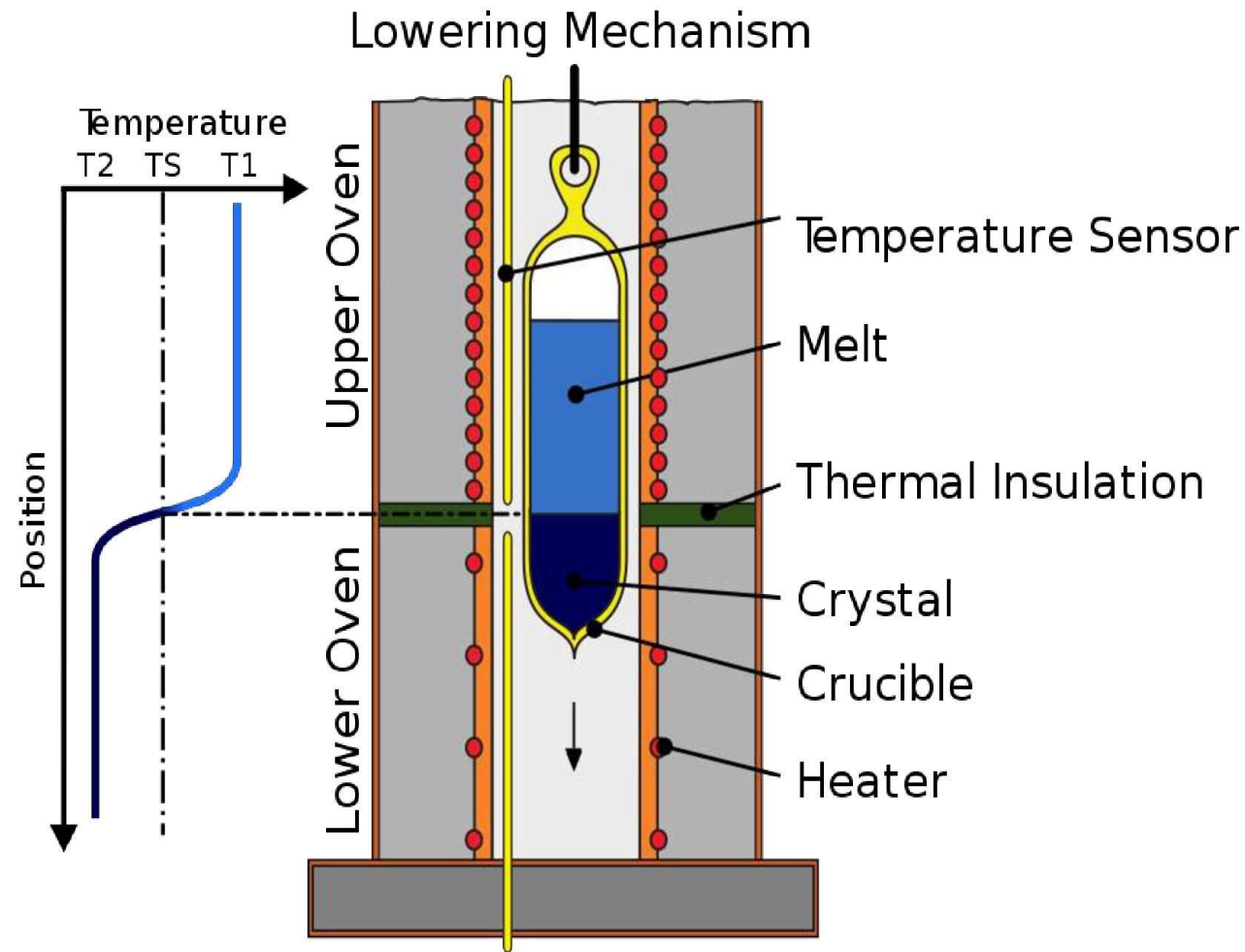


TABLE 29.5 Typical Conditions for Bridgman–Stockbarger Growth

Crystal	T_M (°C)	Growth rate (mm/h)	Crucible
Al_2O_3	2037	2–8	Molybdenum
ZnS	1850	0.5–2	Silica supported by graphite
FeAl_2O_3	1790	5–10	Iridium
GaAs	1238	2–6	Sand-blasted silica
Cu	1083	6–60	Graphite powder
Ge	937	50–150	Graphite- or carbon-coated silica
As	814	5–12	Thick-walled silica
AgBr	434	1–5	Pyrex
NaNO_2	271	3–6	PTFE ^a
K	63.7	1–4	Stainless steel coated with paraffin
Ar	–189.2	0.7–1.5	Mylar

^a PTFE, polytetrafluoroethylene.

The **Verneuil method** also called **flame fusion**, was the first commercially successful method of manufacturing synthetic gemstones, developed by the French chemist Auguste Verneuil. It is primarily used to produce the ruby, sapphire varieties of corundum, as well as the diamond simulants rutile and strontium titanate. The principle of the process involves melting a finely powdered substance using an oxyhydrogen flame, and crystallising the melted droplets into a boule.

Finely powdered RM, oxygen is supplied, travels with the powder down a narrow tube, tube is located within a larger tube, into which hydrogen is supplied. a flame of at least 2,400 °C at its core, powder passes through the flame, it melts into small droplets, which fall onto an support rod, a single crystal, called a boule, starts to form , support is slowly moved downward,

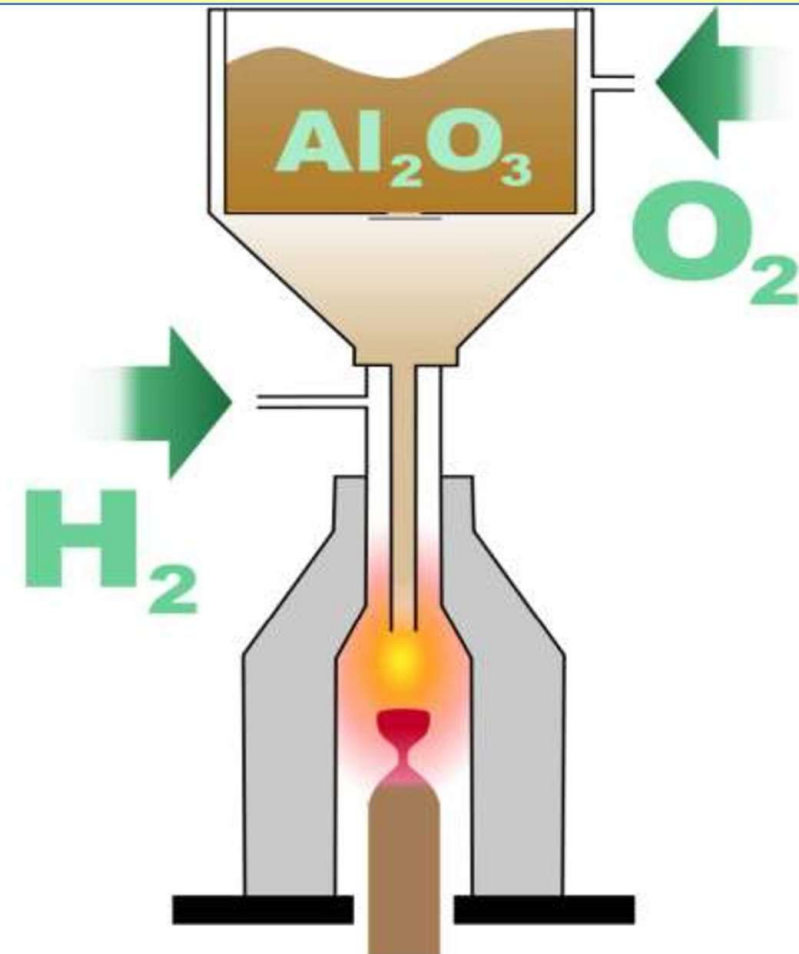


TABLE 29.3 Crystals Grown by Verneuil and Arc-Image Techniques

Material		Comments	T_M (°C)
Al_2O_3	Corundum, sapphire	Growth in a variety of directions; best growth in a cone of directions 60° from c	2040
$\text{Al}_2\text{O}_3\text{: Cr}$	Ruby	Verneuil	2130
MgAl_2O_4	Magnesium-aluminum spinel	Verneuil	1810
$3\text{Al}_2\text{O}_3\cdot 2\text{SiO}_2$	Mullite	Verneuil	1530
CaWO_4	Scheelite	Verneuil	1830
TiO_2	Rutile	Verneuil	2700
ZrO_2	Zirconia	Verneuil	2400
Y_2O_3	Yttria	Verneuil	>1200
MgFe_2O_4	Magnesium (nonstoichiometric) spinel	Arc-image	>1200
NiFe_2O_4	Nickel ferrite	Arc-image	>1200

Hydrothermal Crystal Growth:

Aqueous solution: at high temperature and pressure: to dissolve nutrient: In lower part of the system: Transferred to other part: and deposit upon Seed crystal by epitaxy. : Autoclave is heated from one side: A sharp drop of temperature at perforated baffle: Solvent usually alkaline solution.: Dissolve Nutrient at higher Temp.

Transported by convection through baffle into seed zone: Where temp is lower; Solution super-saturated; deposit on Seeds;
 $P > 600$ atm.
 $T: 300- 600$ °C.

Quartz: 1 M NaOH soln
Dissolution T: 400 °C
Growth T: 350 °C
Pressure: 1430 atm.

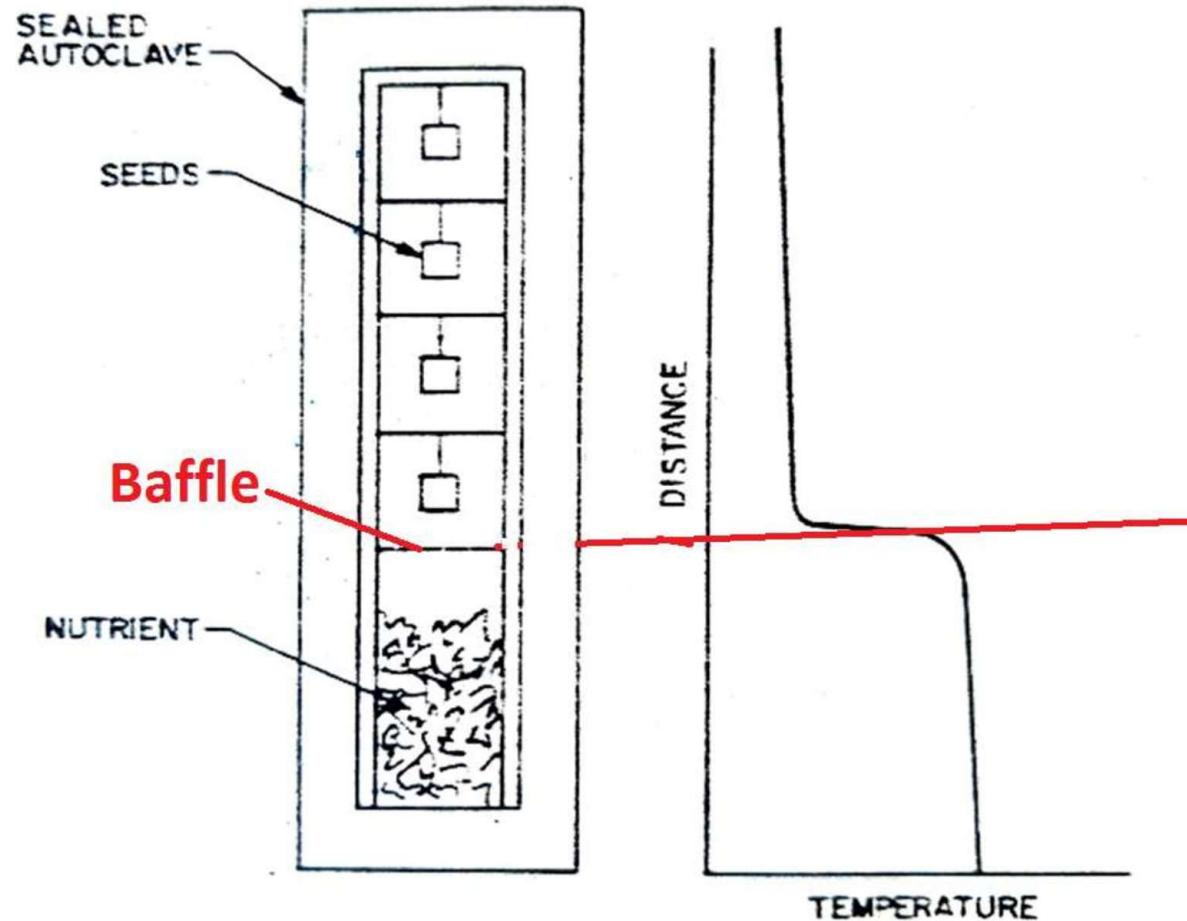
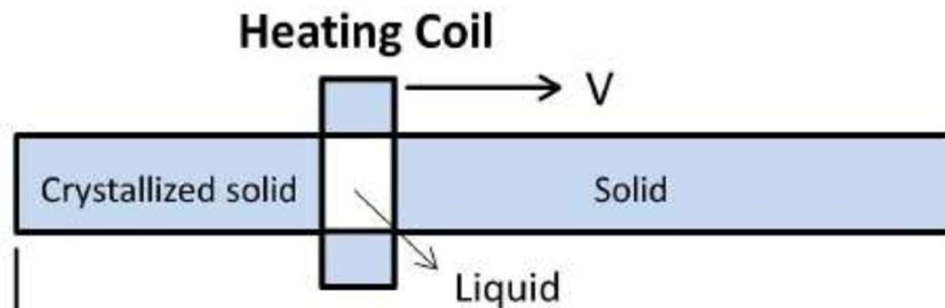
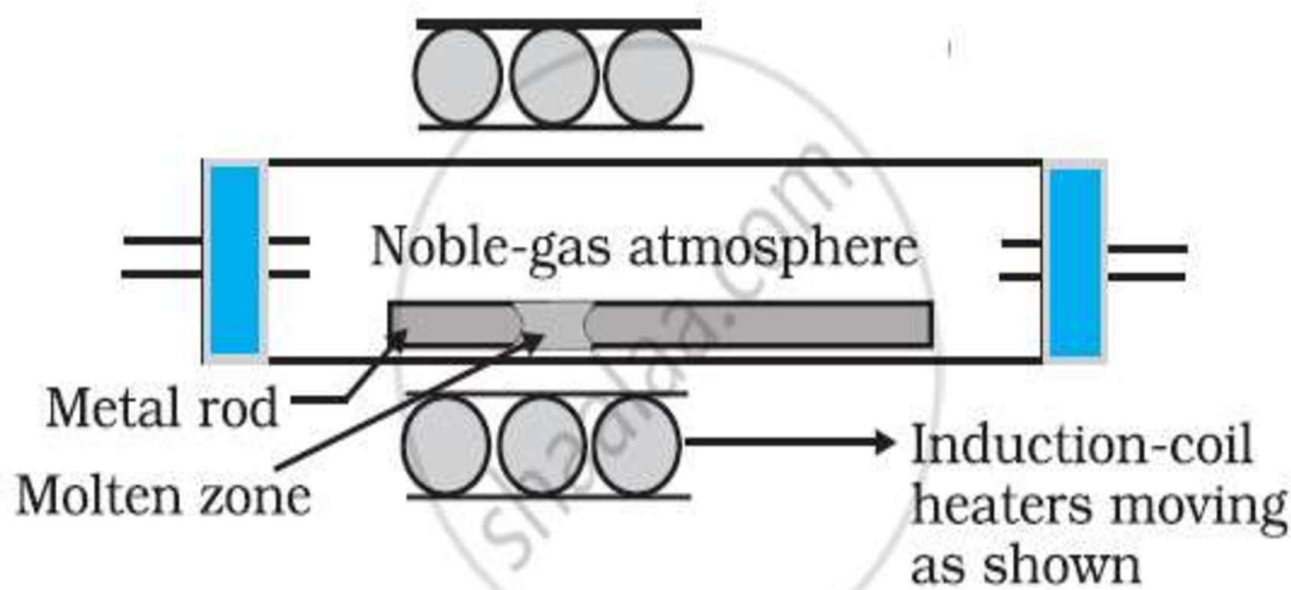


Fig. 11. A hydrothermal autoclave with internal temperature distribution.

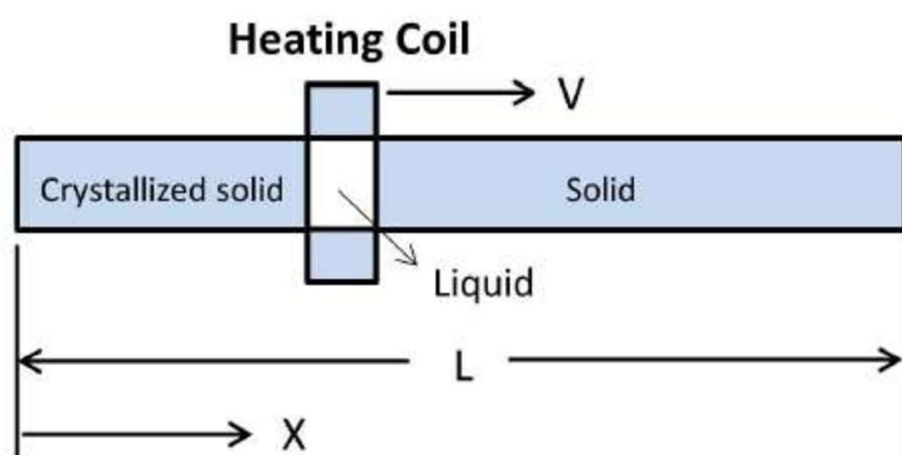
TABLE 29.6 Examples of Hydrothermally Grown Crystals

Crystal	Solvent	Growth zone temperature (°C)	Dissolution zone temperature (°C)	Pressure or degree of fill
$\alpha\text{-SiO}_2$	1 N Na_2CO_3 1.0 M NaOH + 0.025 M Li_2CO_3 + 0.1 M Na_2CO_3	360 374	400 397	80% 88%
LiGaO_2	3.5 M NaOH	385	420	70%
$\text{BiTi}_2\text{O}_{12}$, $\text{Bi}_{12}\text{TiO}_{20}$	KF	550–600	—	>70–80%
$\text{K}(\text{Ta},\text{Nb})\text{O}_3$	15 M KOH	650	690	1000 atm
KNbO_3 , KTaO_3	KOH	400–600	450–680	70–80%
PbTiO_3 , PbZrO_3	KF	570	585–590	50–55%
$\text{Pb}(\text{Ti},\text{Zr},\text{Nb})\text{O}_3$	>10 wt% KF	580	618	83%
$\text{R}_x\text{Al}_y(\text{BOH})_z\text{Si}_z\text{O}_{10}$	H_3BO_3 + NaCl or NaF	400–700	—	1000–3000 atm
AlPO_4 , GaPO_4	6.1 M H_3PO_4 , 3.8 M ADP	150	300	80%
$(\text{Mn},\text{Fe},\text{Zn})_3[\text{Be}_2\text{Si}_6\text{O}_{24}]S_3$	1% NaOH or 8% NH_4Cl	450	480–500	1500–2000 atm
$\text{Na}_2\text{ZnGeO}_4$	30 wt% NaOH	250–300	253–310	50–90%
NiFe_2O_4	0.5 N NH_4Cl	470–480	—	70–75% (1100–1300 atm)
Fe_3O_4	10 M NaOH	500	550	1000 atm
ZnFe_2O_4	NaOH	400	—	—
$\text{Y}_3\text{Fe}_5\text{O}_12$	1–3 M Na_2CO_3 or 1–3 M NaOH	400–750	—	200–1350 atm
	20 M KOH	350	360	88%
$\text{Y}_3\text{Ga}_5\text{O}_12$	1–3 M Na_2CO_3 or 1–3 M NaOH	400–500	—	1000–3000 atm
	K_2CO_3	500	550	~1000 atm
$\alpha\text{-Al}_2\text{O}_3$	2–3 M Na_2CO_3 or 1 M K_2CO_3	390–490	500–540	75–82% (1100–1600 atm)
	10% K_2CO_3 or 10% KHCO_3	530–600	540–640	50–70%
	4 M K_2CO_3	370	390	85%
	HCl	—	—	—
$\text{Y}_3\text{Al}_5\text{O}_12$	2 M K_2CO_3	550	600	1000 atm
CaWO_4	4 wt% NaOH	380	430	60–70%
SrWO_4 , BaWO_4	7–10 wt% NaOH	410–485	450–500	70%
	5–7 wt% NH_4Cl or 15–20 wt% LiCl or 30–40 wt% NaCl	430–485	450–500	65–70%
CdWO_4	7 wt% NH_4Cl or 16–25 wt% LiCl	430–455	450–470	75%
SrMoO_4 , BaMoO_4	5–7 wt% NH_4Cl or 15–20 wt% LiCl or 30–40 wt% NaCl	430–485	450–500	65–70%
ZnO	5.45 M KOH + 0.7 M LiOH	353	467	83%
PbO	1 N LiOH	430	450	60%
ZnS	2–5 M NaOH	350–380	410–560	50–80%

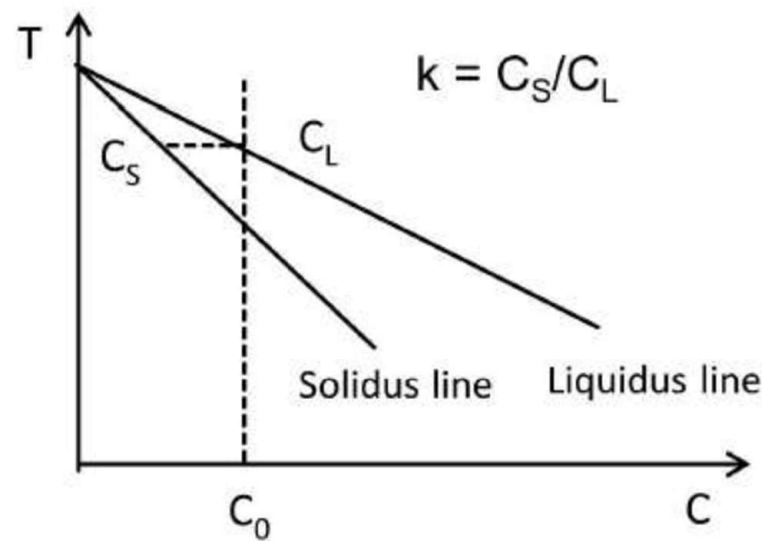
Zone melting (or **zone refining** or **floating-zone process**) is a group of similar methods of purifying crystals, in which a narrow region of a crystal is melted, and this molten zone is moved along the crystal. The molten region melts impure solid at its forward edge and leaves a wake of purer material solidified behind it as it moves through the ingot. The impurities concentrate in the melt, and are moved to one end of the ingot.



The principle is that the segregation coefficient k (the ratio of an impurity in the solid phase to that in the liquid phase) is usually less than one. Therefore, at the solid/liquid boundary, the impurity atoms will diffuse to the liquid region. Thus, by passing a crystal boule through a thin section of furnace very slowly, such that only a small region of the boule is molten at any time, the impurities will be segregated at the end of the crystal. Because of the lack of impurities in the leftover regions which solidify, the boule can grow as a perfect single crystal if a seed crystal is placed at the base to initiate a chosen direction of crystal growth. When high purity is required, such as in semiconductor industry, the impure end of the boule is cut off, and the refining is repeated.

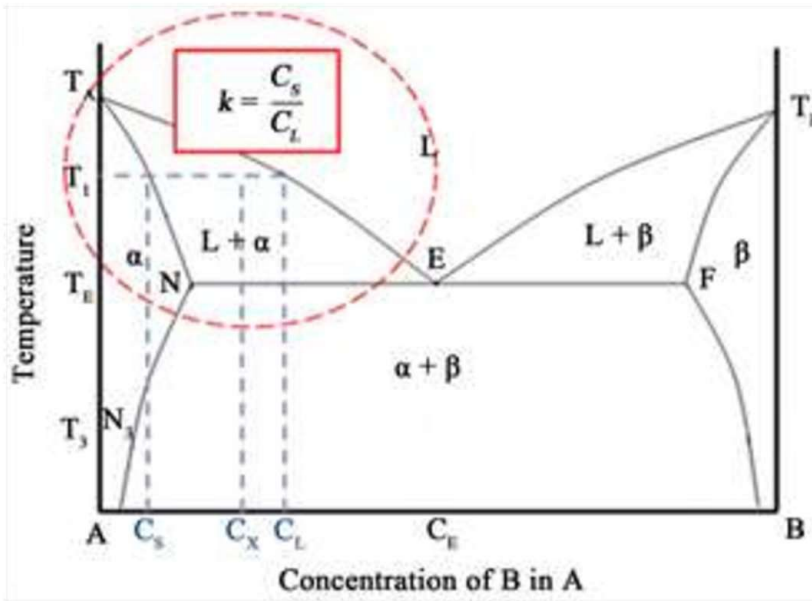


(a)



(b)

Figure 2. Scheme of zone refining process (a) and part of binary phase diagram (b).



Silver in Germanium metal : $k < 1 \sim 4 \times 10^{-7}$
 Al in GaP : $k > 1, \sim 45$
 $K \sim 1$: Fe₃O₄ in Mn₃O₄

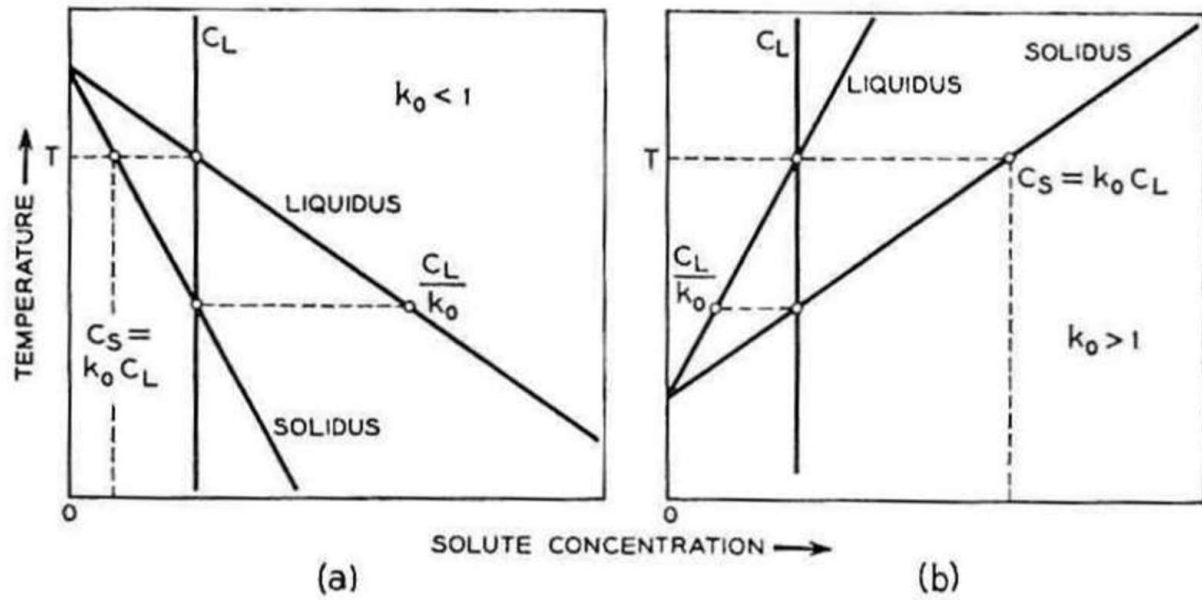
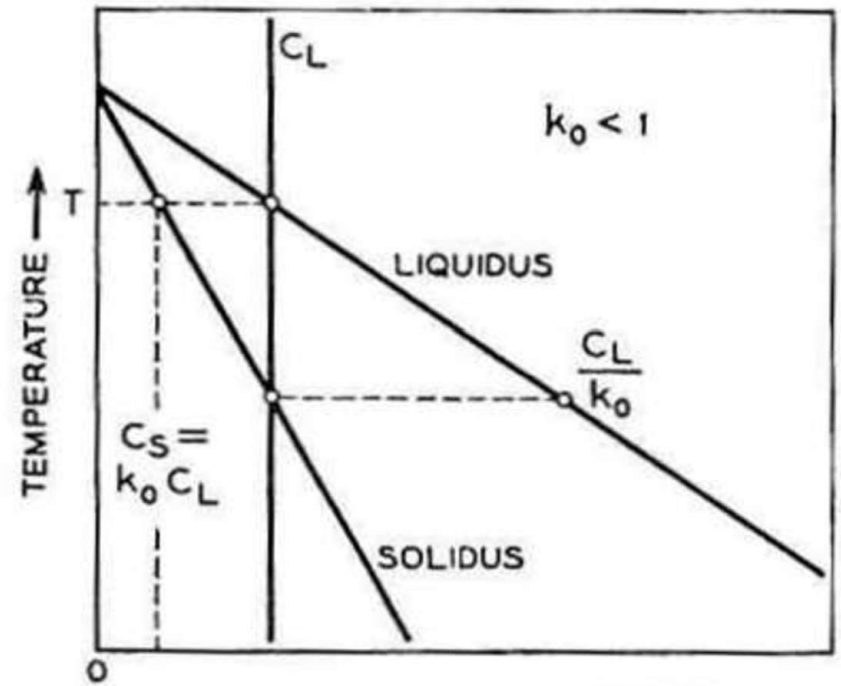
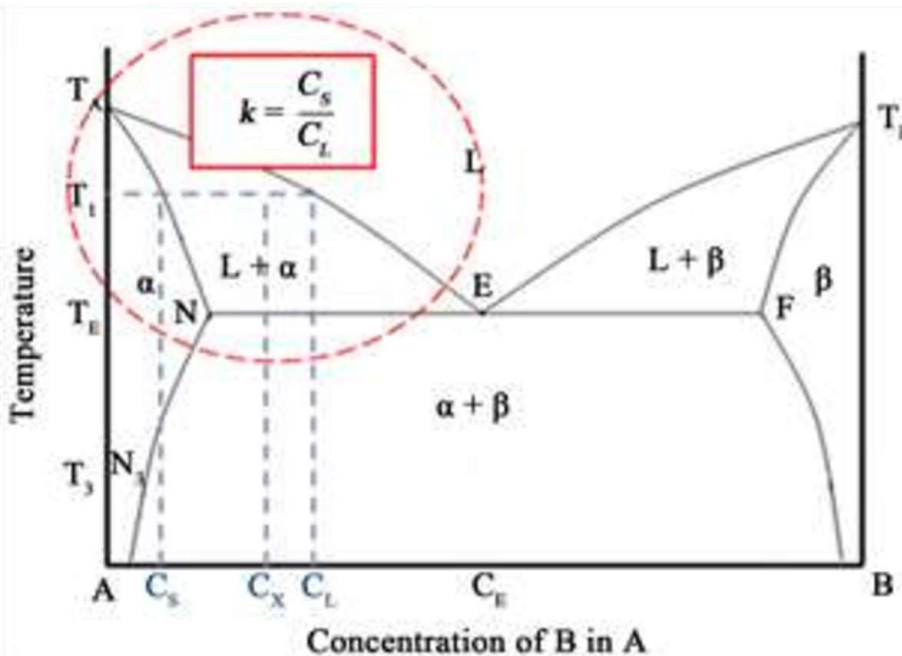


Fig. 2.1. Portions of constitutional diagrams in which the freezing point of the solvent is (a) lowered, (b) raised, by the solute.

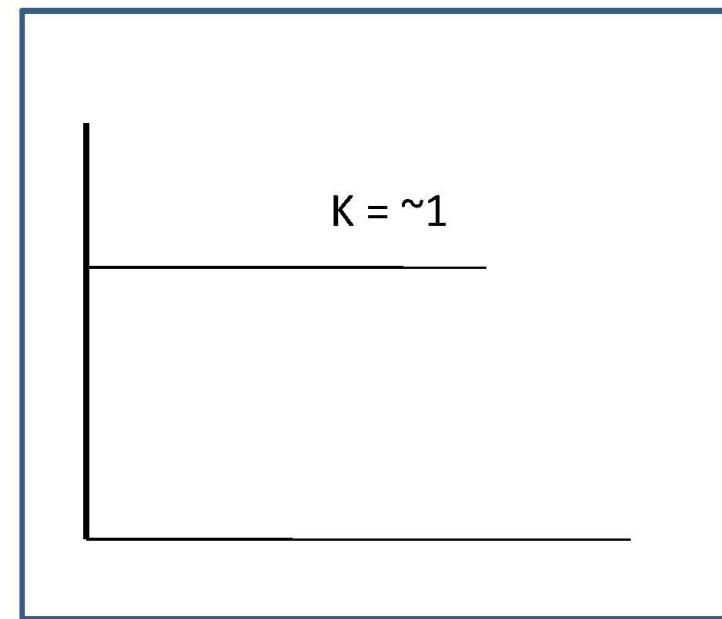
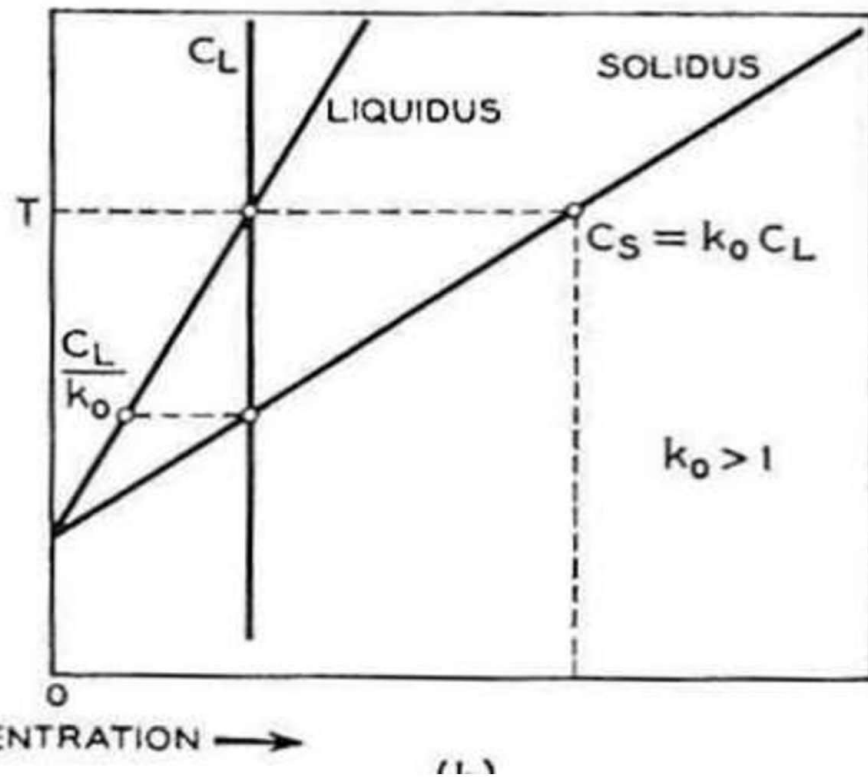
Growth from Nearly Stoichiometric Melt:

- Melting point will suggest , which crystal growing technique to use.
- However, impurity and stoichiometry create serious problem.
- Impurity distribution Co-efficient: $k = (X_s/X_l) = \text{mole fraction impurity in Solid/Liquid at equilibrium}$.
- (a) The case : $k < 1$ (Silver in Germanium $k= 4 \times 10^{-7}$), As Crystal grows, Impurity builds up in the melt, and increasingly incorporated in the crystal.: A compositional gradient. : Bridgman-Stockbarger, Vernuil, methods are not practical. An advantage in CZ techniques is, Growth can be terminated before the formation of second phase or before reaching upper limit of impurity.



SOLUTE CONCE

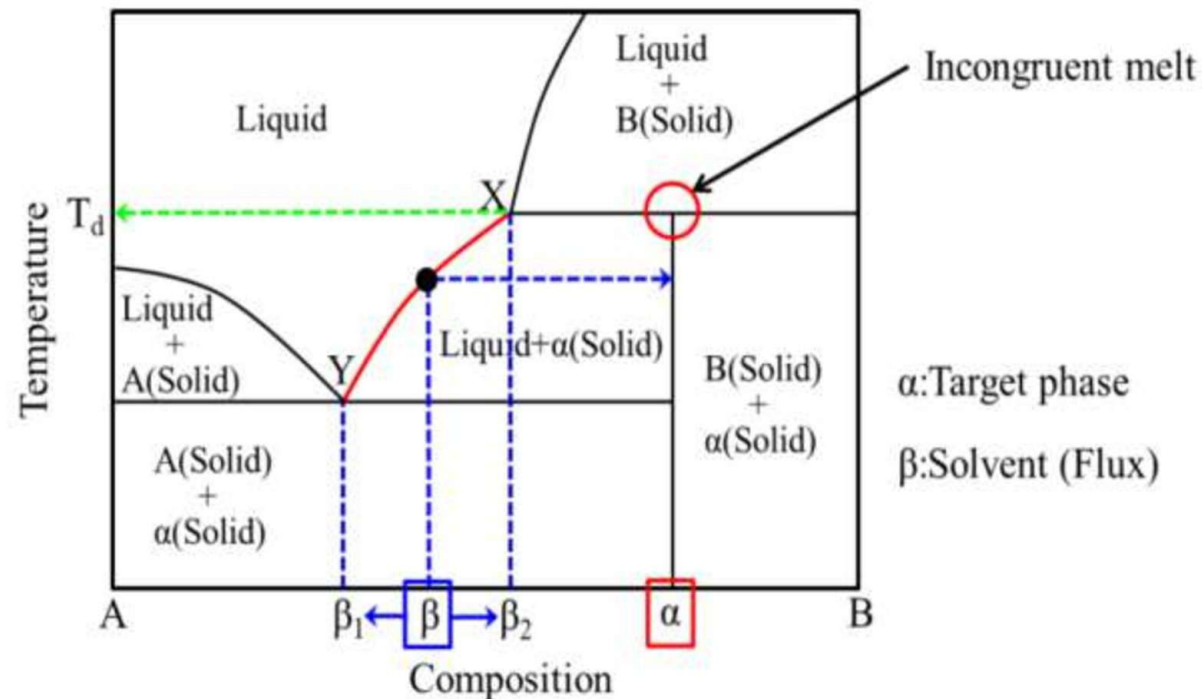
- (C) The case: $k > 1$ (Al in GaP , $k= 45$)
- (d) The case : $k = 1$ Liquid and solid have equal concentration. (Fe_3O_4 in Mn_3O_4) **Zone refining is impossible.** But, this case is most suitable for the growth of solid solution single crystal.



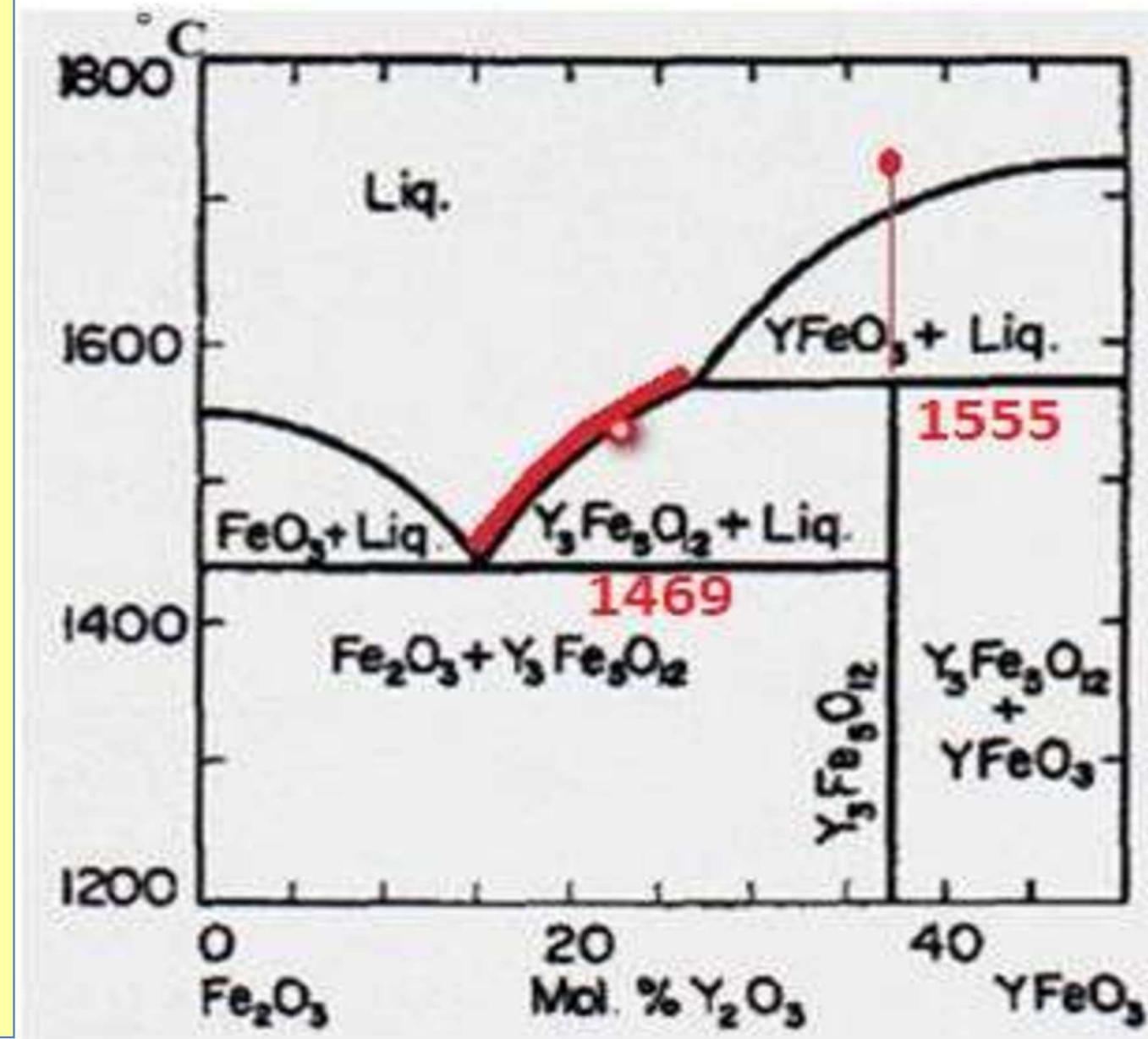
Growth from Non-Stoichiometric Melt:

Three cases arise in which it convenient to grow crystals from non-stoichiometric melts, where melt composition differ substantially in composition from crystal.

- The crystal melts in-congruently.
- The crystal has a solid-solid transition above the lowest liquidus temperature and low temperature form is required.
- One component has high vapor pressure at melting point of crystal.

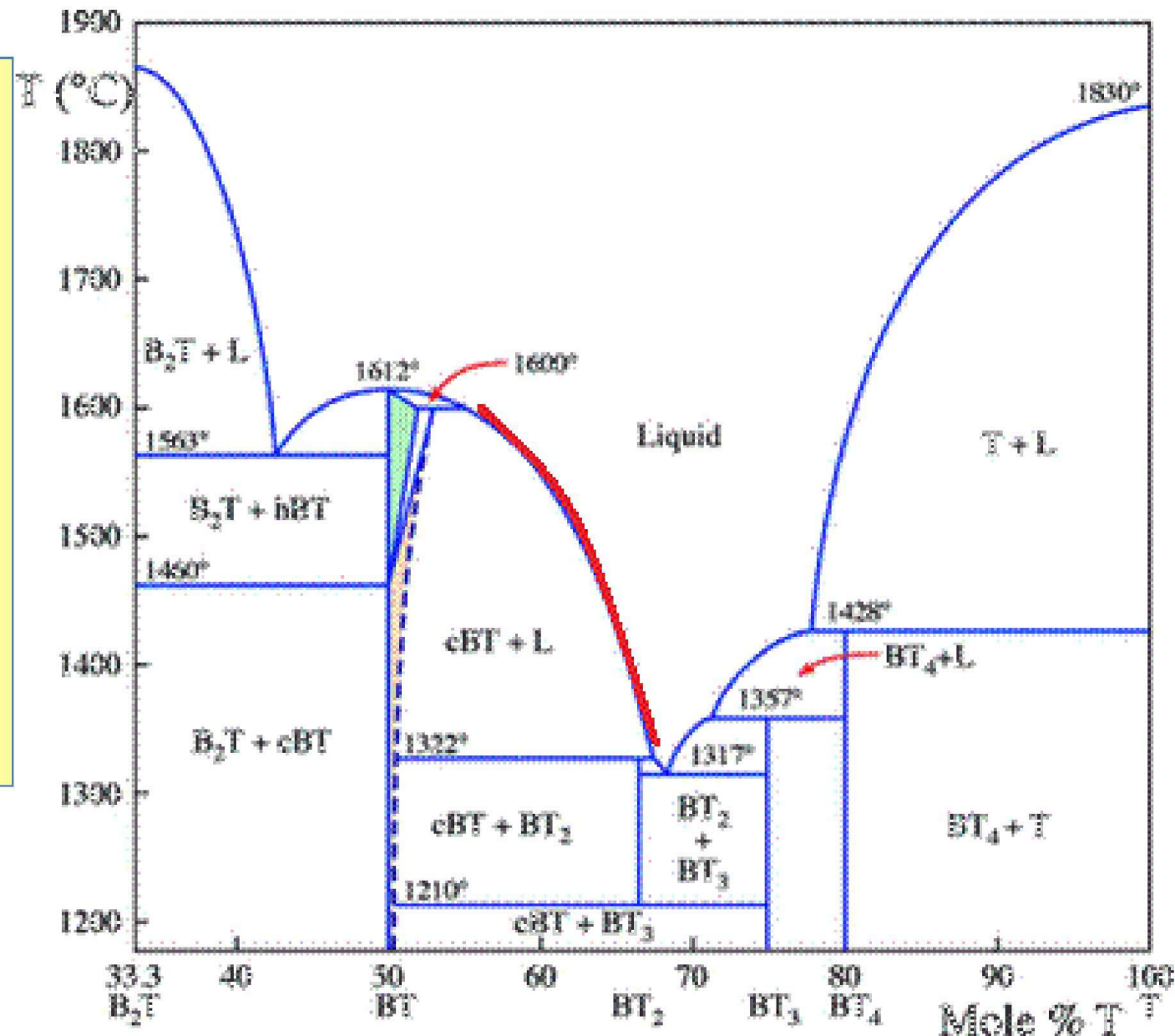


• $\text{Y}_3\text{Fe}_5\text{O}_{12}$
(YIG) Single
crystal: Optical
Isolator;
Magneto-Optic
Device, Phase
shifter,
Oscillator,
Circulator,
Single crystal
is grown from
melt with 14
to 23 mol %
 Y_2O_3 : **CZ, BS**

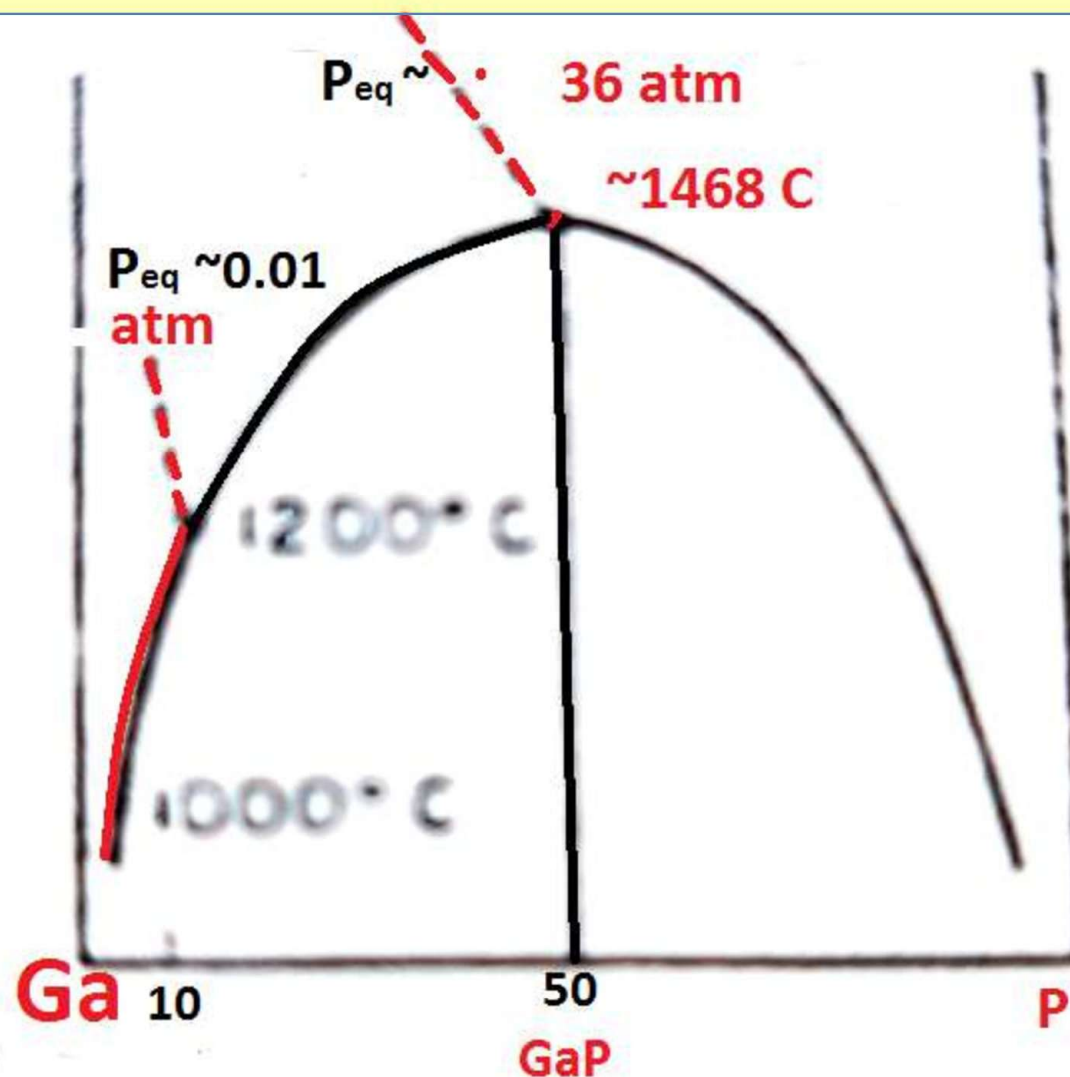


(2) Cubic BaTiO₃: Electro-optic application:

Cubic BT has been grown from melt having 14% excess TiO₂ and at a temperature near 1440 oC. Pulling rate is only 0.5 to 1 mm/h.



- Semiconductors, gallium phosphide (GaP) is an excellent candidate to be part of a high band gap solar cell. GaP crystal can be grown from gallium rich melts in the range shown as heavy liquidus red line.



$\bullet \text{Y}_3\text{Fe}_5\text{O}_{12}$ (YIG)

Single crystal:

Optical Isolator;

Magneto-Optic

Device, Phase
shifter, Oscillator,

Circulator, Single

crystal is grown from
melt with 14 to 23

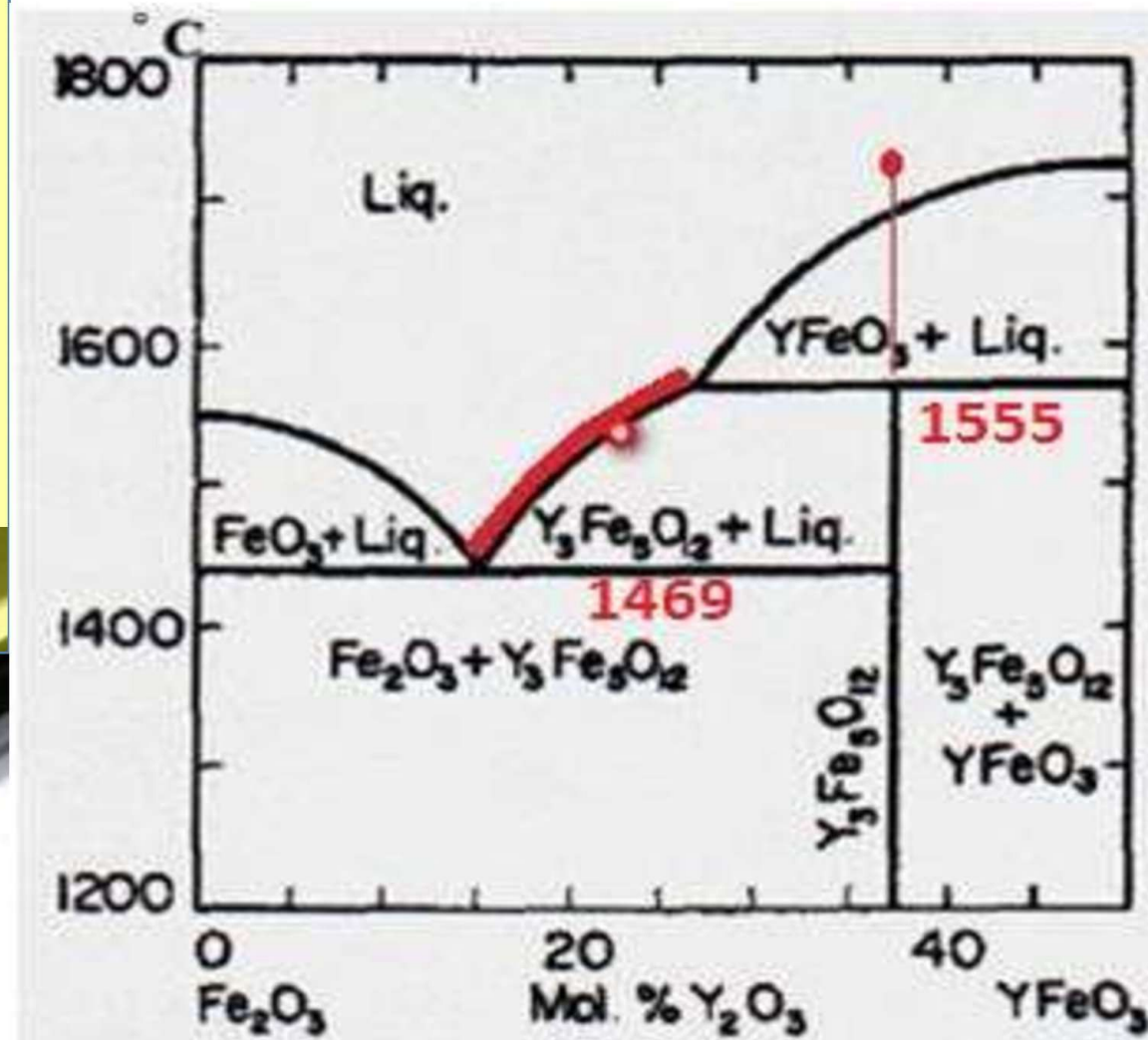
mol % Y_2O_3 : CZ, BS



YIG ($\text{Y}_3\text{Fe}_5\text{O}_{12}$)
Single Crystal

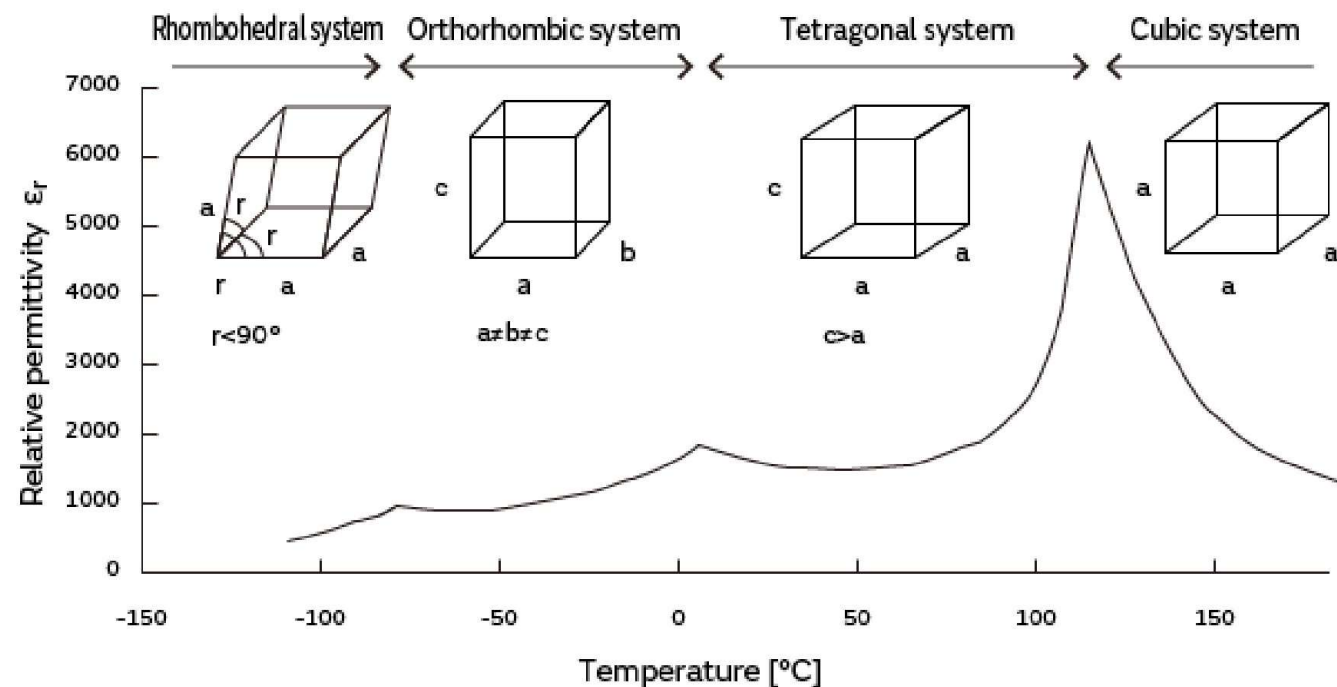
5 Dia. x 70 L, mm

- The crystal melts in-congruently.



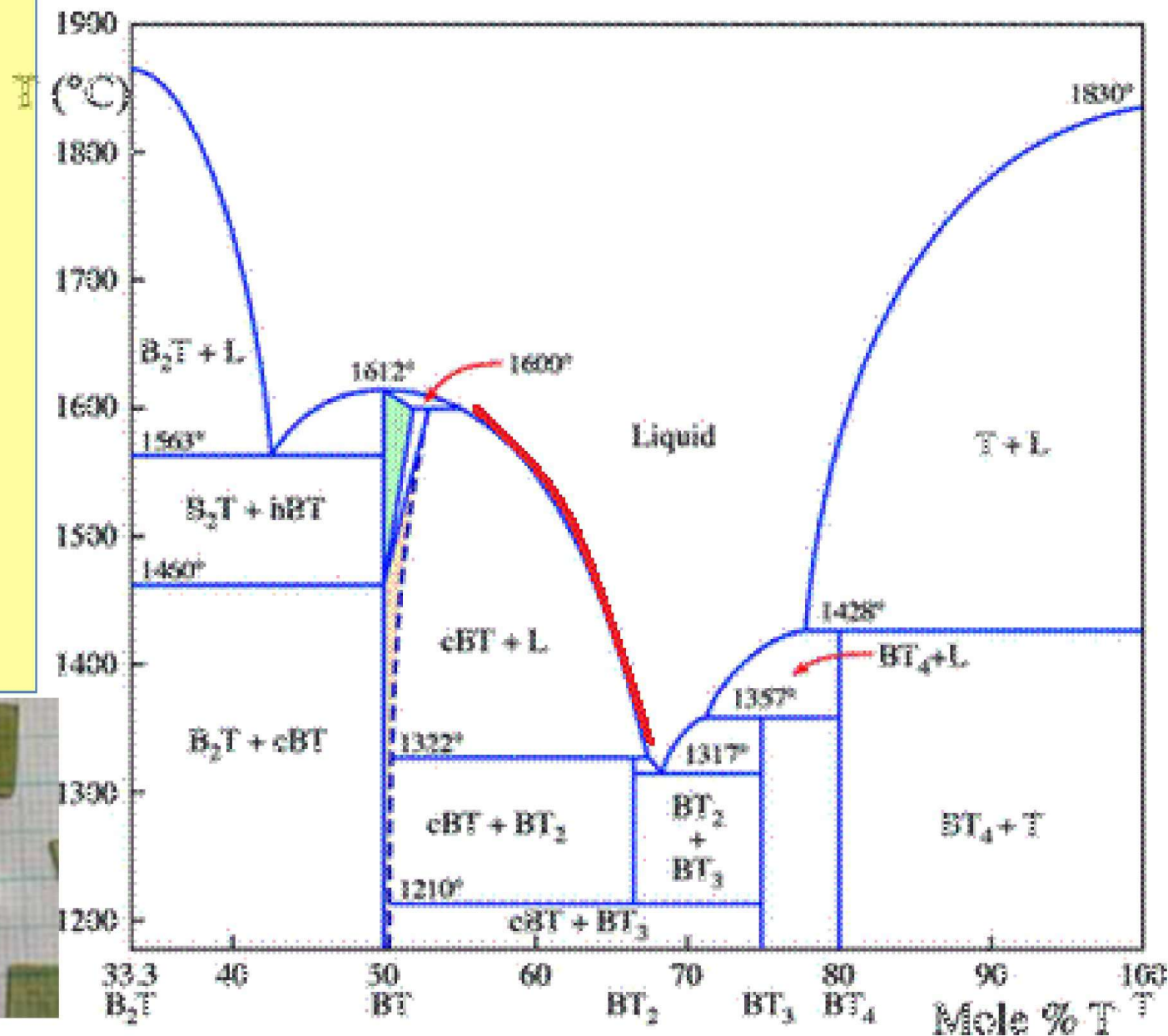
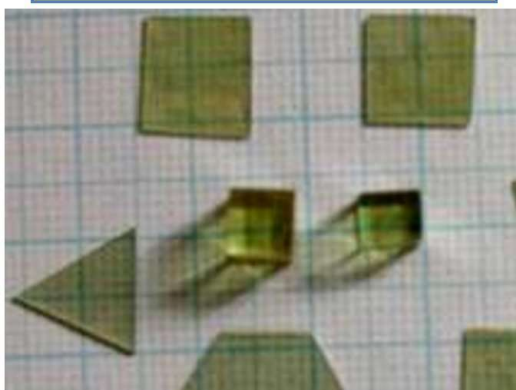
Growth from Non-Stoichiometric Melt:

- The crystal has a solid-solid transition above the lowest liquidus temperature and low temperature form (**Cubic BaTiO₃**) is required.
- One component has high vapor pressure at melting point of crystal.

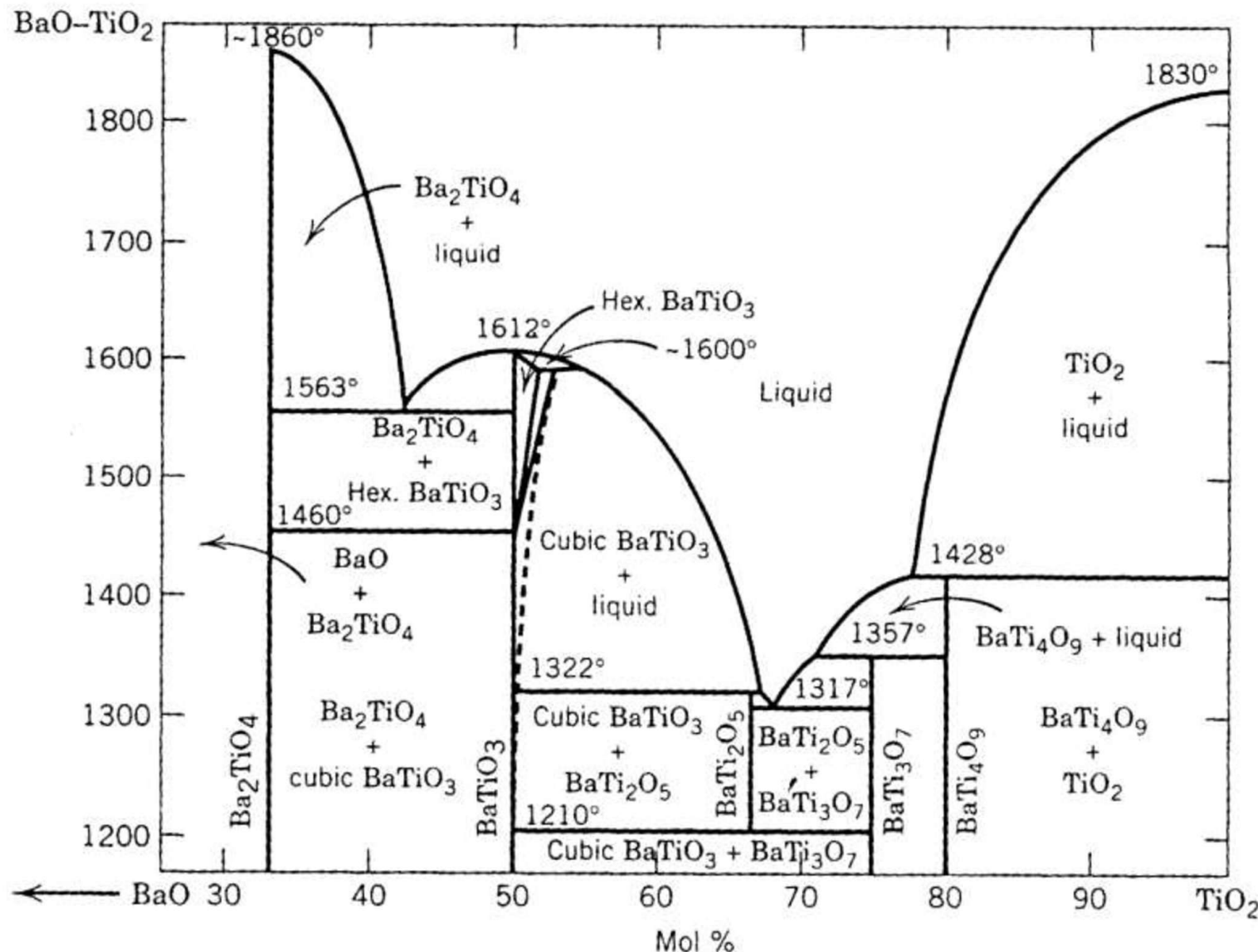


(2) Cubic BaTiO₃: Electro-optic information storage app

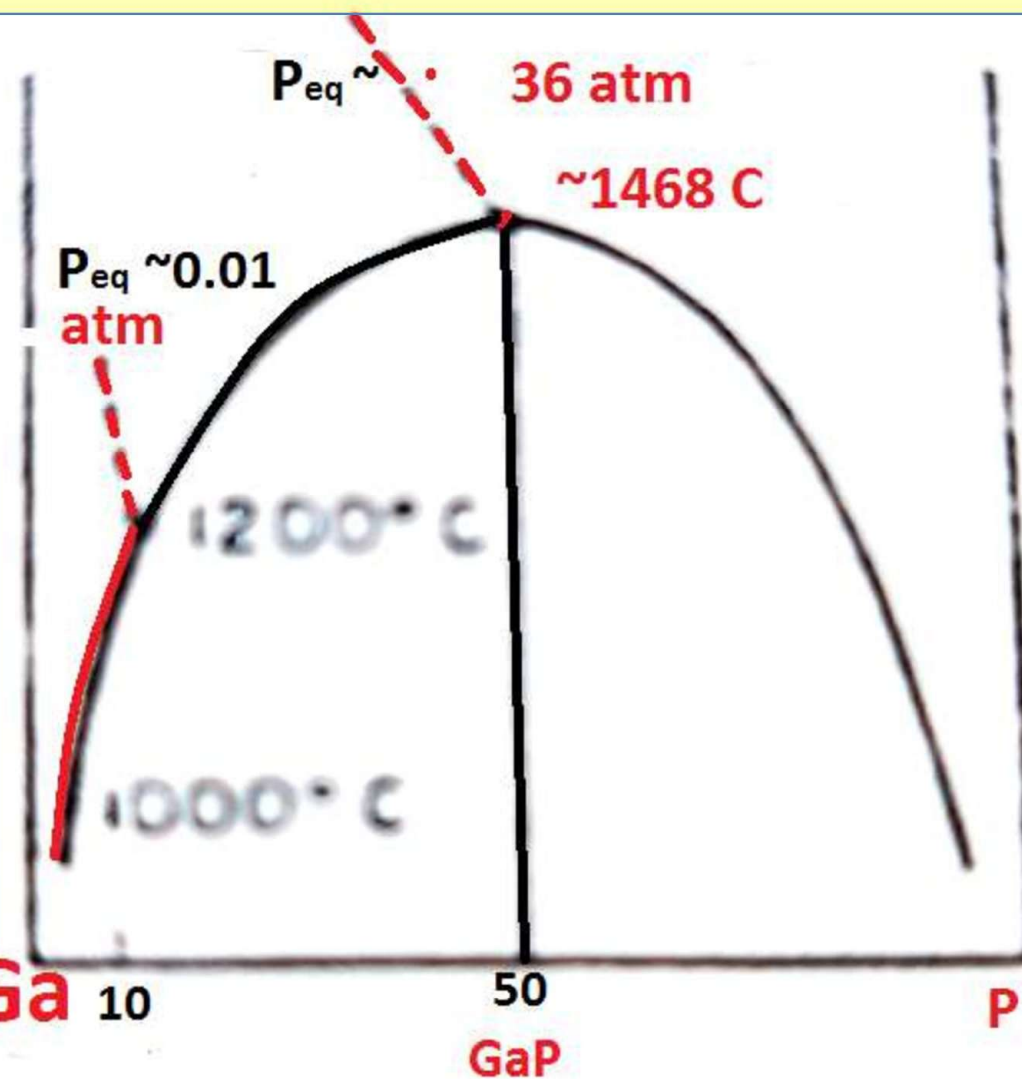
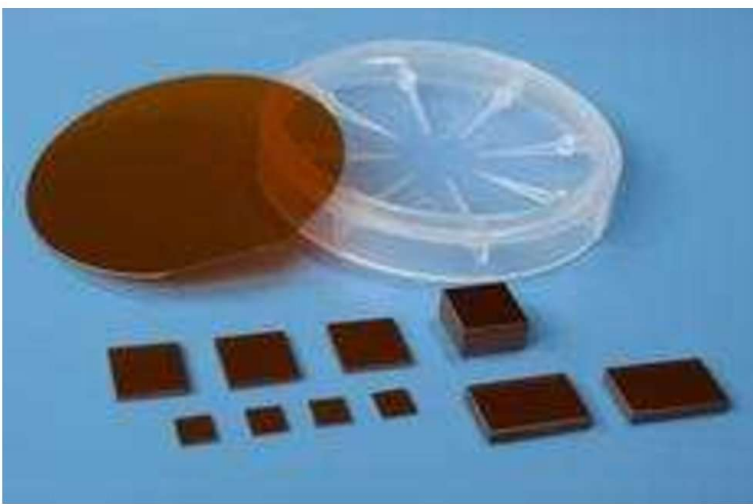
Cubic BT has been grown from melt having 14% excess TiO₂ and at a temperature near 1440 °C. Pulling rate is only 0.5 to 1 mm/h.



BaTi4O9: Microwave Dielectrics: $\epsilon_r \sim 37$, $Q \times f \sim 22,700$ GHz

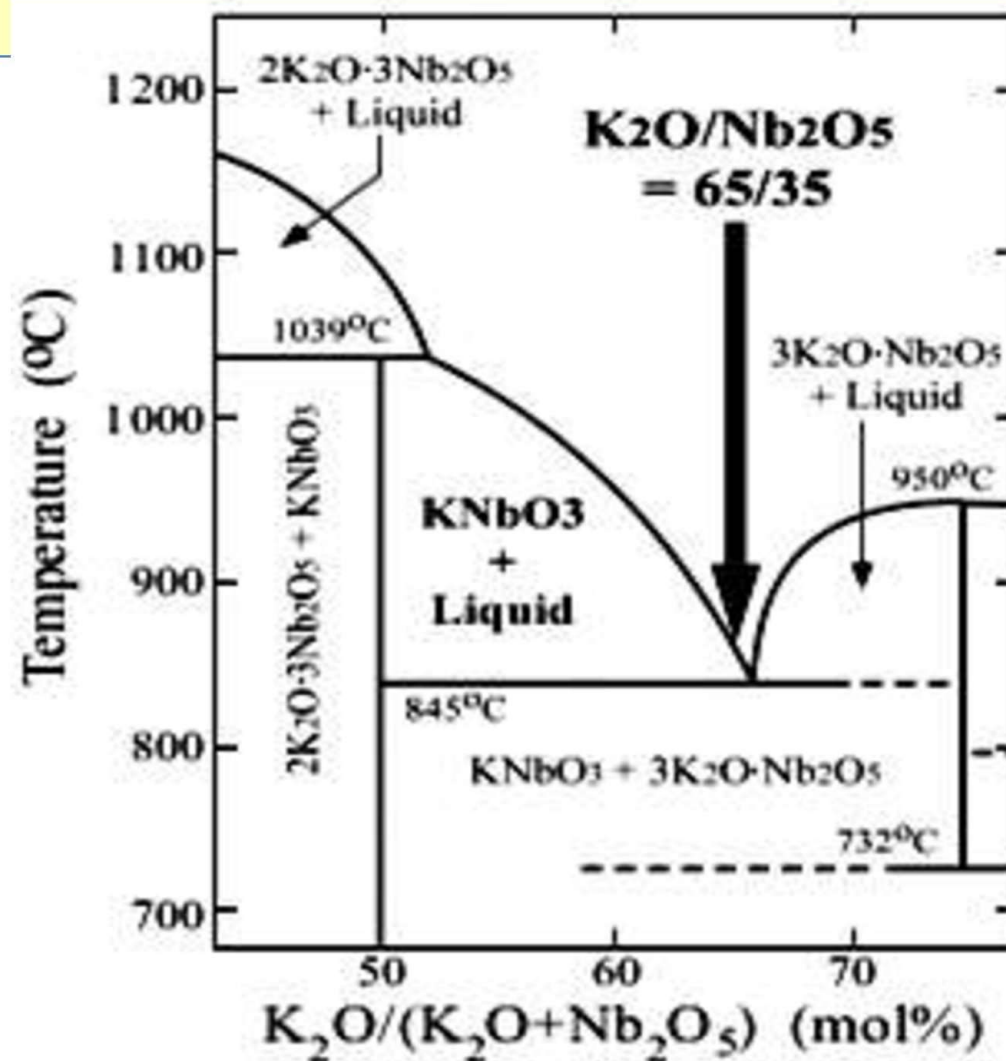


- Semiconductors, gallium phosphide (GaP) is an excellent candidate to be part of a high band gap solar cell. GaP crystal can be grown from gallium rich melts in the range shown as heavy liquidus red line.

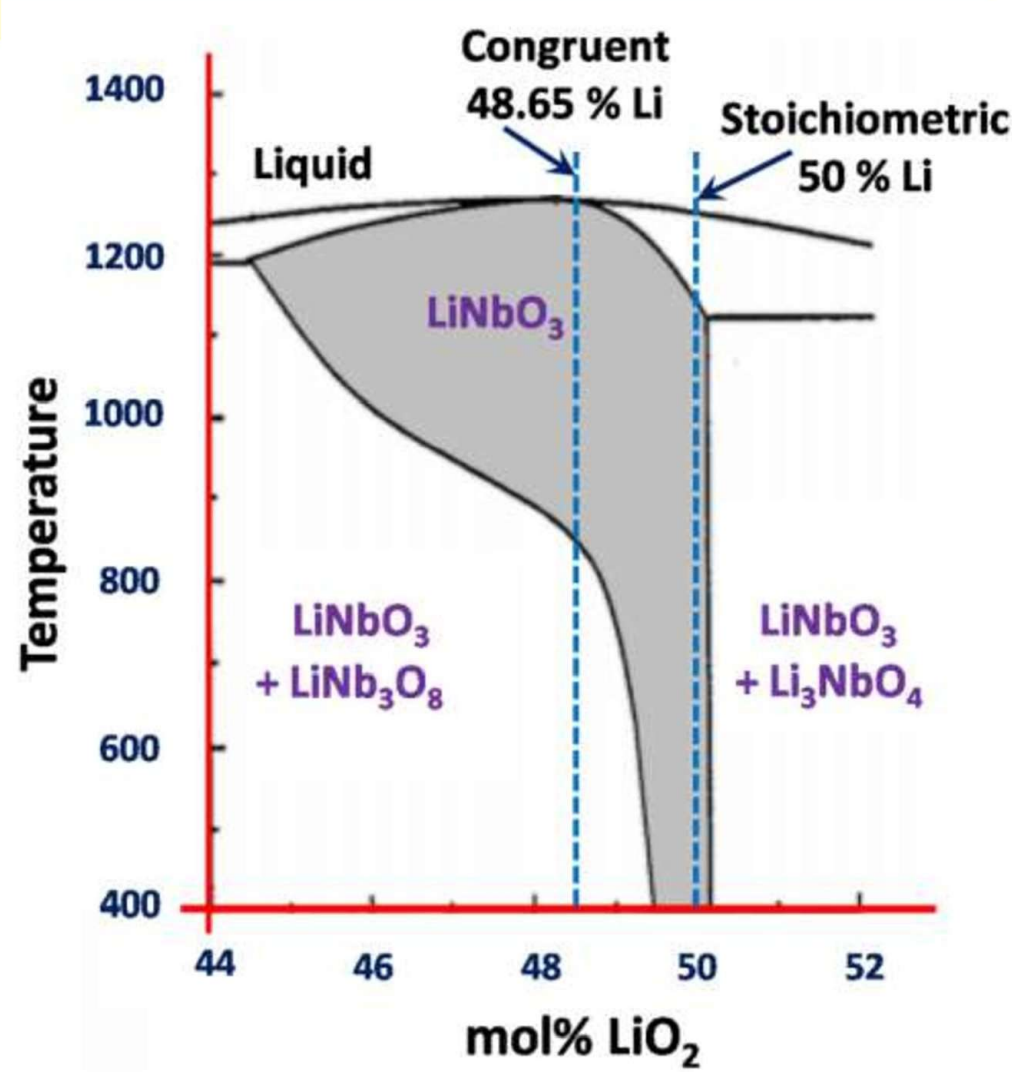


Potassium niobate (**KNbO₃**) single crystal belonging to the perovskite-type ferroelectric of barium titanate family. Due to its excellent electro-optical, nonlinear optical, and photo-refractive properties, it has been widely studied for applications in nonlinear optics and electro-optics devices

KNbO₃ Melts incongruently; Peritectic points differ slightly; **Stoichiometric melt is not possible for Single crystal growth.** Crystals are grown either solution or Flux growth techniques: (Flux grown: grown from foreign liquid solvent in order to lower the temp of growth, (Halides, Borate, Vanadates)



More than 70% of today's radiofrequency filters are based on **LiNbO₃**. Melts Congruently, However single phase SS exists over a range of composition. Con. M. point is not exactly at stoichiometric composition; at Nb-rich; High quality Single Crystal is drawn from Congruent Composition.



Iron-Carbon Alloy Steel: Major Industrial Product: Meta-stable Product

Fe-Fe₃C is characterized by five individual phases: **α -ferrite (BCC) Fe-C SS**, **γ -austenite (FCC) Fe-C SS**, **δ -ferrite (BCC) Fe-C SS**, **Fe₃C (iron carbide) or cementite**. and four invariant reactions namely: eutectoid, eutectic, monotectic and peritectic

- Carbon present in solid iron as interstitial impurity,
- in **α -ferrite** Stable upto 911; carbon soluble is 0.02% at 723: limited solubility is attributed to shape and size of interstitial position in BCC **α -ferrite**; $a=2.866$.: magnetic material below 768

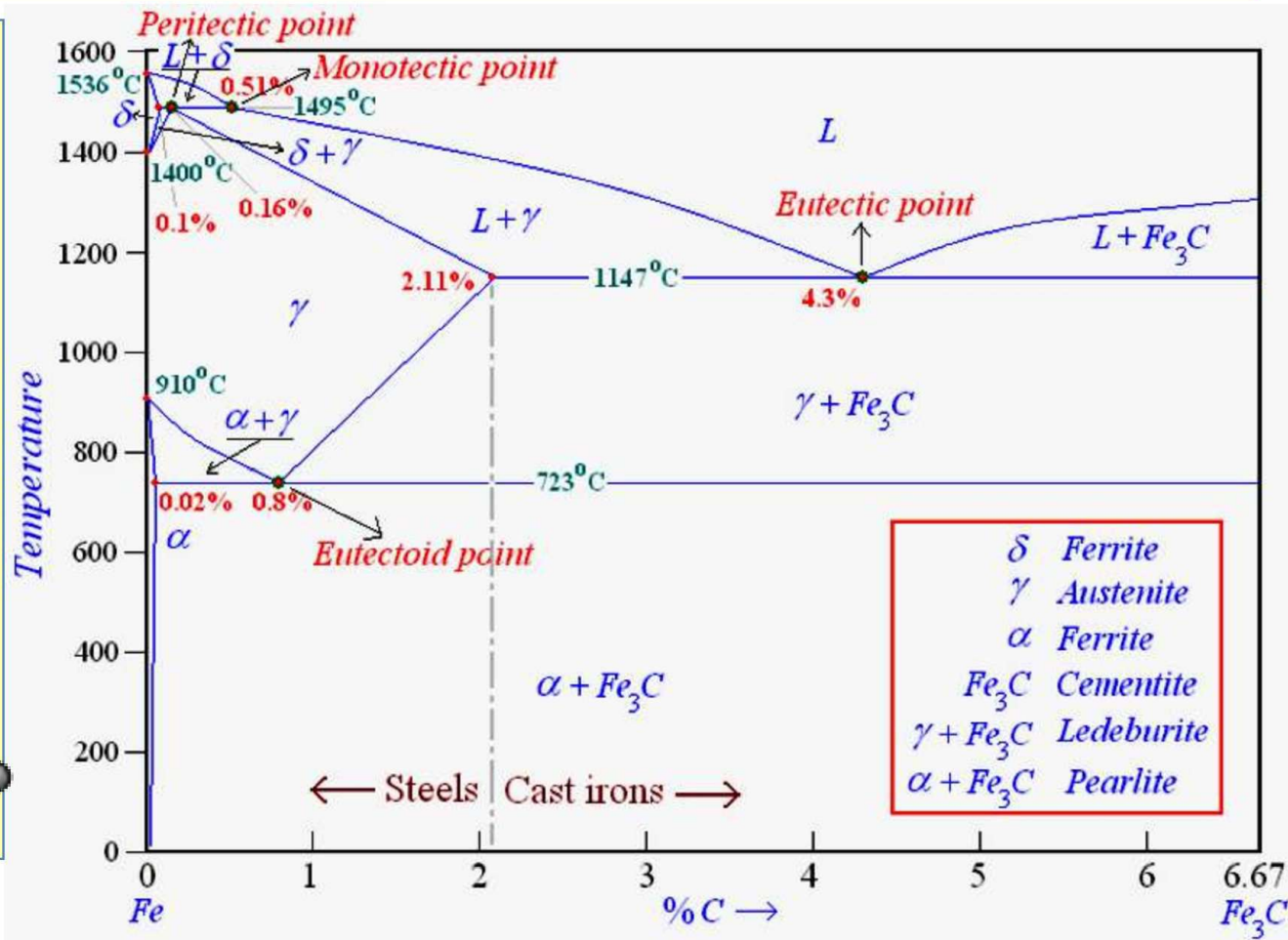
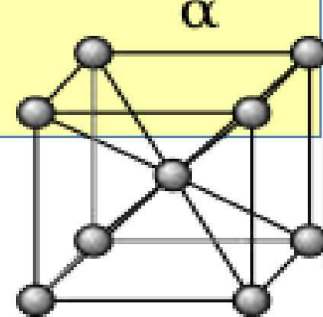
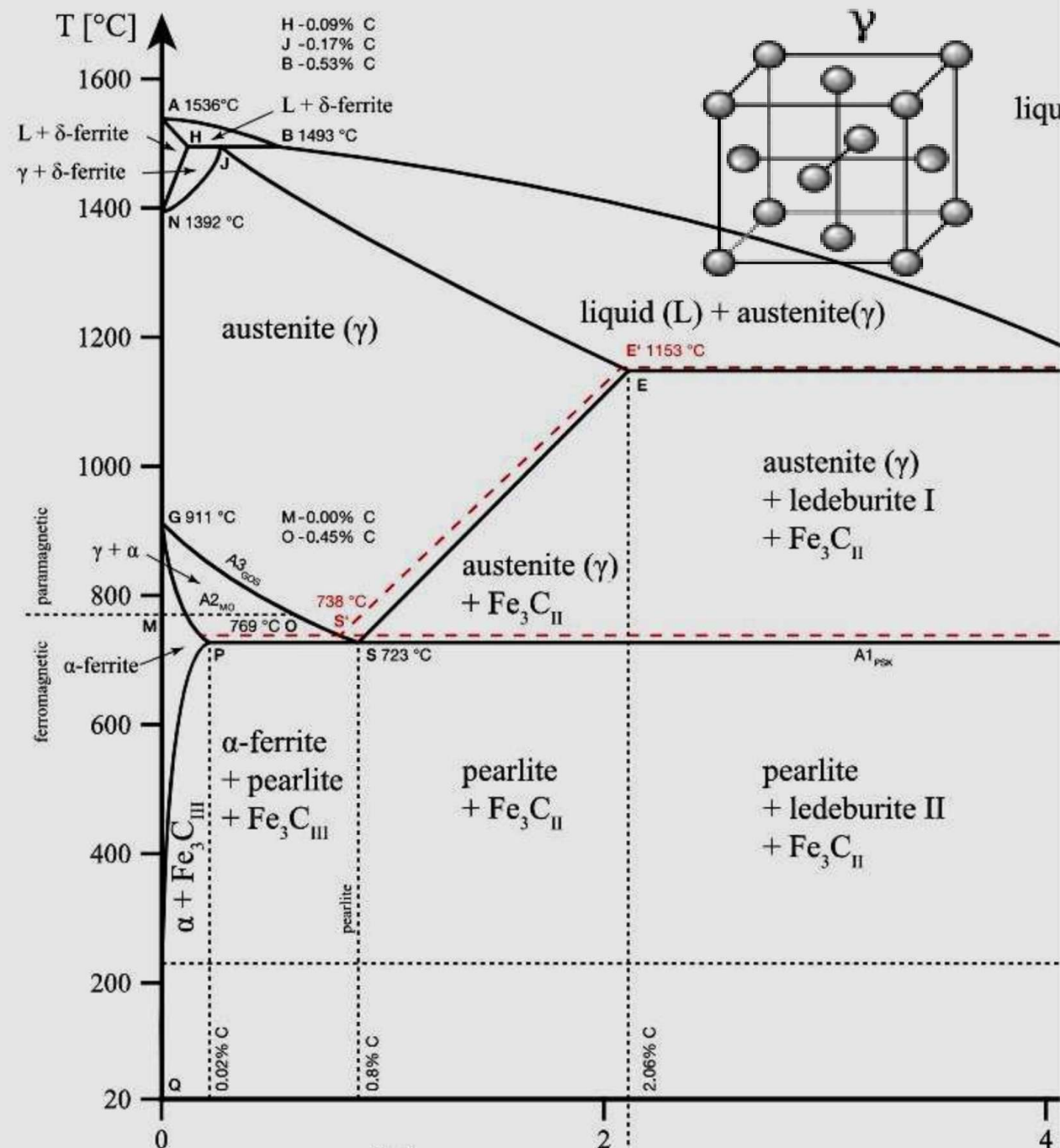


Figure-16: Iron – Iron carbide phase diagram.

- **γ -austenite:** (non-magnetic) FCC: 911 to 1392; Max Solubility: 2.06% @ 1147 C.; Higher solubility: FCC structure ($a=3.592$) interstitial sites; Phase transformation plays very significant role in heat treatment of different steels.

δ -ferrite: BCC

- 1392 to 1536 C
- Max Solubility: 0.09% @ 1493 C.
- **Fe₃C or cementite:** intermetallic compound
- Metastable at ordinary T : thousands of years; hardest and brittle among four; **α -ferrite, on the other hand, is softest;** act as matrix



commercial pure irons (α -ferrite) : C less than 0.008%; steels having %C between 0.008-2.11; while cast irons have carbon in the range of 2.11%-6.67%.

- **Peritectic reaction** at 1495 °C; 0.16% C,
 δ -ferrite + L \leftrightarrow γ -iron (austenite)
- **Monotectic reaction**: 1495 ; 0.51% C,
 $L \leftrightarrow L + \gamma$ -iron (austenite)
- **Eutectic reaction**: 1147 °C ; 4.3 %C,
 $L \leftrightarrow \gamma$ -iron + Fe₃C (cementite)
[ledeburite]
- **Eutectoid reaction** : 723 °C ; 0.8%C,
 γ -iron \leftrightarrow α -ferrite + Fe₃C (cementite)
[pearlite]
- ledeburite transforms into pearlite and cementite.
- mild steels up to 0.3%C, medium carbon steels with C between 0.3%-0.8% i.e. hypo-eutectoid Fe-C alloys)
- steels with carbon higher than 0.8% (high-carbon steels i.e. hyper-eutectoid Fe-C alloys) consists of pearlite and pro-eutectoid cementite.

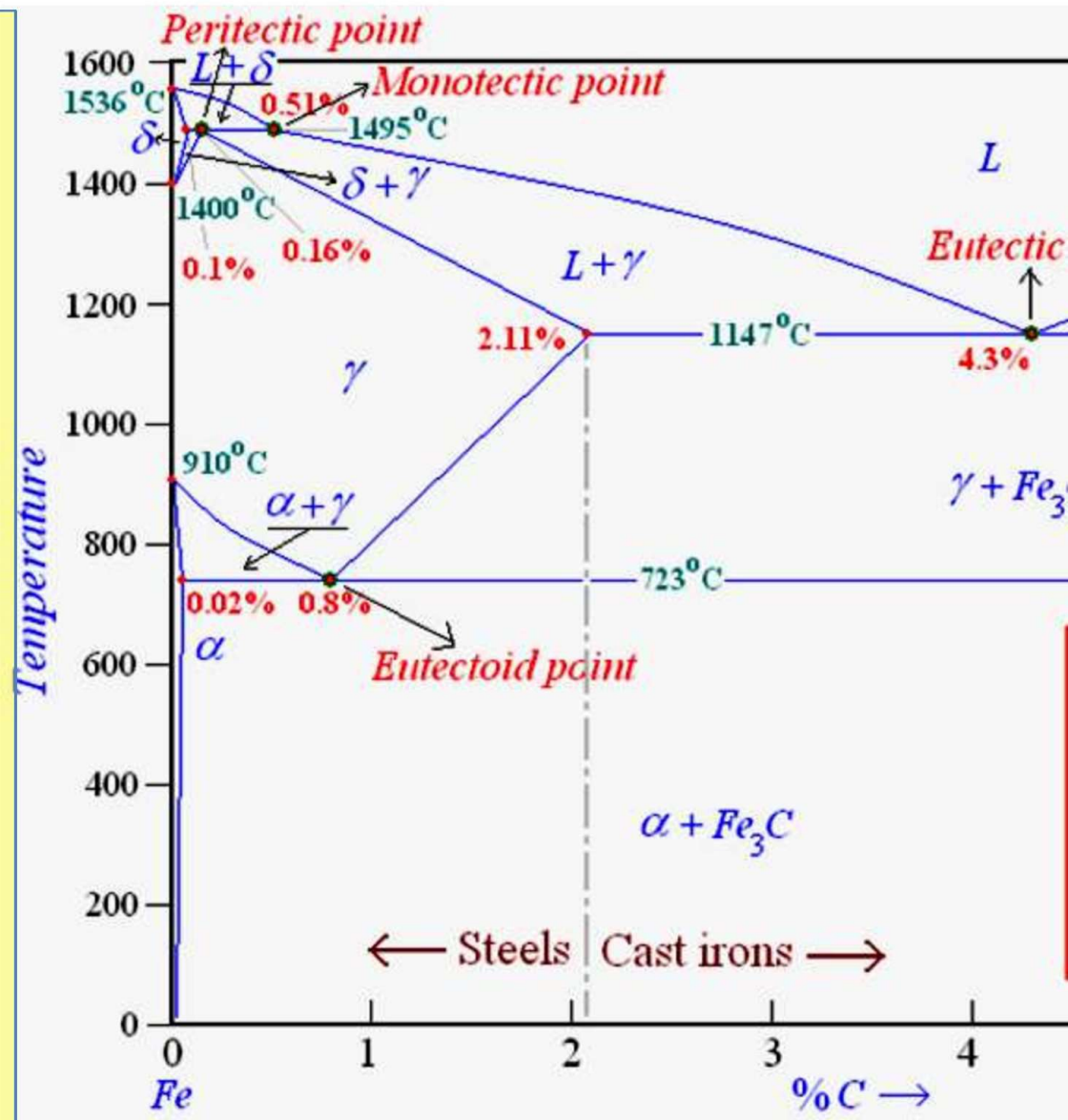
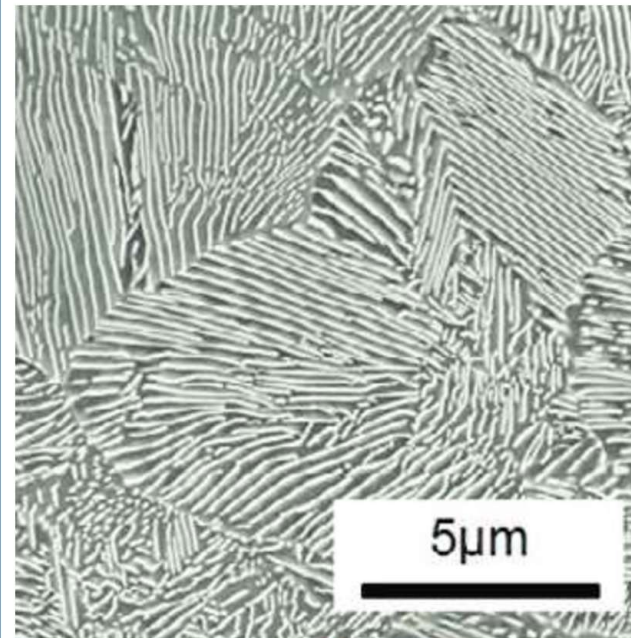


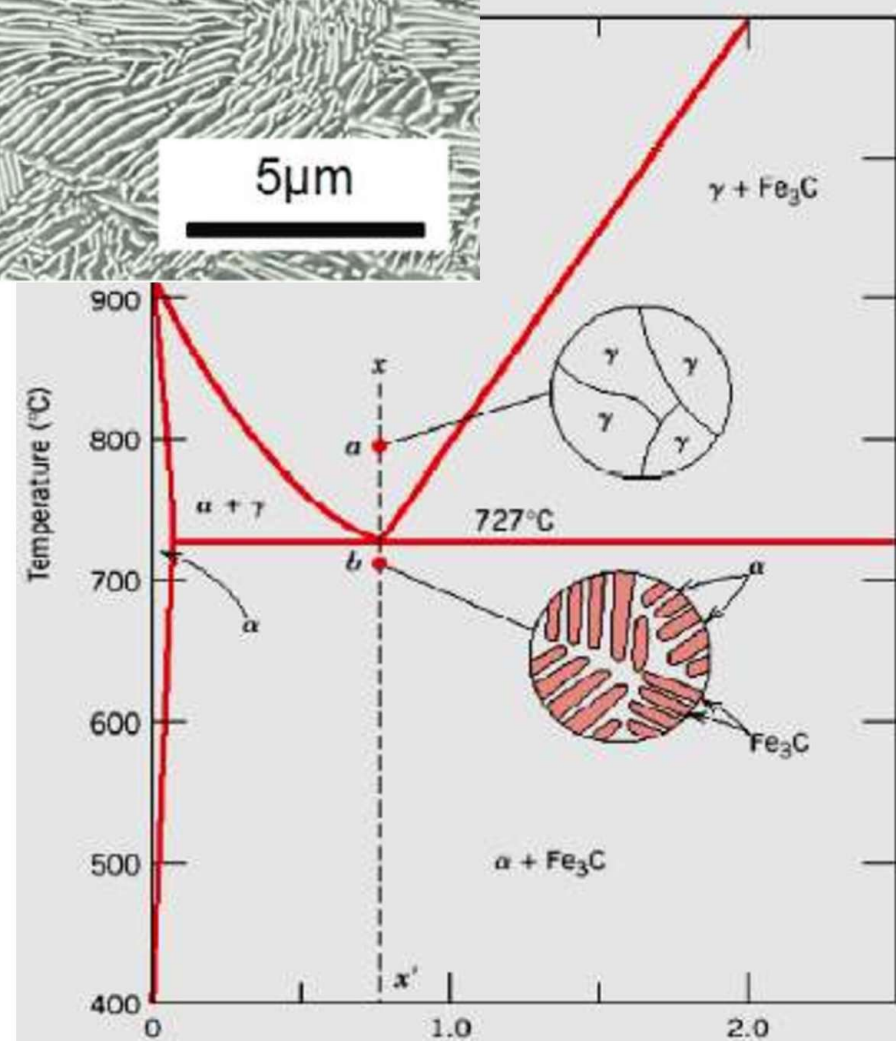
Figure-16: Iron – Iron carbide phase diagram

•Eutectoid Structure:

- alternate thin layers of **α -ferrite (~88%) and Fe₃C, cementite (~12%). Called Pearlite**
- great importance in heat treatment of steels.
- almost always cooled from the austenitic region to room temperature.
- first pro-eutectoid phase (either **α -ferrite or cementite) forms up to eutectoid temperature.**
- With further cooling below the eutectoid temperature, remaining austenite decomposes to eutectoid product called pearlite, mixture of thin layers of **α -ferrite and cementite**.



eutectoid steel (I)

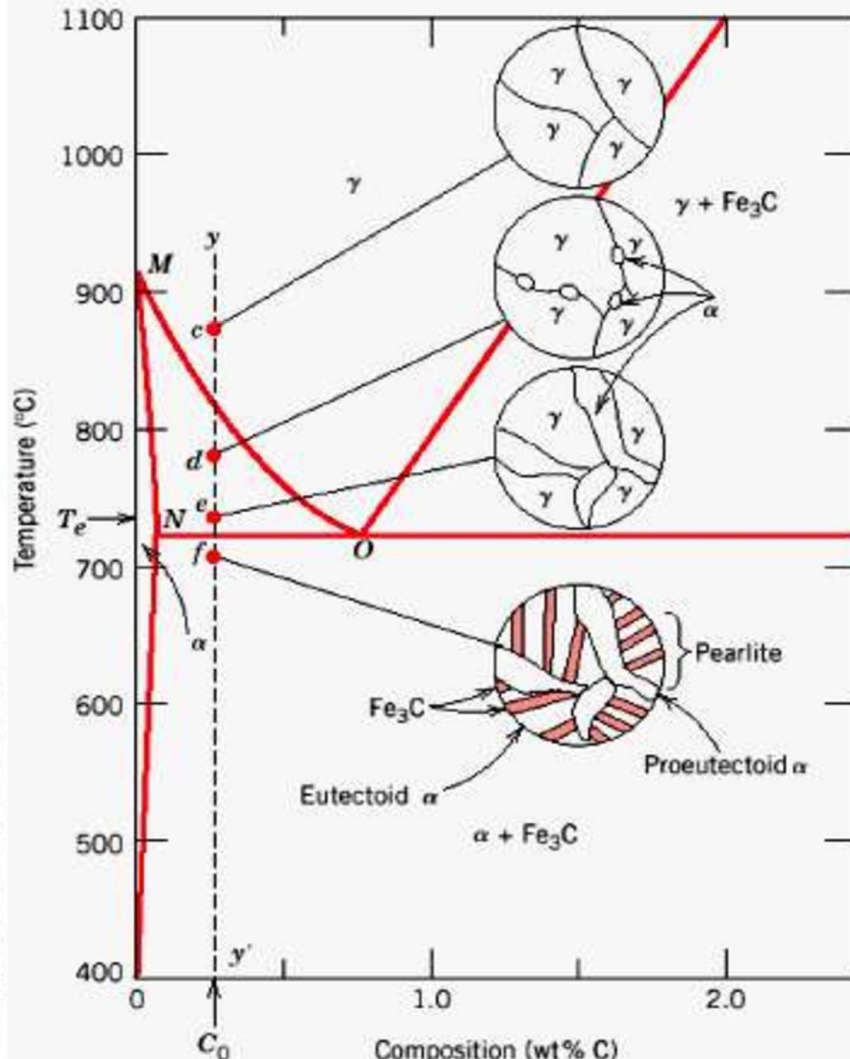
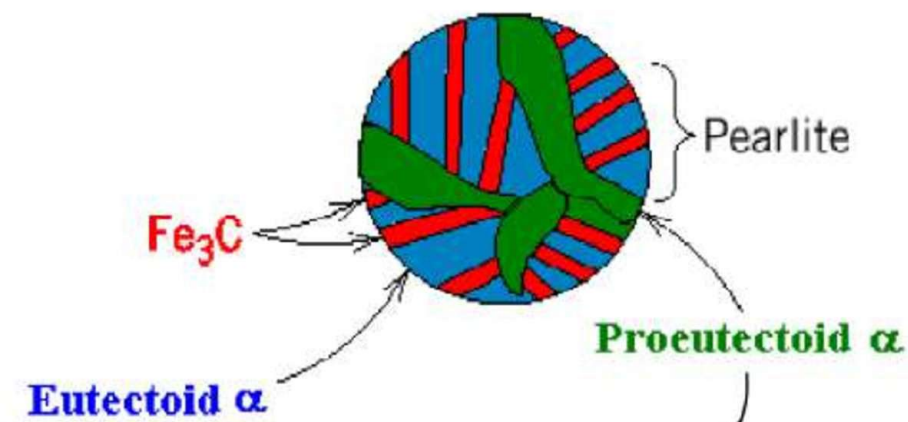


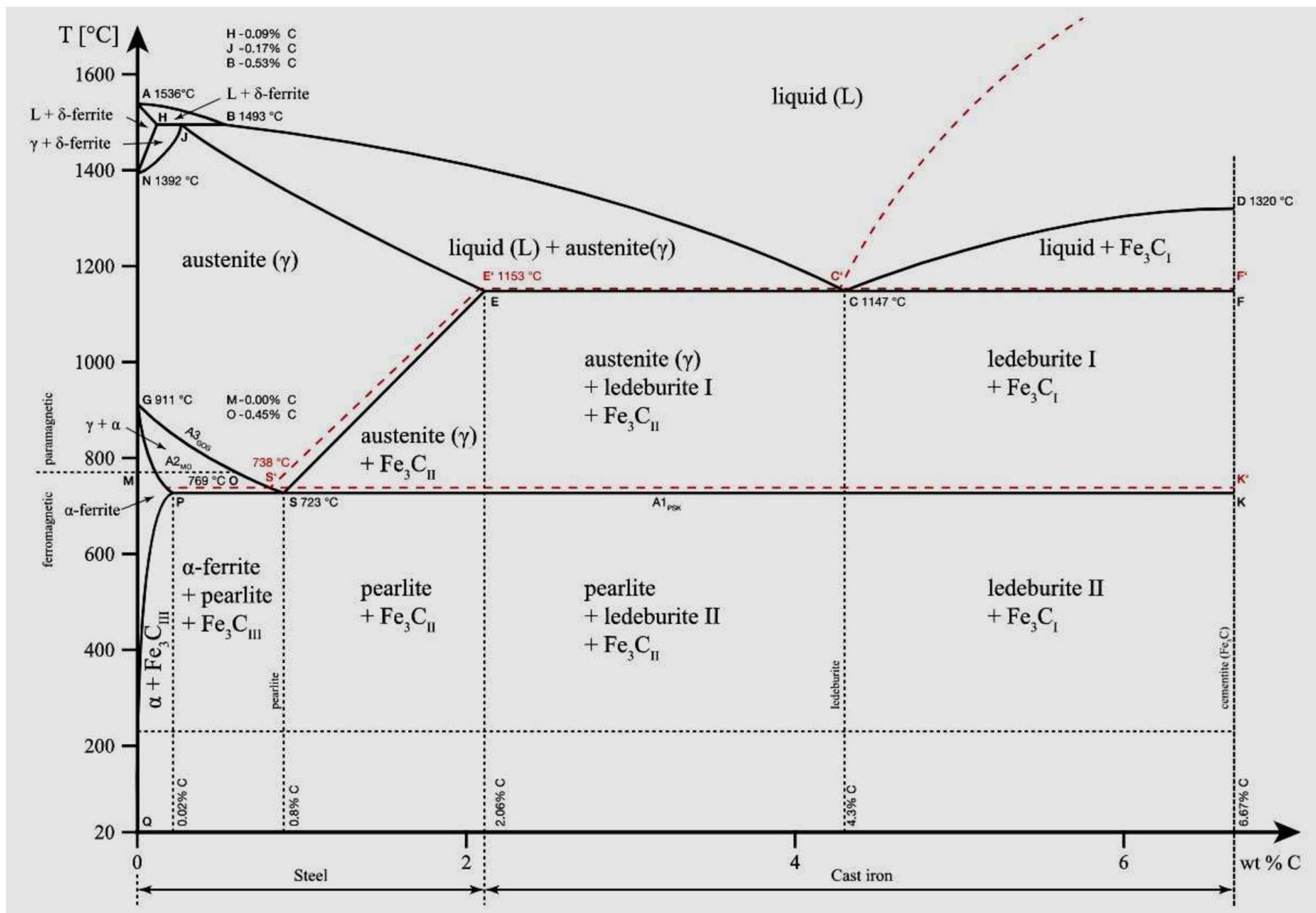
Microstructure of hypoeutectoid steel (I)

Compositions to the left of eutectoid (0.022 - 0.76 wt % C) **hypoeutectoid** (*less than eutectoid* -Greek) alloys.

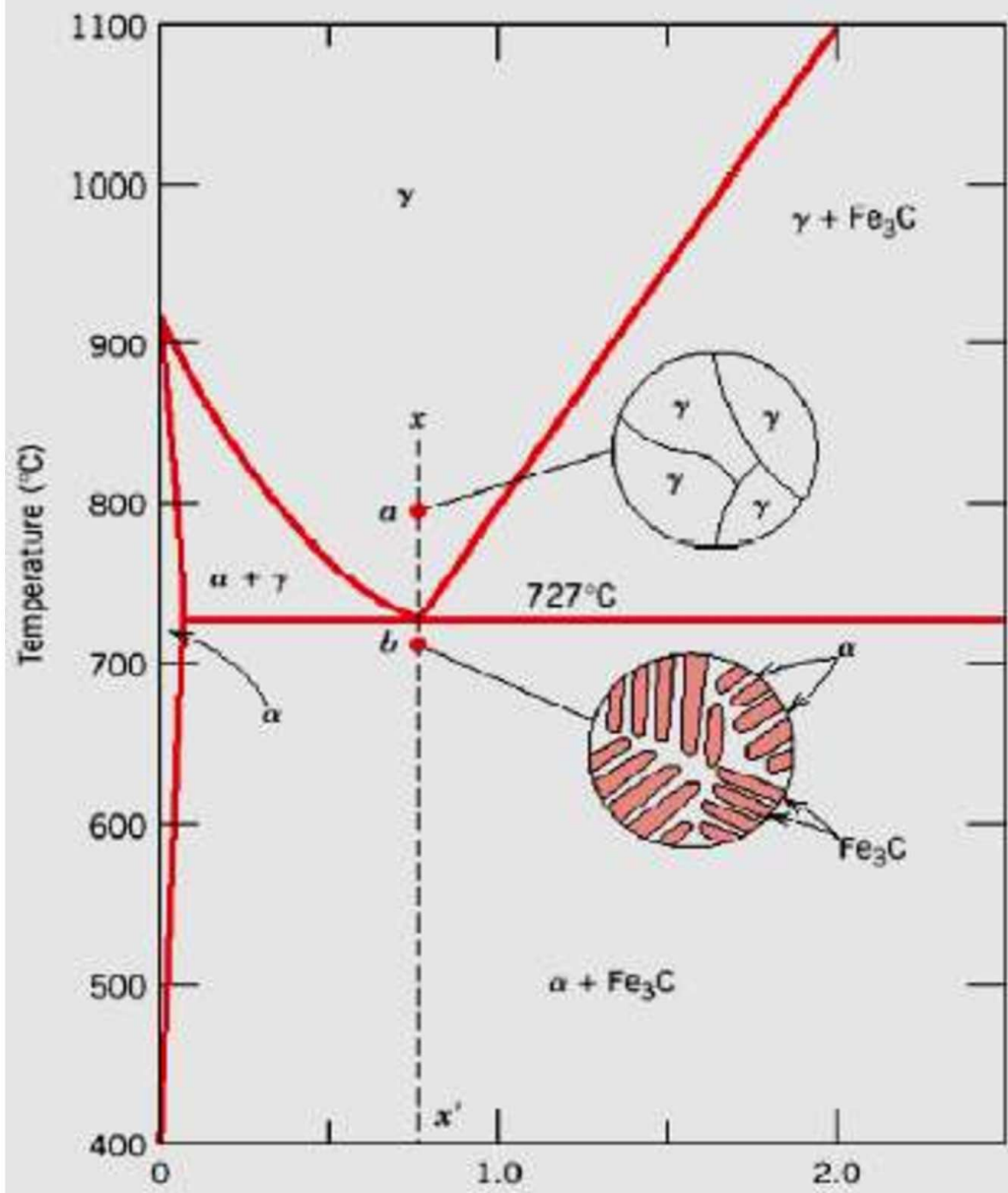


Hypoeutectoid alloys contain proeutectoid ferrite (formed above the eutectoid temperature) plus the eutectoid perlite that contain eutectoid ferrite and cementite.





Microstructure of eutectoid steel (I)

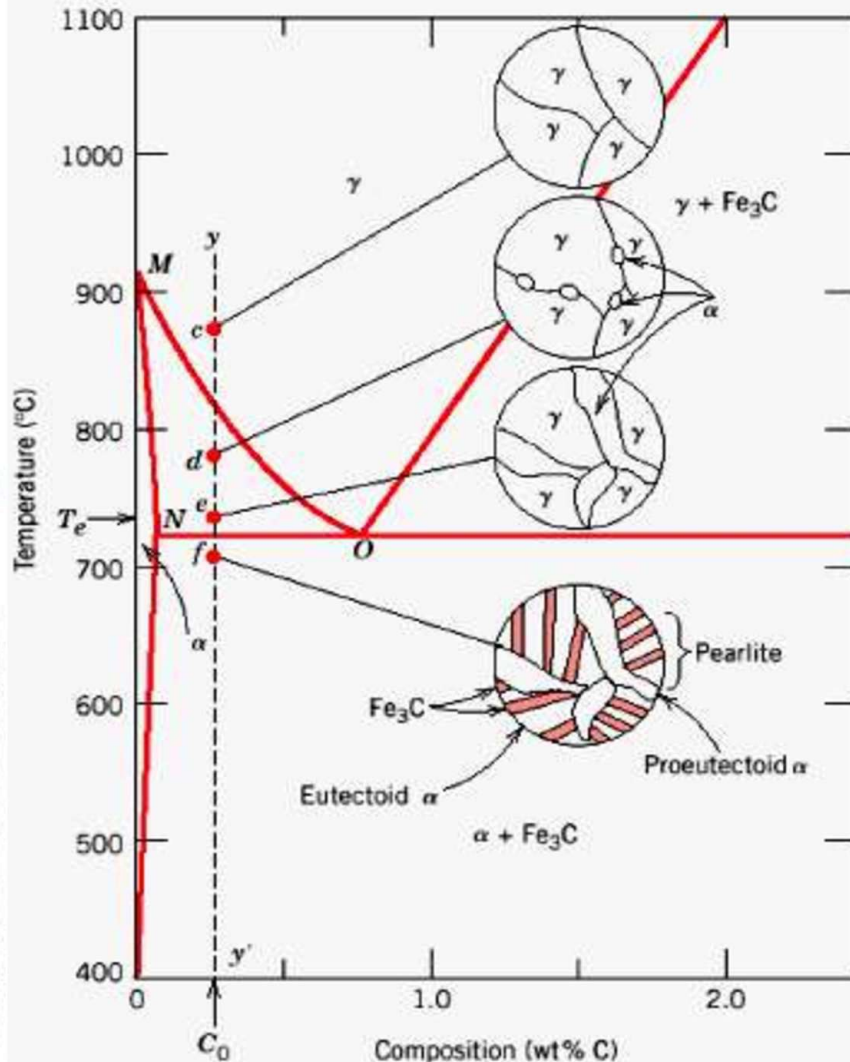
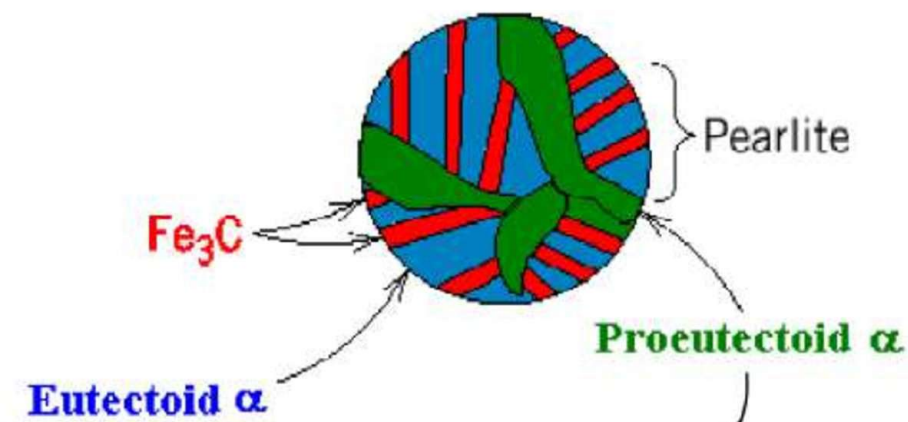


Microstructure of hypoeutectoid steel (I)

Compositions to the left of eutectoid (0.022 - 0.76 wt % C) **hypoeutectoid** (*less than eutectoid* -Greek) alloys.

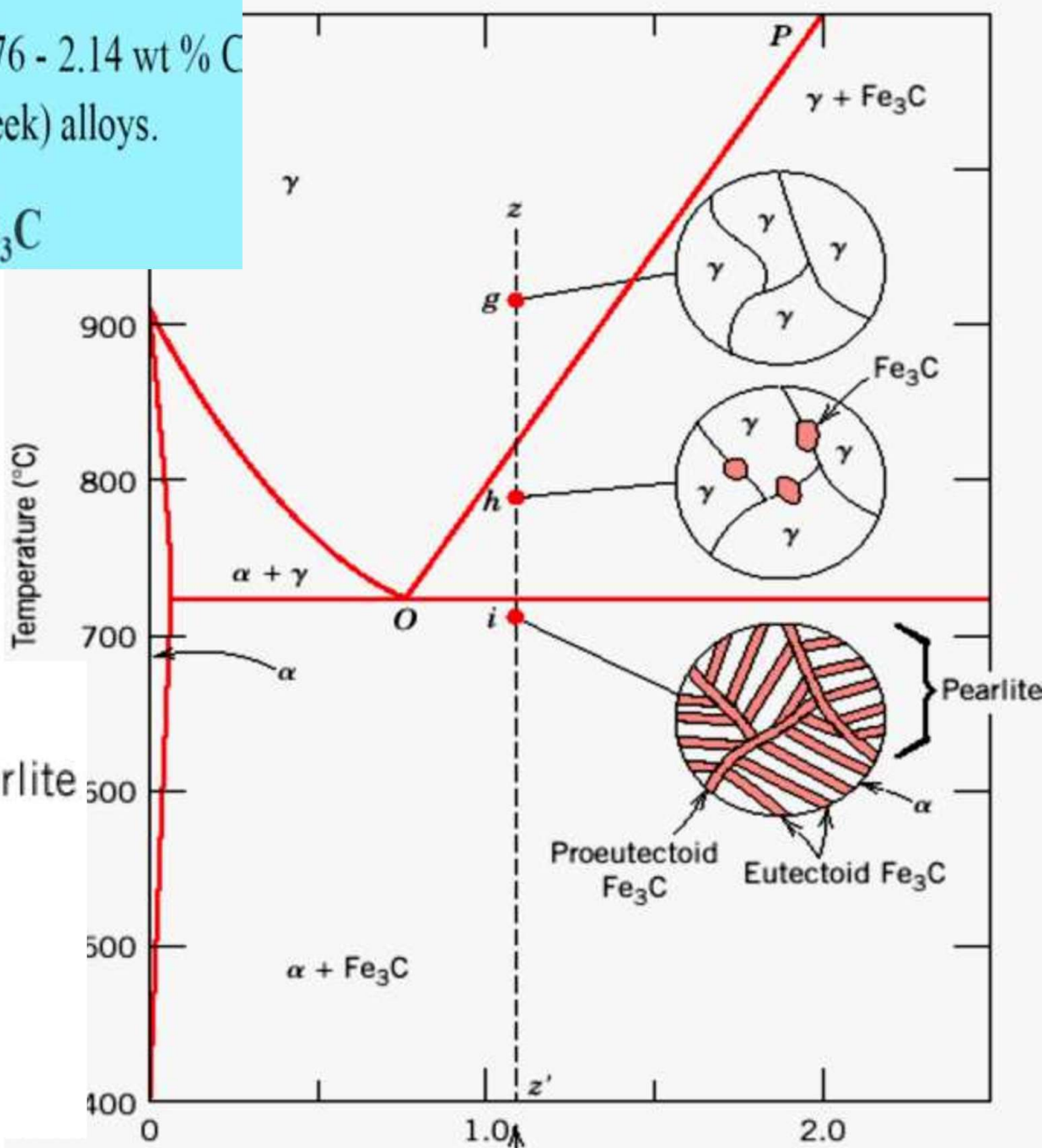
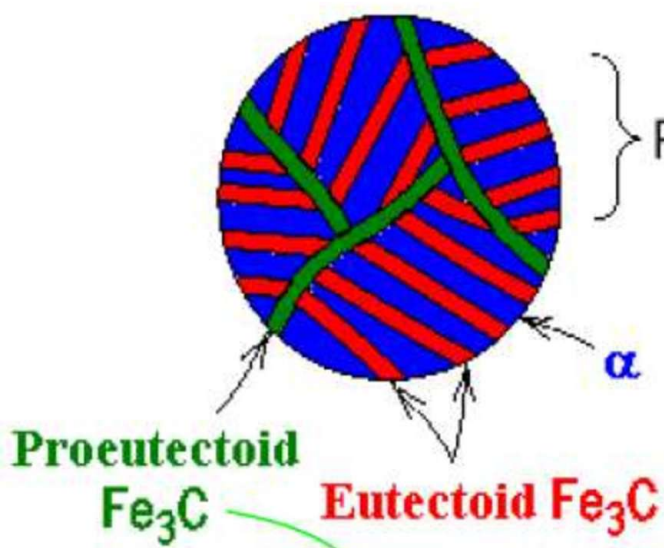
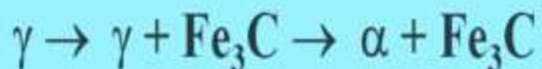


Hypoeutectoid alloys contain proeutectoid ferrite (formed above the eutectoid temperature) plus the eutectoid perlite that contain eutectoid ferrite and cementite.



Microstructure of hypereutectoid steel (I)

Compositions to the right of eutectoid (0.76 - 2.14 wt % C) hypereutectoid (*more than eutectoid* -Greek) alloys.

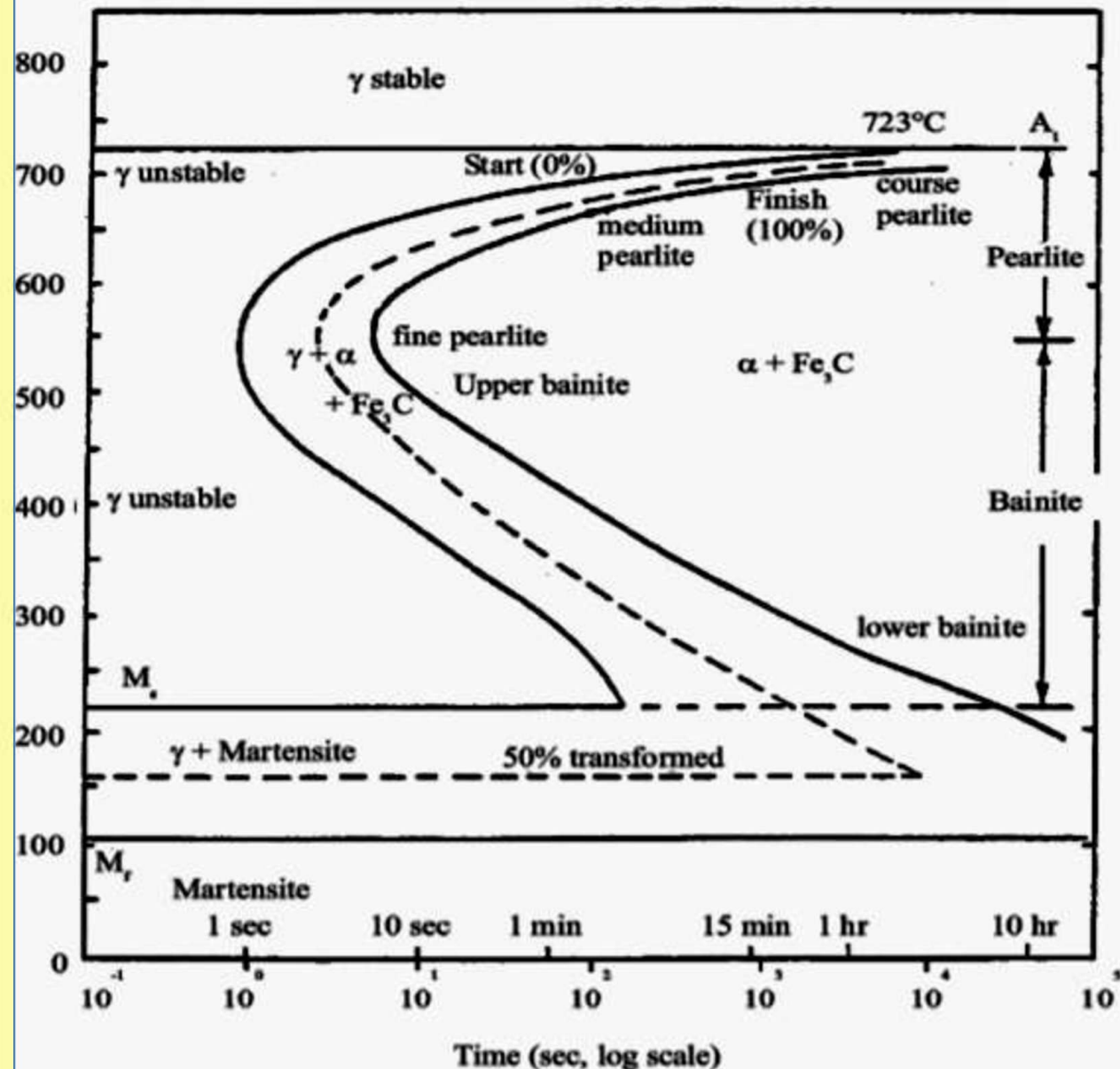


- Time-Temperature-Transformation

Diagram: Pearlite: above 550 C.

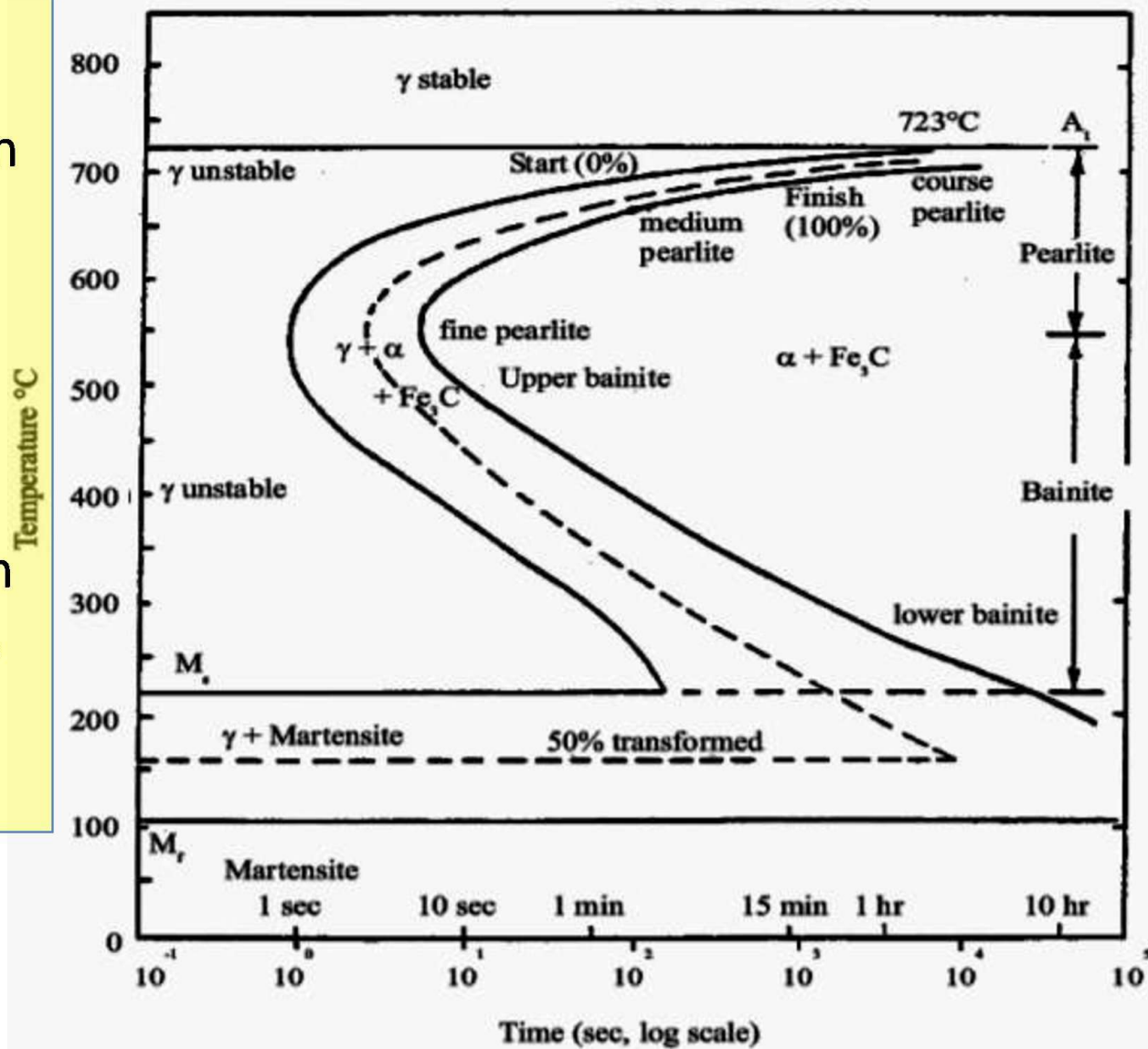
- Between 220-500: Bainite: Cementite+ Ferrite grow as extremely fine needle: So Ferrite phase is under highly strained:
- Strain due to excess C trapped in ferrite.;

Isothermal treatment

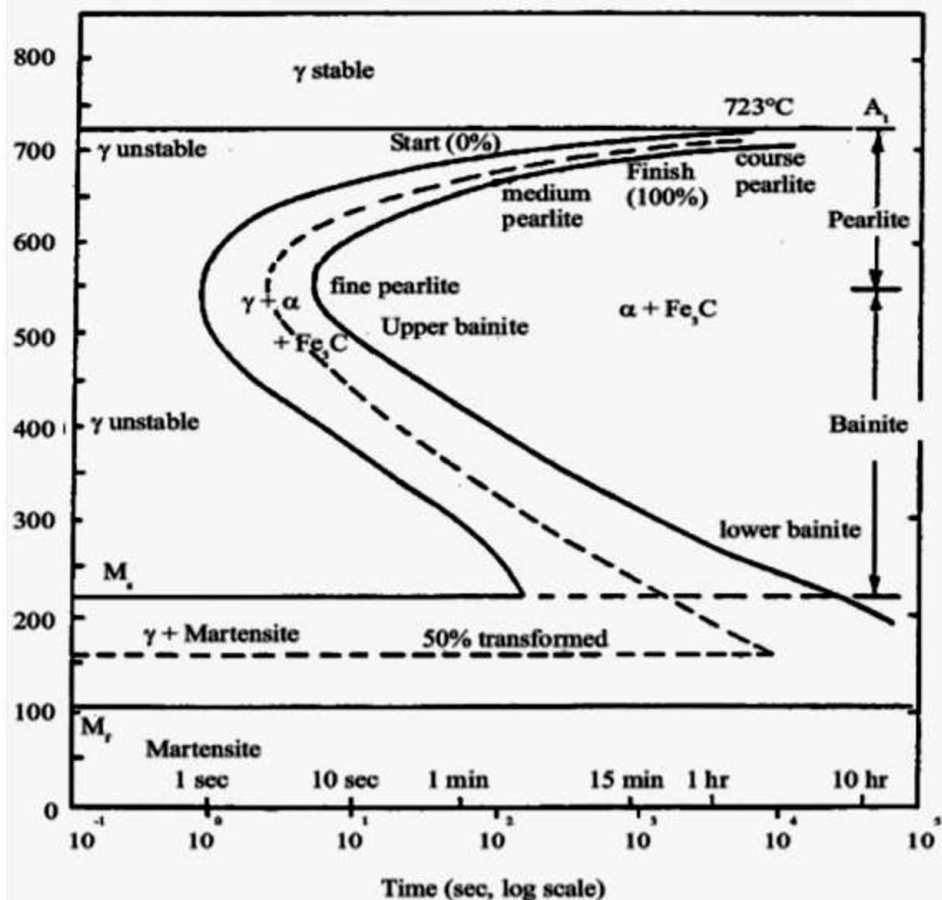


- Below 220 C: Austenite transform very rapidly to new phase: **Martensite** (*meta-stable*), rapid enough so that diffusion of carbon can be arrested. : No diffusion involved in the transformation: time independent
- Shearing and extension of austenite lattice.: Ms and Mf: @ speed of sound: Instantaneous

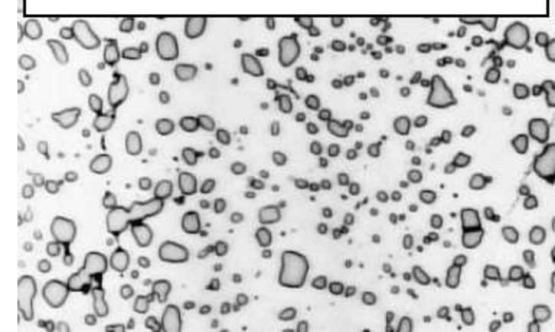
Isothermal treatment



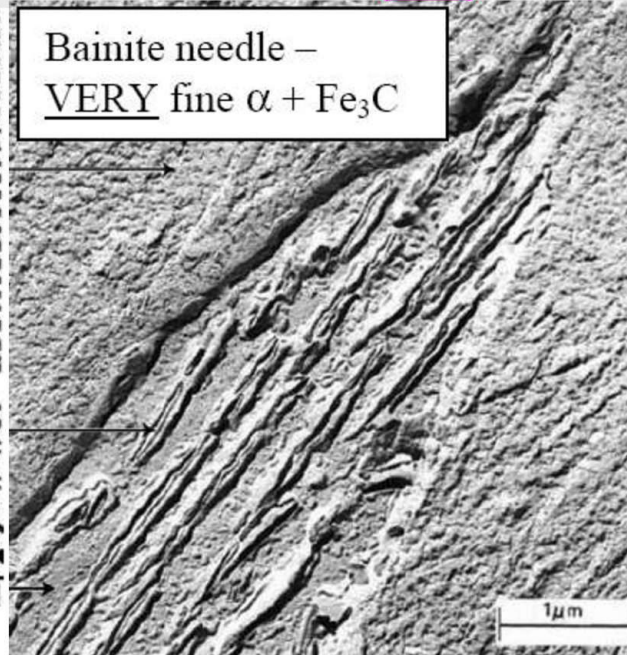
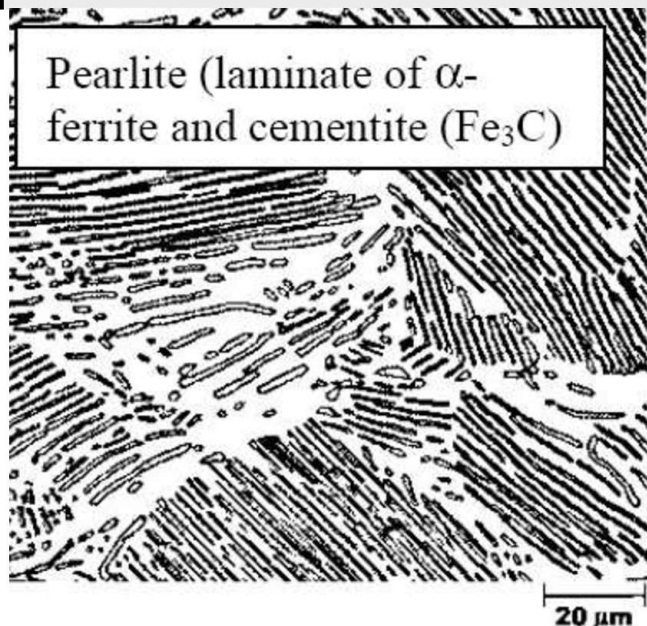
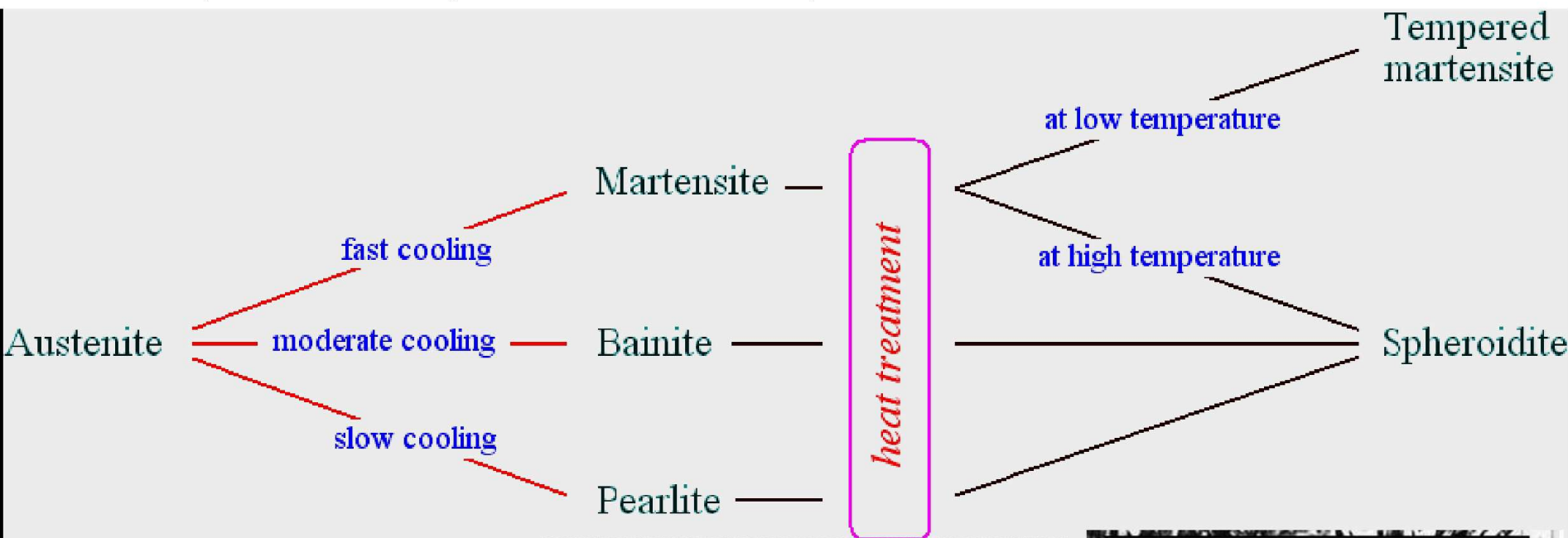
- coarse pearlite; fine pearlite: thinner layers **α -ferrite**
- Upper bainite: coarse, irregular shaped cementite particles in **α -ferrite plates.**
- lower bainite: **α -ferrite needlelike shape,**
Lower bainite is considerably harder than upper bainite.
- Martensite: body centered tetragonal (not BCC) ; **extremely hard**, applicability is limited by **brittleness**: *tempering*: below eutectoid temperature to permit diffusion of carbon atoms;
Martensite loses its tetragonality and becomes BCC ferrite; improved machinability; During tempering, carbide particles attain spherical shape; **spheroidite**; softest yet toughest structure;



Spheroidite: spheres of Fe_3C in a ferrite matrix. Very soft, ductile, weak.

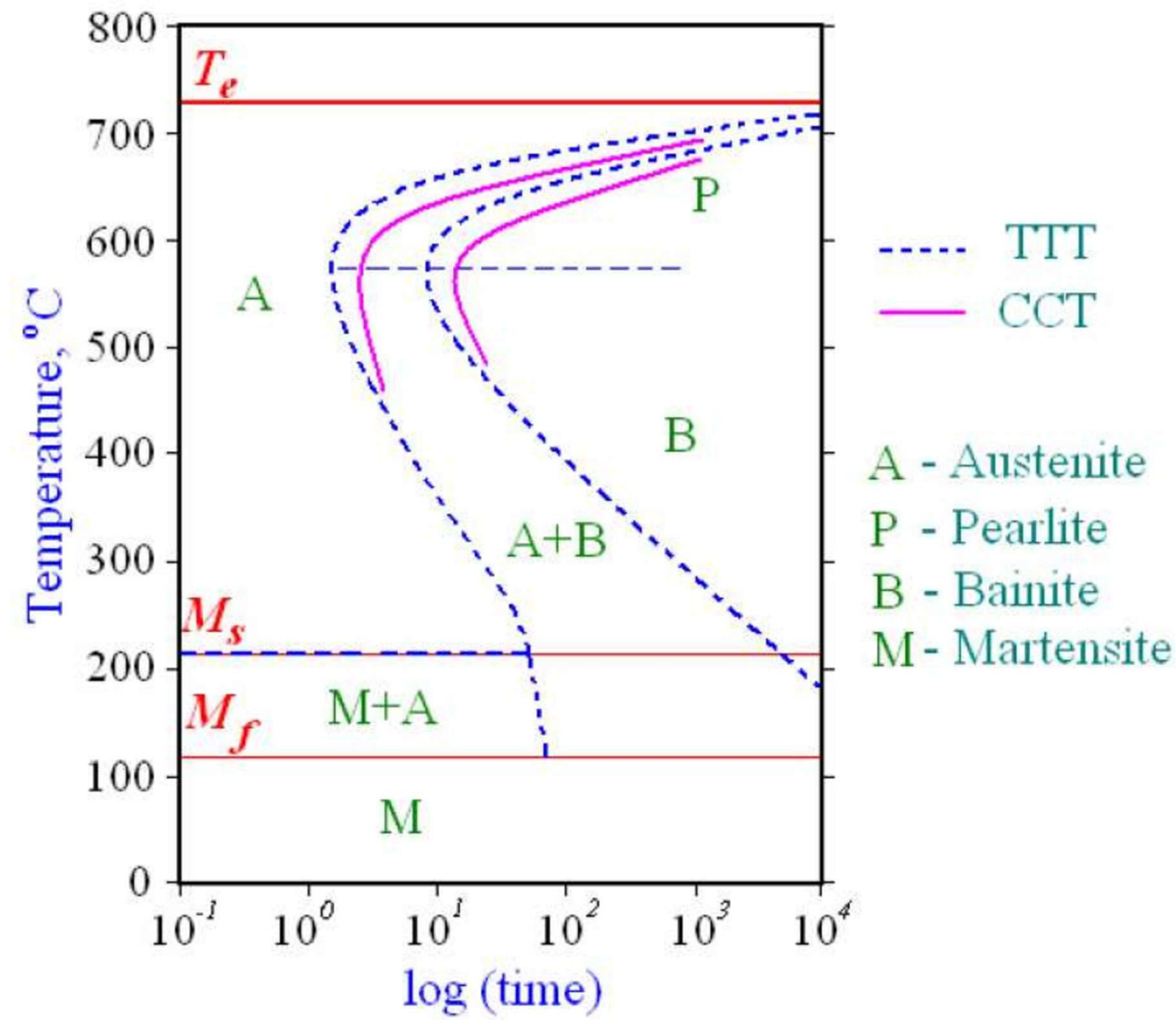


The tempering heat treatment is also applicable to pearlitic and bainitic structures. This mainly results in improved machinability.

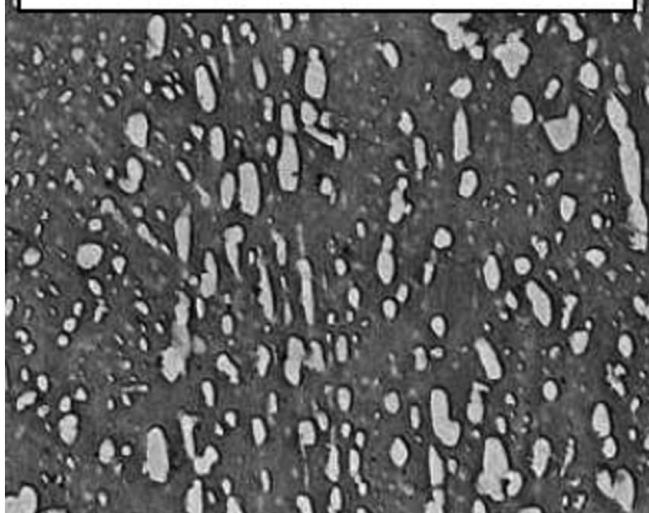


Both TTT and Continuous Cooling Transformation (CCT) diagrams are, in a sense, phase diagrams

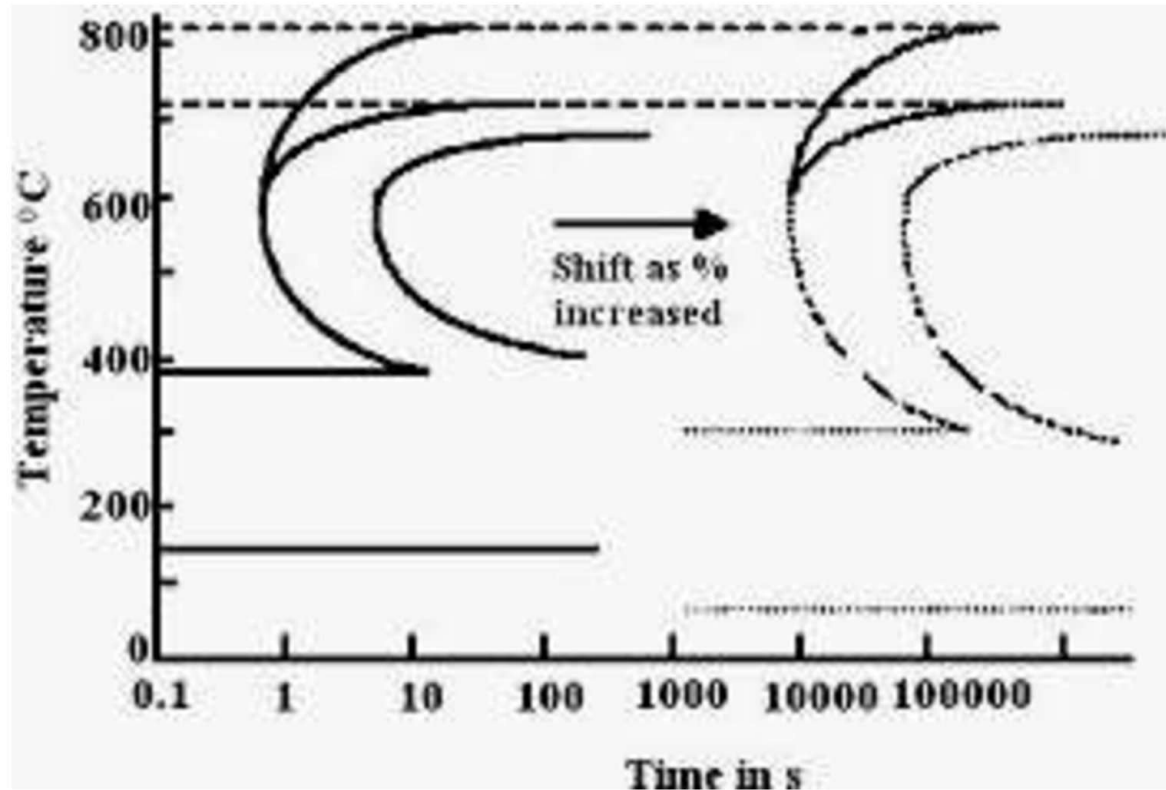
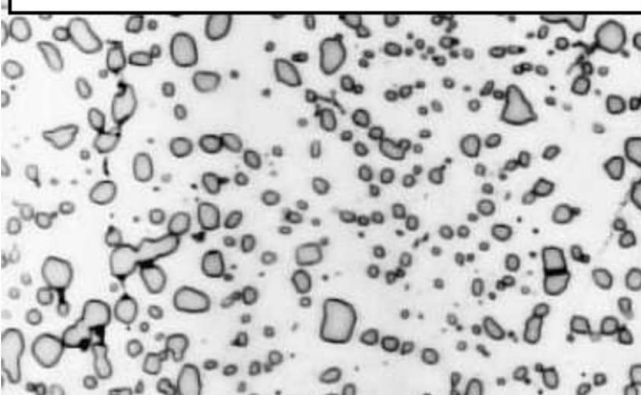
TTT diagrams are less of practical importance since: constant T; CCT diagrams are generally more appropriate;
Normally, bainite will not form during CCT; Thus, as shown in figure-20, region representing austenite-pearlite transformation terminates just below the nose.



Tempered Martensite:
Very fine spheres of
 Fe_3C in a ferrite matrix.
Very hard, some
toughness.



Spheroidite: spheres of Fe_3C in a ferrite matrix. Very soft,
ductile, weak.

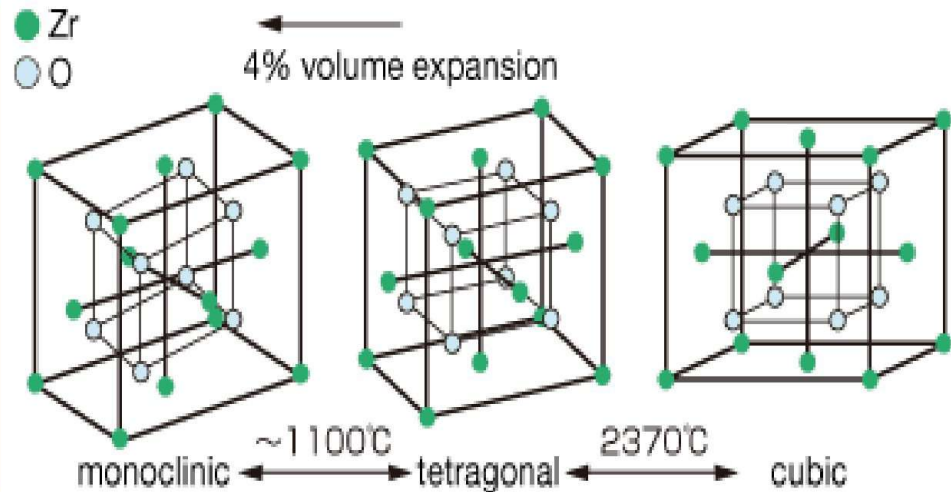


Zirconia is found in Baddeleyite: a rare zirconium oxide mineral (ZrO_2 or zirconia), occurring in a variety of monoclinic prismatic crystal forms. It is transparent to translucent, has high indices of refraction, and ranges from colorless to yellow, green, and dark brown.

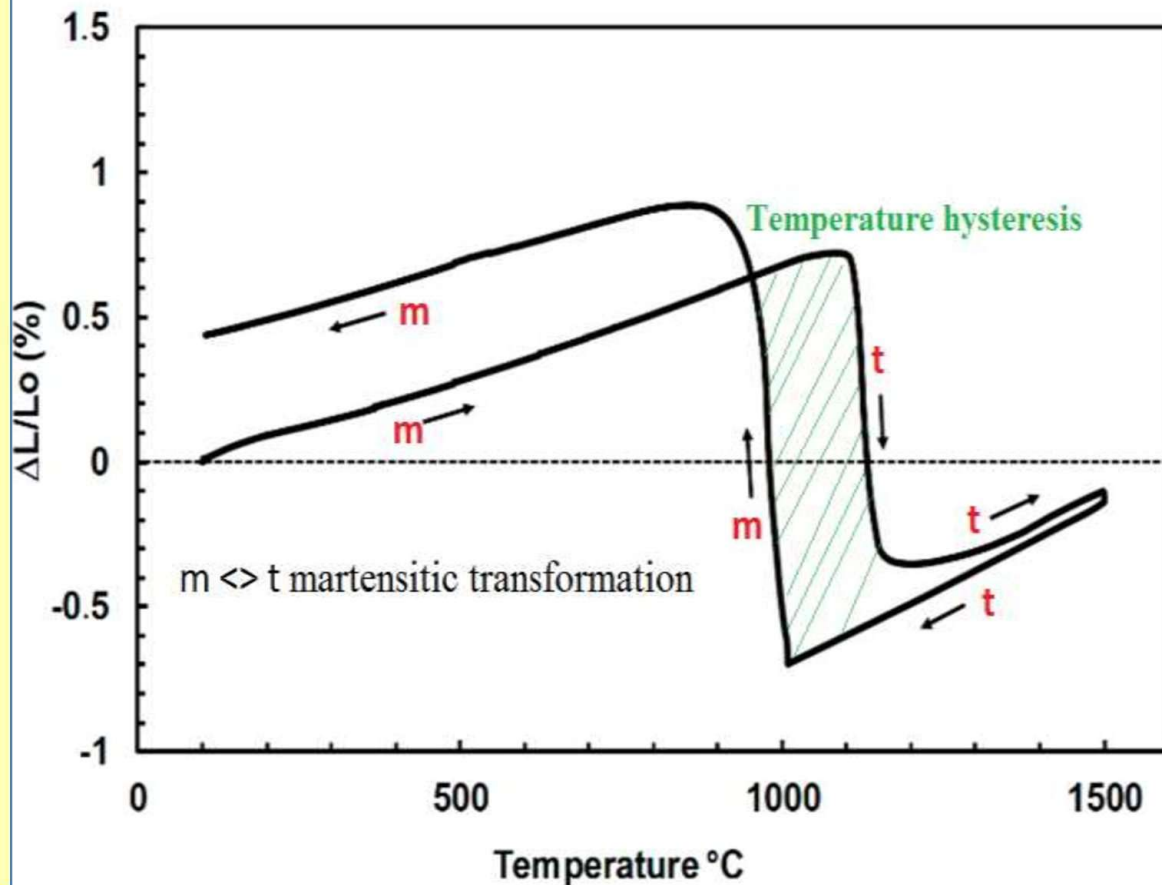
Uses:

- **Major application:** Stabilized Zirconia is used for Refractory application, Crucible, nozzle, etc., Foundry sand and flours, Ceramic pain pigments., Abrasives, Grinding Ball
- **Advanced Engineering applications:** Extrusion Dies for hot Cu drawing, machinery wear parts, piston cap.
- Yttria-stablised zirconia (YSZ) : oxygen sensors
- thermal barrier coatings in jet aircraft engines
- Bioceramics: Hip joint prostheses, Dental application

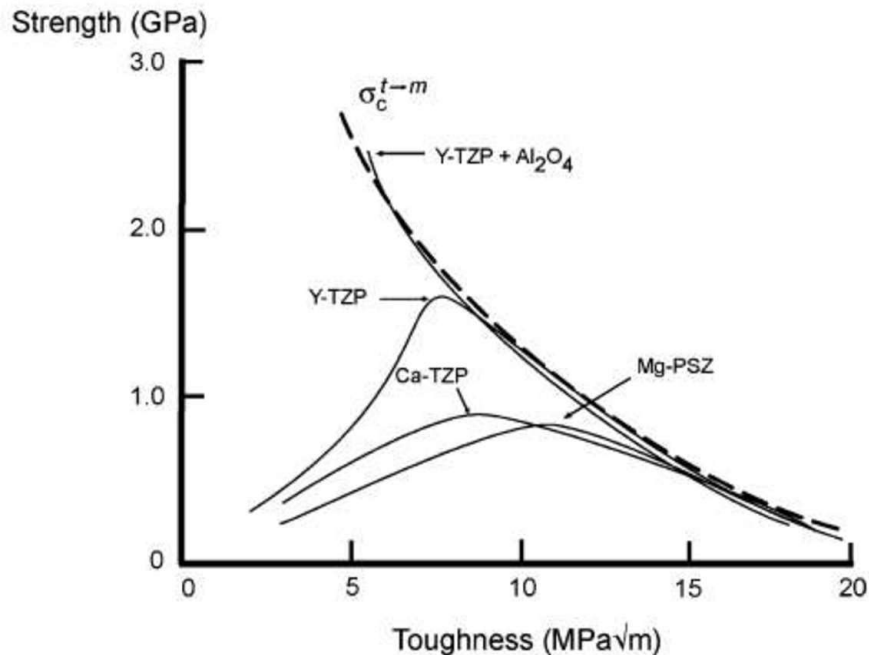
Monoclinic (*m*) at room temperature and pressure -> transforms to **tetragonal (*t*)**, by ~ **1170 °C** and then to a **cubic (*c*)** fluorite structure starting about **2370 °C**; melting by **2716 °C**.



t to m: athermal martensitic : a large temperature hysteresis;
Diffusionless, great speed: leads to disintegration of sintered undoped zirconia parts.
FSZ, PSZ, TZP



The simplest, most commonly “understood” toughening mechanism concept involves crack-tip shielding (from the applied stress) by the compressive dilatational stress associated with transformation.



An increase in the resistance to crack growth (i.e. toughness) during crack extension has been termed R-curve behavior.

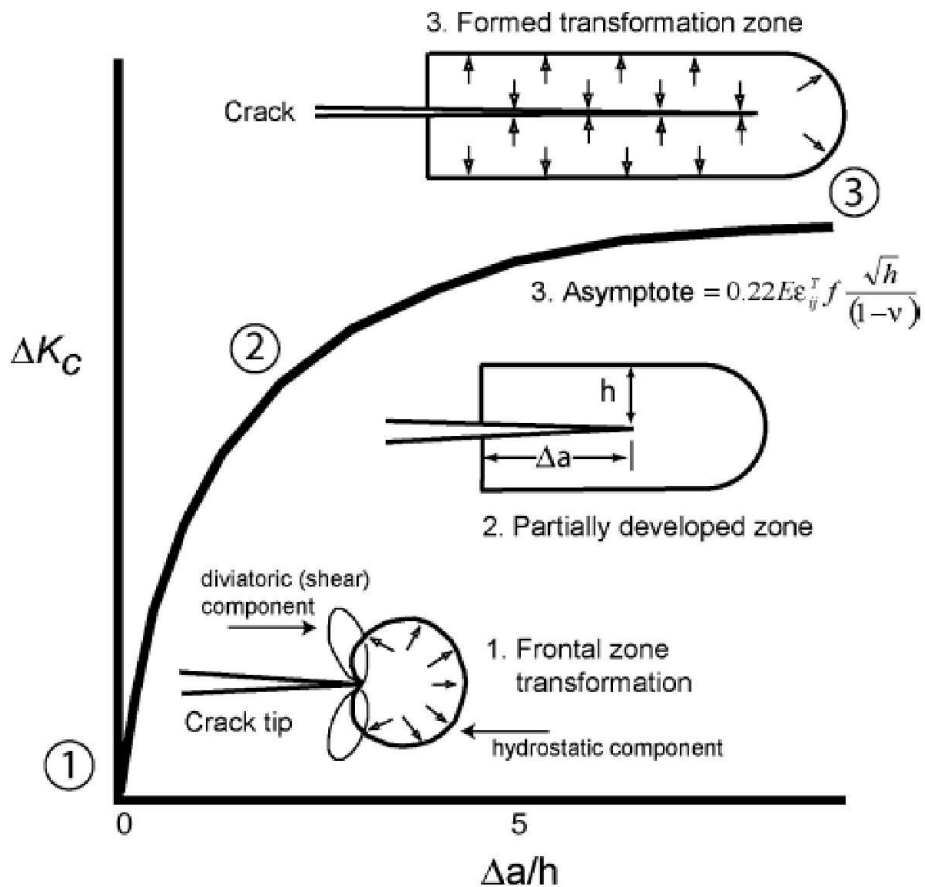
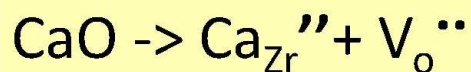


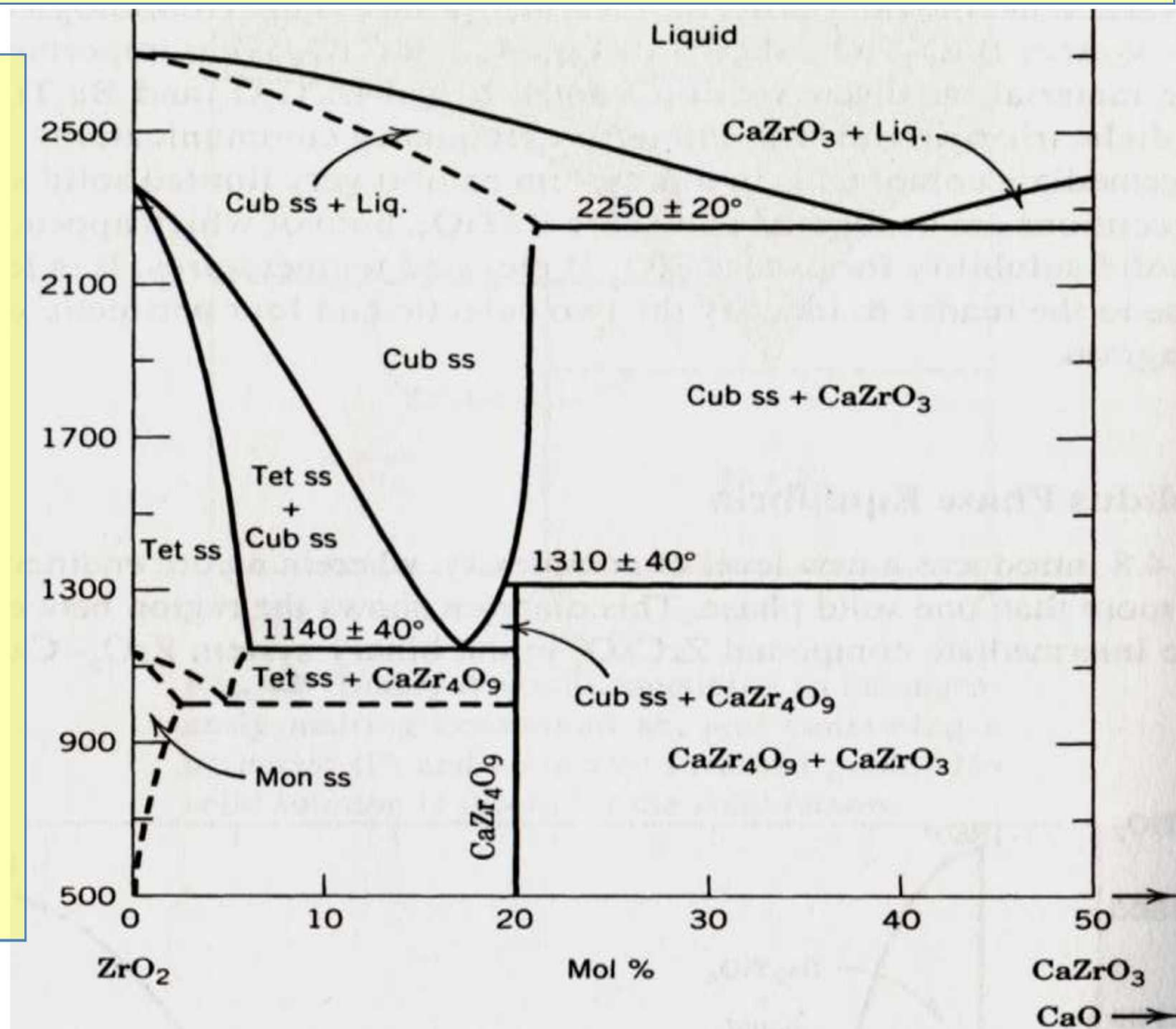
Fig. 2 – Schematic views of transformation zone and toughness increment (ΔK_C) development with crack extension, recreated with permission per description of Evans [2] and Evans and Heuer [5].

Engineering Application require: PSZ, Stabilizer: Ca, Mg, Ce, Y (Ionic Rad.<40%), Phase Diagram: Composition, Heat Treatment Phase Stability, Many transformation Sluggish: Eutectoid transformations are important. **Example: ZrO₂-CaO Phase Diagram:**



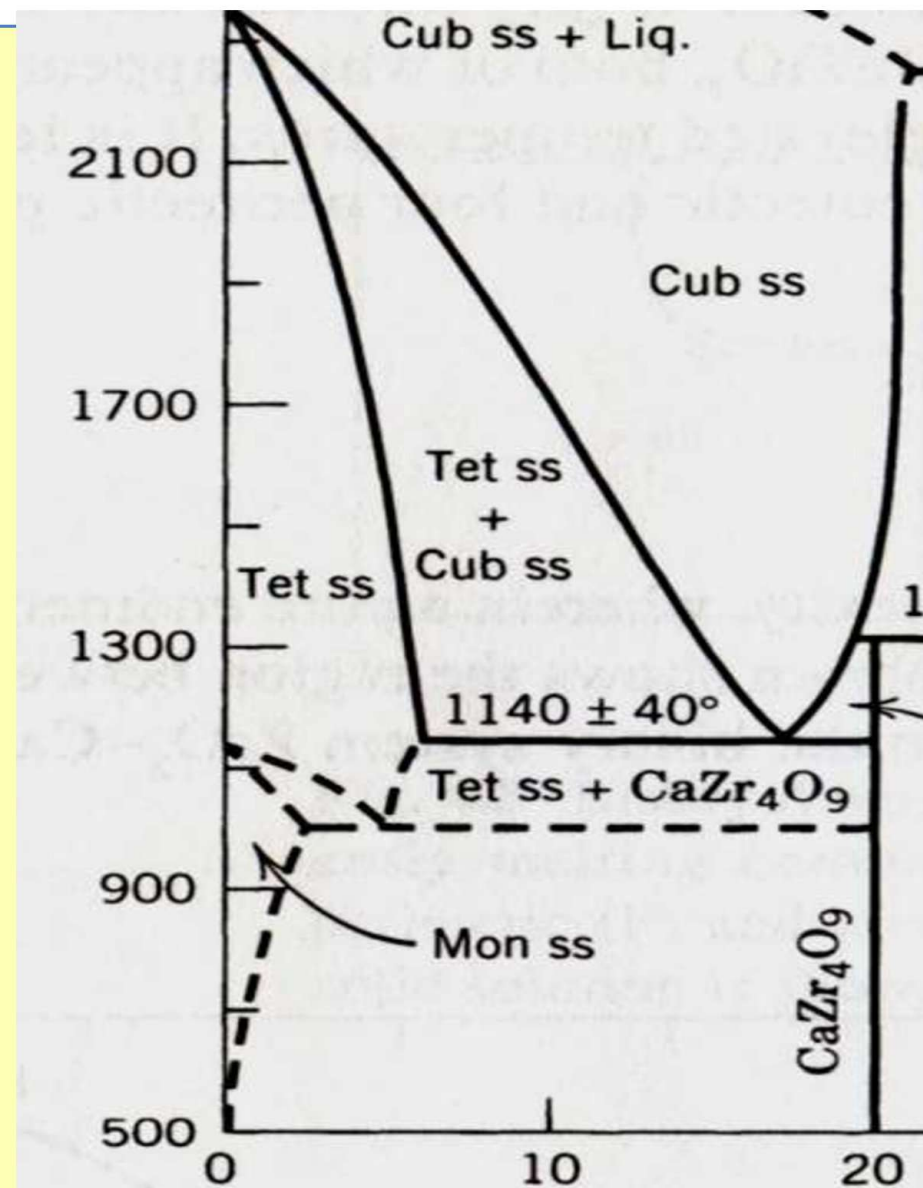
Stability of CaZr_4O_9 @ 20 mol% CaO, is not clear.

- $\text{Ca}_6\text{Zr}_{19}\text{O}_{44}$ @ 27 mol% CaO also proposed by others.
- Eutectoid composition and temperature: Also reported differently.



- Eutectoid composition and temperature: ~ 17 Mol% CaO @ 1140 (+-) 40 is more reliable. Eutectoid T: Very sluggish

- Not usually seen in conventional heat treatment, Meta-stability extended.
- $Css \rightarrow Tss + CaZr_4O_9$
- Large Cubic Field (advantage) + Sluggish Eut. Tr. : Results FSZ by rapid cooling.
- Is the basis of Ca-FSZ Solid Electrolyte
- In actual: Cubic Matrix containing finely nucleated t-particle.
- Suitable heat treatment “aging”, allows the growth of transformable (by stress from a propagating crack) metastable t-phase.



Silica Refractory: Raw Materials: Quartzite, Silica Sand: Purity: Al₂O₃ and Alkali;

TiO₂ and Fe₂O₃ are not as much objectionable as Al₂O₃ and Alkalies.

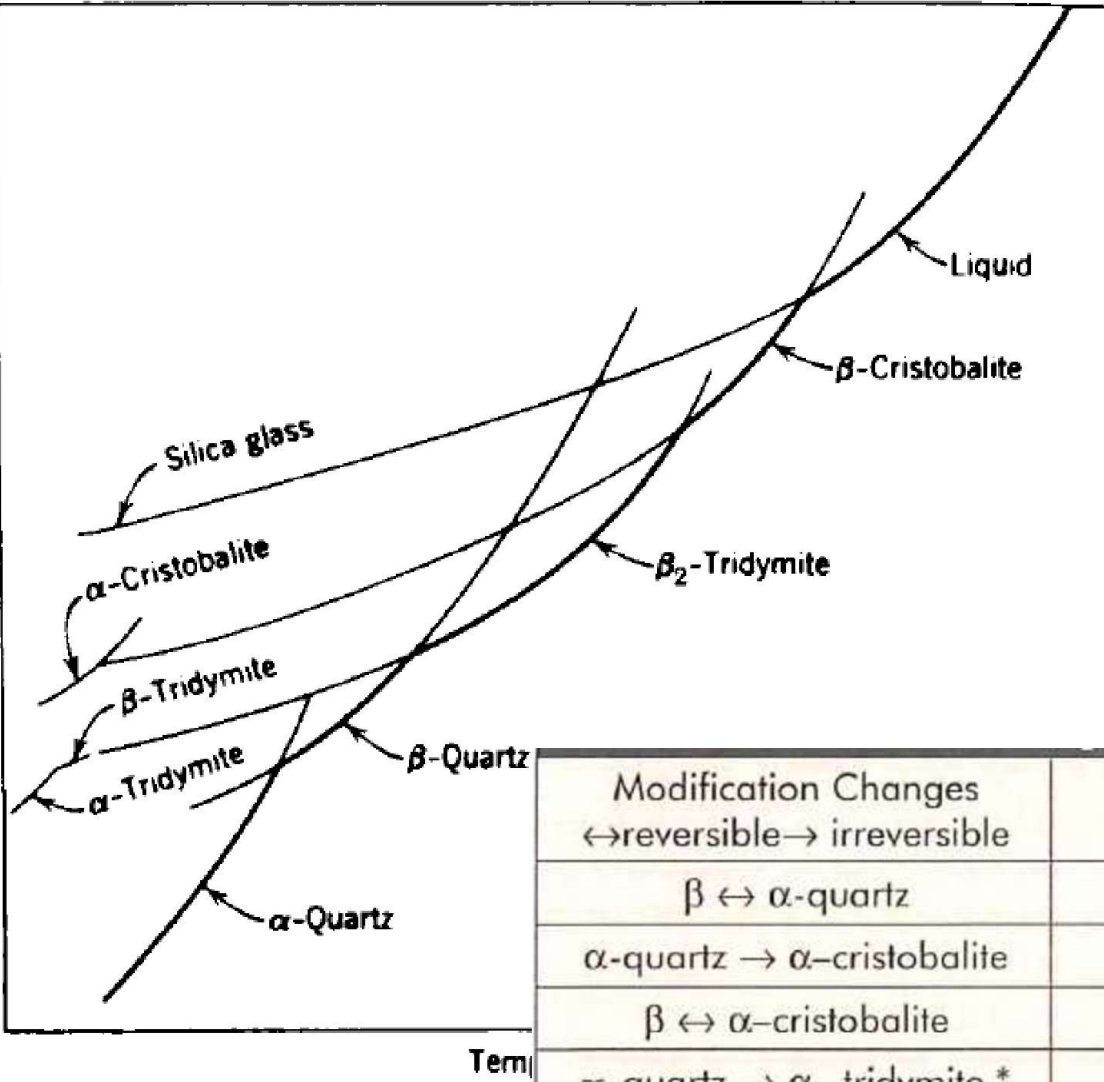
: 2-4 % CaO as slaked lime: Firing Temp: @1500 C.:

Fired Silica Brick: Cristobalite, Tridymite, Residual Quartz, Glass.

Tridymite brick: Better strength and thermal shock resistance.

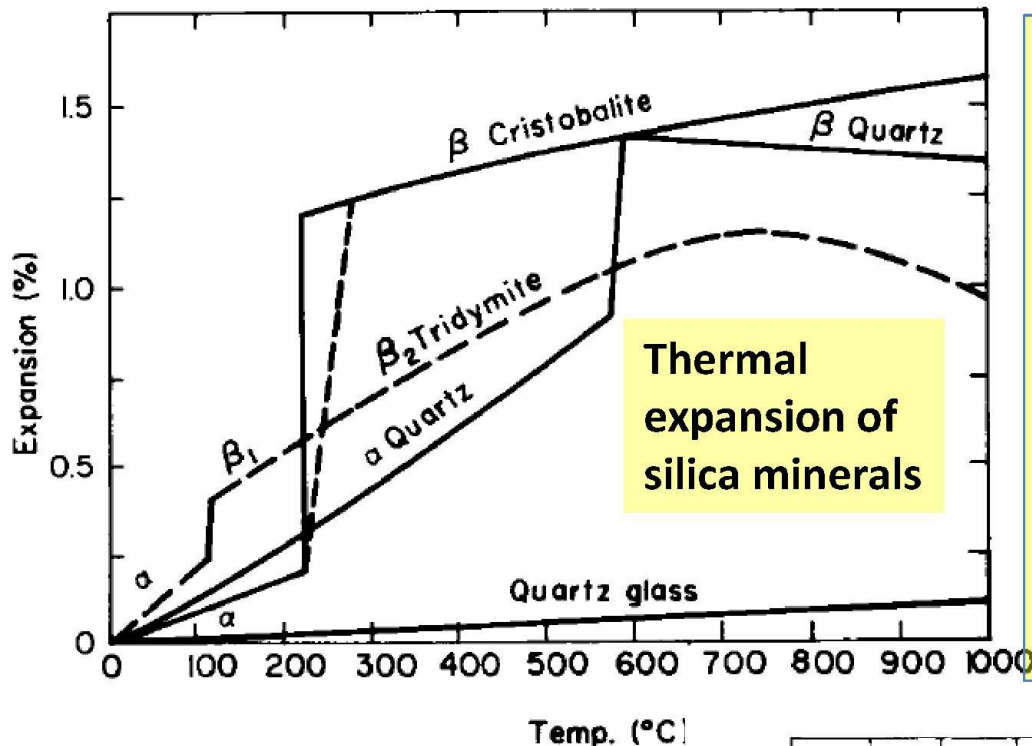
Application	Bulk Density [g/cm ³]	Apparent Porosity [vol.-%]	Cold Crushing Strength [MPa]	Refractoriness Under Load (differential) (DE) T05 [°C]	Thermal Expansion 1000 °C [%]	Thermal Conductivity 1000 °C [W/m·K]
Coke oven	1.78–1.90	18–23	30–60	1610–1650	1.3	1.8–2.2
Glass furnace	1.81–1.85	19.5–21.5	30–40	1630–1670	1.4–1.5	1.8–1.9

Pressure

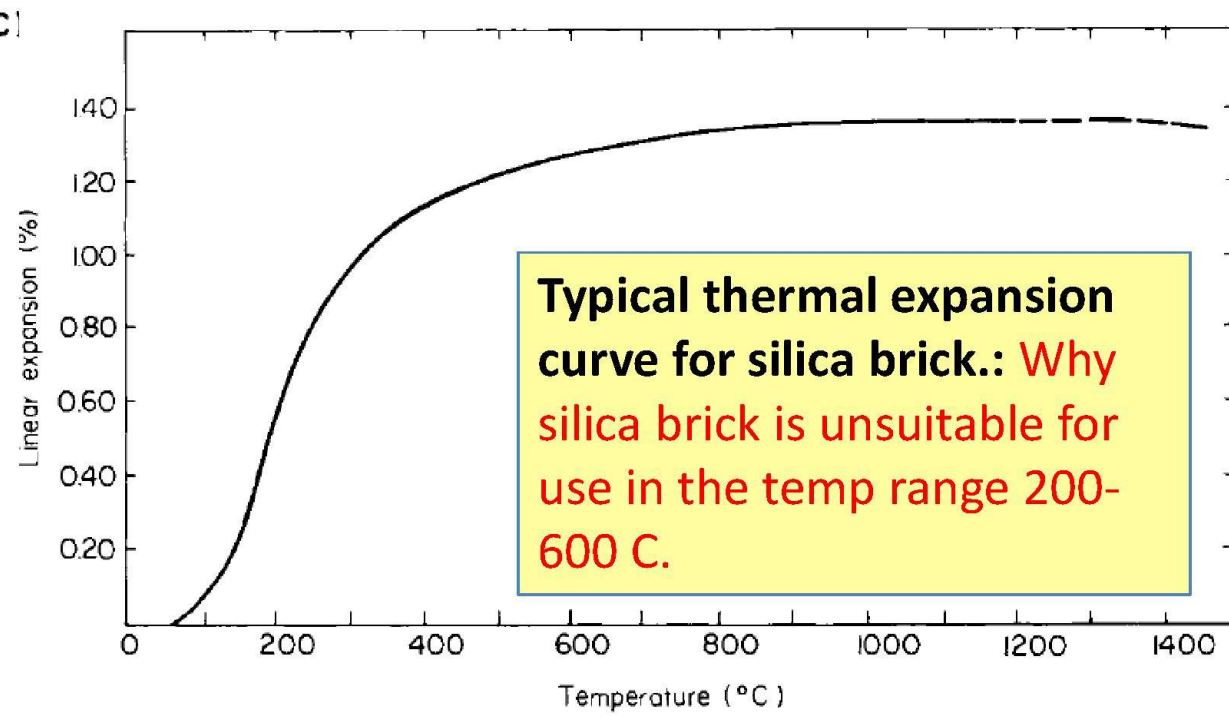


Silica Refractory:
Firing: sequences of
phase transformation

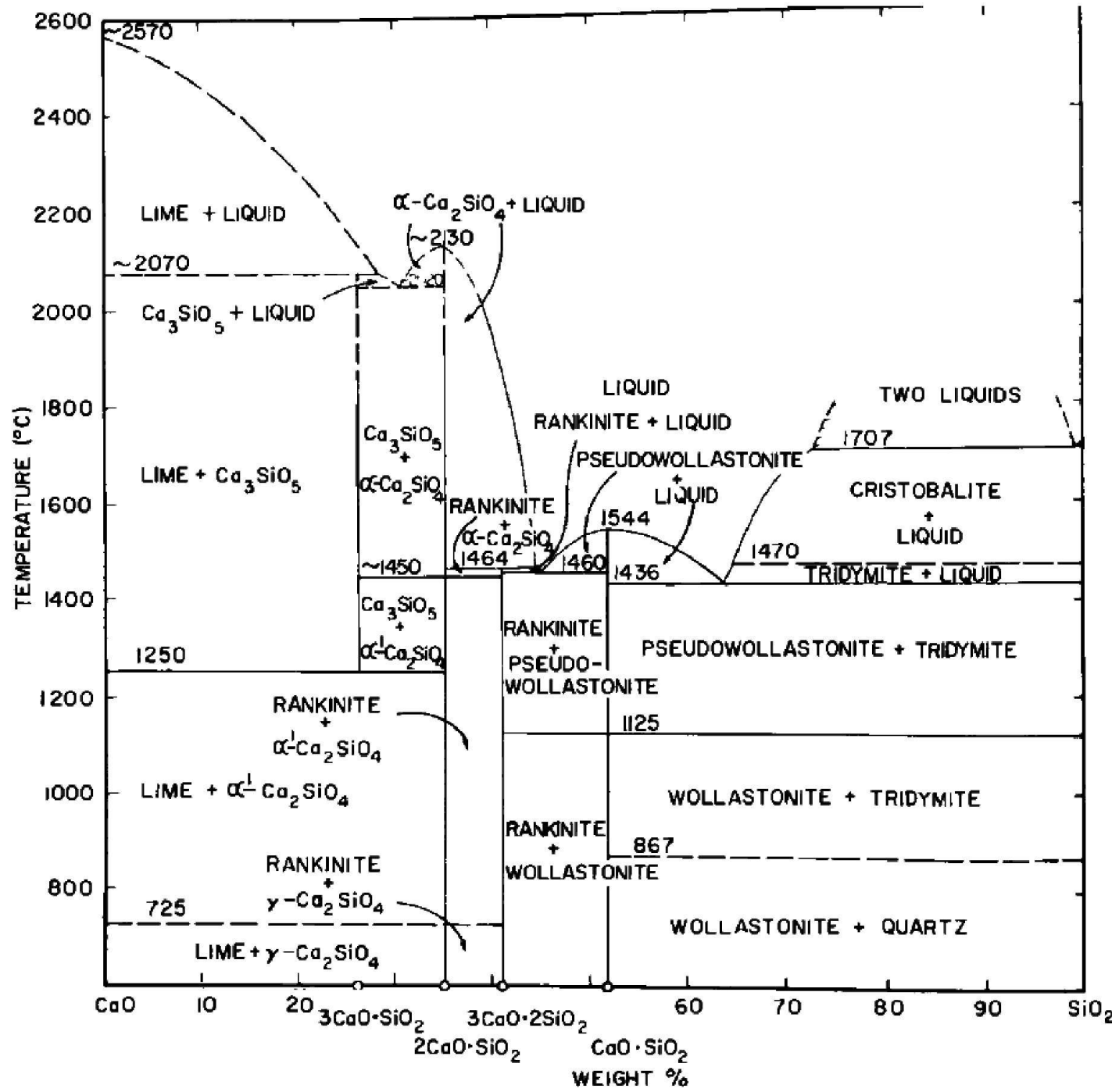
Modification Changes ↔reversible→ irreversible	Transformation Temperature [°C]	Volume Change [%]
$\beta \leftrightarrow \alpha$ -quartz	573	0.8–1.3
α -quartz → α -cristobalite	1250 ($\approx 1050^*$)	17.4
$\beta \leftrightarrow \alpha$ -cristobalite	≈ 260	2–2.8
α -quartz → α -tridymite *	≈ 870	14.4
$\gamma \leftrightarrow \beta \leftrightarrow \alpha$ -tridymite *	117–163	0.5
α -tridymite → α -cristobalite *	1470	0
α -cristobalite → melt	1713 ± 10	–
α -tridymite → melt **	1670 ± 10	–
fused silica → α -cristobalite	above $\approx 1150^*$	≈ 0.9



The ability of the brick to withstand temperatures so close to its melting point has been attributed in a general to the characteristic of silica to form immiscible liquids with lime and with iron oxide. A brick containing 1 % of Al₂O₃ plus alkalies will not withstand as high a temperature as one containing only 0.5% or less.

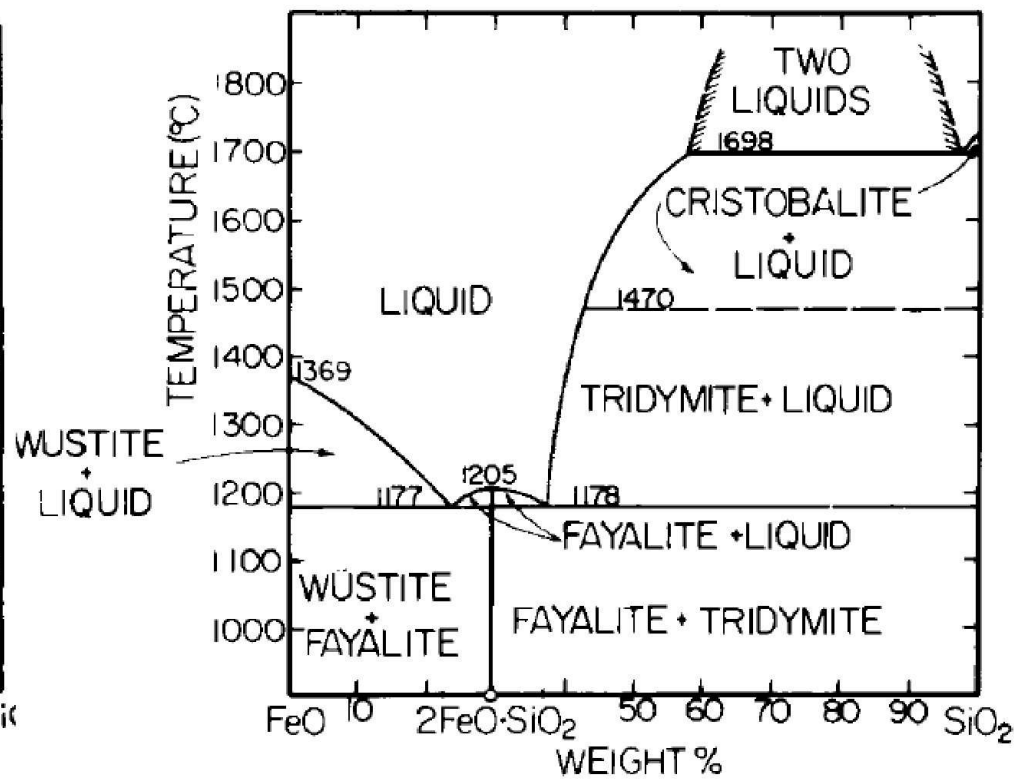
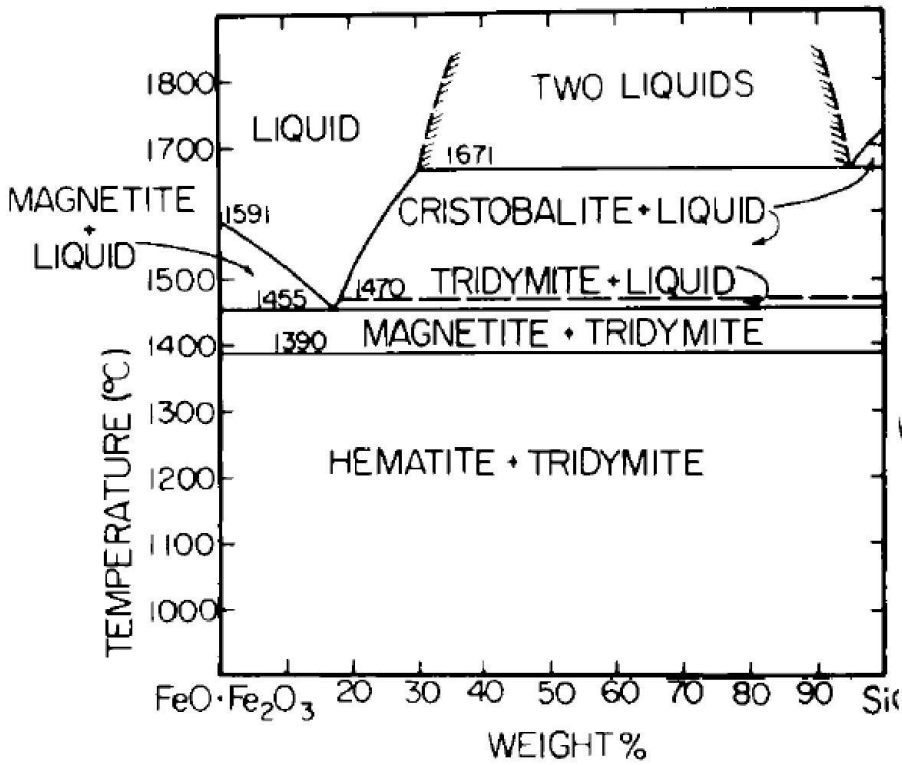


silica forms
 two immiscible
 liquids with lime;
 cristobalite is
 stable in the
 presence
 of these at 1707°C
 • very near to the
 melting point of
 SiO_2 .
 • immiscible
 liquids are
 favorable to the
 refractory
 behavior of
 cristobalite.

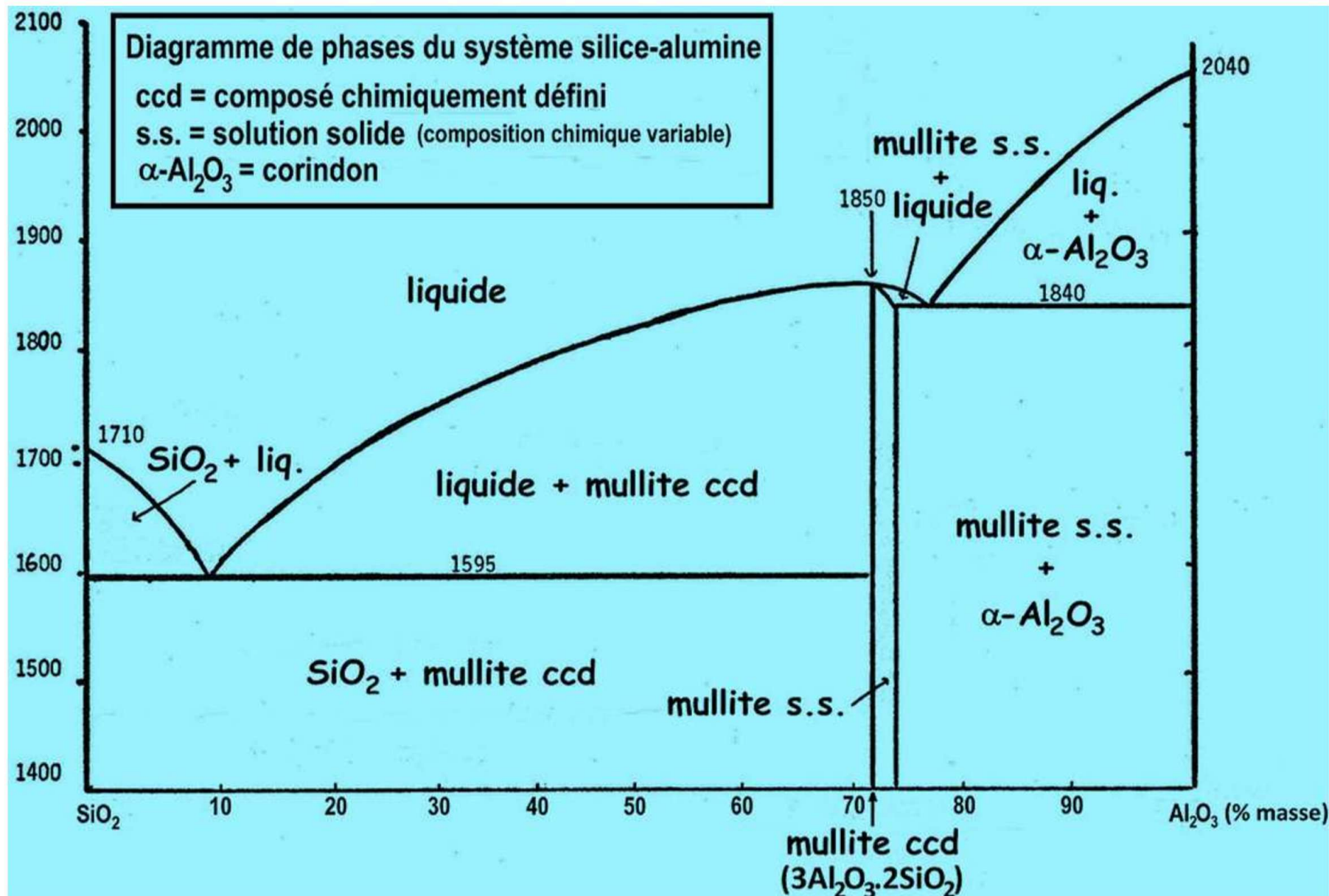


silica forms two immiscible liquids with Iron oxide; cristobalite is stable in the presence of these at 1671°C

- immiscible liquids are favorable to the refractory behavior of cristobalite.

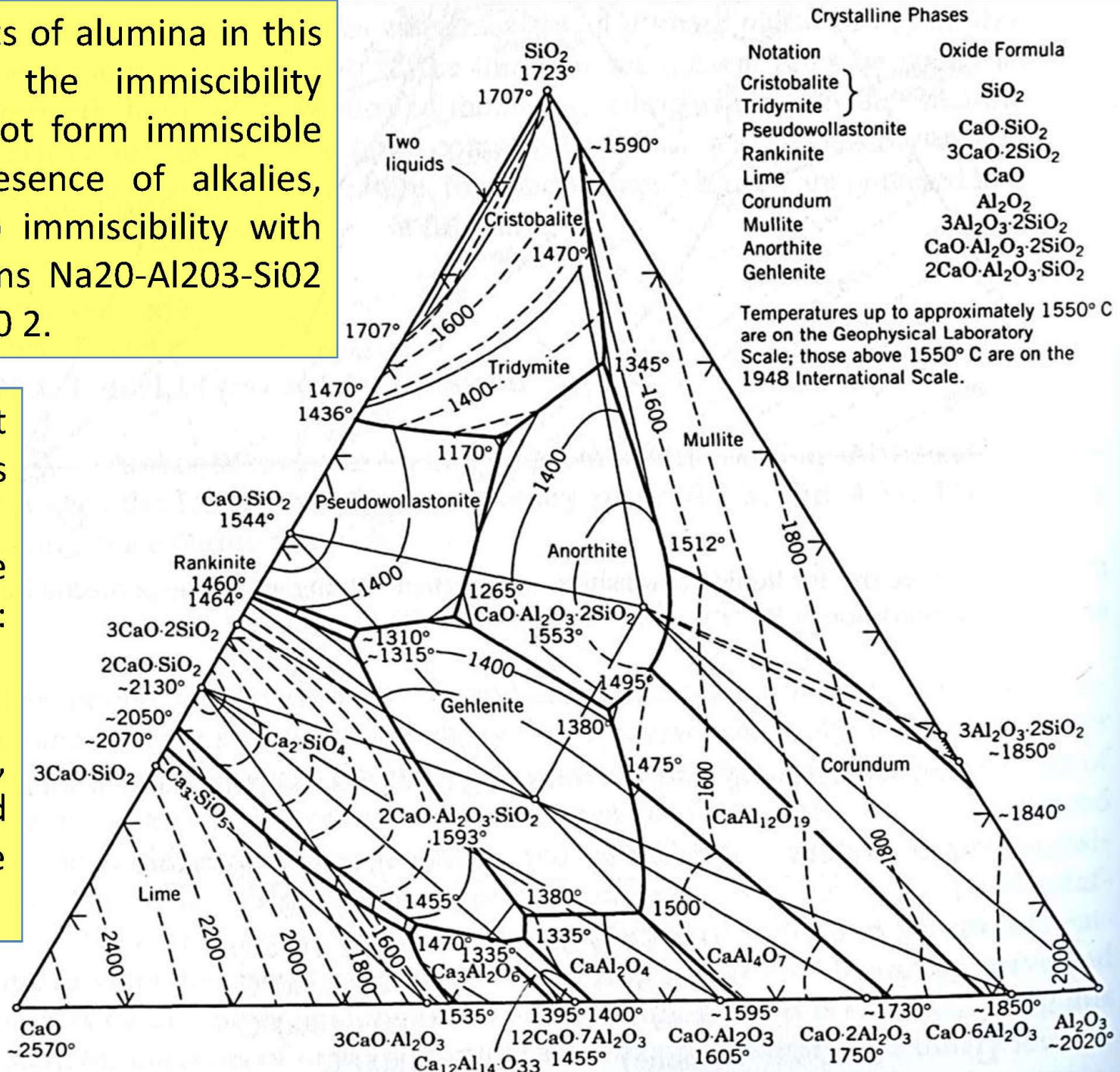


Silica does not form immiscible liquids with alumina.



Even small amounts of alumina in this system eliminate the immiscibility field. Silica does not form immiscible liquids in the presence of alkalies, hence there is no immiscibility with silica in the systems Na₂O-Al₂O₃-SiO₂ and K₂O-Al₂O₃-SiO₂.

very small amount of alumina that is present plus about 2% lime, the first liquid to form: eutectic composition between tridymite, anorthite, and pseudowollastonite at 1170°C



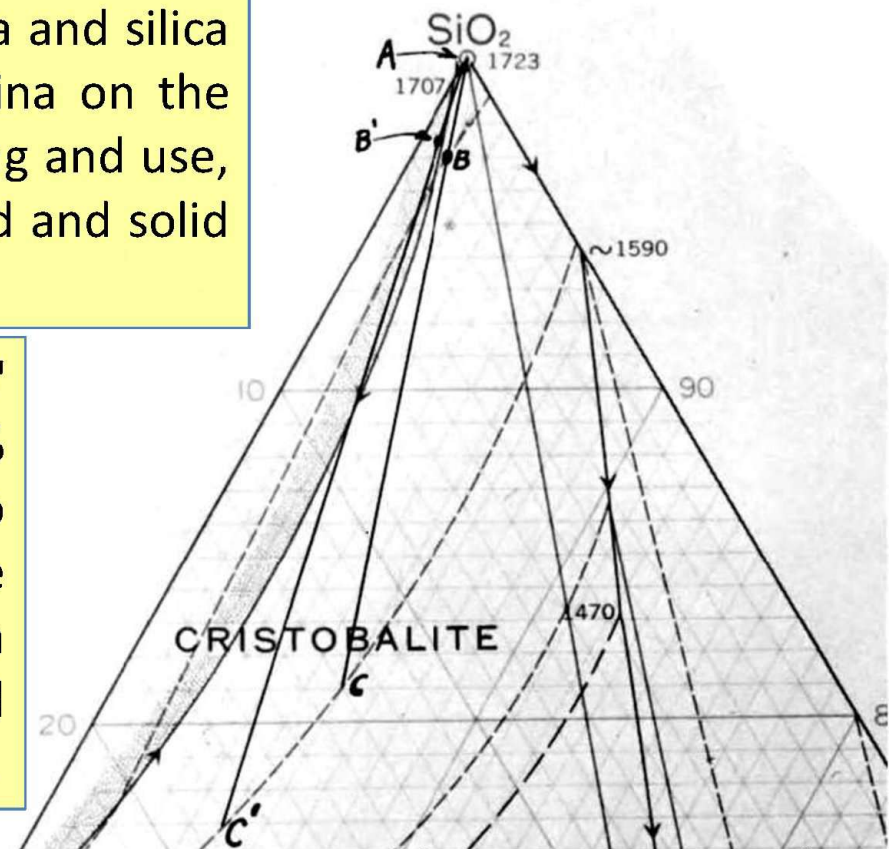
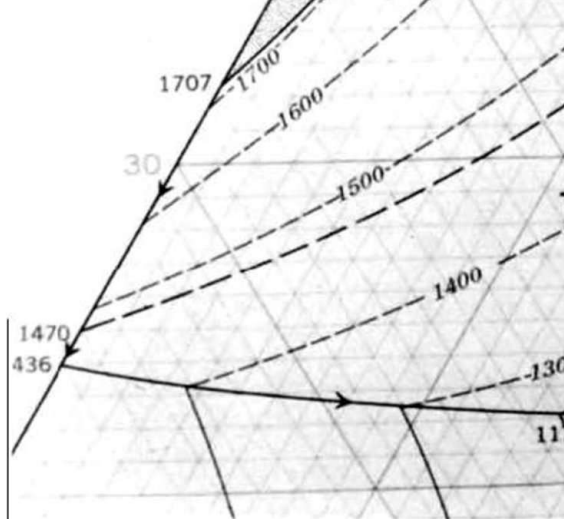
The phase diagram of the system lime-alumina and silica is very useful in studying the effect of alumina on the liquid development in a silica brick during firing and use, and for the calculation of the amount of liquid and solid present at temperatures of use.

For example, consider compositions B and B' on Fig. 15. These contain 1 % and 0.5% alumina, respectively, and 2% lime. To determine the amount of liquid in these compositions as an example, a line is drawn from the apex A (silica) through B or B' and then on to the 1600°C isotherm, (point C or C').

The proportions of the liquid and solid are then determined from distance measurements AB, AC, and BC wherein:

$$\text{AB/AC} \times 100 = \% \text{ liquid in composition B at } 1600^\circ\text{C}$$

$$\text{BC/AC} \times 100 = \% \text{ solid in composition B at } 1600^\circ\text{C}$$



SiO₂-Al₂O₃ Phase Diagram: Wide application in Refractory Technology. : Explain many Refractories

Only binary phase: Mullite; Two eutectics; @ 1595 and @ 1840; Mullite has limited SS of Al₂O₃. ;

Refractory:

Silica: < 2% Al₂O₃

Fire Brick:

Siliceous: 14-22% A

F.B. : 22-38%

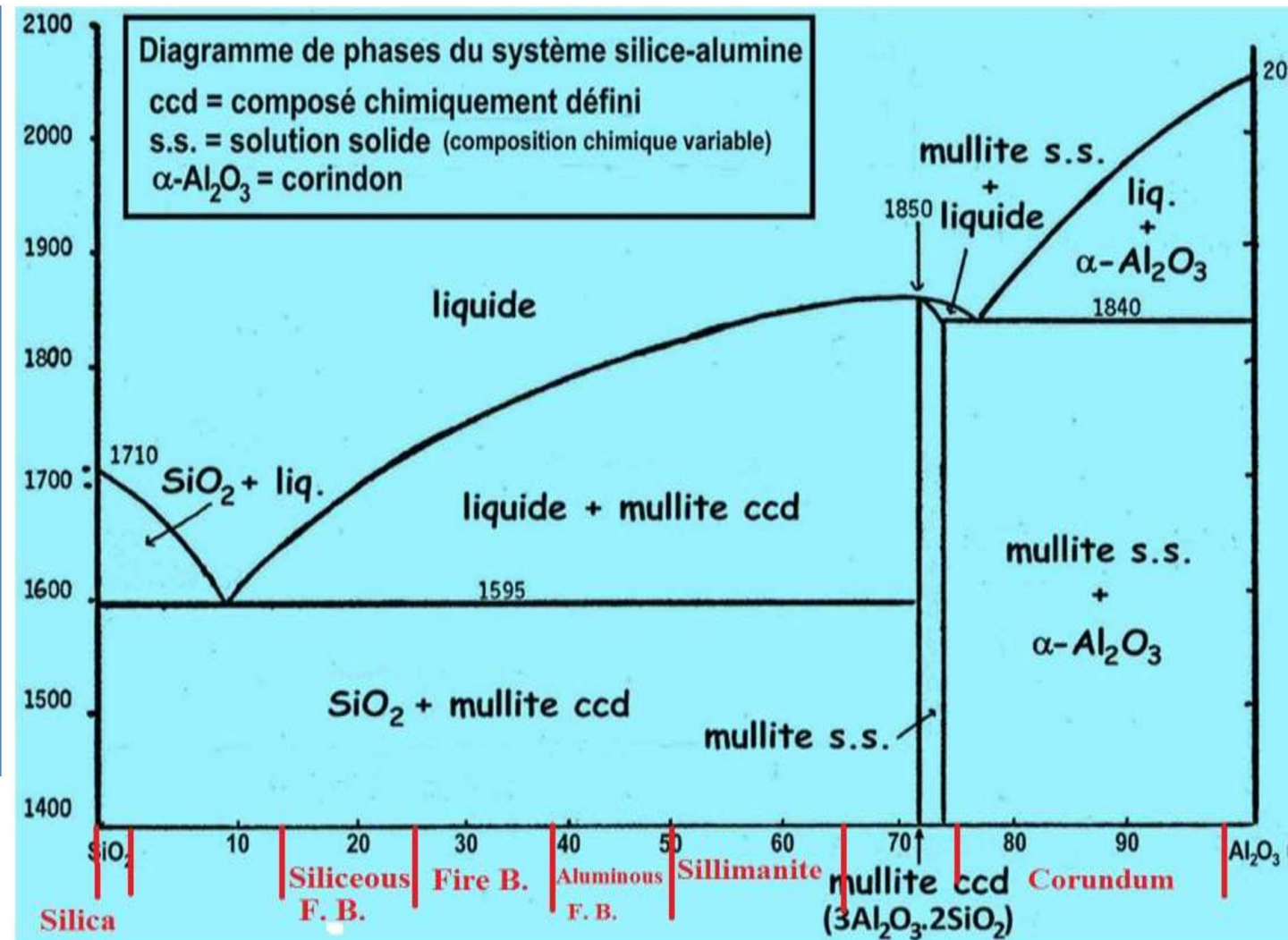
Aluminous FB: 38-50 % Al₂O₃.

High Alumina:

Sillimanite: 50-65%

Mullite: 65-75%

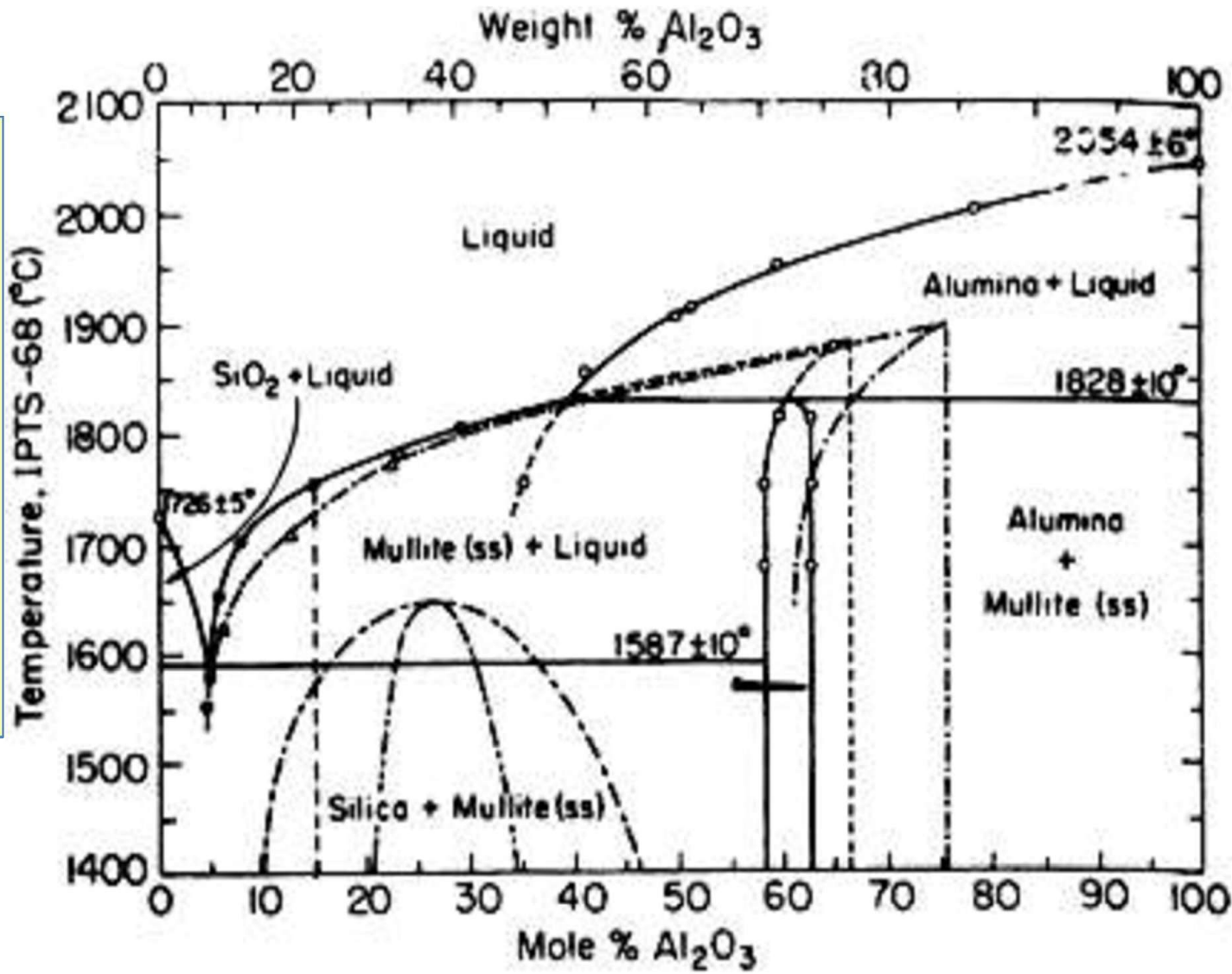
Corundum: 75-98%



Incongruently Melting Mullite: (Aksay & Pask)

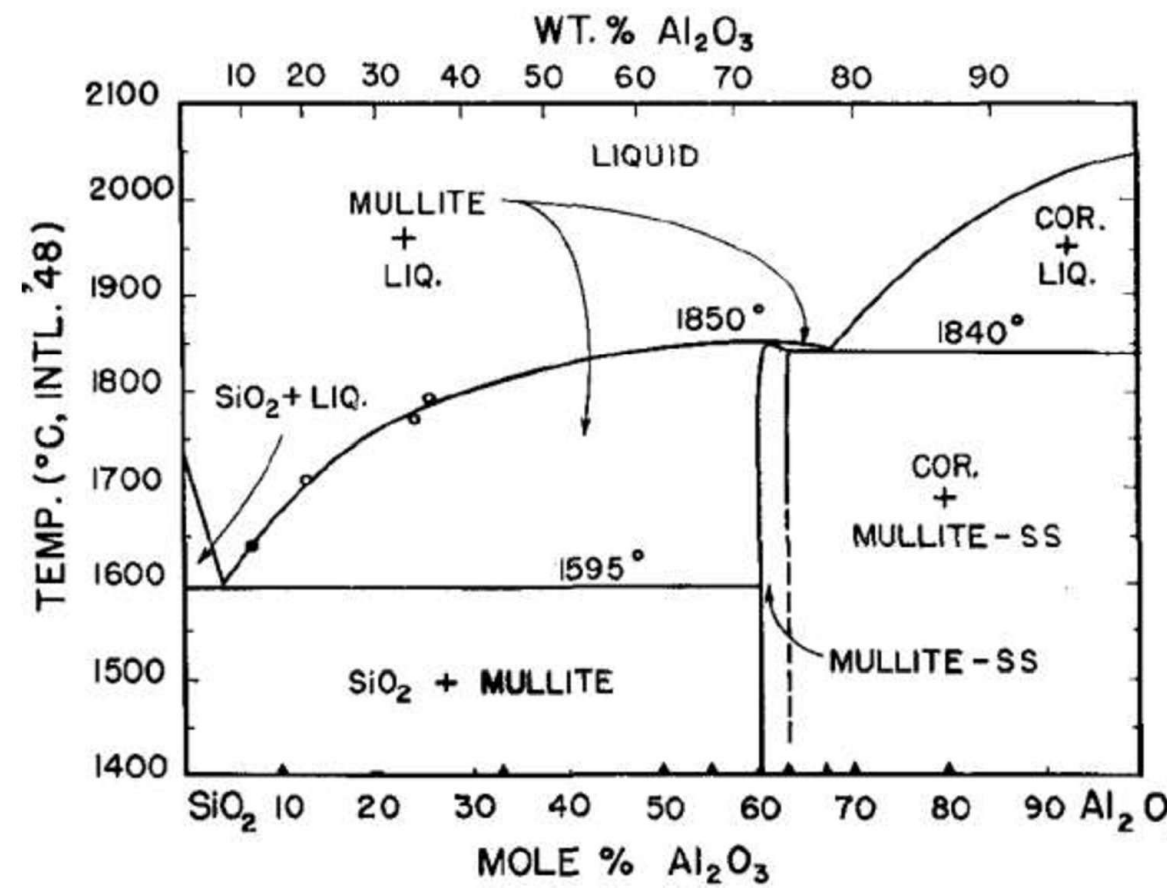
Mullite: $\text{Al}_2^{\text{VI}}(\text{Al}^{\text{IV}}_{2+2x}\text{Si}_{2-2x})\text{O}_{10-x}$; IV and VI represent four and six-fold coordination. x= amount of missing oxygen. x; 0.17 to 0.59.

Al_2O_3 : 70.5 to 83.6 wt%,
However, Normal
x; 0.25 (3:2 Mull)
To
x; 0.4(2:1 Mull;
77.2 wt%)
Many meta-
stable extension.

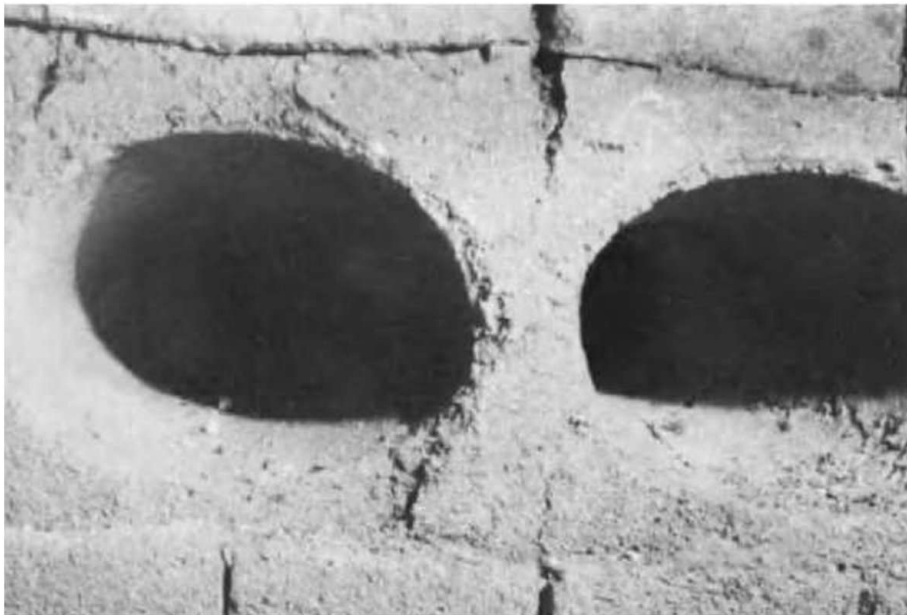


- Compositions between mullite and cristobalite will develop liquid at 1595°C. Al₂O₃ is powerful flux for silica: Eutectic 1595 @7% Al₂O₃. *
- Melting of compositions between 5 and 72% alumina increase with their alumina contents; will form liquid in some degree at temperatures above 1595°C.

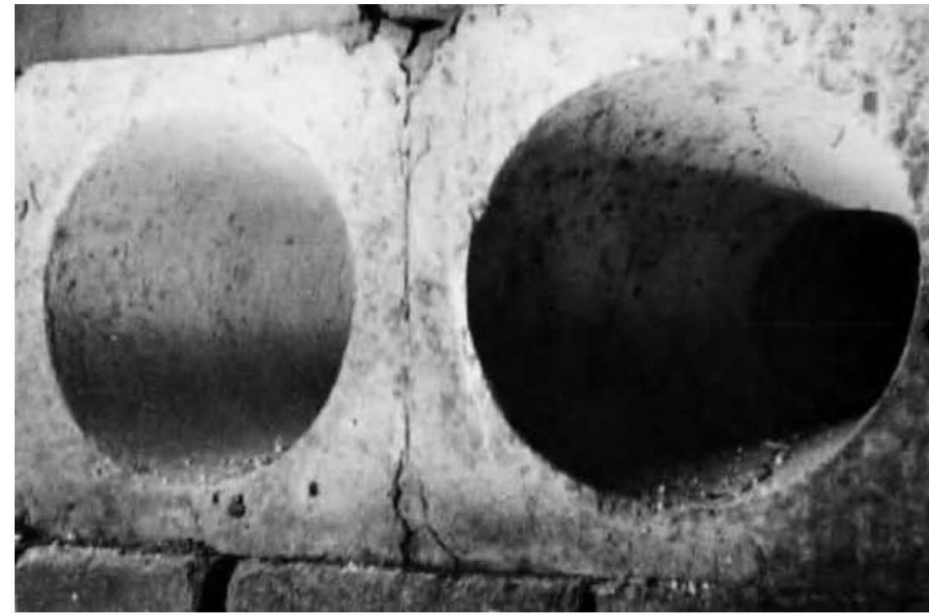
- Compositions: more than 72% alumina develop liquids above 1840°C
- compositions in mullite and corundum field: used with assurance up to 1840°C.
- compositions close to pure alumina: used well above 1840°C.



- alumina-silica diagram: 68% Al₂O₃ blocks developed liquid at 1590°C and continued to increase liquid content at temperatures above this. life of these blocks was less than two weeks
- 90 % alumina block :near to Al₂O₃: on the diagram: no liquid developed below 1840°C.: Decrease in repair delay: Although the unit cost of these refractories: very high,



68% alumina burner blocks after
two weeks service at 1700°C.



90% alumina burner blocks after
four weeks service at 1700°C.

Table 8.6 Typical properties of fireclay refractories

	<i>Firebrick</i>	<i>Aluminous fireclay</i>
Composition (wt%)		
SiO_2	59	53
Al_2O_3	25	42–43.5
TiO_2	0.6	1.4–1.7
Fe_2O_3	5.9	0.9–2.0
$\text{CaO} + \text{MgO}$	0.6	0.25–0.7
$\text{K}_2\text{O} + \text{Na}_2\text{O}$	2.3	0.5–0.8
Apparent porosity (%)	20	12–17
Bulk density (g cm^{-3})	2.12	2.3
Cold crushing strength (MPa)	31	42–59
Bend strength (MPa)	2–10	7–10
Refractoriness ($^{\circ}\text{C}$)	1595–1605	1740–1780
Thermal expansion ($\times 10^{-6} \text{ }^{\circ}\text{C}^{-1}$) from 20 to 1200°C	5.1	5.1
Major phases	Aluminosilicate glass, mullite	Aluminosilicate glass, mullite

Table 8.7 Typical properties of alumina refractories

	<i>Sillimanite</i>	<i>Mullite</i>	<i>Bauxite-based high-alumina</i>
Composition (wt%)			
SiO ₂	39–42.5	23.2	6.5–9.5
Al ₂ O ₃	55.4–59	74.2	82.5–88.2
TiO ₂	0.3–0.5	0.2	2.4–3.5
Fe ₂ O ₃	1.0–1.2	0.7	1.5–2.0
CaO + MgO	0.2–0.3	0.1	0.4–0.5
K ₂ O + Na ₂ O	0.3–0.4	1.0	0.2–0.3
Apparent porosity (%)	13–16	13–17	17–21
Bulk density (g cm ⁻³)	2.5	2.6	2.75–2.9
Cold crushing strength (MPa)	27–60	60–65	55–100
Bend strength (MPa)	7–11	7–14	5–14
Refractoriness (°C)	1750–1810	1880	1860–1920
Thermal expansion ($\times 10^{-6} \text{ }^{\circ}\text{C}^{-1}$) from 20 to 1200°C	6.5	4.5–6	7.3–10.2
Major phases	Mullite, glass	Mullite, glass	Corundum, mullite, glass

Effect of Alkali content on alumino-silicate refractory.

- The high potash content of plastic fireclay is largely responsible for the low refractoriness of Fire Brick.
 - Alkalies are a major problem in attaining high-temperature stability and good hot load bearing ability in alumina-silica refractories.

	Flint fireclay	Plastic fireclay
Percent raw clay basis	0	0
Loss at 105°C	1.35	2.28
Ignition loss	12.90	7.69
SiO_2	45.20	60.07
Al_2O_3	36.77	22.57
Fe_2O_3	1.30	2.38
CaO	0.50	0.68
MgO	0.08	0.64
TiO_2	1.80	1.60
P_2O_5	0.02	0.07
Na_2O	0.00	0.11
K_2O	0.52	1.71
MnO	Trace	Trace
S	0.04	0.95
C	0.35	0.22
PCE	33	27

Firebrick

Composition (wt%)

SiO ₂	59
Al ₂ O ₃	25
TiO ₂	0.6
Fe ₂ O ₃	5.9
CaO + MgO	0.6
K ₂ O + Na ₂ O	2.3

Apparent porosity (%)

20

Bulk density (g cm⁻³)

2.12

Cold crushing strength (MPa)

31

Bend strength (MPa)

2–10

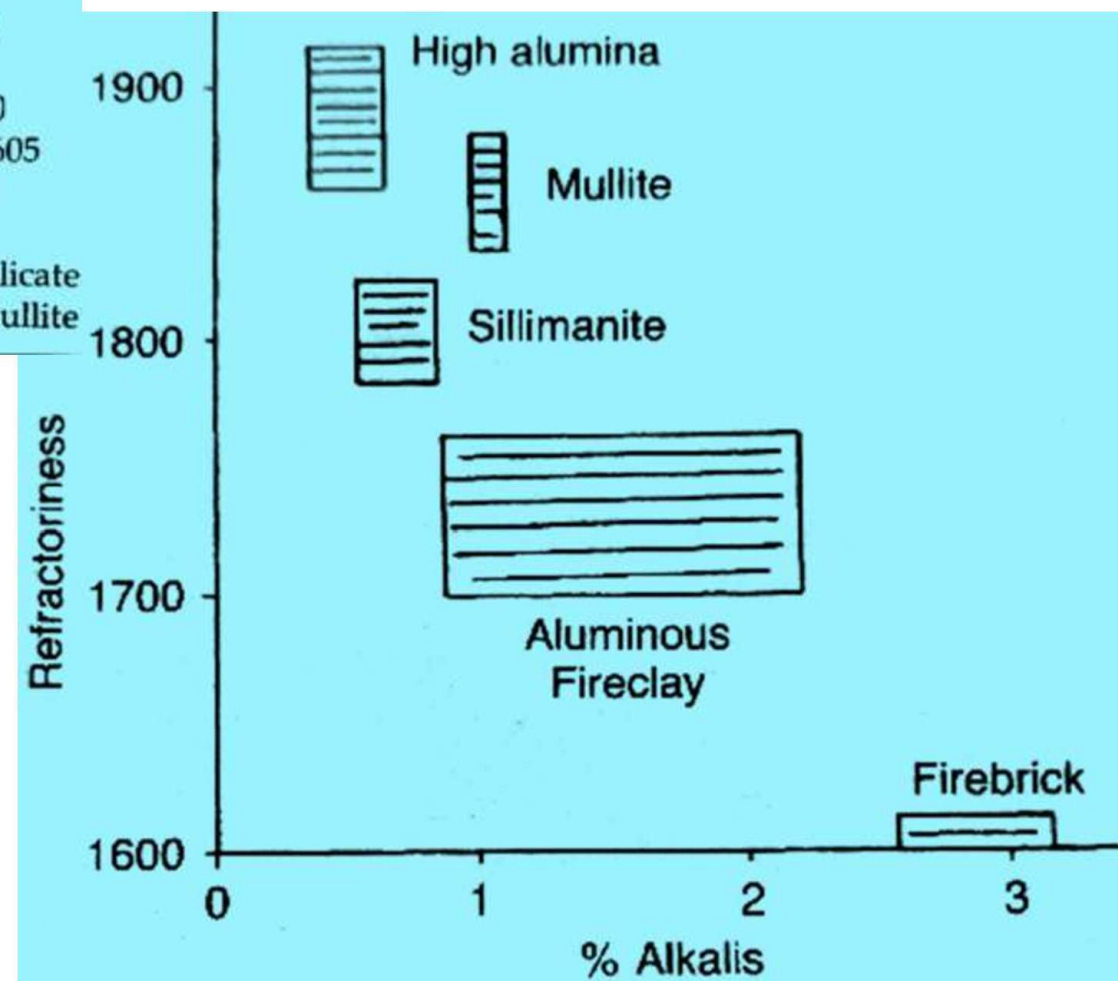
Refractoriness (°C)

1595–1605

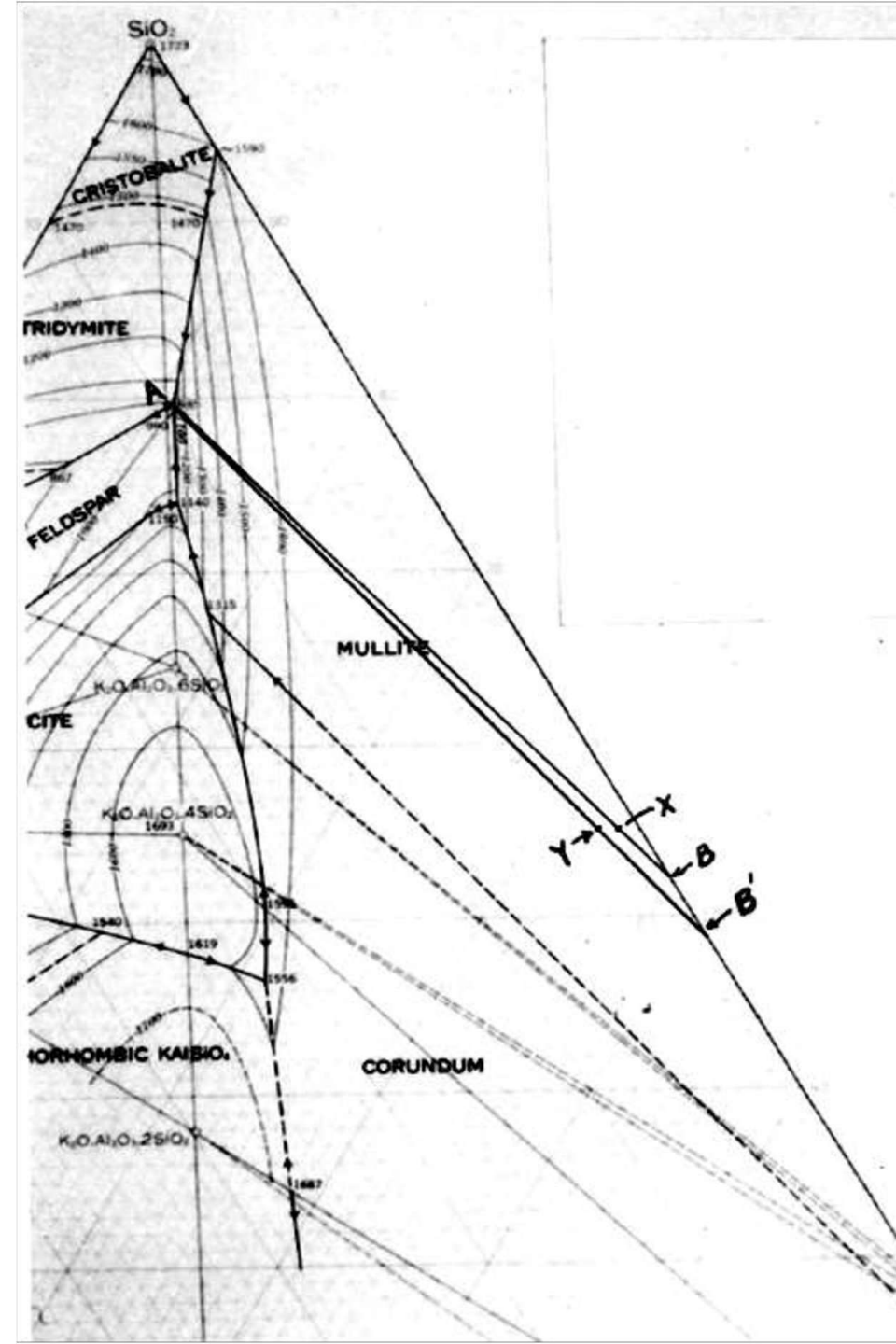
Thermal expansion ($\times 10^{-6} \text{ }^{\circ}\text{C}^{-1}$)
from 20 to 1200°C

5.1

Major phases

Aluminosilicate
glass, mullite

- A part of the phase diagram of the system K₂O-Al₂O₃-SiO₂
 - Compositions X and Y spotted thereon represent compositions of two otherwise pure clays in their fired condition. X contains 1 % K₂O whereas Y contains 2 % K₂O.
 - lie in the mullite field; first liquid to form; 985°C eutectic at point A.
 - X ~ 11.5% liquid; Y ~22.5% liquid
 - Y would deform to a greater extent; So; X=more refractory,
 - 2 % K₂O would require less fire, ~1200 C is sufficient.
 - 1 % K₂O ~1500°C might be required.



	Sillimanite	Mullite	Bauxite-based high-alumina
Composition (wt%)			
SiO ₂	39–42.5	23.2	6.5–9.5
Al ₂ O ₃	55.4–59	74.2	82.5–88.2
TiO ₂	0.3–0.5	0.2	2.4–3.5
Fe ₂ O ₃	1.0–1.2	0.7	1.5–2.0
CaO + MgO	0.2–0.3	0.1	0.4–0.5
K ₂ O + Na ₂ O	0.3–0.4	1.0	0.2–0.3

- Iron Oxide in A-S Brick should not be totally ignored.
- around 1.5 to 2%.
- Under oxidizing conditions: may not be seriously detrimental.
- FeO·Fe₂O₃-Al₂O₃-SiO₂ PD
- there is no liquid formed in this system much below 1400°C.

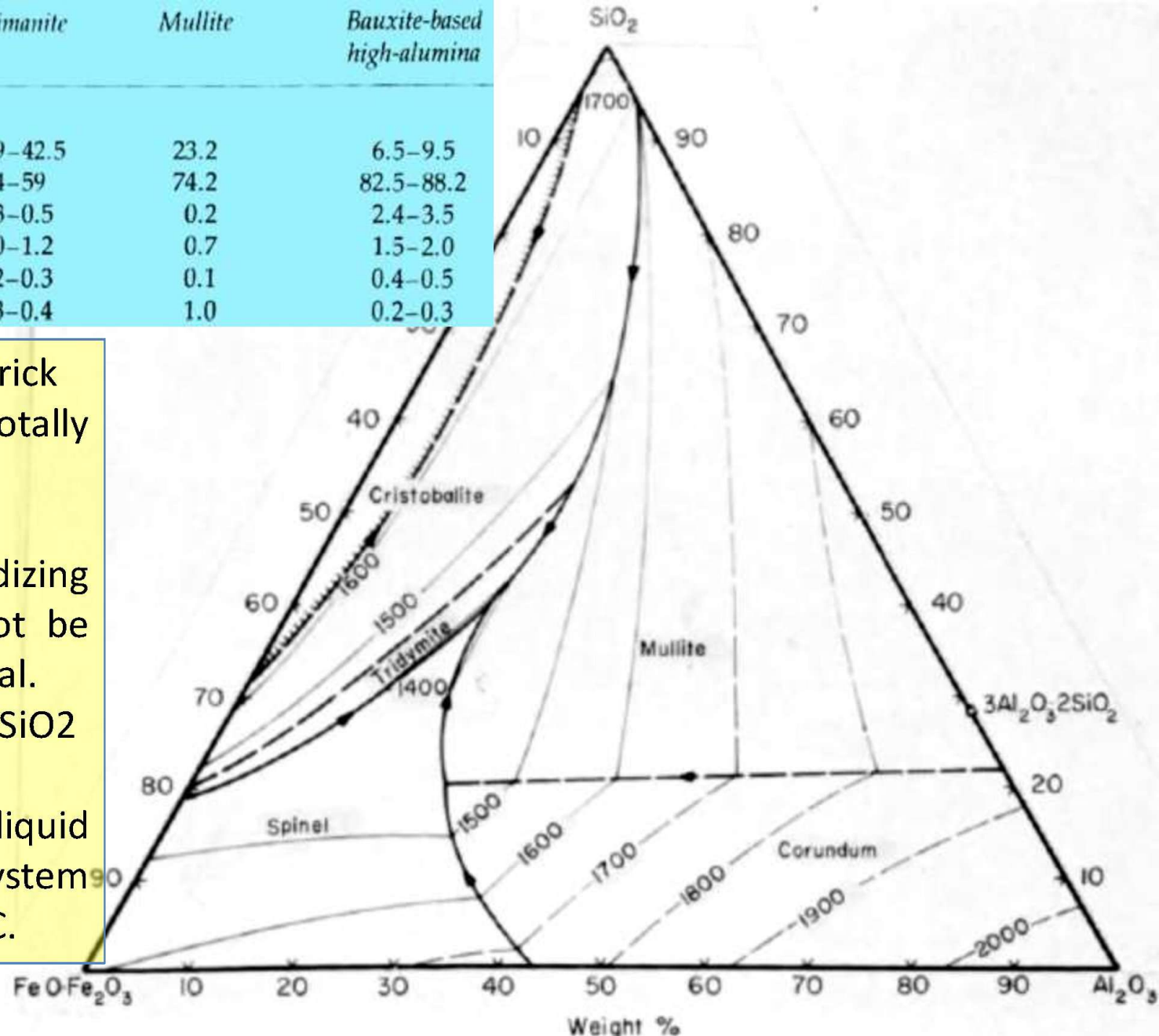
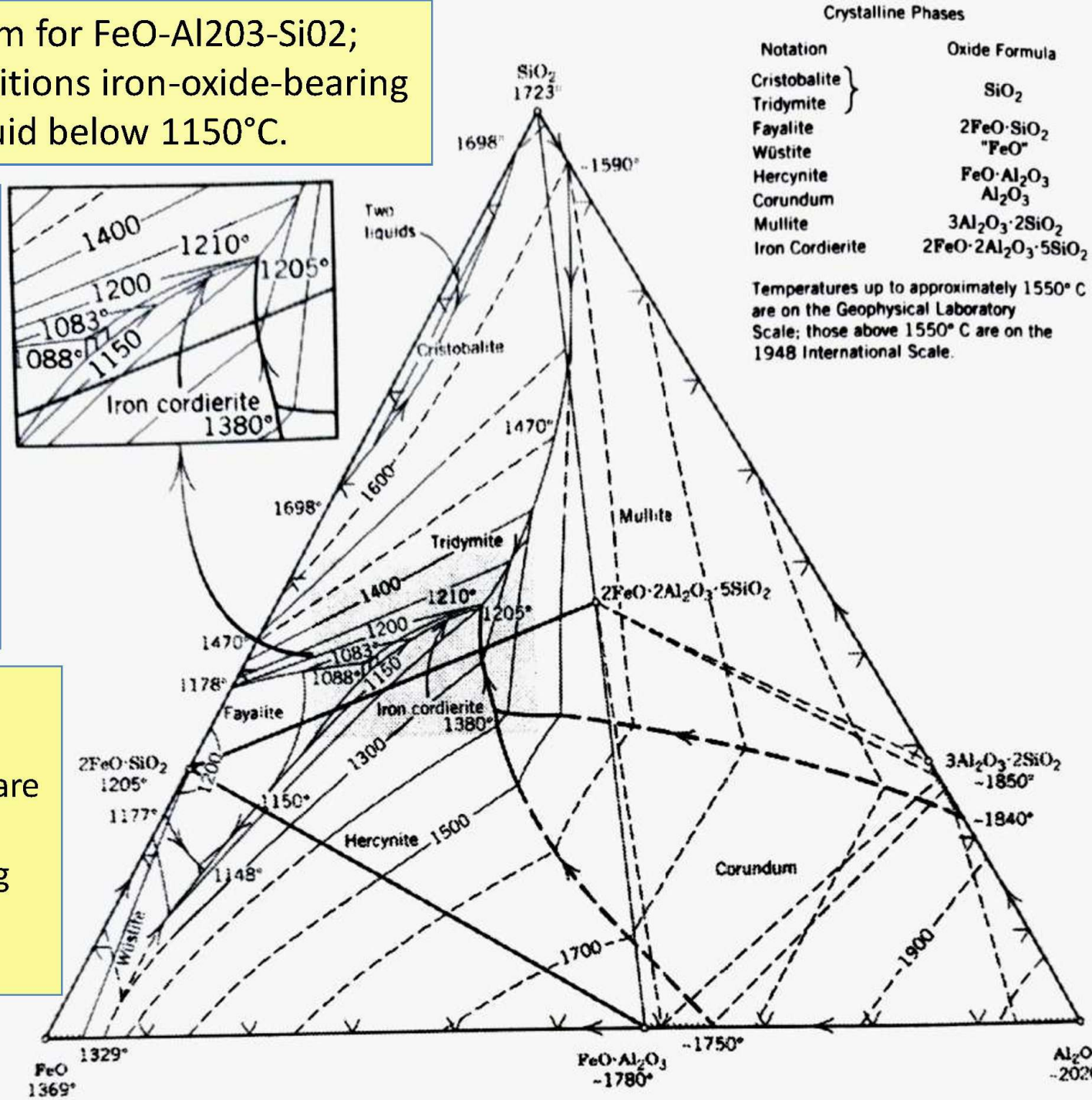


Fig. 5. Phase relations at liquidus temperatures in the system iron oxide-Al₂O₃-SiO₂ in air. Based mainly on Muan, (1957). Reprinted from Muan and Osborn (1965).

- However, the diagram for FeO-Al₂O₃-SiO₂; under reducing conditions iron-oxide-bearing brick will develop liquid below 1150°C.

Clay brick and other alumina-silica compositions are often employed in furnaces where **iron oxide appears as scale or dust**.: open-hearth checkers or reheating furnaces in the steel industry.

- **Advantage of high-alumina brick:**
Liquidus temperatures are generally higher in all compositions containing substantial amounts of alumina.



BASIC REFRactories Basic refractories are made almost exclusively from three raw materials: **magnesia, chrome ore, and dolomite.**

Lime: its tendency to hydrate in moist atmospheres and because it **reacts with iron oxide** at relatively low temperatures, its **use as a refractory is very limited.**

85 % basic refractories: in the steel industry : open hearths, basic oxygen vessels, and electric furnaces. other 15% : copper industry.

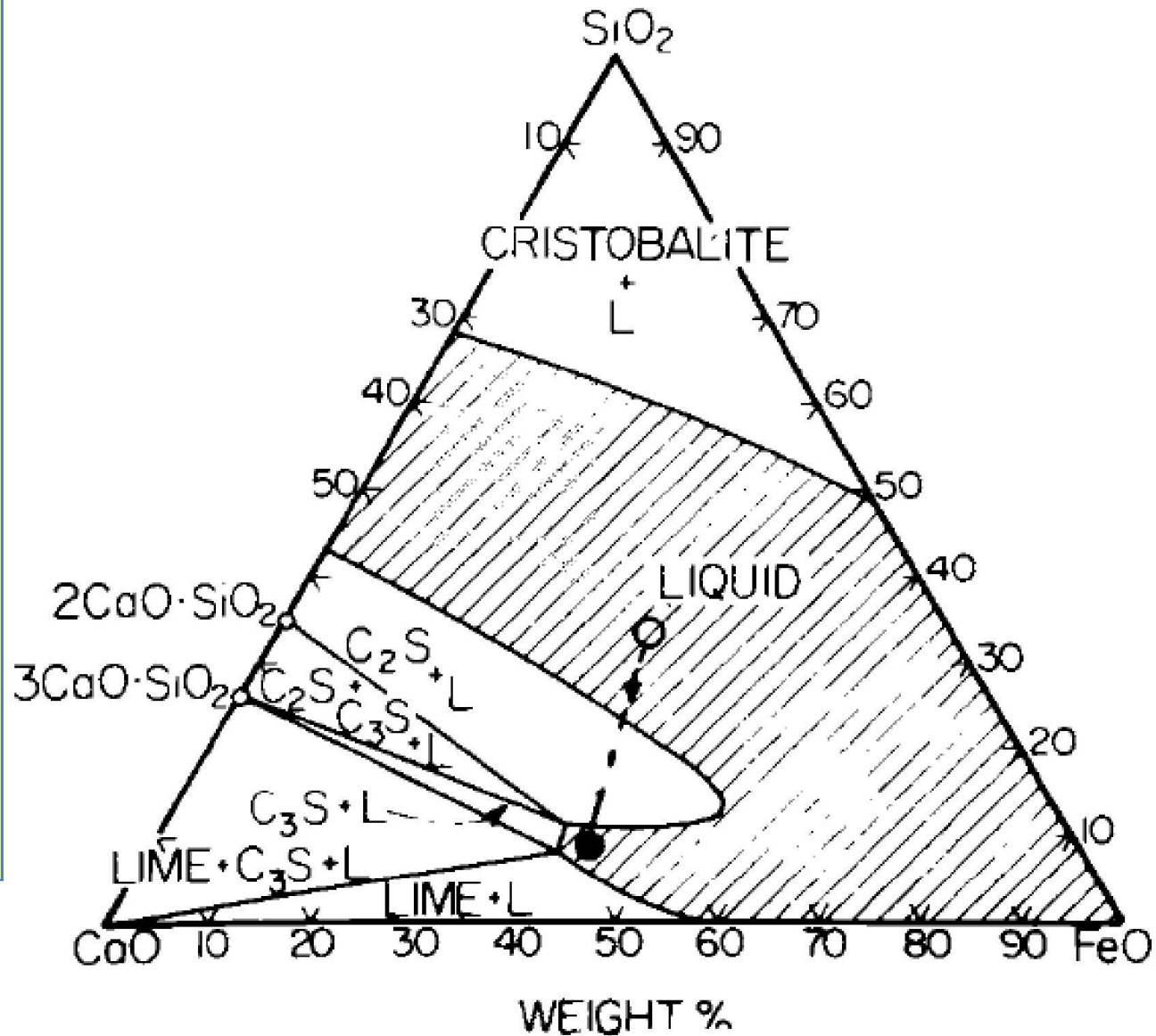
Table 2: Chemical composition and major phases of typical LD slag generated integrated steel plant in India

Blast furnaces: Basic refractories are unsuitable: Hydration due to water vapor or water that might result from a leak in the cooling system.
basic oxygen process: burns the carbon, silicon and manganese: basic slags developed
slags : lime, iron oxide, manganese oxide, magnesium oxide, and silica.

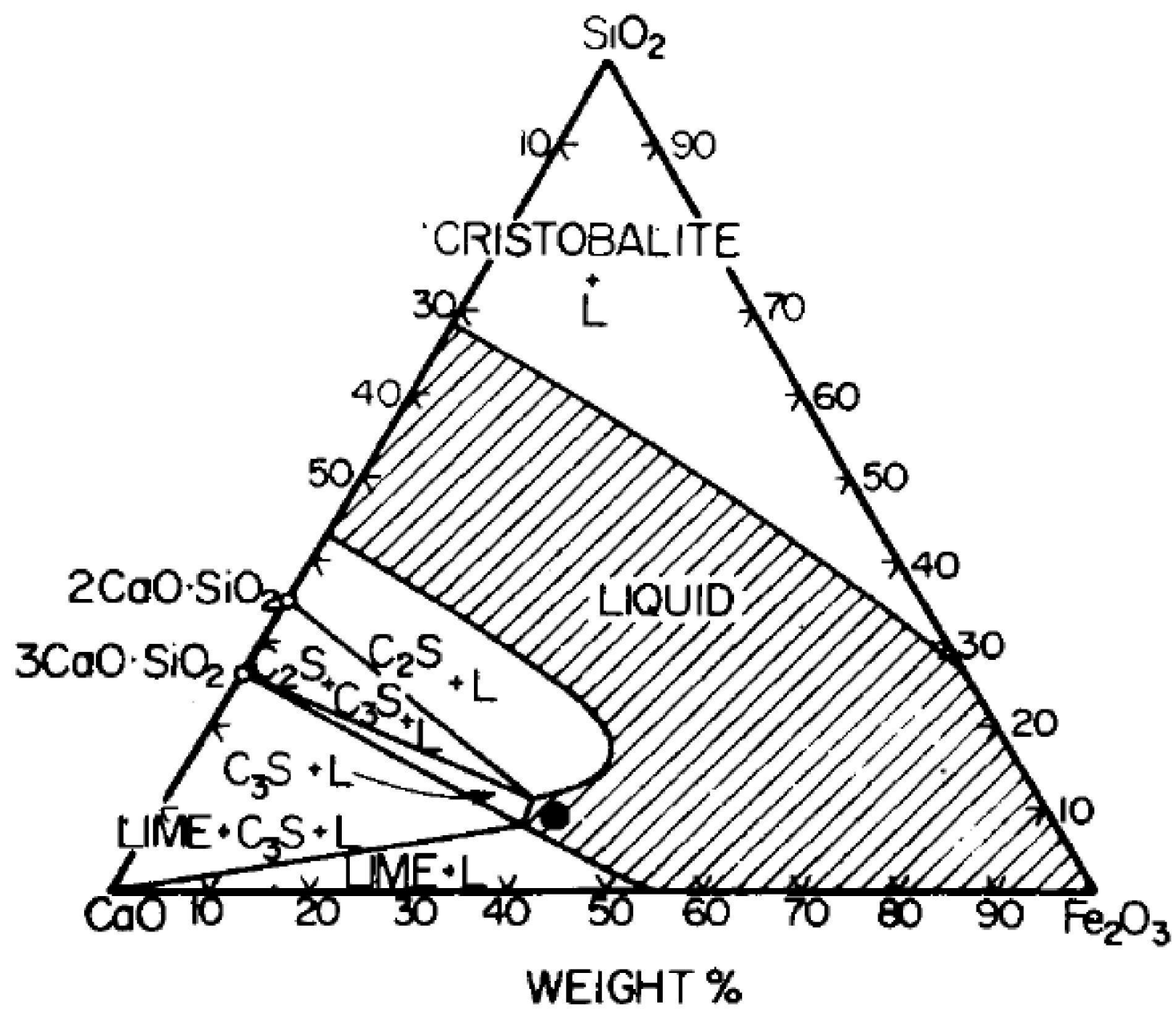
Chemical Composition	Major Phases and wt. %
SiO ₂ - 12.16%	Tricalcium silicate (C ₃ S), Ca ₃ SiO ₅ - 0–20%
Al ₂ O ₃ - 1.22%	Dicalcium silicates (C ₂ S), Ca ₂ SiO ₄ - 30–60%
FeO - 26.30%	Other silicates - 0–10%
CaO - 47.88%	Magnesiocalciowustite - 15–30%
MnO - 0.28%	Dicalcium aluminoferrite (Ca ₂ (Fe, Al, Ti) ₂ O ₅ - 10–25%
MgO - 0.82%	Magnesium type phase (Fe, Mn, Mg, Ca) O - 0–5%
P ₂ O ₅ - 3.33%	Lime phase (Ca, Fe) O - 0–15%
S - 0.28%	Periclase (Mg, Fe) O - 0–5%
Na ₂ O - 0.036%	Fluorite CaF ₂ - 0–1%
K ₂ O - 0.071%	-

Phase diagrams for lime-iron oxides and silica: slags which develop early; contain 35 % or more iron and manganese oxides.

Low lime-silica ratio of 1:1 or less; progress of the heat, lime enters the slag; final slags: lime-silica ratio as high as 3 or 4,

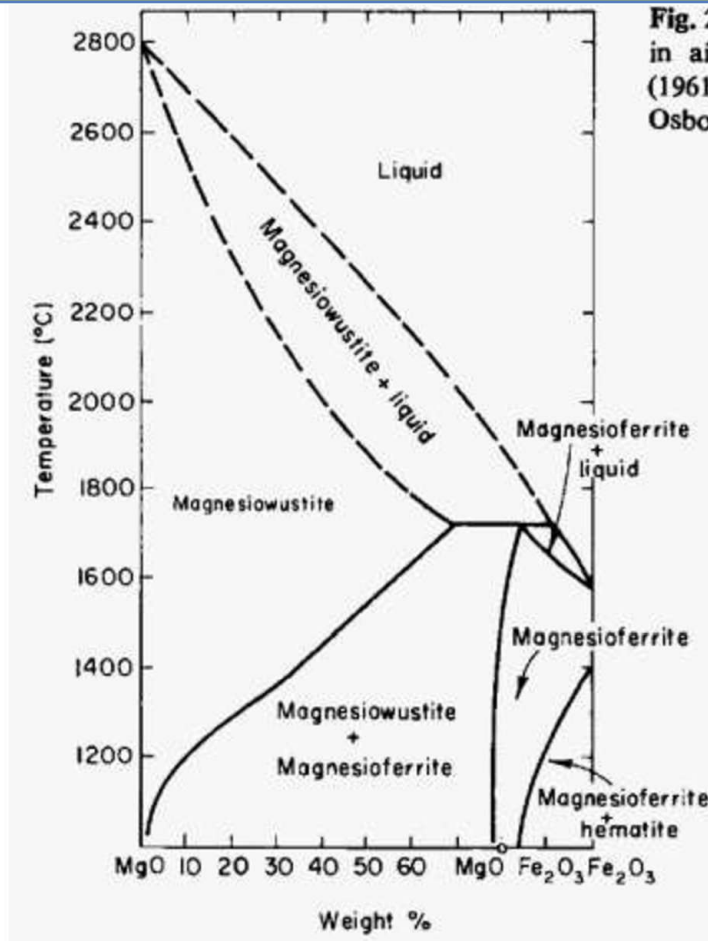
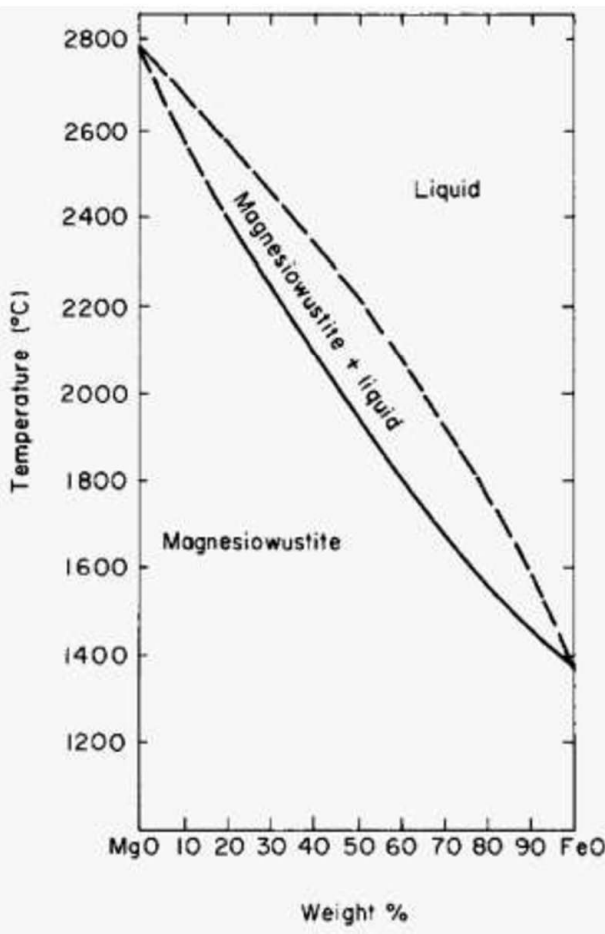


1600°C isothermal section in the system $\text{CaO}-\text{FeO}-\text{SiO}_2$ in contact with metallic iron. dotted line represents the course of approximate composition changes from early slag to finish slag.

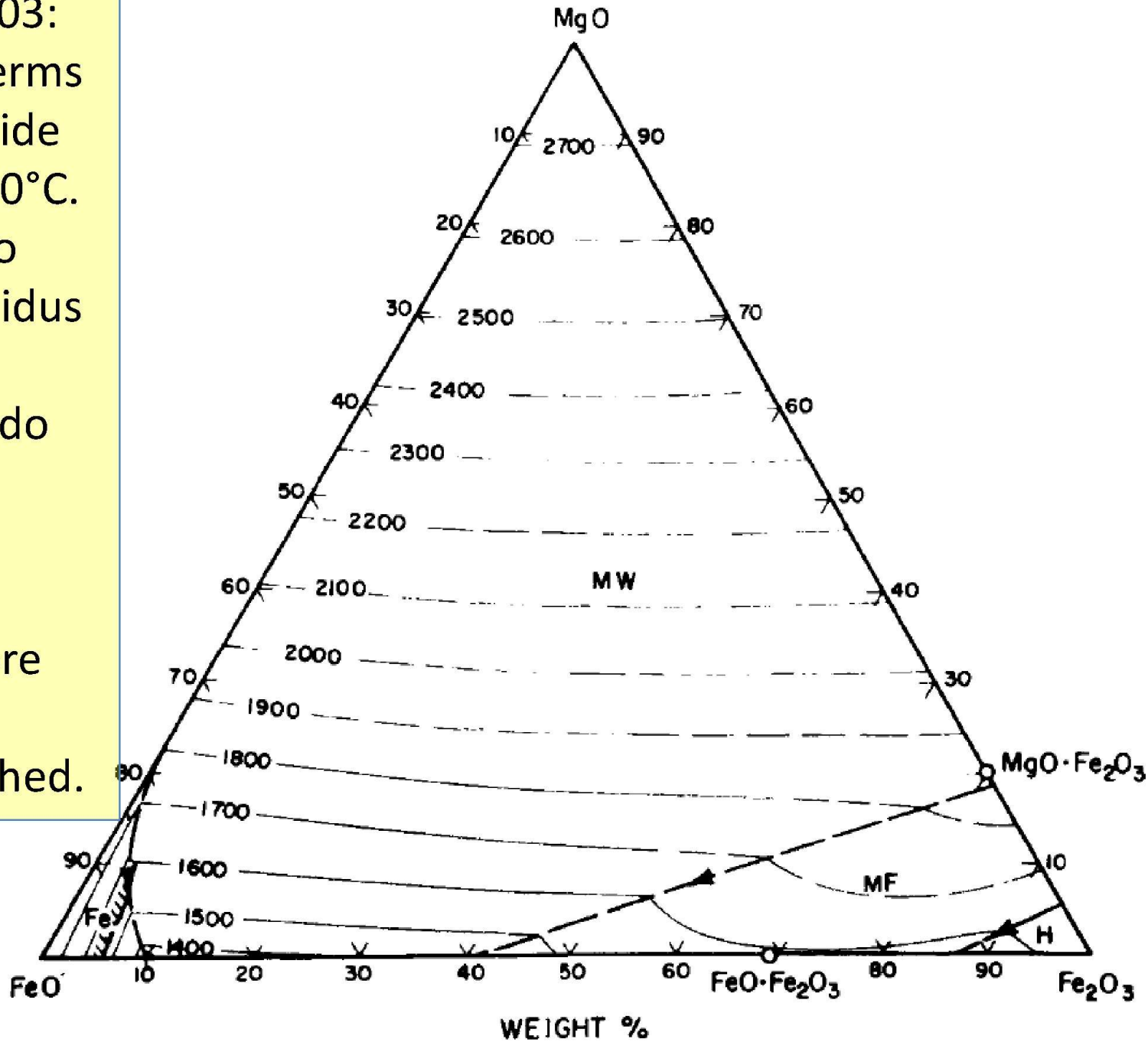


1600°C isotherm section in the system CaO -iron oxide-silica in air.

iron oxide is considered to be a universal high-temperature solvent for most mineral. Iron-rich basic slags: Magnesium and chromium oxides are resistant to the solvent action of iron oxide at high temperatures; important as refractories capable of absorbing 60% or more of iron oxide in solid solution and at the same time remain refractory: Phase diagrams for MgO-FeO, MgO-Fe₂O₃



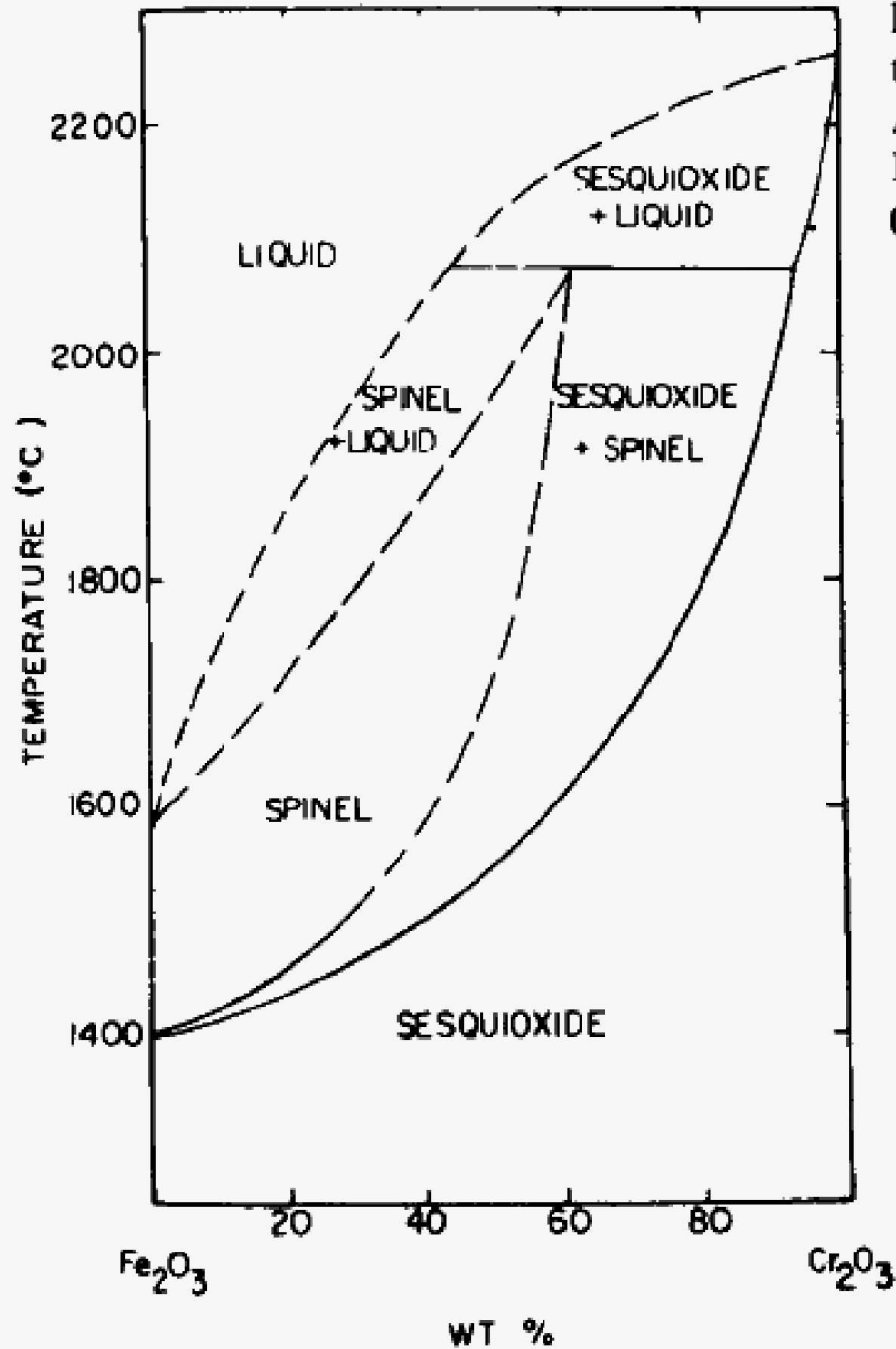
MgO-FeO-Fe₂O₃:
liquidus isotherms
at 60% iron oxide
are above 2000°C.
• diagrams also
show that liquidus
temperatures
in this system do
not fall below
1600°C until
compositions
containing more
than 80% iron
oxide are reached.



FeO-Fe₂O₃-Cr₂O₃:

Chromium oxide ably resists the fluxing action of iron oxide

Cr₂O₃ raises the liquidus continuously from that of Fe₃O₄ to well over 2200°C, the melting point of Cr₂O₃.



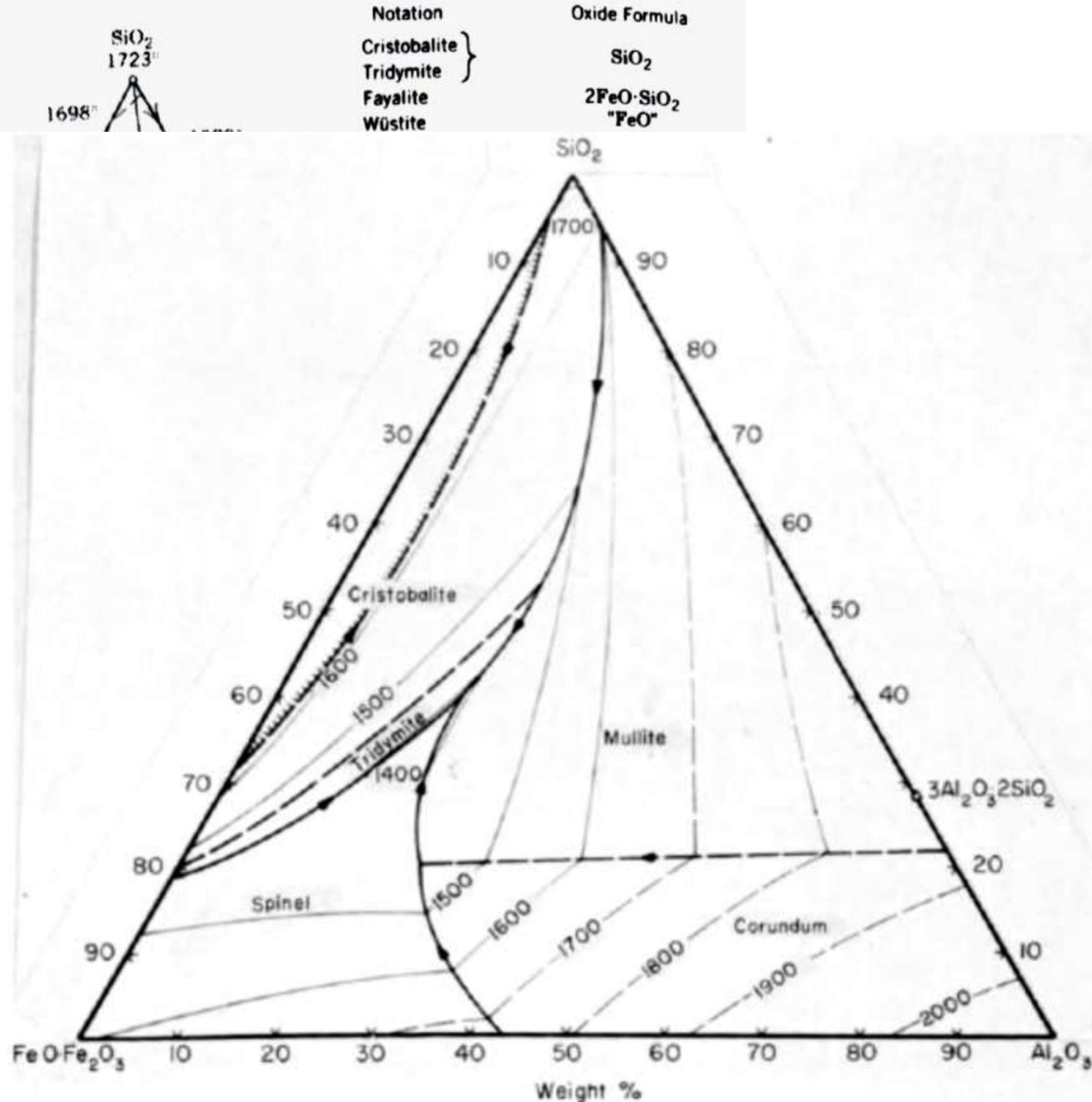
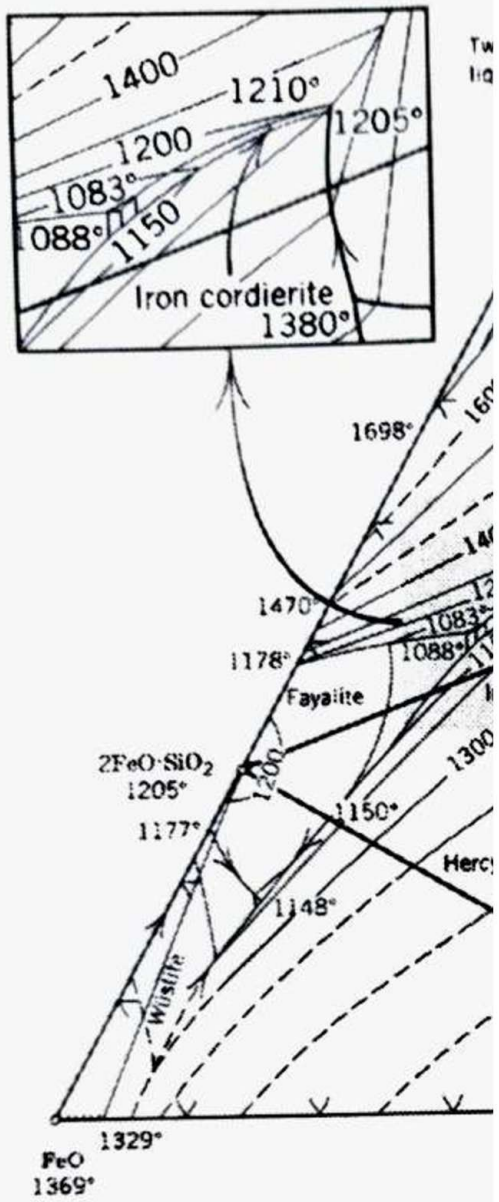


Fig. 5. Phase relations at liquidus temperatures in the system iron oxide- Al_2O_3 - SiO_2 in air. Based mainly on Muan, (1957). Reprinted from Muan and Osborn (1965).

Magnesia

Refractory: Dead

Burned MgO

powder+ Sulphite

Lye = Pressing @

100 Mpa -> Drying

@ <60 °C, controlled
humidity -> Firing @

1500-1900 °C Tunnel

Kiln; 3- 5 days: Brick
~ 15 vol% porosity. :

Used in Glass

Chequers, Sn-

melting Hearth,

Cement R.

Table 8.10 Typical properties of fired basic brick

Chemical analysis (wt%)

MgO 91–97

Fe₂O₃ 0.4–5

Al₂O₃ 0.1–2

CaO 1–3

SiO₂ 0.8–2

B₂O₃ <0.02

Apparent porosity (%) 12–20

Bulk density (g cm⁻³) 2.88–3.0

Cold crushing strength (MPa) 35–70

Thermal conductivity (W m⁻¹ K⁻¹) mean
at 900 °C 4

MOR (MPa)

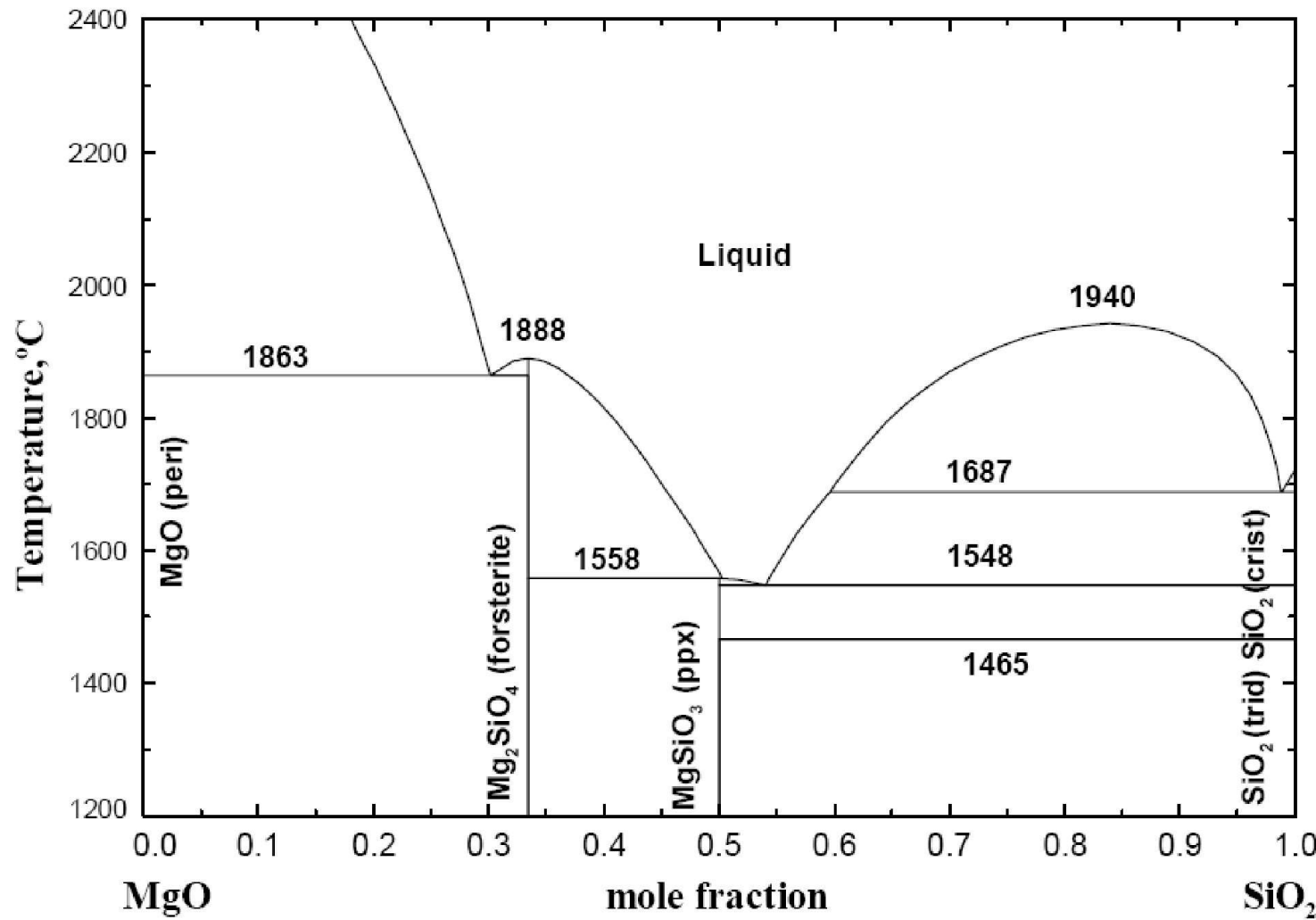
RT 15–20

1400 °C 0–15

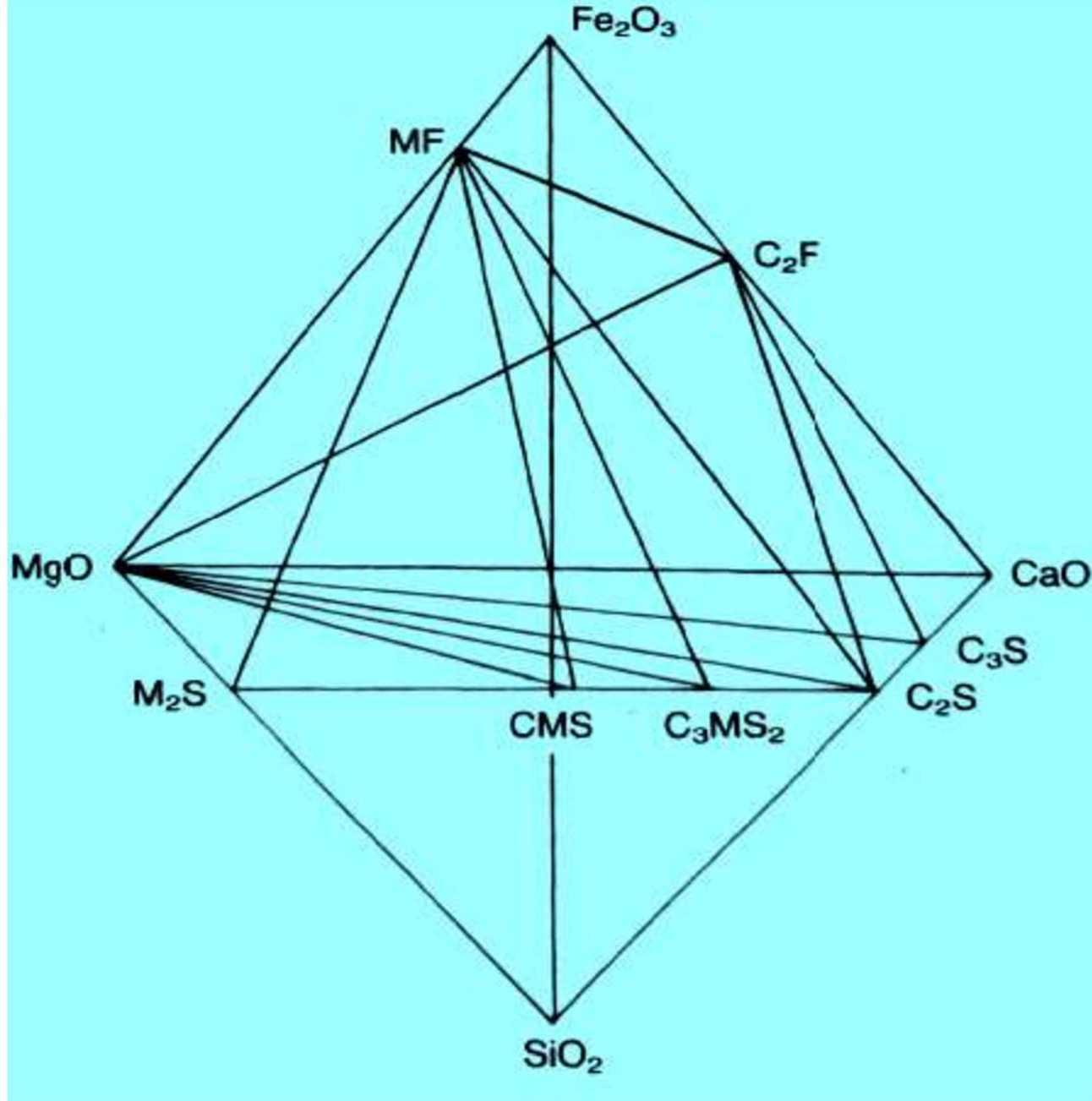
1600 °C 0–5

Magnesia Refractory: Impurities: SiO₂, Al₂O₃, Fe₂O₃, Cr₂O₃, FeO, CaO, B₂O₃:

Silicate Bonding: Low viscosity, compared to Silica Brick; MgO brick fails @10% liquid compared to 30% liquid in case of Silica brick



MgO-CaO-SiO₂-
Fe₂O₃ Phase
Diagram:
Secondary phases
are shown in the
diagram



Factors affecting properties: (a) C/S molar ratio of the bonding phase, (b) Impurity content, in particular B₂O₃, (c) Grain size of MgO

As the grain size increases, the penetration of slag through the grain boundaries can be minimised.

Table 8.11 Common second phases in basic refractories

<i>Mineral</i>	<i>Formula</i>	<i>Abbreviation</i>	<i>T_m (°C)</i>
Periclase	MgO	M	2800
Forsterite	2MgO.SiO ₂	M ₂ S	1890
Monticellite	CaO.MgO.SiO ₂	CMS	1495
Merwinite	3CaO.MgO.2SiO ₂	C ₃ MS ₂	1575
Dicalcium silicate	2CaO.SiO ₂	C ₂ S	2130
Dicalcium ferrite	2CaO.Fe ₂ O ₃	C ₂ F	1435
Magnesium ferrite	MgO.Fe ₂ O ₃	MF*	1750
Magnesio-chromite	MgO.Cr ₂ O ₃	MK*	2400
Spinel	MgO.Al ₂ O ₃	MA*	2135

* All have the spinel crystal structure and are mutually soluble.

C/S~1: a significant amount of liquid forms at relatively low temperature in the bond between the magnesia clinker as a consequence of the low melting point ($T_m = 1495$ C) of the CaOMgOSiO₂ composition, leading to a decrease in refractoriness.

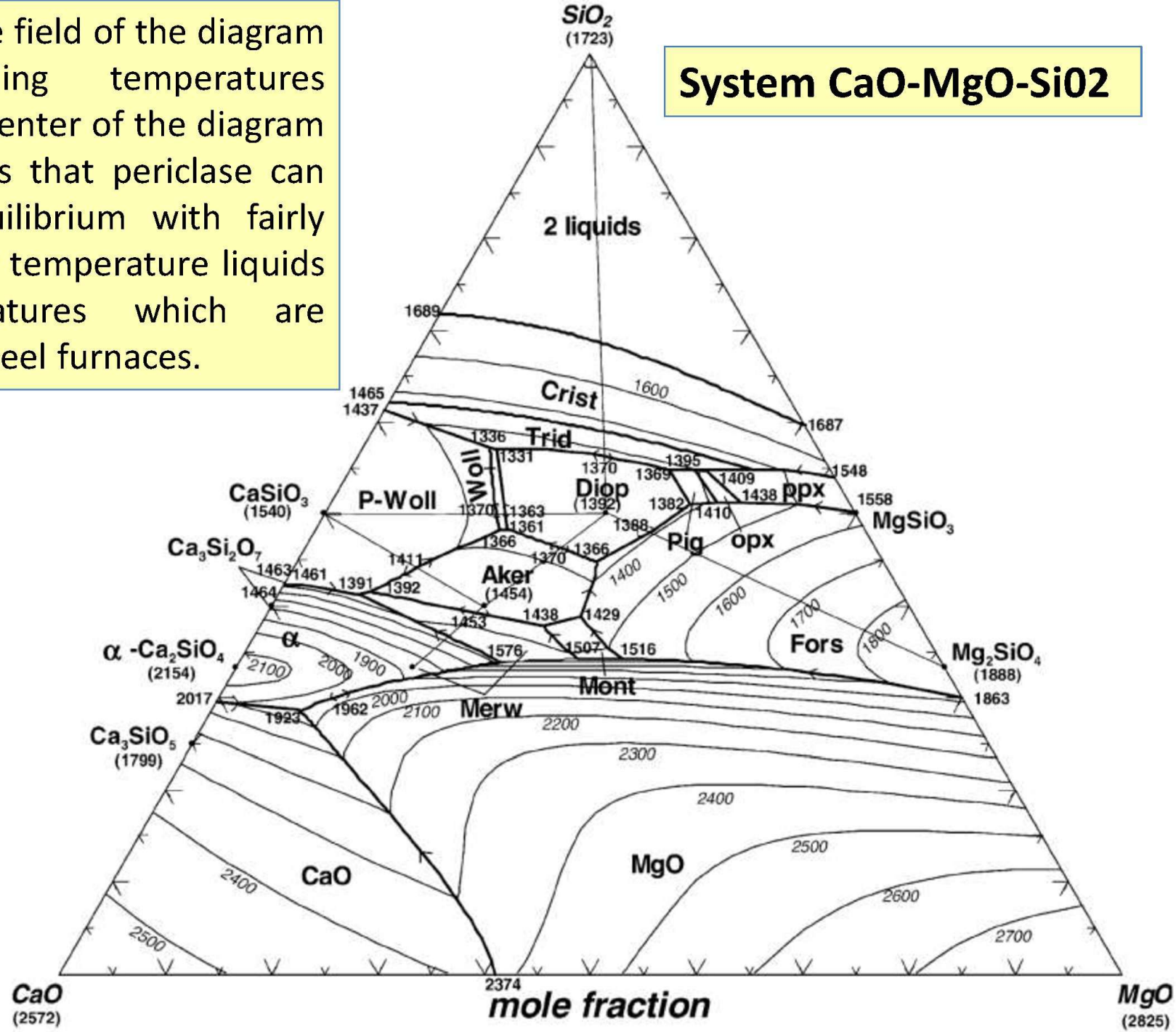
C/S: ~2 contains generally more refractory crystal phases such as 2CaOSiO₂ ($T_m = 2130$ C) and (3CaO.MgO.2SiO₂) ($T_m = 1575$ C) at grain boundaries on cooling

Table 8.12 Effect of CaO/SiO₂ ratio on the second phases found in basic refractories

<i>C/S ratio</i>	<i>Phase formed</i>	<i>Typical firing temperature (°C)</i>	<i>Comments</i>
<1	CMS, M ₂ S, (MA, MK, MF), MgO (ss)	1550	Towards C/S = 0 have M ₂ S, towards C/S = 1 form CMS liquid
1:1.5	CMS, C ₃ MS ₂ , (MA MK, MF), MgO (ss)	1600	Less CMS more C ₃ MS ₂
1.5:2	C ₂ S, C ₃ MS ₂ , (MA MK, MF), MgO (ss)	1700–1750	Increased refractoriness. Dusting from β-γ C ₂ S
≥2	C ₂ S, (C ₂ F, C ₄ AF, i.e. Ca phases), (MA, MK, MF), MgO (ss)		Low T_m Ca-phases form
>2 < 3	C ₃ S, (Ca phases), MgO (ss)		Close to Portland cement
>3	CaO, (Ca phases), C ₃ S, MgO (ss)		Free lime present, i.e. hydrating

The periclase field of the diagram shows falling temperatures toward the center of the diagram and indicates that periclase can exist in equilibrium with fairly siliceous low temperature liquids at temperatures which are attained in steel furnaces.

System CaO-MgO-SiO₂

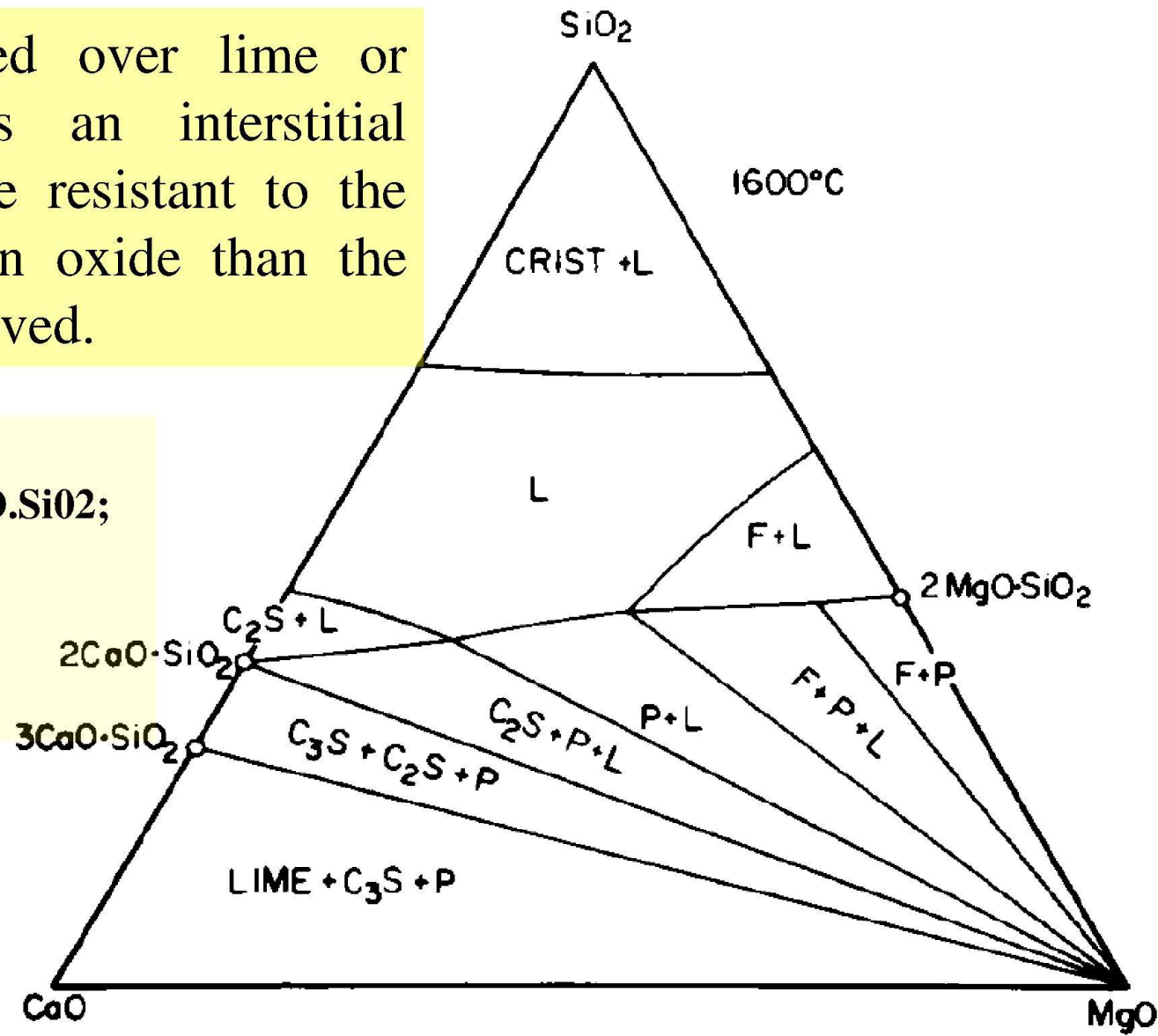


1600°C isothermal section of the system CaO-MgO-SiO₂

Periclase refractory: contains no liquid up to 1600°C: compositions would be selected from areas F + P and C3S + C2P + P or lime + C3S + P.

Forsterite is preferred over lime or calcium silicates as an interstitial mineral as it is more resistant to the fluxing action of iron oxide than the calcium silicates involved.

F is forsterite, 2 MgOSiO₂;
M is monticellite, CaO.MgO.SiO₂;
C₂S is 2CaO.SiO₂;
C₃S is 3 CaO.SiO₂;
P is periclase, MgO;
and L is liquid.



C/S: ~ 3 is used in commercial composition: as CaO has SS in MgO: so G.B. C/S ~2. B₂O₃ must be <0.02%: as it produce liquid @ 1200 oC. Sea-water MgO has higher B₂O₃.

MOR

Table 8.13 Variation of MOR at 1300°C with C/S ratio in basic bricks (Hancock, 1988)

<i>C/S ratio</i>	<i>Hot MOR (MPa)</i>
1.5	3.6
2.0	11.4–15
3.0	6.4

Too much liquid: Checker-works

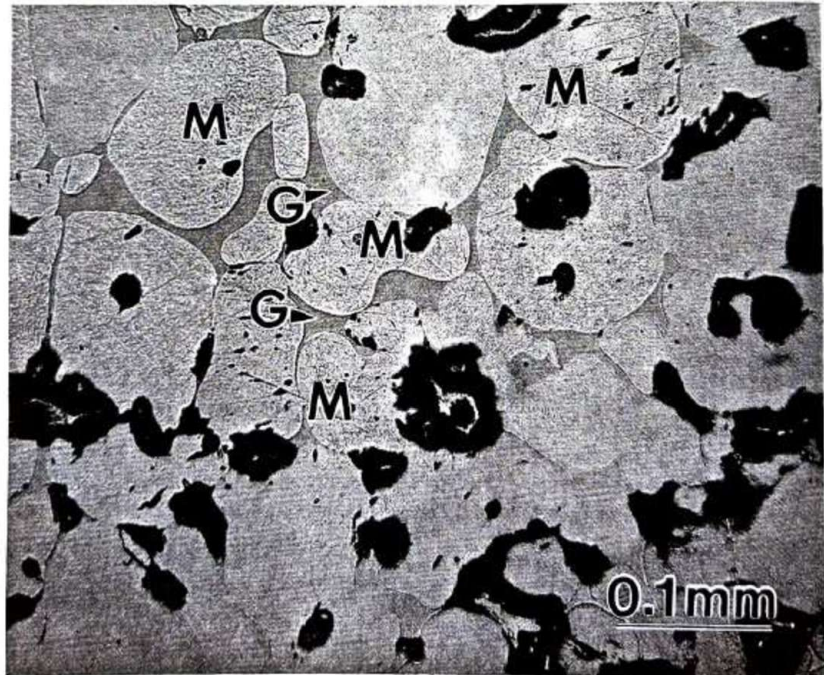


Fig. 8.10 Reflected light micrograph of unetched magnesia brick with $C/S \rightarrow 1$. Large MgO grains (M) are held together by a bond phase of small MgO grains in a CMS composition glass (G). The large amount of liquid formed is indicated by the rounded morphology of the MgO in the bond phase (lower figure). Black features are pores. (Micrograph courtesy of K. Pirt, Hepworth Refractories Ltd, Worksop, UK.)

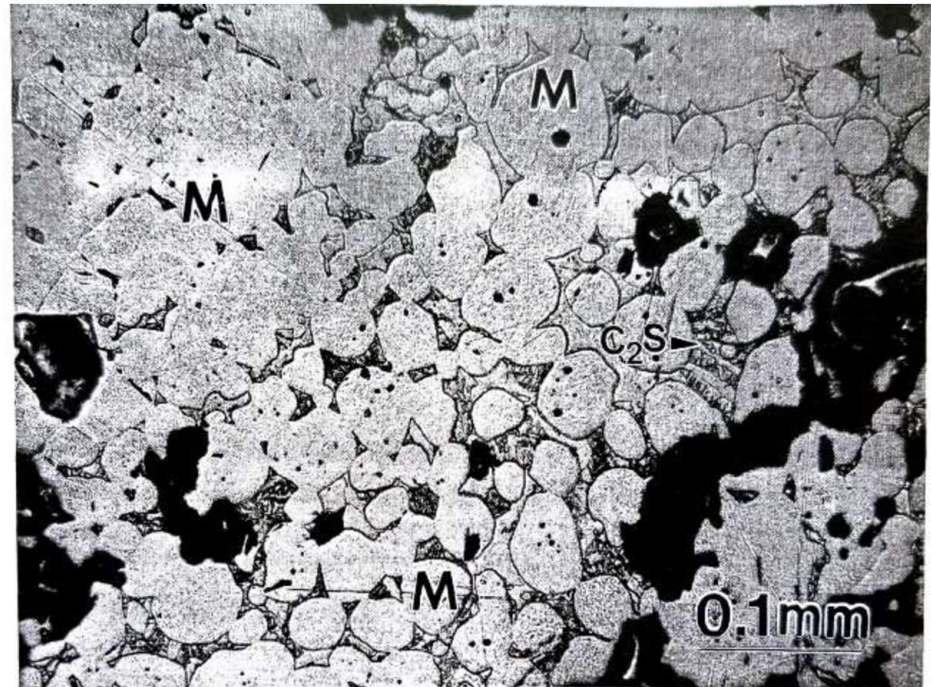


Fig. 8.11 Reflected light micrograph of unetched magnesia brick with $C/S \rightarrow 2$. The bonding phase between the MgO grains (M) is made up of glass and polycrystals of phases such as C₂S. (Sample supplied by R. Webster, Dyson Refractories Ltd, Sheffield, UK.)

Direct-bonded MgO-chrome (spinel) refractories

Silicate-bonded magnesia bricks: high thermal expansion coefficient coupled with poor thermal spalling resistance. When combined with chromium oxide: thermal shock resistance and other properties are improved. When the R₂O₃ content is above 15%, second phase bridges of spinel form between MgO and Cr₂O₃ grains, i.e. CrO₃ +MgO -» MgCr₂O₄, These bridges give direct bonding, i.e. solid-solid bonds of MgO-spinel, Cr₂O₃-spinel and spinel-spinel between the ceramic grains without any interrupting films of silicate, often termed spinel bonding.

Bricks are fabricated by three routes:

1. **High firing** in which MgO and Cr₂O₃ powders are mixed, pressed and fired about 1700°C.
2. **Prereacting or presintering** where fine, lightly calcined MgO and Cr₂O₃ ore are pressed to pellets and prefired at 1800°C to get all the chromia in solution before crushing and resintering at 1700°C or Lower.
3. **Prefusing** where the MgO and Cr₂O₃ are melted, cooled and crushed to give a fused grain which is sintered at 1700°C.

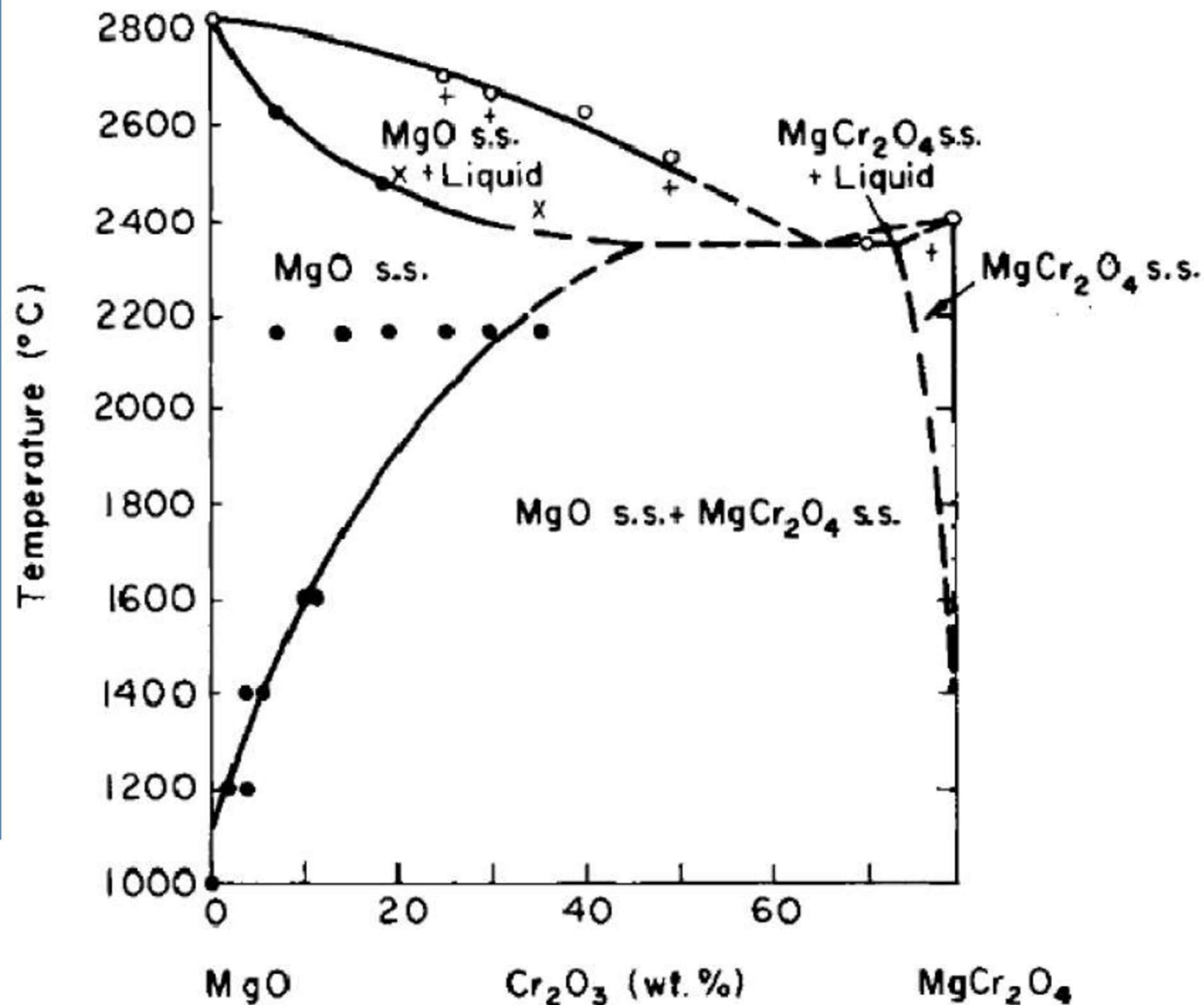
Silica content must be kept <3% or else a silicate liquid forms around the spinel so isolating the spinel bond and losing its beneficial effect on properties.

Direct-bonded MgO- MgAl₂O₄ spinel refractories:

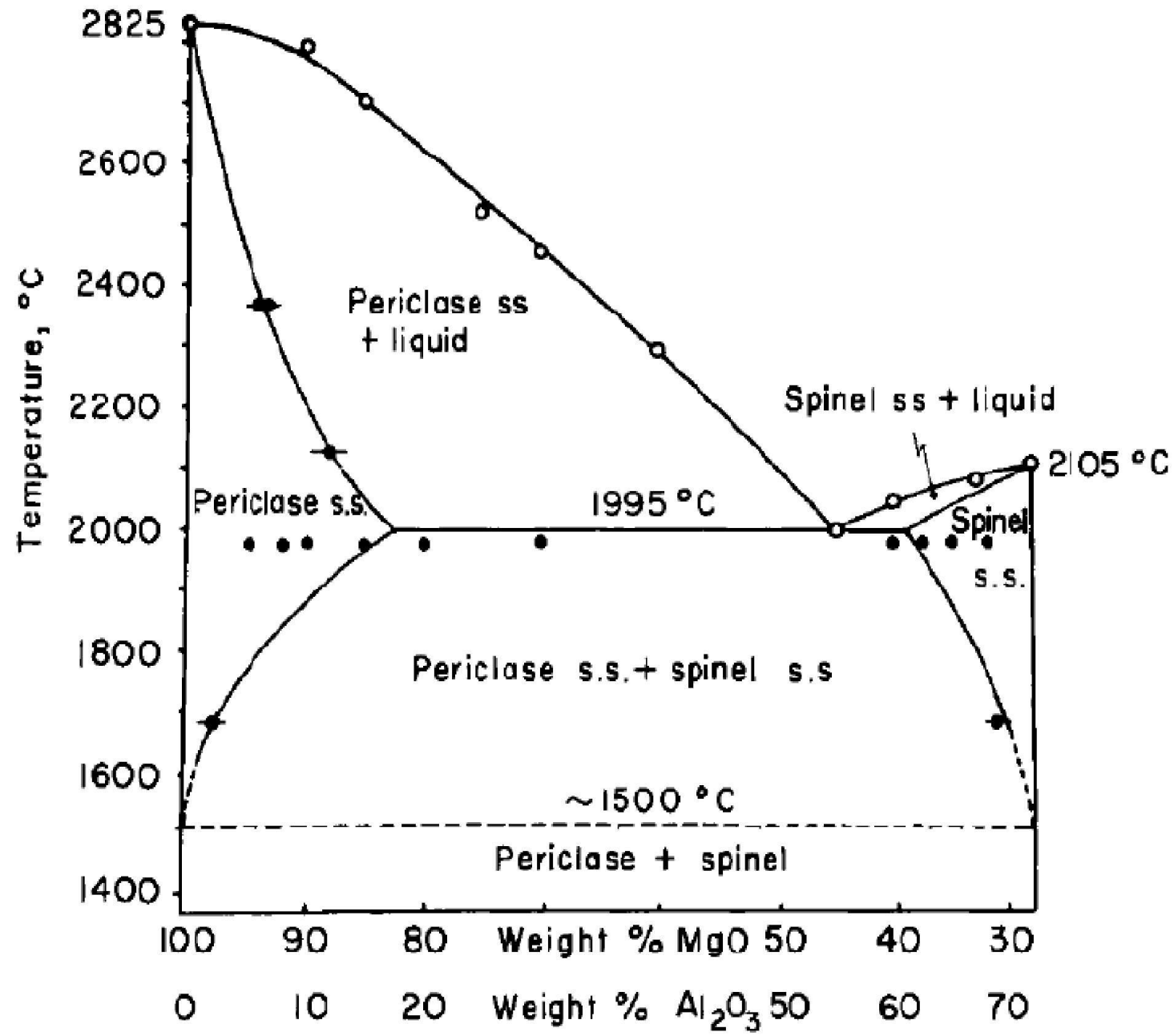
Recent legislation on the disposal of Cr-containing materials has led to development of MgAl₂O₄ spinel-bonded MgO bricks with improved strength at high temperature and better thermal shock resistance than MgCr₂O₄-bonded bricks.

The most commonly used processing route is to add preformed MgAl₂O₄ spinel to the MgO grain prior to firing.

Figure, show that the formation of solid solution of spinels and periclase is appreciable when samples are fired in the temperature range of normal refractory firing processes, namely, 1400°C to 1600°C.



The contact of the grains of periclase and the spinel permits ion migration and the formation of strong solid solution bonds.



Sintering of Al₂O₃: MgO additive: APD

- A small additions of MgO (0.25 wt%) to Al₂O₃ produced polycrystalline **translucent alumina** with theoretical density at 1700-1800 C in H₂ atmosphere (**Lucalox: Coble-1961**).

The specific mechanisms; microstructural homogenizer:

1. MgO reacts with Al₂O₃ to form **MgAl₂O₄**, which pin the boundaries and prevent abnormal grain growth.
2. MgO in solid solution segregates at the grain boundaries and reduces the boundary mobility by a **solute-drag mechanism**, thereby preventing abnormal grain growth.
3. MgO in solid solution enhances the densification rate through an increase in the lattice diffusion coefficient for Al ions that are believed to be the rate-controlling diffusing species.

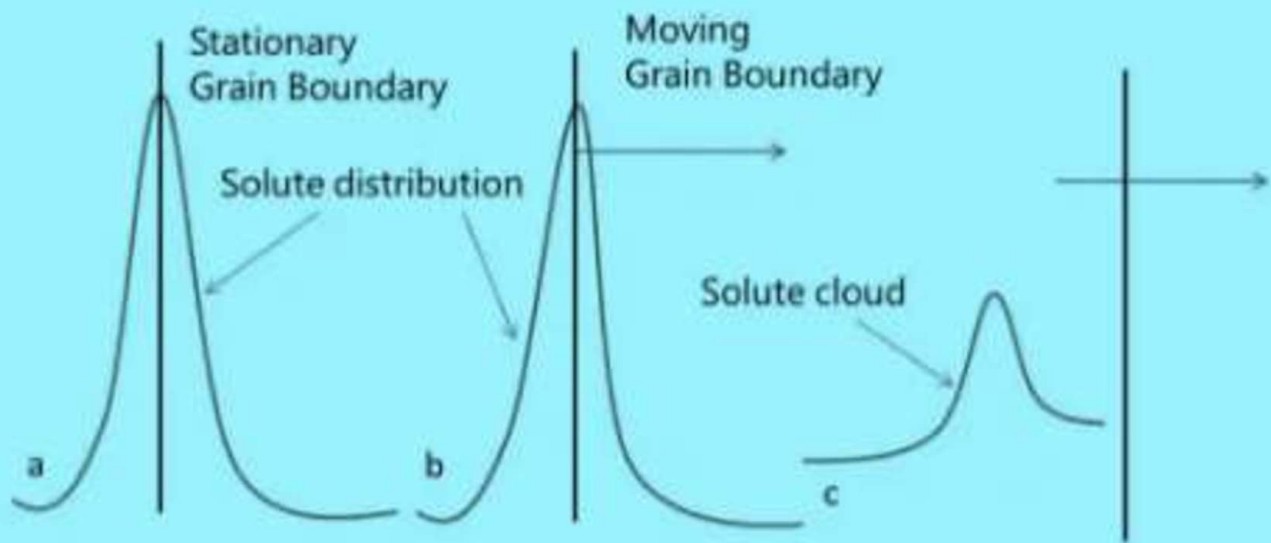
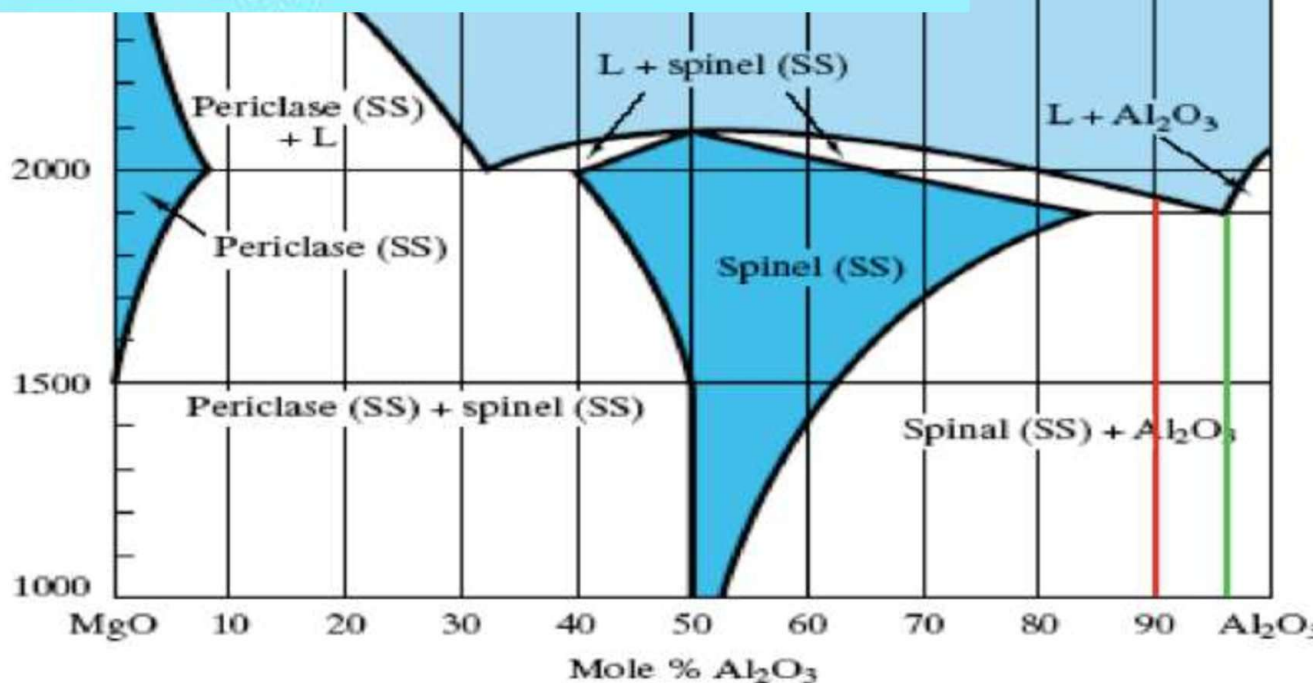


Figure : Distribution of the solutes across the boundary (a); Asymmetric distribution due to a moving boundary (b); Left out solute cloud and boundary break away event approaching the mobility of a clean boundary (c).



Carbon-bonded Basic Bricks:

Doloma (Mg,Ca)O fired or carbon-bonded is often used in Europe in place of MgO. **Pitch is added** to the fired ore and mixture **heated to 100°C to soften the pitch, pressed at 100 MPa and tempered at 400 °C** to carborize the pitch, stabilized the structure and remove volatiles. The bricks are fired in situ. On firing in reducing atmosphere the pitch further reacts to provide **carbon bonding**.

- Oxide-graphite bricks have now replaced the traditional aluminosilicate and basic bricks in many applications and may contain **4- 30 wt% natural graphite** as well as **carbon from the pitch bond** or additional **carbon black**. 20wt% graphite is $\sim 50\text{vol\%}$ (due;low density).
- **Phenolic resin binders** based on cross-linked synthetic polymers may be used in place of pitch to counter the carbon bond since some pitches produce carcinogenic fumes on preheating.
- **MgO-graphite (Graphite content 5- 20 wt%)** is used in BOF and EAF steelmaking furnace linings. MgO-Gr. Has replaced fired magnesia and unfired doloma bricks in BOF furnace.

Purpose of steel making

- Pig iron usually contains 3-4% of carbon, 2-4% of silicon, 1-2% of manganese and 1-1.2% of phosphorous.
- which makes it very brittle and not useful directly as a material except for limited applications
- Primary Steel making is about refining pig iron to reduce these impurity amounts
- Typical MS composition

Carbon	0.16-0.18%
Silicon	0.40% max
Manganese	0.70-0.90%
Sulphur	0.040% Max
Phosphorus	0.040% Max

Why basic lining?

- The refining of the impurities specially P and S require the slag to be basic in nature.
- If the slag is not basic, these elements cannot be kept in the slag and revert back into the melt
- Thus most modern steel refining operations utilize a basic process, i.e create a basic slag, by adding fluxes appropriately
- If the refractory lining of the furnace is not basic as well then the slag and lining will react with each other, causing unacceptable lining wear

The Basic Oxygen Practice

This process produces steel at a spectacular rate of over 300 tons/hr; carried out in the refractory-lined-vessels resembling a top-blown Bessemer converter. The vessel is tilted for charging and for discharging the final product. The **charge is ~ 30% scrap and 70% liquid metal** from a blast furnace. **Limestone** containing a small percentage of dolomite is also charged as a **requisite to form slag**.

- **Oxygen is blown through water cooled lances** to burn the silicon and carbon and some iron to carry on the process.
- As the process requires basic slags to remove sulfur and phosphorous, the slags and their chemistry and functions are almost identical to those of the open hearth slags. The refractories that line the furnace must withstand the chemical attack of basic slags.
- The BOF employs calcined or sintered dolomite and magnesite or combinations of the two.
- These combinations may be fired or not, but for most of the lining, tar or pitch bonds and graphite play an important part in the life of the vessel lining.

Presence of high levels of carbon in MgO and doloma refractory improve their properties and resistance to slag attack. Suggested mechanisms of carbon are :

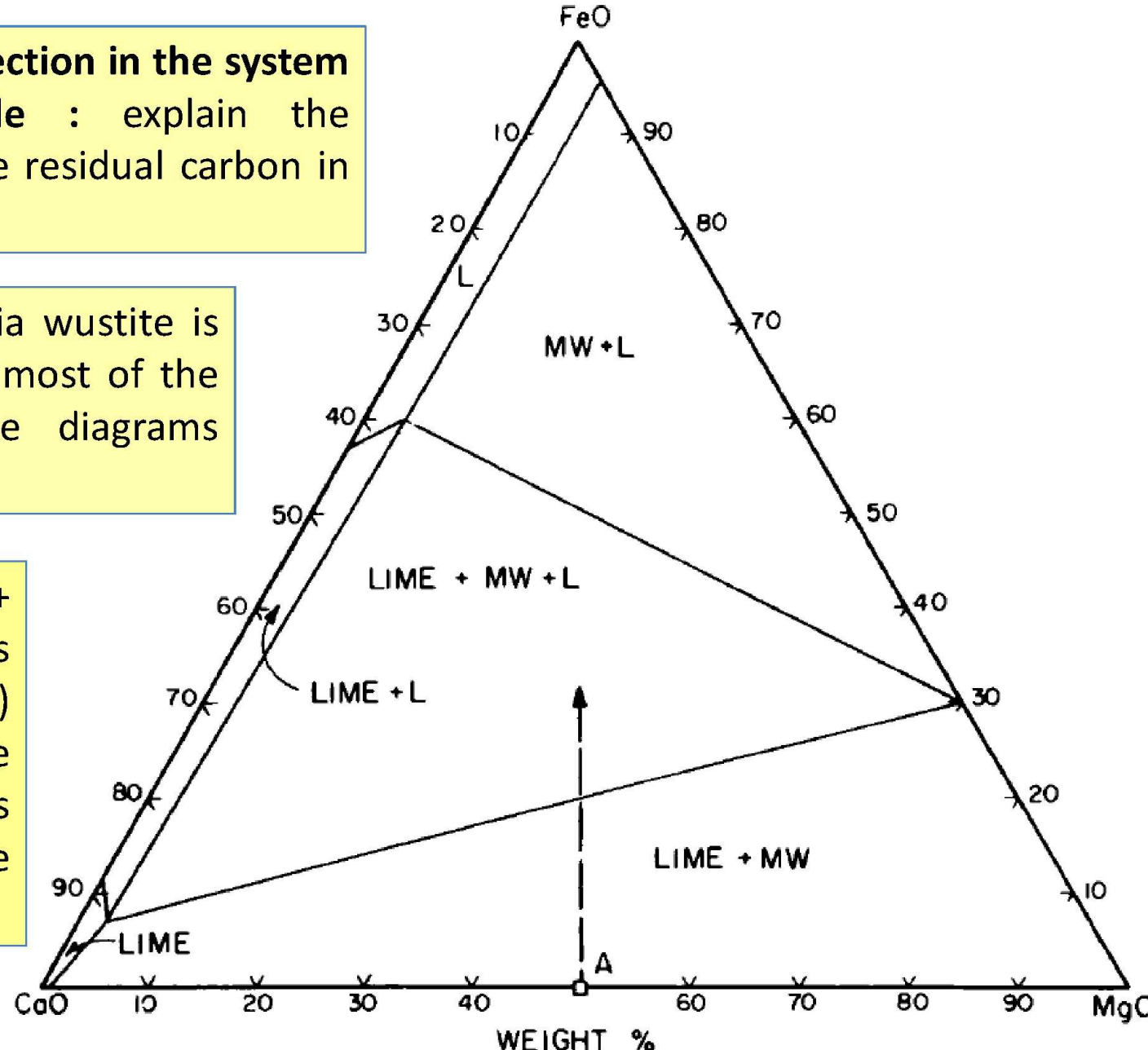
- C is **non-wetting** for most molten metals and slags and so liquid infiltration and slag attack is reduced.
- C reduces, for example, MgO to Mg vapour at high temperature which re-oxidizes and deposits as a dense layer of secondary periclase at slag-brick interface which prevent slag/metal ingress.
- C reduces iron oxide to FeO and then Fe metal so that it does not attack the MgO-CaO and form low melting phases.
- CO gas (form on oxidation of carbon) and /or Mg vapour (from reduction of MgO) provide and over-pressure which resists slag/metal ingress.

1500°C isothermal section in the system

CaO-MgO-iron oxide : explain the important role of the residual carbon in the refractory

Area lime + magnesia wustite is very broad whereas most of the other areas of the diagrams contain some liquid.

The large area lime + MW (lime plus magnesia wustite) are the result of the reducing conditions provided by the carbon

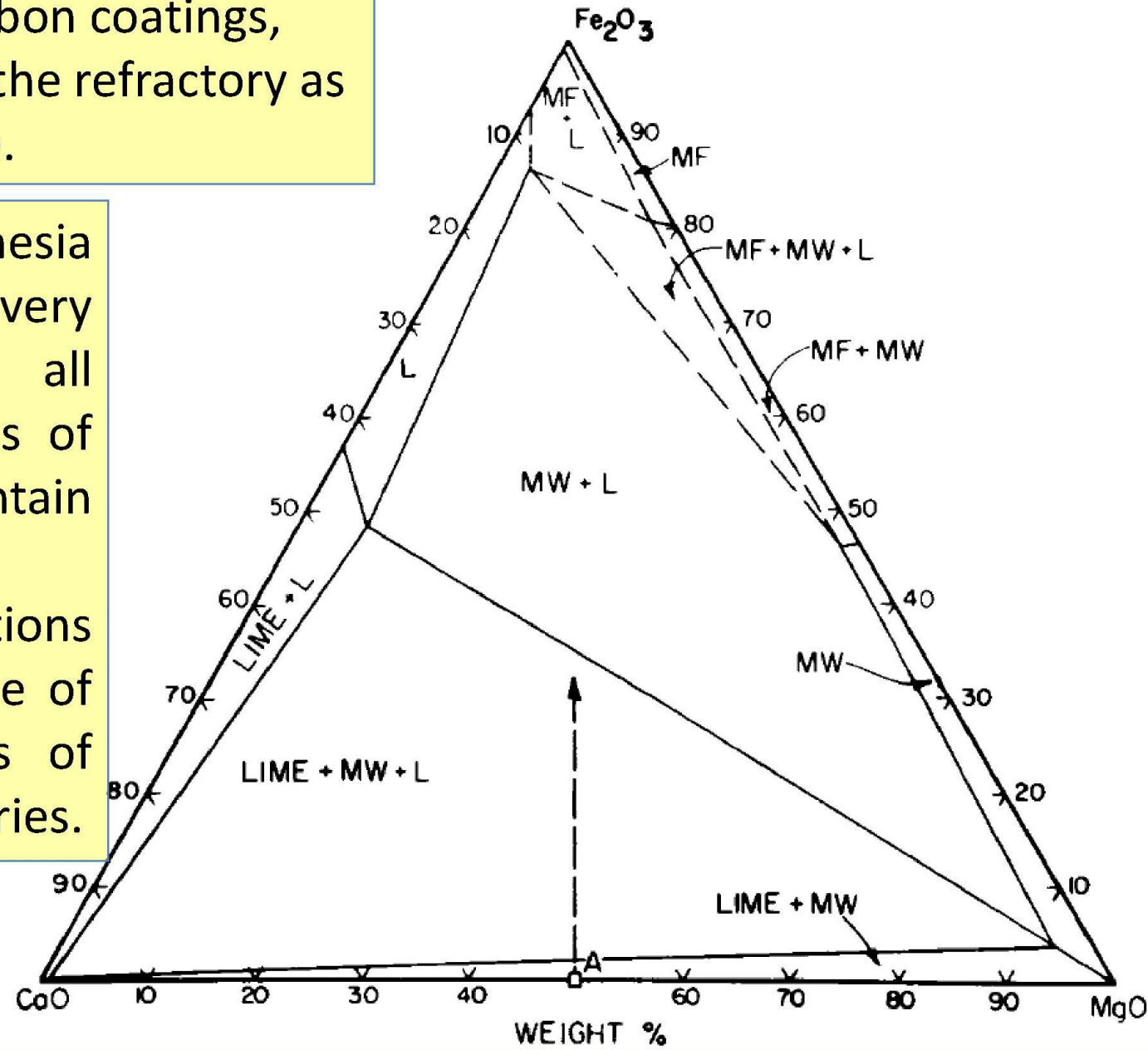


1500°C isothermal section in the system **CaO-MgO-iron oxide**

Without these carbon coatings,
conditions within the refractory as
indicated in Figure.

lime + magnesia
wustite area is very
restricted and all
other major areas of
the system contain
liquid.

These conditions
favor rapid decline of
the refractoriness of
dolomitic refractories.



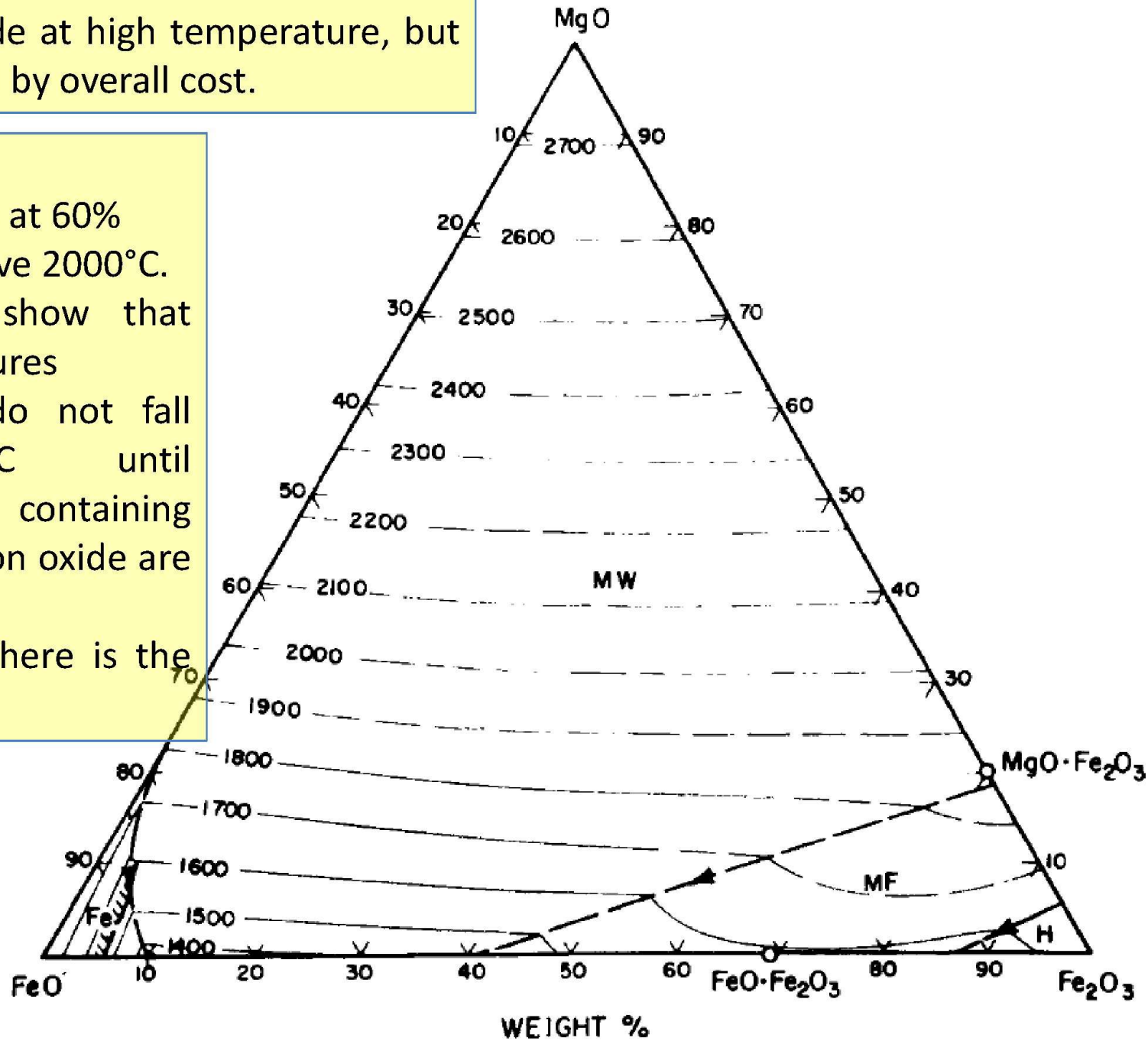
1500°C isothermal section in the system CaO-MgO-iron oxide in air

Magnesite is known for its resistance to the action of iron oxide at high temperature, but its use is governed by overall cost.

MgO-FeO-Fe₂O₃:

liquidus isotherms at 60% iron oxide are above 2000°C.

- diagrams also show that liquidus temperatures in this system do not fall below 1600°C until compositions containing more than 80% iron oxide are reached.
- In FeO corner, there is the formation of Fe

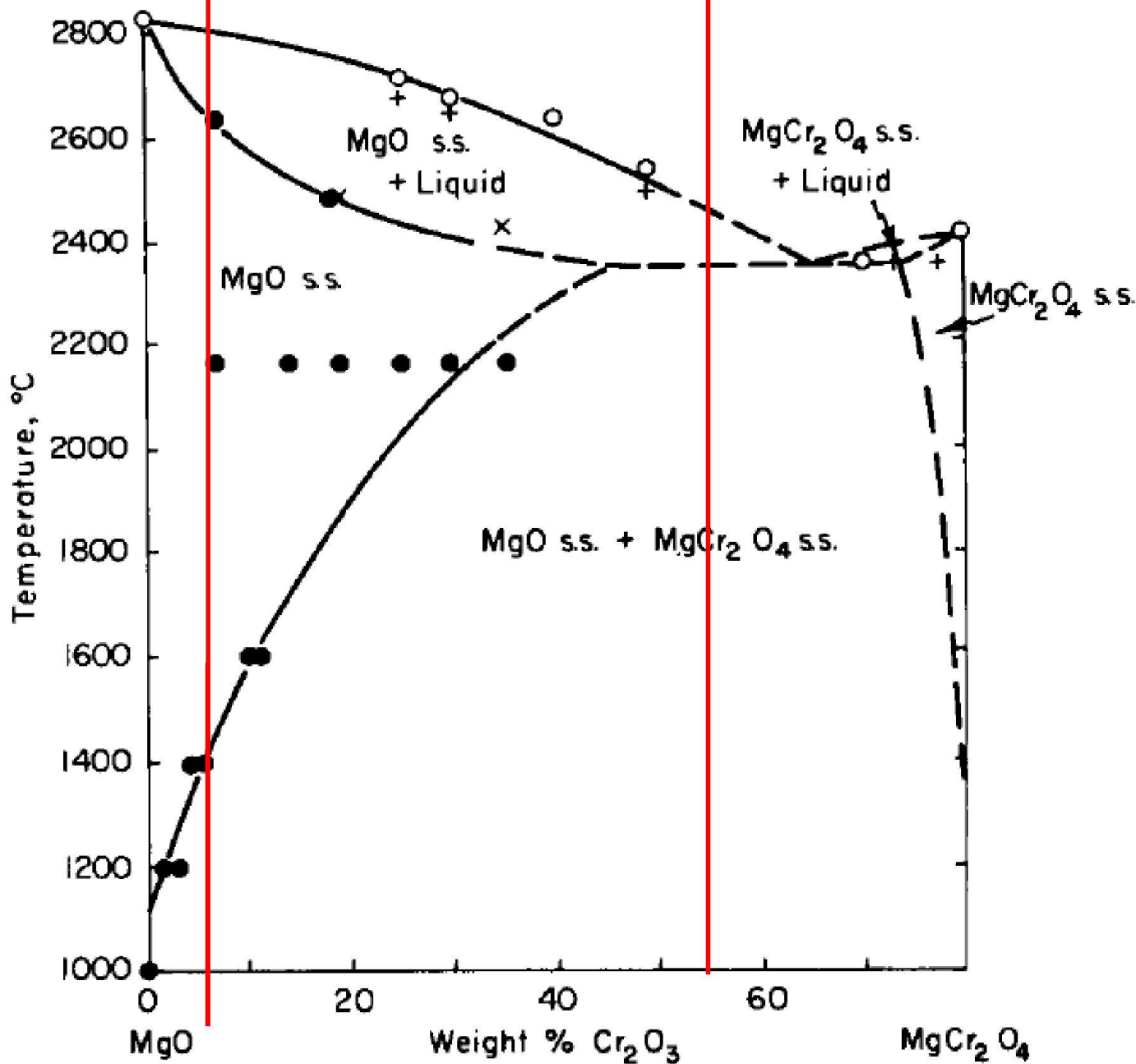


MgO-Spinel Fusion-Cast Refractory:

The MgO-MgAl₂O₄ and the MgO-MgCr₂O₄ systems are examples in which the phases melt congruently and where a simple eutectic is present and a limited solid solution occurs.

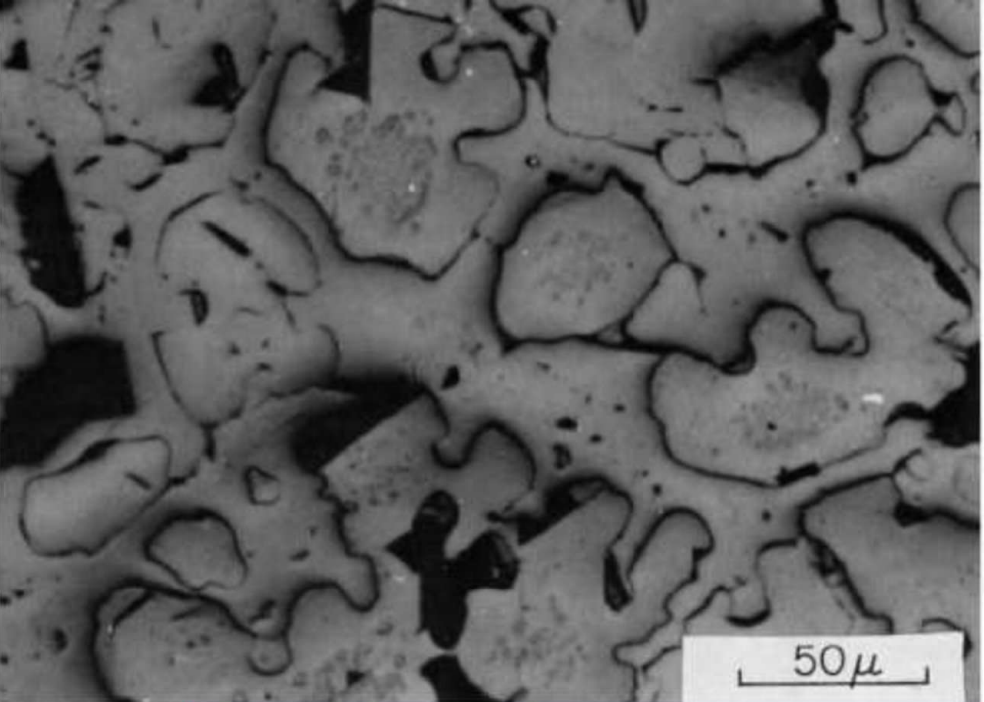
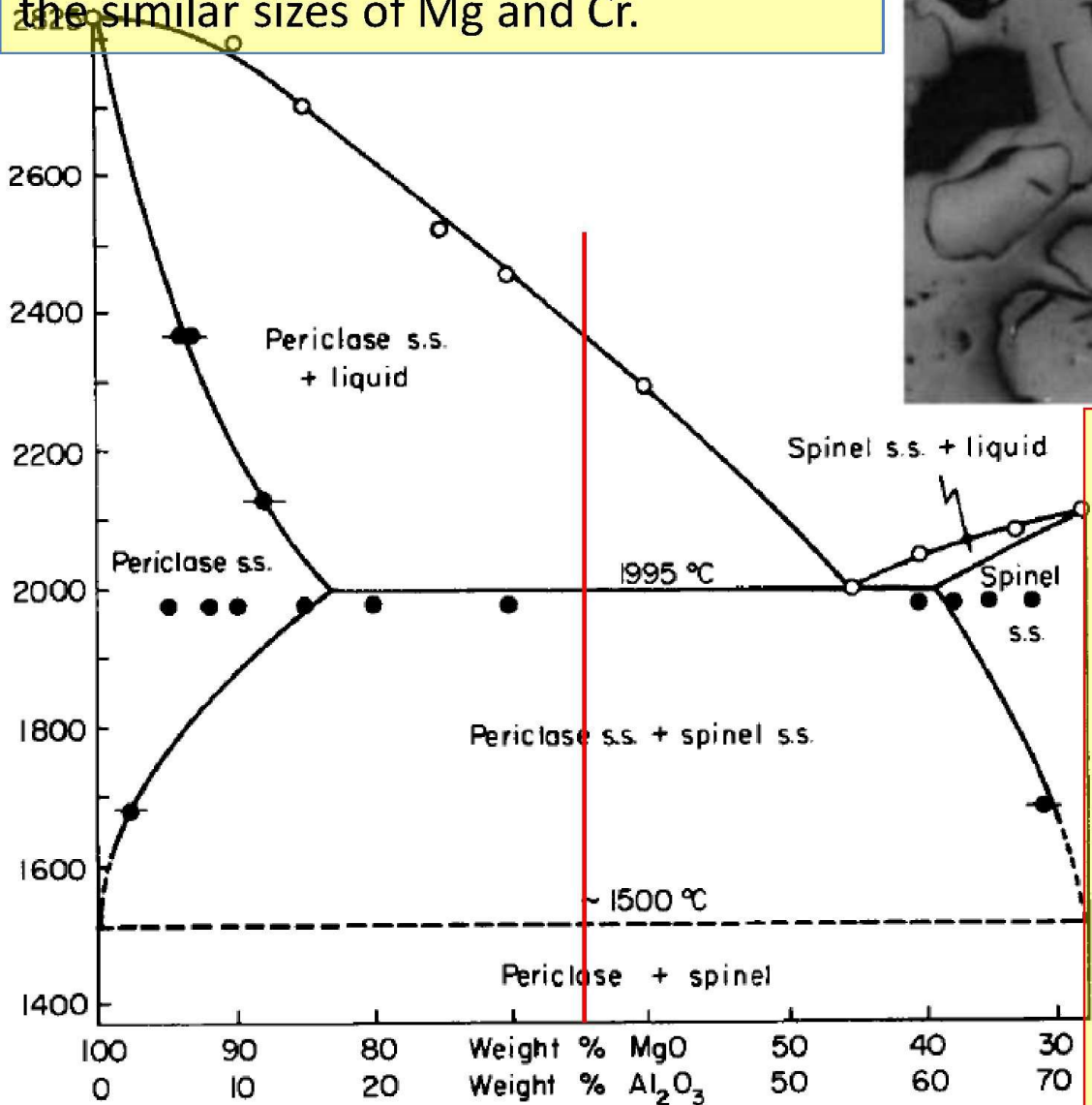
Fusion-cast refractories in different parts of this type of system have essentially different microstructure and properties.

1. Compositions containing **less than the maximum amount of solute ions**: microstructure: mainly **large crystals of the Periclase**, crystals of the precipitated P-phase, some amount of the **exsolved spinel phase at grain boundaries**.
2. **more than the maximum amount of solute ions** is fused and chill cast, the resulting microstructure contains an **intergranular low-melting phase**.



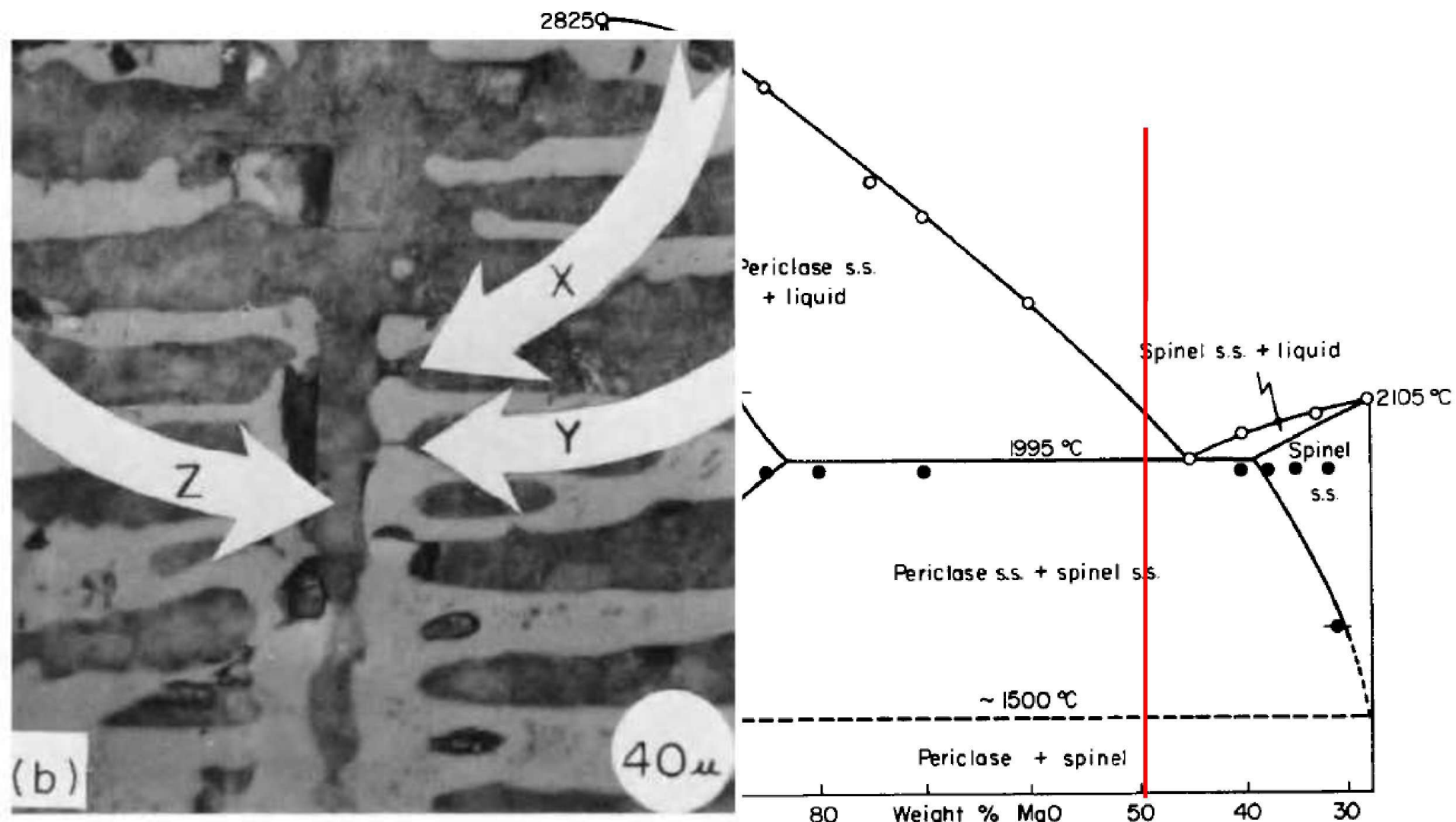
Phase diagram of $\text{MgO}-\text{MgCr}_2\text{O}_4$ system

Al-ions are less soluble in the periclase lattice than are Cr-ions: due to the larger differences in the ionic sizes between Al and Mg when compared to the similar sizes of Mg and Cr.



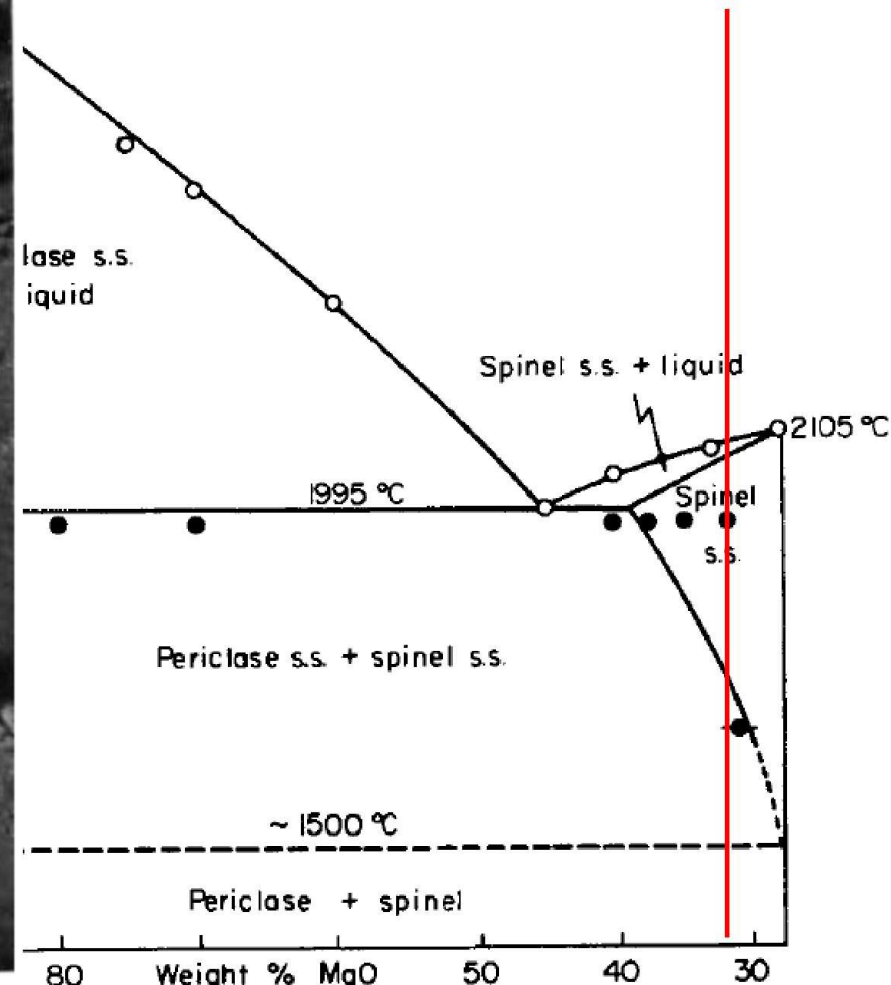
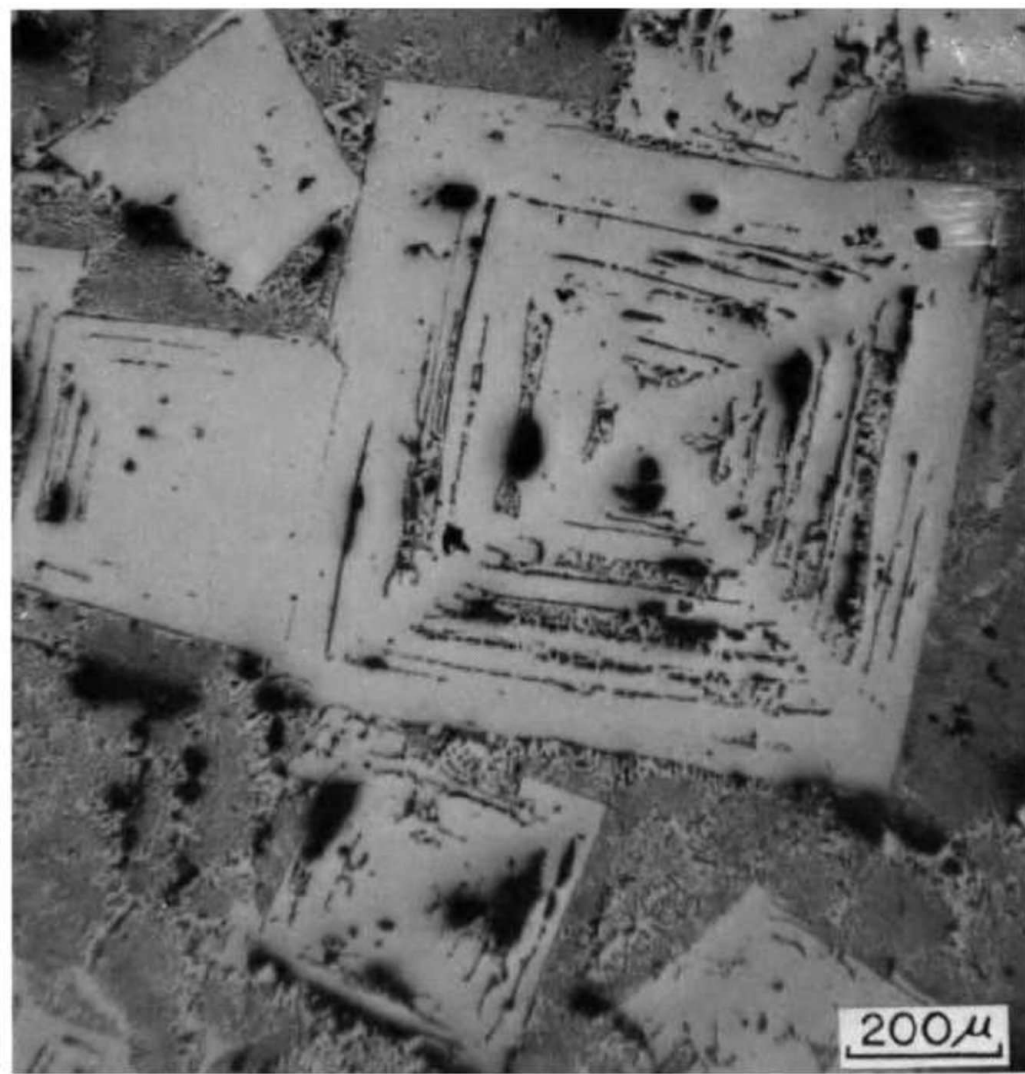
65/35 $\text{MgO}/\text{Al}_2\text{O}_3$ fusion-cast ceramic: the periclase crystals are coated by a spinel phase.: the primary periclase crystals appear to serve as crystallization sites for the periclase that is crystallizing out from the eutectic composition. Second phase appears to break up the microstructure and increase the formation of equiaxial primary crystals.

The primary periclase phase in compositions near the eutectic point crystallizes dendritically.: Photomicrographs of polished sections of ~ 50 wt % MgO-50 wt % Al₂O₃ fusion-cast body. The dendrite (black phase) is periclase and the background is the eutectic structure,



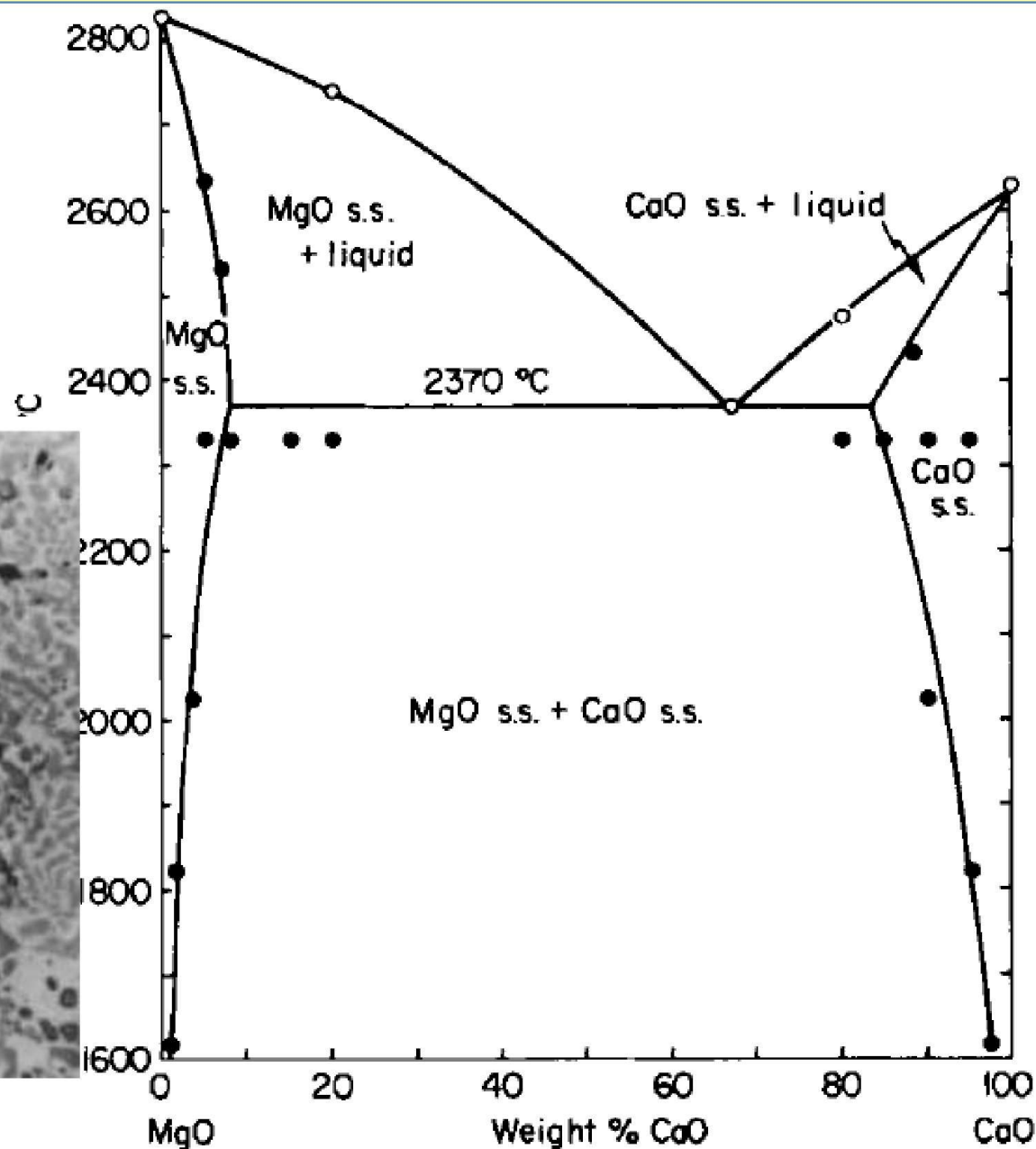
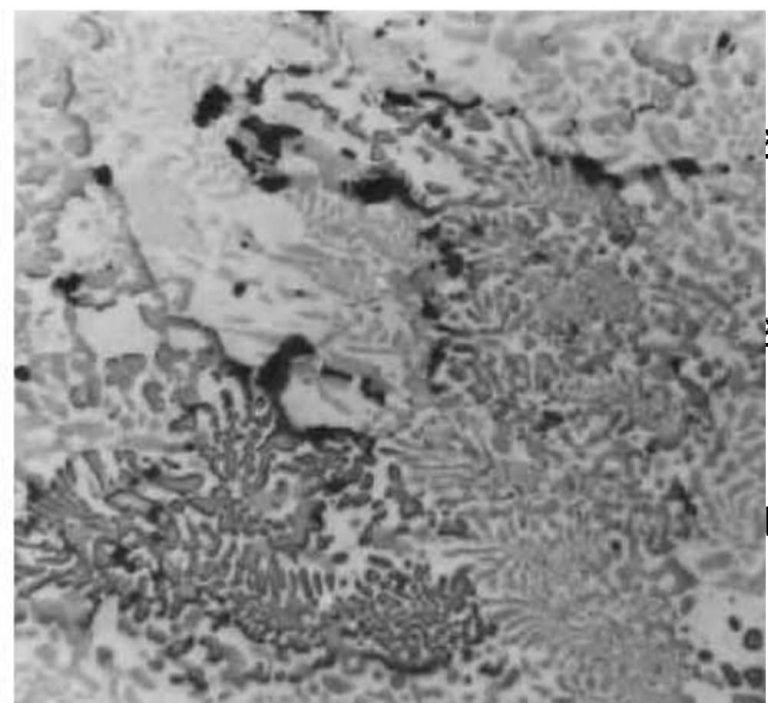
spinel-rich side of the eutectic: shows the primary spinel crystals, characterized by the fourfold symmetry, surrounded by eutectic structure:

Photomicrograph of 68% Al₂O₃- 32% MgO fusion-cast refractory, which contains large primary spinel crystals surrounded by the eutectic composition.

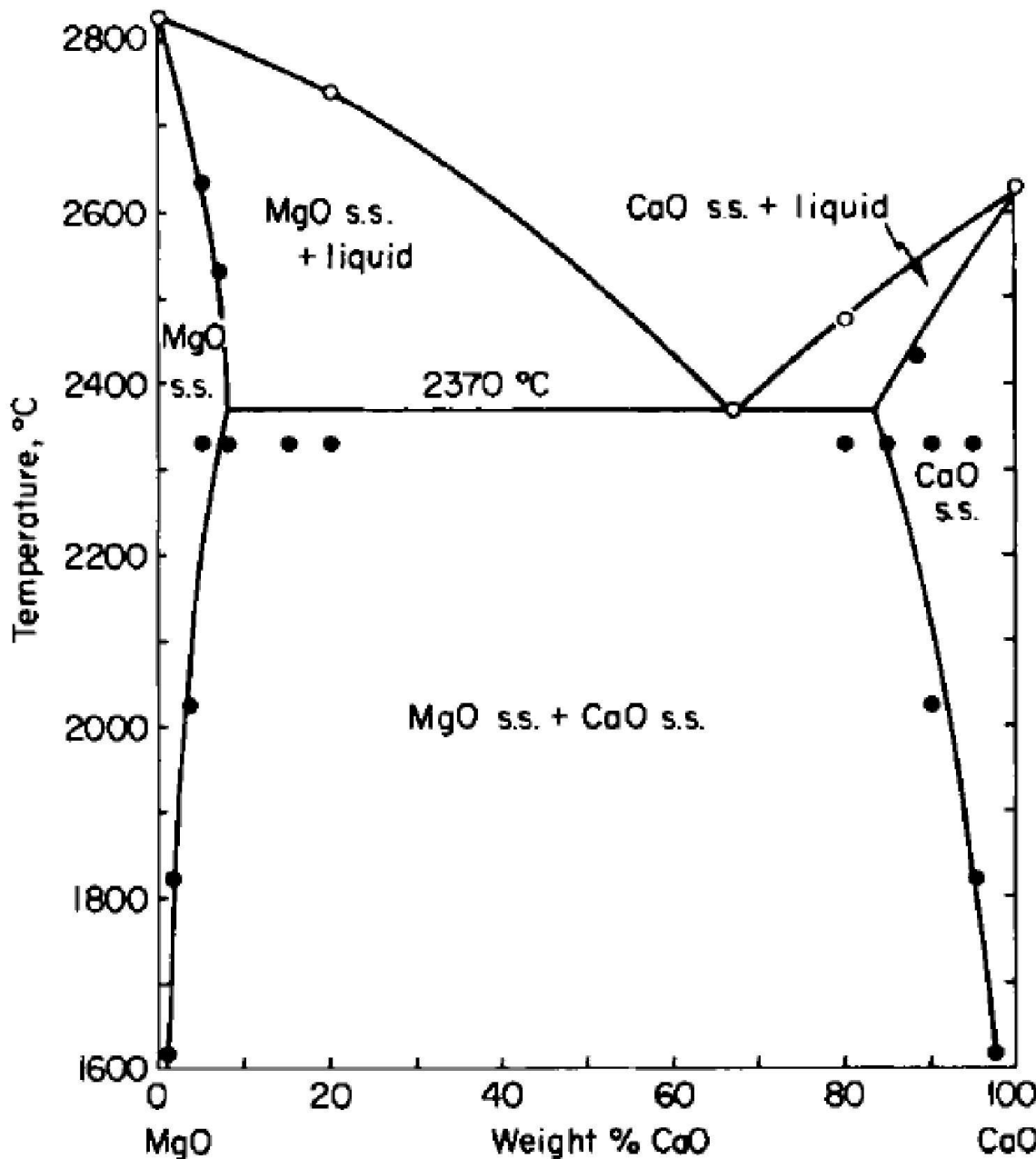


Fusion-cast refractories composed of MgO-CaO: shows a simple eutectic and very limited solid solution

The microstructure of the compositions near the eurectic can be described as finely disseminated, rounded to rodlike, periclase crystals in a CaO matrix



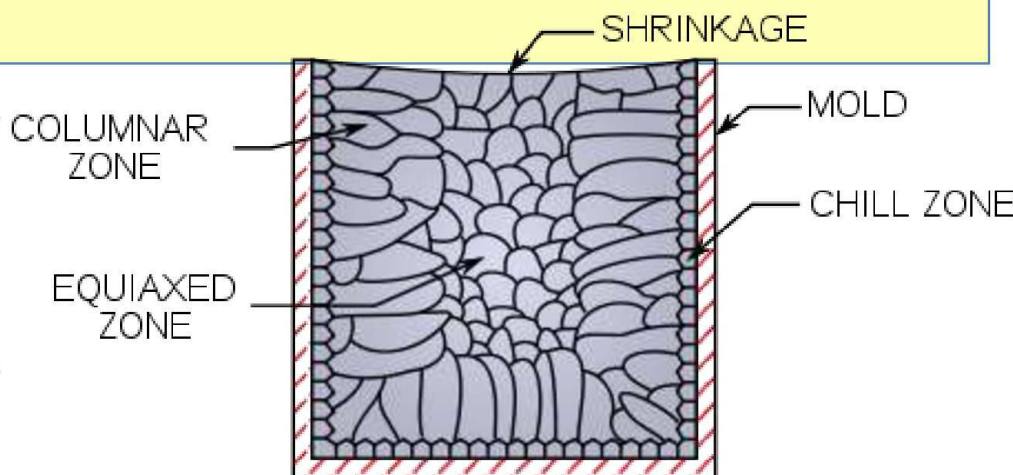
Fusion-cast CaO-MgO refractories are very resistant to corrosion by basic slags (lime/silica ratio greater than 2/1), and they have good high-temperature strength and thermal shock resistance.



Fuse Cast Al_2O_3 - ZrO_2 and Al_2O_3 - ZrO_2 - SiO_2 Refractory:

- (1) Fusion cast **alumina-zirconia** ceramics form **excellent abrasion-resistant** grains used in snagging steel and other metal ingots,
- (2) fusion-cast alumina-zirconia-silica (**AZS**) refractories are the most widely used for lining **glass melting furnaces**. The alumina-zirconia-based fusion-cast refractories are very insoluble in molten glass, allowing production of high-quality glass.
- (3) **Pure alumina** crystallizes in a columnar-oriented structure. **Voids** form between the **columnar crystals**; these are primarily due to shrinkage that occurs when alumina liquids solidify. Materials with this structure are **very weak and have very poor resistance to thermal shock**.

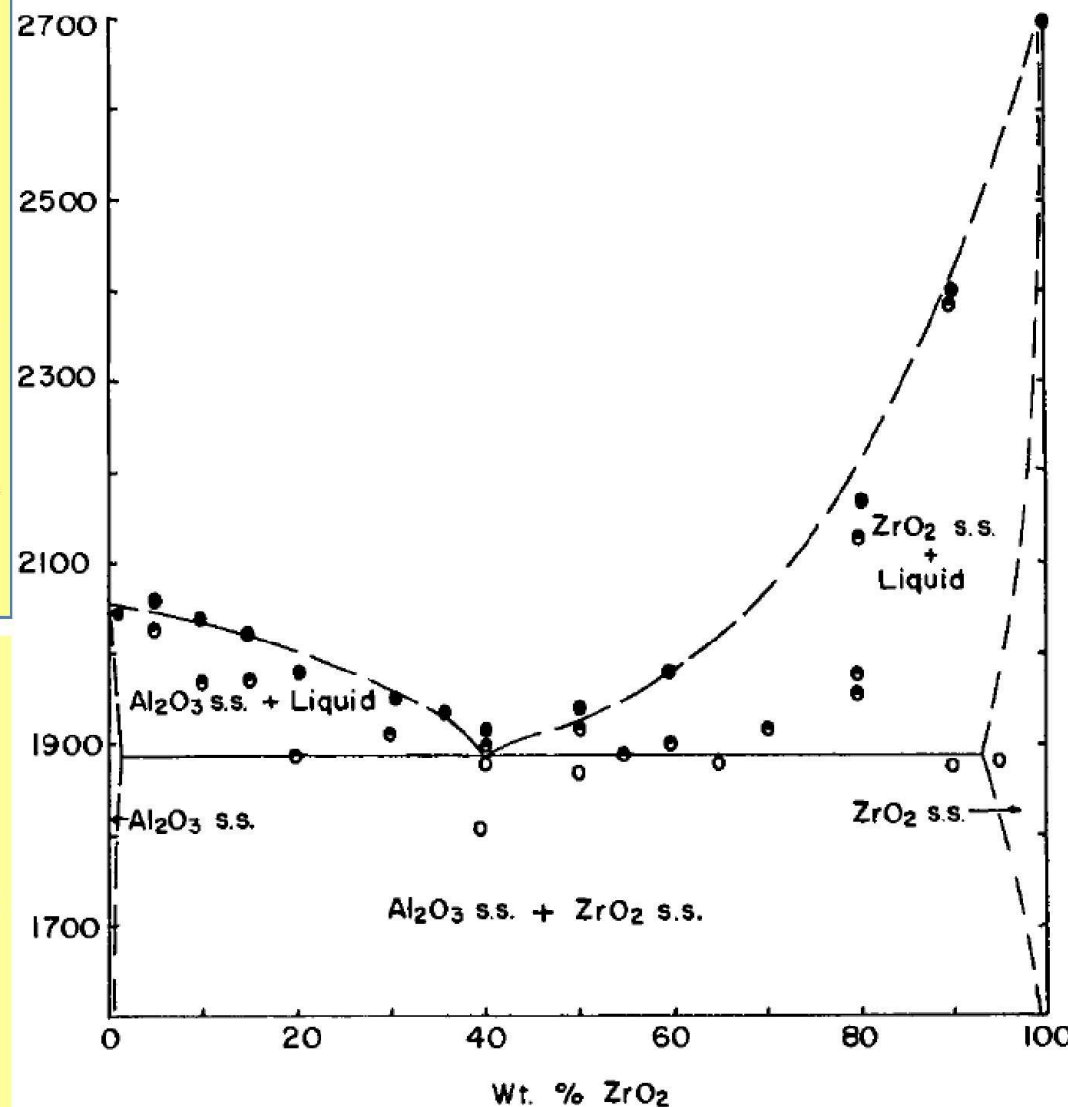
- (4) ZrO_2 is added to alumina, the structure becomes more equiaxial.



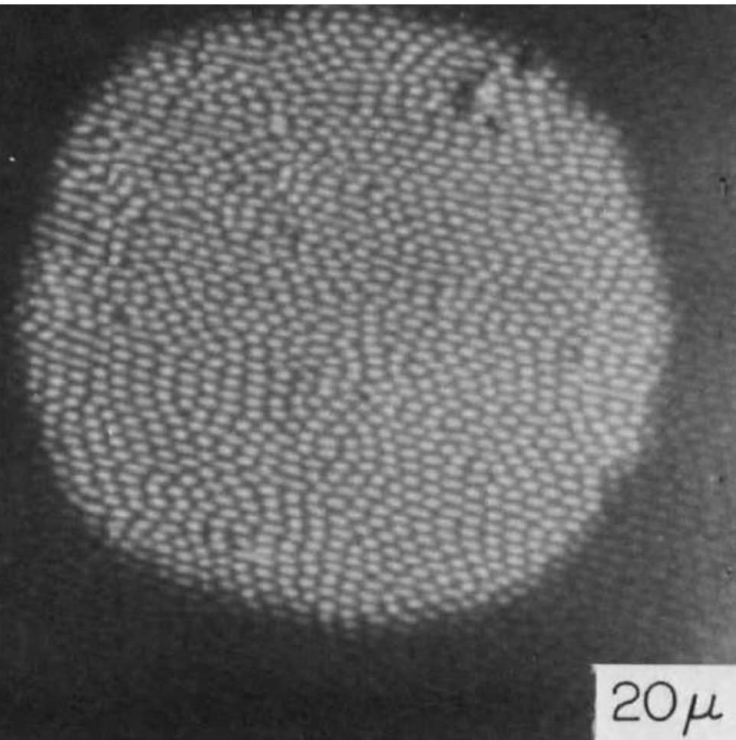
Alumina-zirconia is a simple eutectic system that has very limited solid solution at high temperatures

Compositions that fall between alpha-alumina and the eutectic contain primary crystals of alumina surrounded by the eutectic composition; consists mainly of alumina crystals with included rodlike zirconia crystals

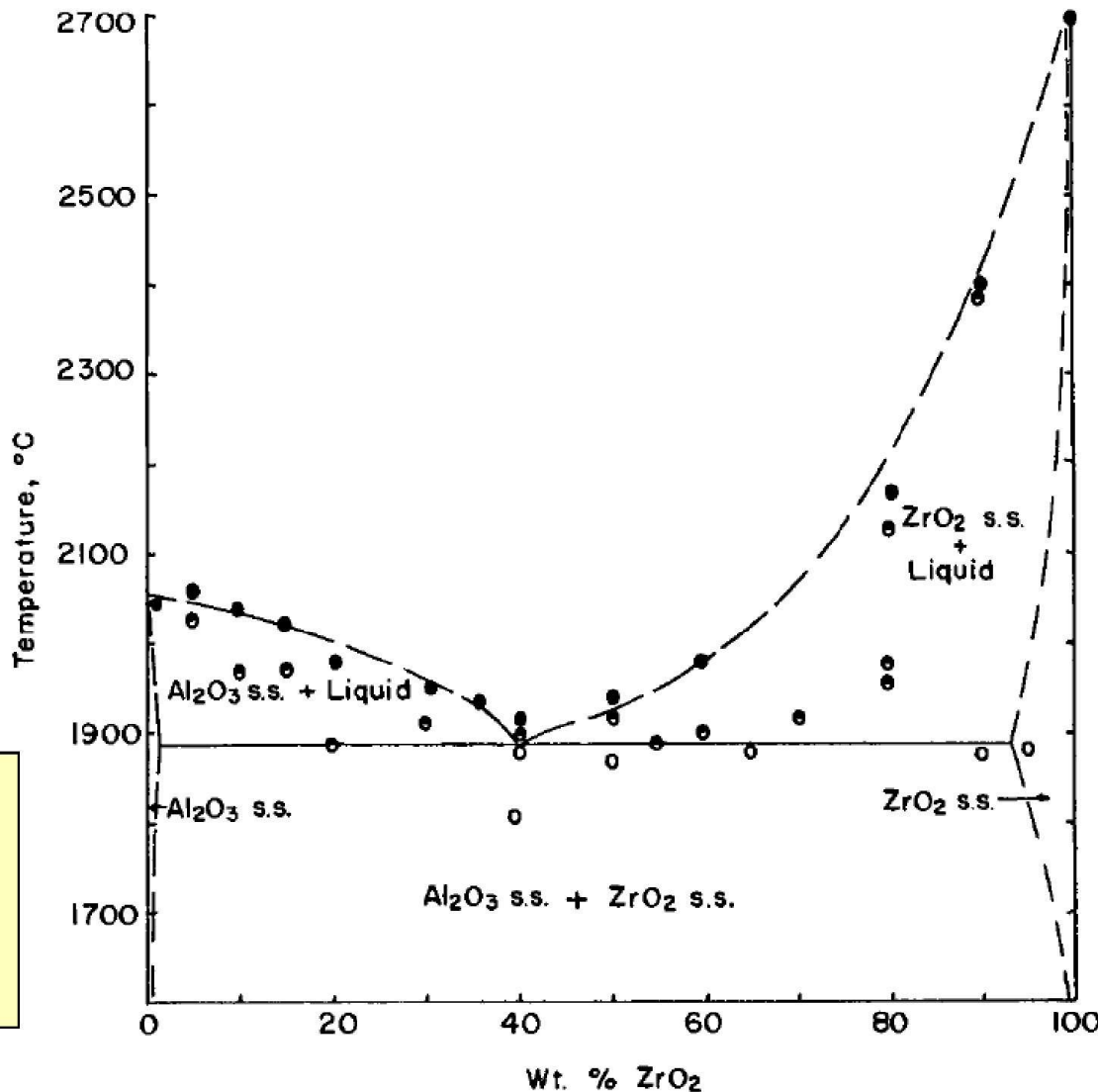
Compositions that fall between the eutectic and pure zirconia have microstructure consisting of primary zirconia surrounded by the eutectic phases



The finely divided eutectic structure gives these fusion-cast materials their high impact strength and toughness, which permits their use in snagging operations.



Eutectic structure of the Al₂O₃-ZrO₂ system : the white phase (rods) is ZrO₂ and the dark background is Al₂O₃.



Fused Cast AZS Refractory

Typical AZS composition contain
45-51 wt% Al_2O_3 , **33-41 %**
 ZrO_2 , **10-15 wt%** SiO_2 , **1-1.5**
wt% Na_2O .

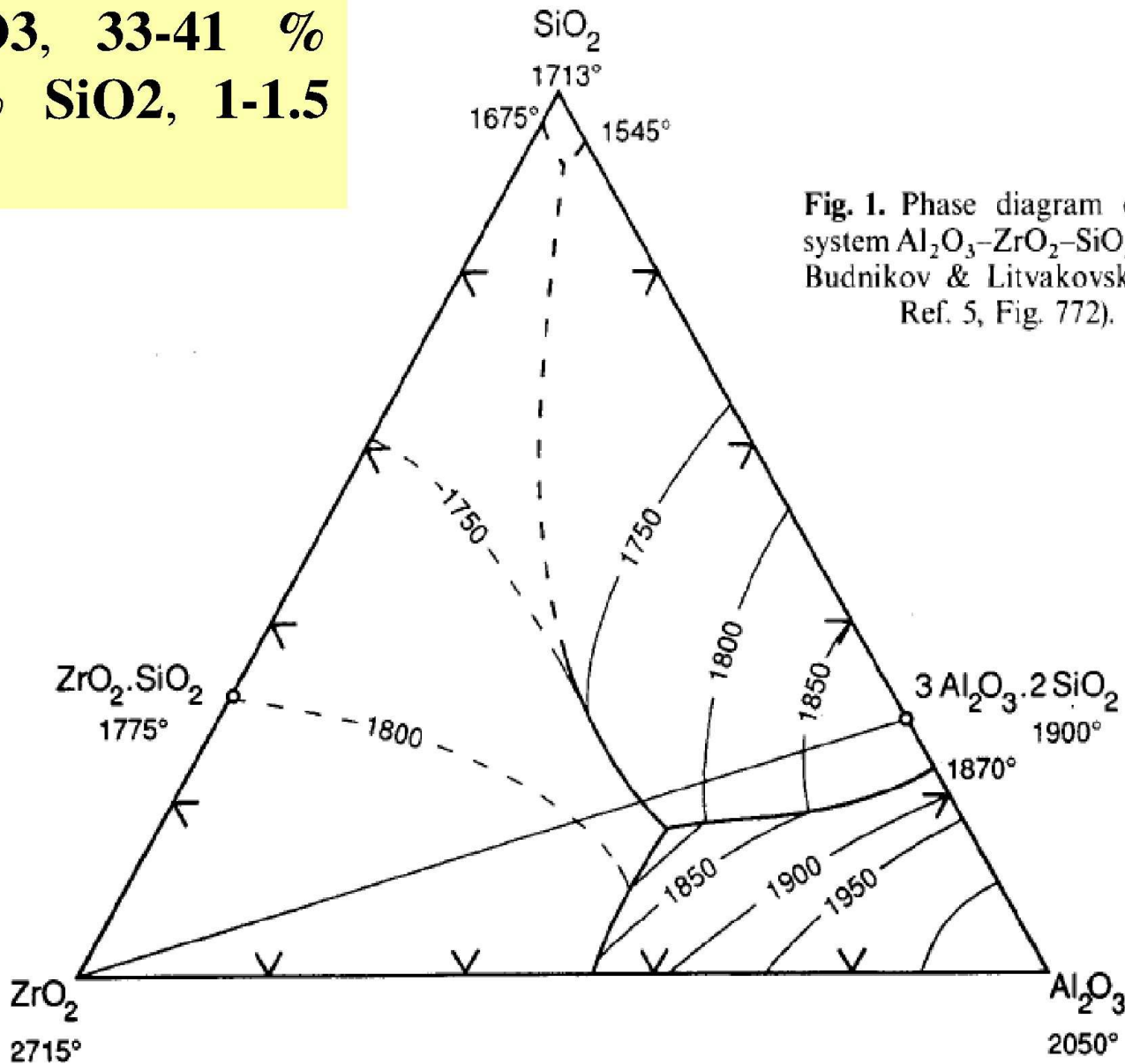


Fig. 1. Phase diagram of the system Al_2O_3 - ZrO_2 - SiO_2 , after Budnikov & Litvakovskii (see Ref. 5, Fig. 772).

Chemical composition of the melt at starting point: 41 mass-% ZrO_2 , 46 mass-% Al_2O_3 and 12 mass-% SiO_2 .

Crystallisation of baddeleyite along the red line: Mineral phase and chemistry at the end of the red line: 13,8 mass-% baddeleyite in 86,2 mass-% residual melt

Crystallisation of baddeleyite and corundum along the green line. Chemistry at the end of the blue line: 18,7 mass-% baddeleyite and 5,0 mass-% corundum in 76,2 mass-%

At the eutectic point baddeleyite, corundum and mullite should crystallize at a constant temperature of 1726 °C

But in reality only baddeleyite and corundum crystallise and a vitreous phase freezes due to the sodium content. 40,2 mass-% ZrO_2 , 41,3 mass-% Al_2O_3 18,5 mass-% vitreous phase

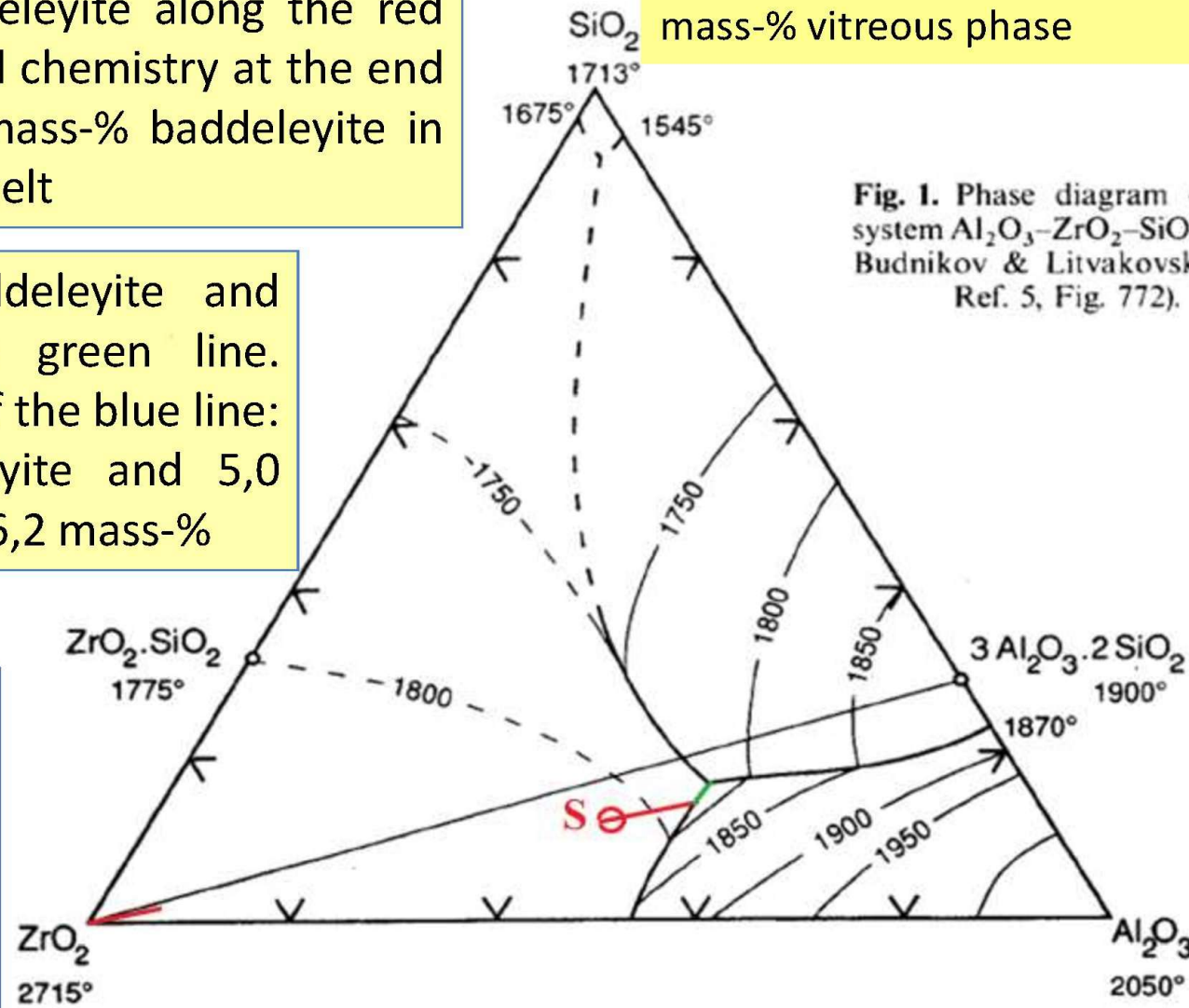
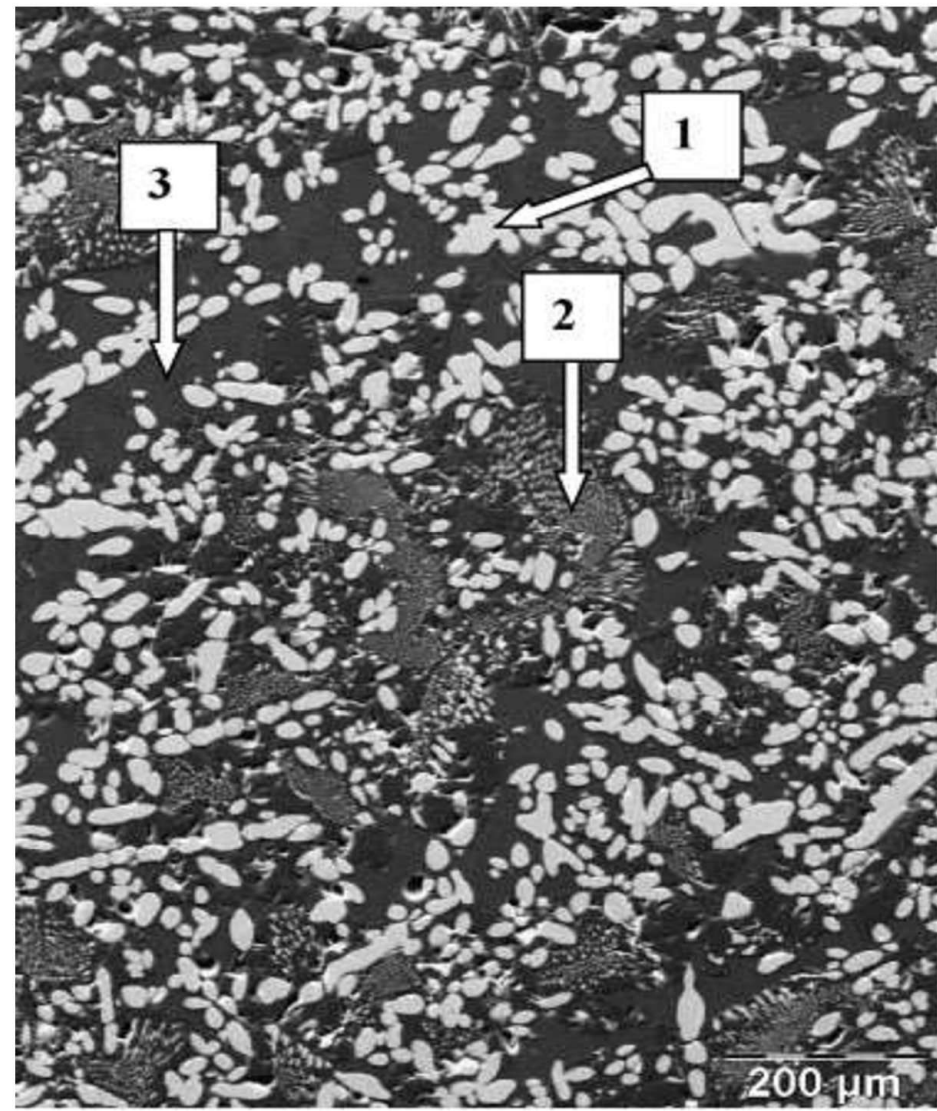
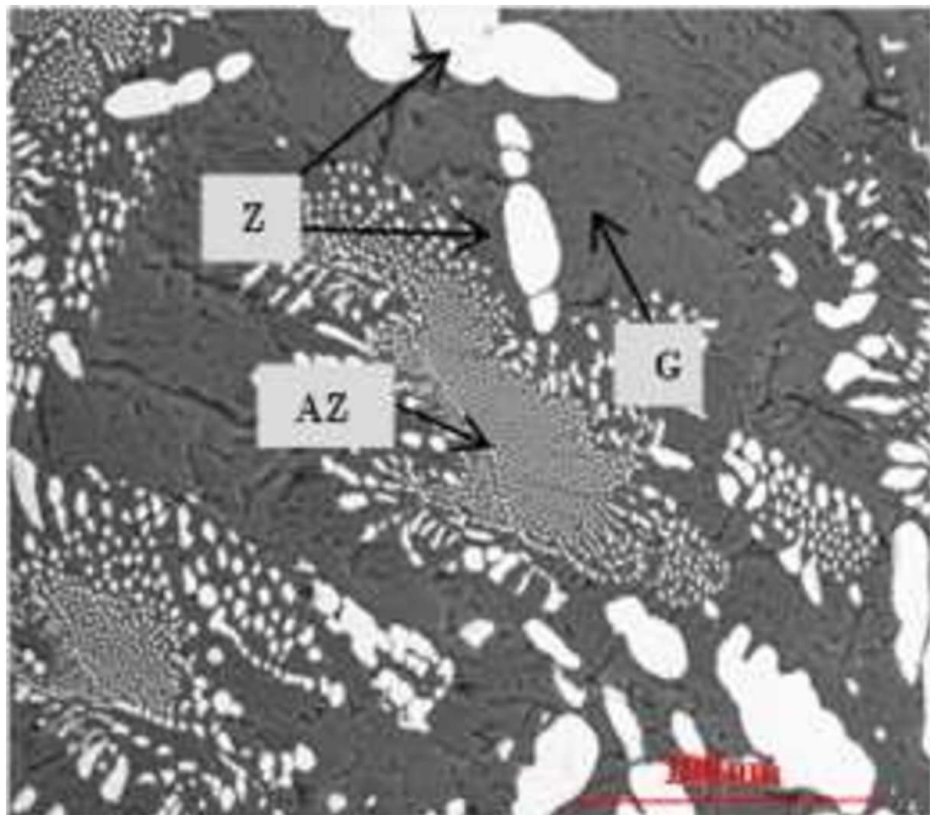


Fig. 1. Phase diagram of the system Al_2O_3 - ZrO_2 - SiO_2 , after Budnikov & Litvakovskii (see Ref. 5, Fig. 772).

Microstructure of AZS with primary ZrO_2 (Z/1), $Al_2O_3-ZrO_2$ eutectics (AZ/2) and glassy phase (G/3).



The proposed revised diagram:

- the larger extent of the zirconia primary-phase field, down to significantly lower zirconia contents;
- the higher alumina content of the mullite solid solution:
- the ternary invariant point relating zirconia, alumina and mullite is of the eutectic type and occurs between 1700 and 1710°C, significantly lower than previously reported

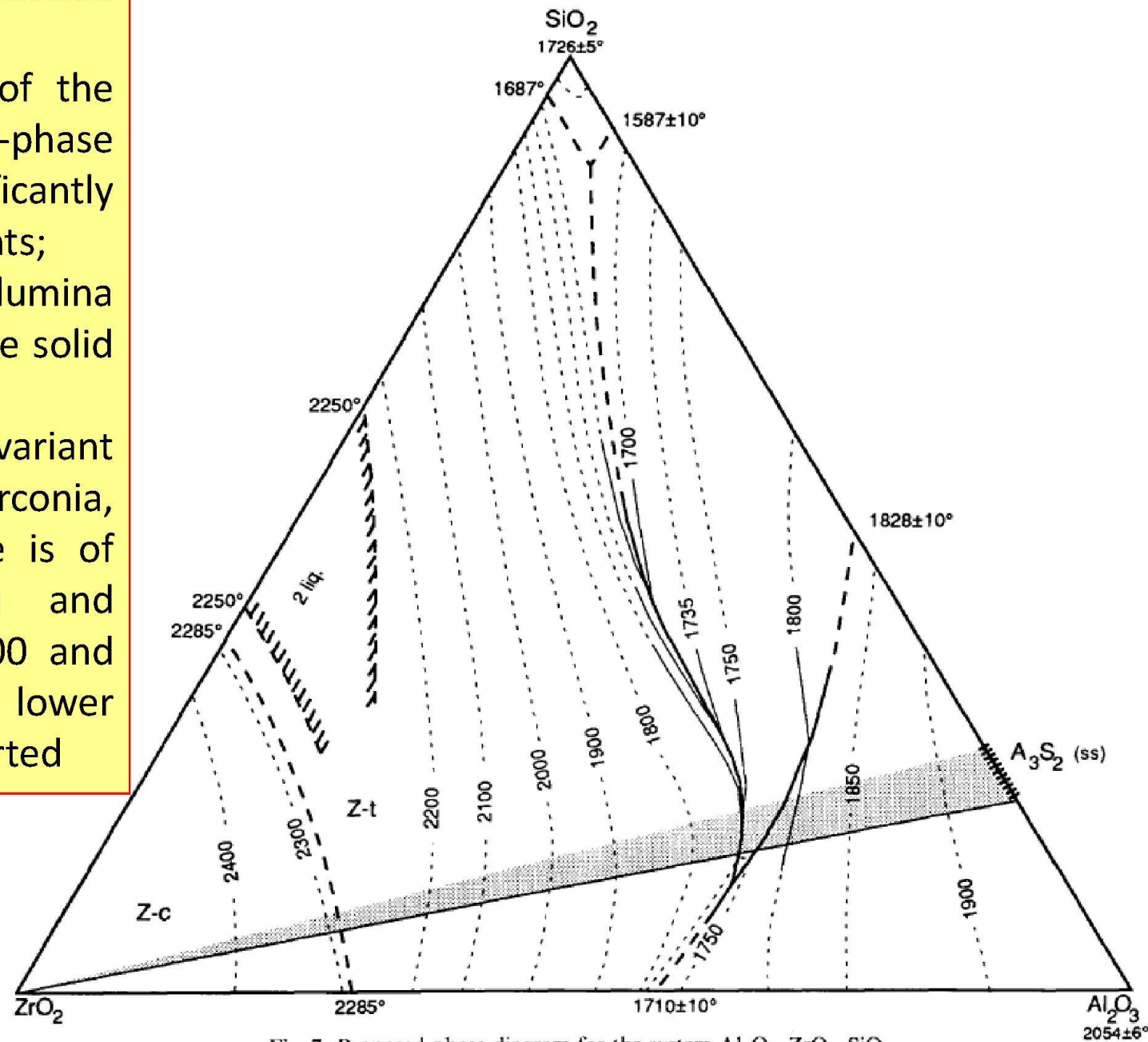


Fig. 7. Proposed phase diagram for the system Al_2O_3 - ZrO_2 - SiO_2 .

Table 1
Modification and volume changes of SiO₂

Modification Changes ↔reversible→ irreversible	Transformation Temperature [°C]	Volume Change [%]
$\beta \leftrightarrow \alpha$ -quartz	573	0.8–1.3
α -quartz → α -cristobalite	1250 (\approx 1050 *)	17.4
$\beta \leftrightarrow \alpha$ -cristobalite	\approx 260	2–2.8
α -quartz → α -tridymite *	\approx 870	14.4
$\gamma \leftrightarrow \beta \leftrightarrow \alpha$ -tridymite *	117–163	0.5
α -tridymite → α -cristobalite *	1470	0
α -cristobalite → melt	1713 ± 10	–
α -tridymite → melt **	1670 ± 10	–
fused silica → α -cristobalite	above \approx 1150*	\approx 0.9

* in presence of
impurities

Formation of tridymite only occurs in the presence of

** rapid heating

Table 2
**Material properties of dense
silica bricks**

Application	Bulk Density [g/cm ³]	Apparent Porosity [vol.-%]	Cold Crushing Strength [MPa]	Refractoriness Under Load (differential) (DE) T05 [°C]	Thermal Expansion 1000 °C [%]	Thermal Conductivity 1000 °C [W/m·K]
Coke oven	1.78–1.90	18–23	30–60	1610–1650	1.3	1.8–2.2
Glass furnace	1.81–1.85	19.5–21.5	30–40	1630–1670	1.4–1.5	1.8–1.9

IV. SILICA BRICK

Silicon is the most abundant element next to oxygen, and silica is therefore found widely in nature, usually as quartz. Its characteristics are varied and interesting to the technologist. Quartz is converted to several polymorphic forms depending upon temperature. The physical properties of these forms as well as those of the fused material are distinctive and merit the efforts of those who have amassed volumes of scientific information on this very useful and interesting mineral.

Silica bricks are one of the unique products that have been used very successfully in industry for many years. In the last decade, however, steel-making processes have radically changed. This has affected refractory requirements, with the result that the market for silica brick has been reduced to less than half the volume that was formerly used. There still exists, however, a sizable market for silica brick in the glass-melting furnaces of the nation and in other high temperature industrial units. In the year 1967, 71,214,000 silica bricks were sold in the United States for refractory purposes. The value of these bricks was \$14,702,000 (U.S. Bureau of Census, 1967).

For many years silica bricks were used very successfully in open-hearth roofs and other important applications in the steel industry. Their success was due to the fact that they could be used under load at high temperatures

close to the melting point of pure silica. The low expansion characteristics of the high-temperature polymorphs of silica was another practical advantage in the open-hearth roof where wide swings of temperature take place during the operation cycle. Not until the industry required temperatures above the melting temperature of silica were they replaced.

The raw material for silica bricks is derived from well-bonded sandstones, quartzite, and quartz pebbles such as the Sharon Conglomerate. These raw materials must have high purity, particularly in respect to their content of alumina and alkalies. Titania and iron oxide are objectionable but not as much so as alumina and the alkalies. In the manufacture of silica brick the rock is crushed and sized. This is then bonded with 2 to 4% CaO as slaked lime. The bonded bricks are fired at temperatures around 1500°C.

The process of firing permanently converts almost all of the quartz to other polymorphic forms of silica. Quartz has a density of 2.65 g/cc, whereas the density of a silica brick is approximately 2.33 to 2.34 g/cc. The brick expand during the firing process. Most of the fired brick is cristobalite and tridymite, but a small amount of glass and some residual quartz are always present. When a substantial portion of the final product is tridymite, it will have good strength and somewhat better heat-shock resistance. Special attention is therefore directed toward developing as much tridymite as is practicable in preference to cristobalite.

The diagrams Fig. 8 by Kingery (1960) and Fig. 9 by LeChatelier (1913, 1914) illustrate the equilibrium conditions in the silica system as applied to silica bricks during firing. See also Sosman (1927a), Kingery (1960), and Chesters (1957). They do not in themselves indicate the rate of inversion from one polymorphic form to another: this being important, as will be seen in the following paragraphs.

When the brick is heated to 573°C, alpha quartz (the common form) converts rapidly to beta quartz. If beta quartz is cooled, it reverts to alpha quartz readily, but when heating is continued to 870°C, another inversion point (beta quartz to beta₂ tridymite) is reached. This inversion is sluggish and does not occur readily; instead the next high-temperature form develops. This is beta cristobalite. Between 873°C and 1470°C, cristobalite may be considered to be metastable for, if the brick were held at temperatures between 870° and 1470°C for a longer period of time, the previously formed cristobalite would eventually invert to tridymite. This would entail considerable furnace time and expense and it is therefore not often done. When the brick are cooled, quartz is not reproduced and the ratio of tridymite and cristobalite existing at high temperature remains upon cooling. The high-temperature forms of tridymite and cristobalite do, however, invert to their respective lower-temperature forms—265°C for the low cristabolite form and 163° and 117°C for the low tridymite inversions. The low inversion for cristobalite is accompanied by a 2.8% volume change. Its reconversion must be dealt with carefully when heating furnaces that contain structural elements of silica bricks.

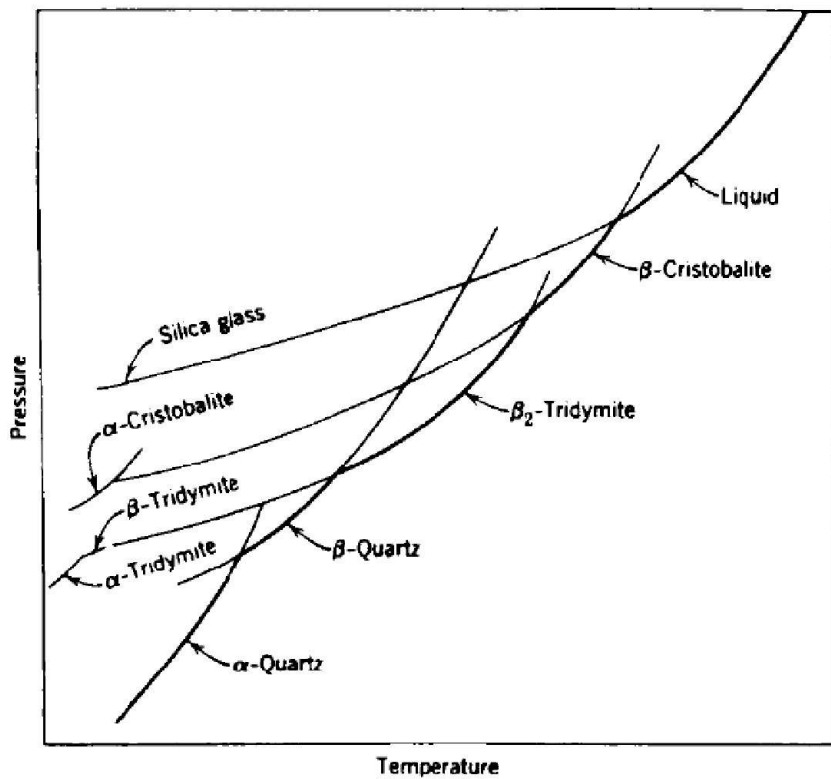


Fig. 8. Equilibrium relations of the minerals in the silica system. Reprinted from Kingery (1960).

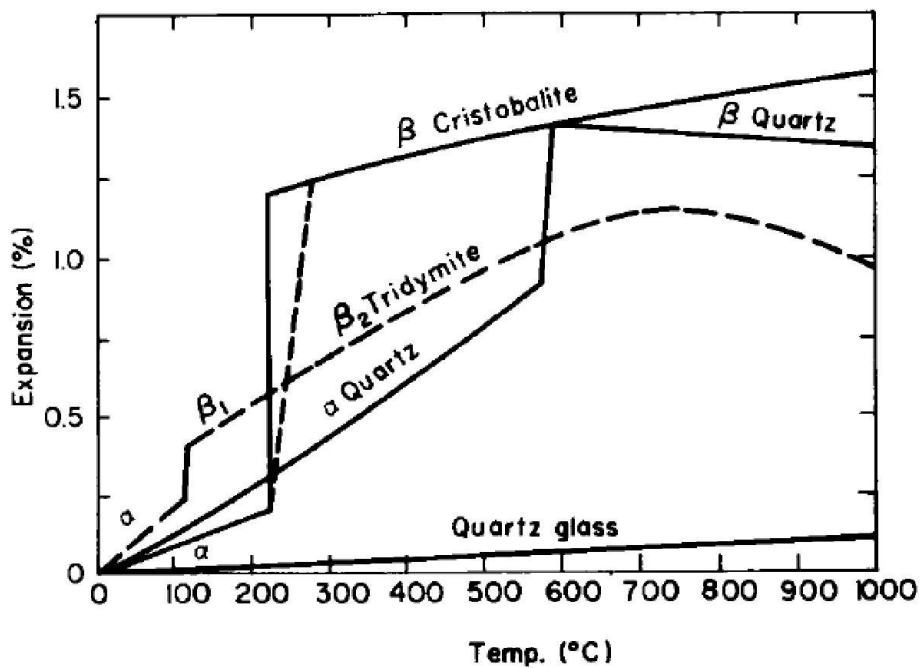


Fig. 9. Thermal expansion of silica minerals (after LeChatelier). Reprinted from Chesters (1957).

Heating schedules have been developed which are successful. These employ slow heating rates in the temperature range of the high expansion inversions (Kraner and Jewart, 1952). As the high-temperature form of cristobalite has a very low coefficient of expansion, it is largely responsible for the almost zero expansion of silica brick above 500°C, as shown in Fig. 10. This is the typical expansion curve of a commercial silica brick.

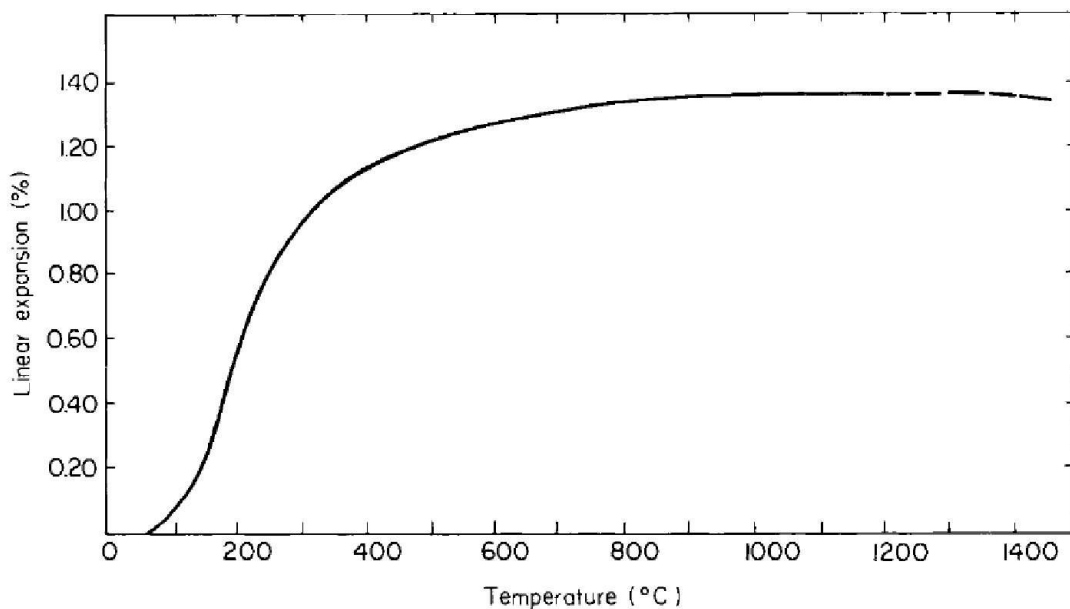


Fig. 10. Typical thermal expansion curve for silica brick.

The large expansion of the brick below 400°C makes it unsuitable for use in units such as blast furnace stoves and other regenerators in the range between room temperature and 500°C.

As cristobalite does not melt until 1723°C and, as good silica raw materials are rather plentiful, silica bricks can be used at temperatures very close to the melting point of pure silica. In a used silica brick taken from an open-hearth roof, one will find the hot face to have been completely converted to cristobalite.

In a vigorously operated open hearth furnace, the efficient operator will always maintain hot face temperatures at or very near the melting point of the brick. A brick containing 1% of Al_2O_3 plus alkalies will not withstand as high a temperature as one containing only $\frac{1}{2}\%$ or less. It is known that as much as 25% more steel has been made in a given length of time in a furnace under a 0.5% alumina silica roof as compared with a furnace that was

operated with a 1% alumina roof. If a furnace is operated with a split roof with one-half being a 0.5% alumina brick and the other half being 1% alumina, the low-alumina half will last approximately twice as long as the higher-alumina half. This has been demonstrated in practice. The use of a complete roof of low-alumina brick allows the operator to run his furnace at higher temperatures thereby producing steel at a faster rate. In split-roof trials, the producing rate is limited by the lower refractoriness of the higher-alumina brick.

The ability of the brick to withstand temperatures so close to its melting point has been attributed in a general way to the purity of the rock. More specifically, as Greig (1927a, b) pointed out in 1927, it was due in large measure to the characteristic of silica to form immiscible liquids with lime and with iron oxide.

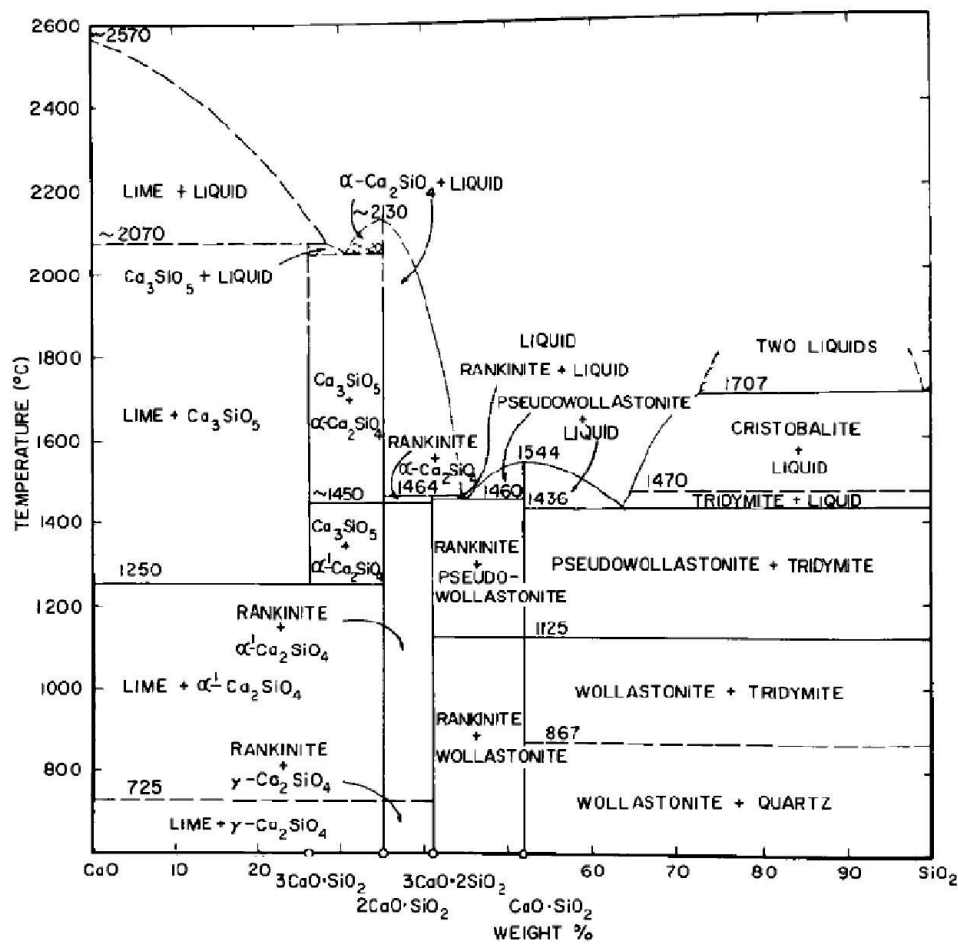


Fig. 11. Phase diagram for the system CaO-SiO₂. Based mainly on the work of Day et al. (1906). Reprinted from Muan and Osborn (1965).

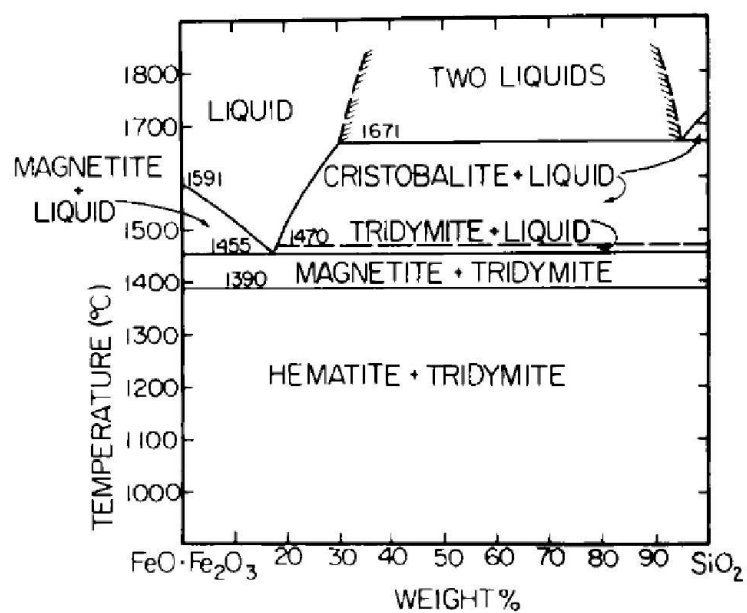


Fig. 12. The phase relations for iron oxide–silica in air plotted on the Fe_3O_4 – SiO_2 join (Muan, 1958). Reprinted from Muan and Osborn (1965).

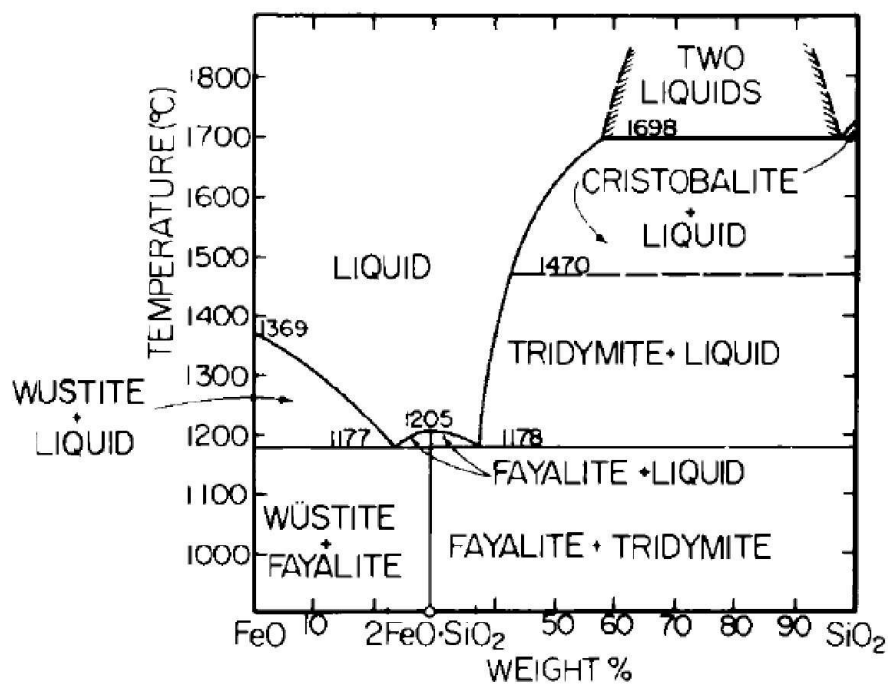


Fig. 13. The phase relations for iron oxide– SiO_2 in contact with metallic iron plotted on the FeO – SiO join (Bowen and Schairer, 1932). Reprinted from Muan and Osborn (1965).

The lime-silica diagram, Fig. 11 (Day *et al.*, 1906), shows that silica forms two immiscible liquids with lime and that cristobalite is stable in the presence of these at 1707°C, this being very near to the melting point of cristobalite. The lime content of the composition reaches approximately 28 %. The diagrams for iron oxides and silica, Figs. 12 and 13 indicate that the same situation prevails wherein immiscible liquids are favorable to the refractory behavior of cristobalite. The ternary systems of silica and common divalent oxides such as FeO, MnO, and MgO also show this immiscibility area as an extensive plateau. See Fig. 17. Silica does not form immiscible liquids with alumina. This was shown in the alumina-silica diagram, Fig. 1, and in the CaO-Al₂O₃-SiO₂ phase diagram, Fig. 14 (Rankin and Wright, 1915). The latter shows the relationships that apply to silica brick. Even small amounts of alumina in this system eliminate the immiscibility field.

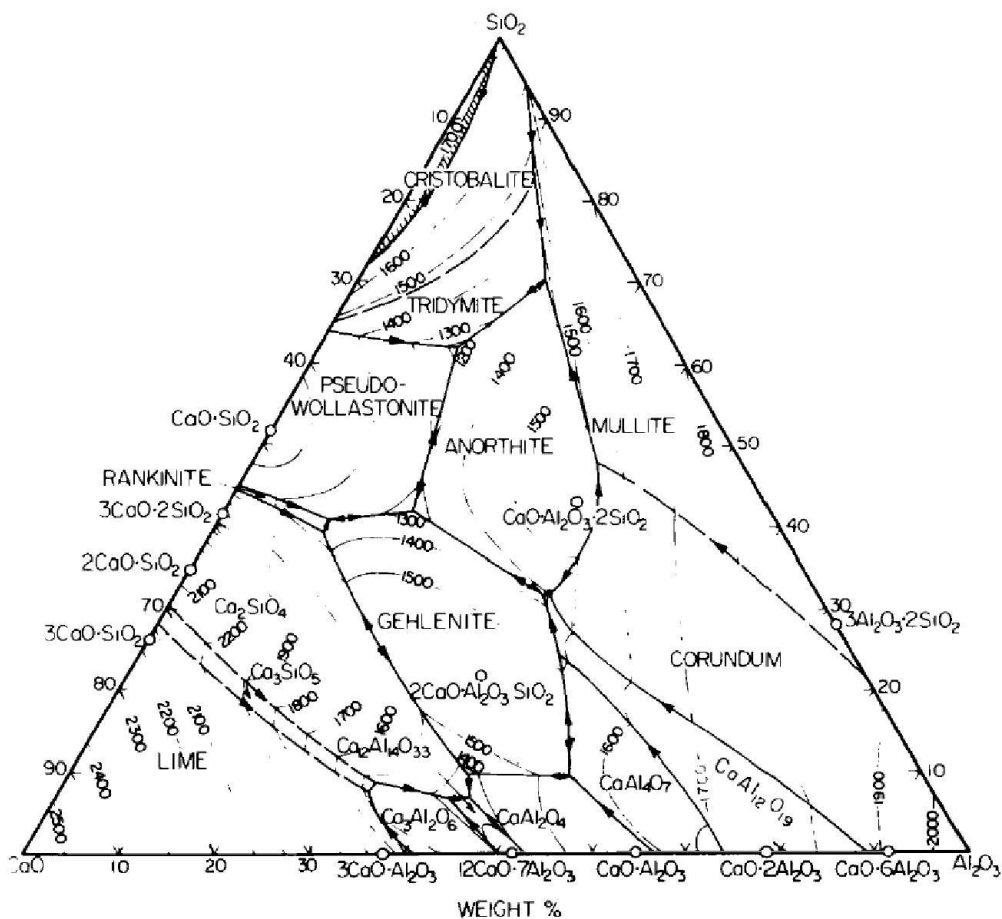


Fig. 14. Phase diagram for the system CaO-Al₂O₃-SiO₂. Mainly from Rankin and Wright (1915) and Grieg (1927, pp. 1, 133). Reprinted from Muan and Osborn (1965).

Silica does not form immiscible liquids in the presence of alkalies, hence there is no immiscibility with silica in the systems $\text{Na}_2\text{O}-\text{Al}_2\text{O}_3-\text{SiO}_2$ and $\text{K}_2\text{O}-\text{Al}_2\text{O}_3-\text{SiO}_2$.

The extent of liquid phase development in silica brick at high temperatures is determined by the use of the lime-alumina-silica phase-equilibrium diagram, Fig. 14 (Rankin and Wright, 1915; Kraner, 1944). The brick is

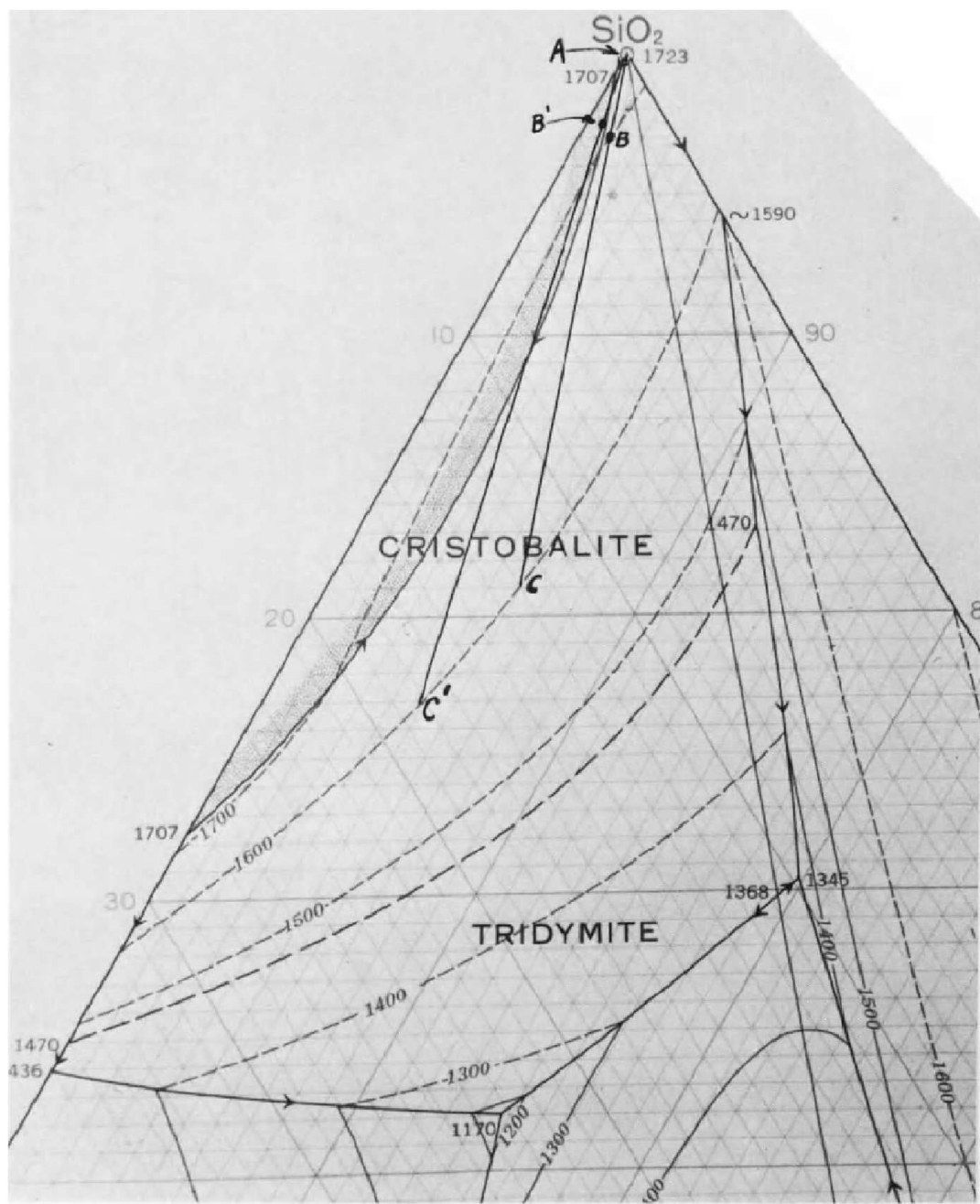


Fig. 15. Partial diagram of the system lime-alumina-silica.

largely silica. With the very small amount of alumina that is present plus about 2% lime, the first liquid to form when the brick is fired will be the eutectic composition between tridymite, anorthite, and pseudowollastonite at 1170°C. With increased temperature the composition of the liquid changes following the boundary line between pseudowollastonite and tridymite dissolving lime and silica simultaneously. When the lime-alumina ratio of this liquid reaches that of the brick composition, further heating carries only silica into solution until the maximum temperature of the firing process is reached. Meanwhile the mineral constitution of the brick has been established for the temperature attained.

The phase diagram of the system lime-alumina and silica is very useful in studying the effect of alumina on the liquid development in a silica brick during firing and use, and for the calculation of the amount of liquid and solid present at temperatures of use. For example, consider compositions B and B' on Fig. 15. These contain 1% and 0.5% alumina, respectively, and 2% lime. To determine the amount of liquid in these compositions as an example, a line is drawn from the apex A (silica) through B or B' and then on to the 1600°C isotherm, (point C or C'). The proportions of the liquid and solid are then determined from distance measurements AB, AC, and BC wherein

$$AB/AC \times 100 = \% \text{ liquid in composition B at } 1600^\circ\text{C}$$

$$BC/AC \times 100 = \% \text{ solid in composition B at } 1600^\circ\text{C}$$

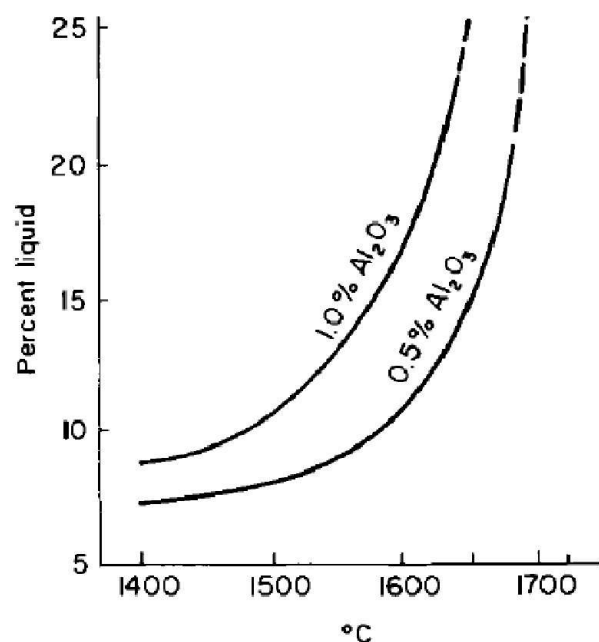


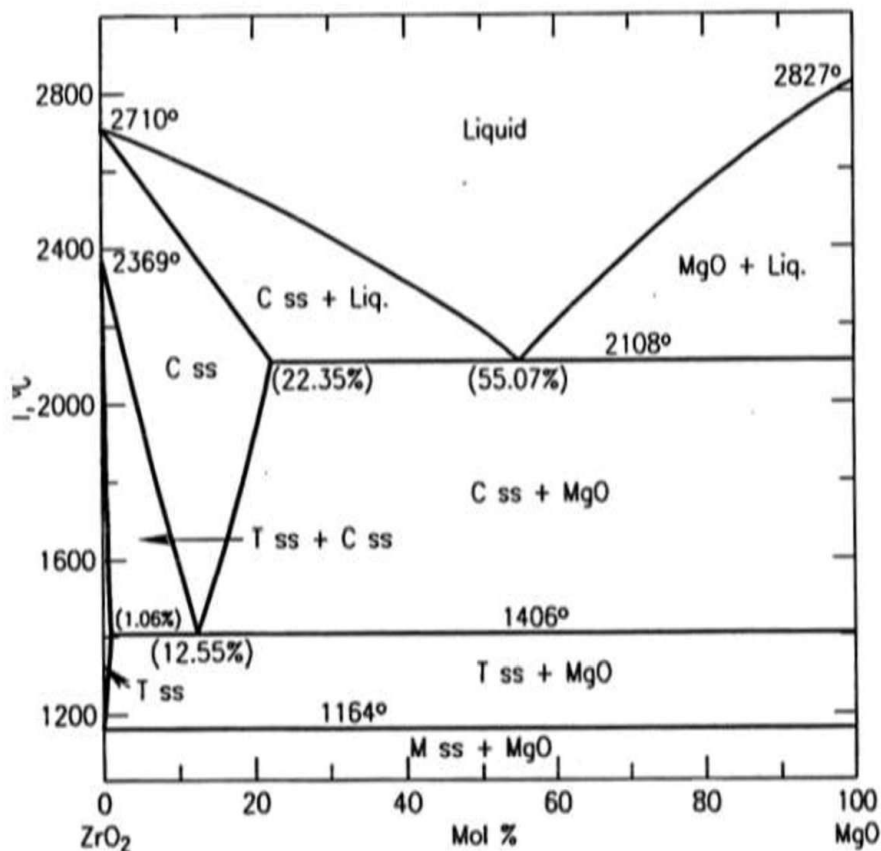
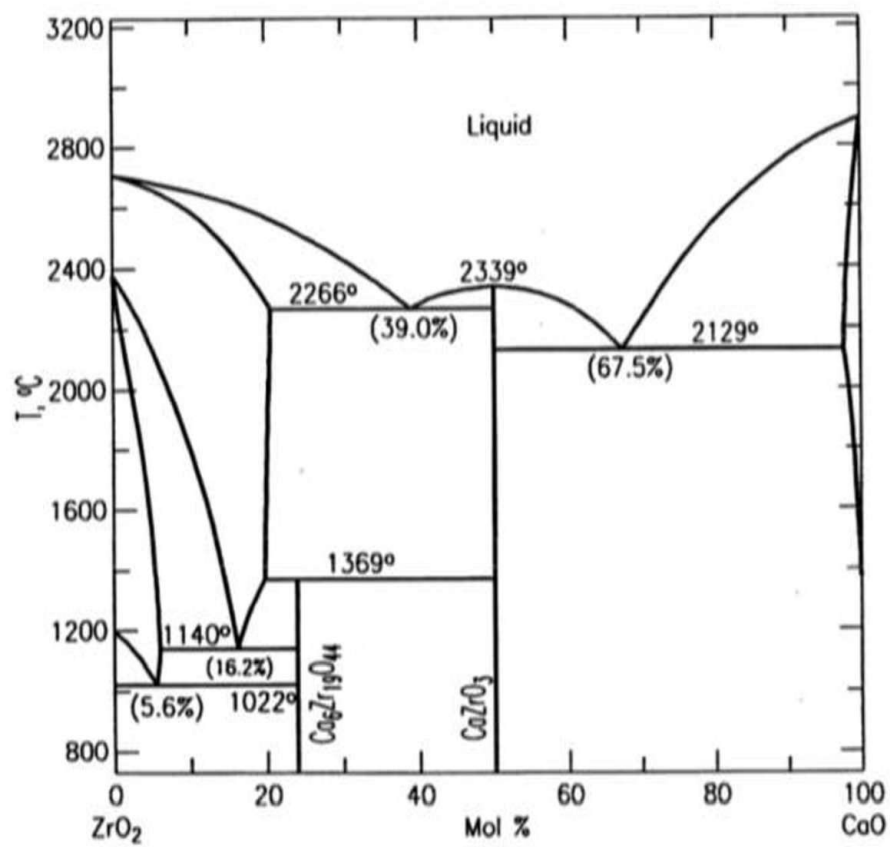
Fig. 16. Liquid content of silica bricks at elevated temperatures.

From such measurements and calculations one may obtain data as shown in Fig. 16 for bricks containing other percentages of alumina and at other temperatures.

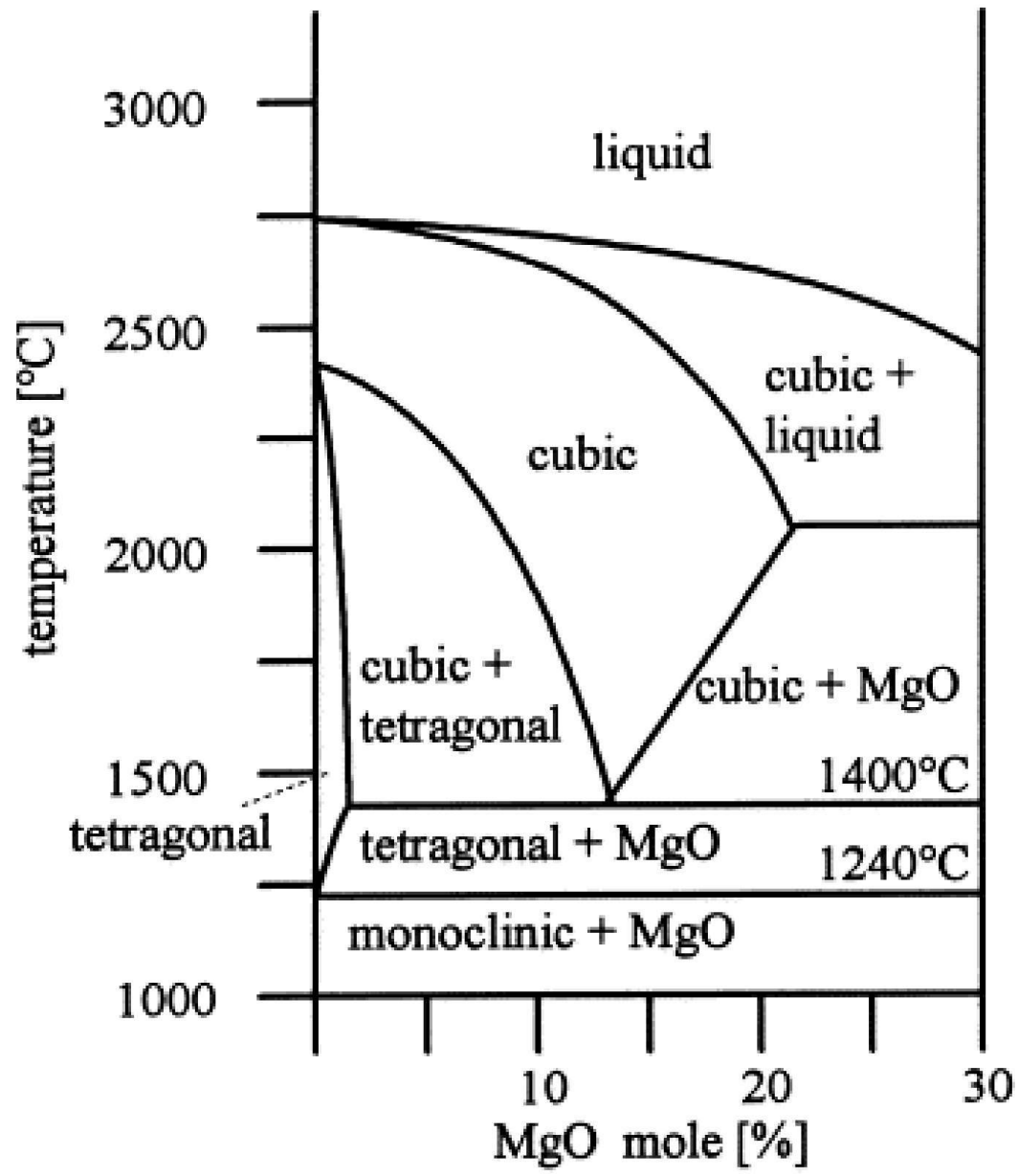
The sharp increase in the liquid development at temperatures above 1600°C as illustrated in this figure very impressively indicates the effect of alumina on the refractoriness of silica brick at temperatures of use.

Liquids containing high percentages of silica are quite viscous, and this may be a factor in retarding crystallization. It is also sufficient to rule out the PCE test as a practical one for testing the refractoriness of silica brick (Kraner, 1944). The viscosity is not sufficient, however, to improve the hot load bearing ability of silica brick at high temperatures. In work performed on silica bricks of various alumina contents, it was shown that when the liquid content of a silica brick reached 18%, failure would occur in the hot-load test under a load of 25 psi (Kraner, 1944).

Zirconia Stabilization

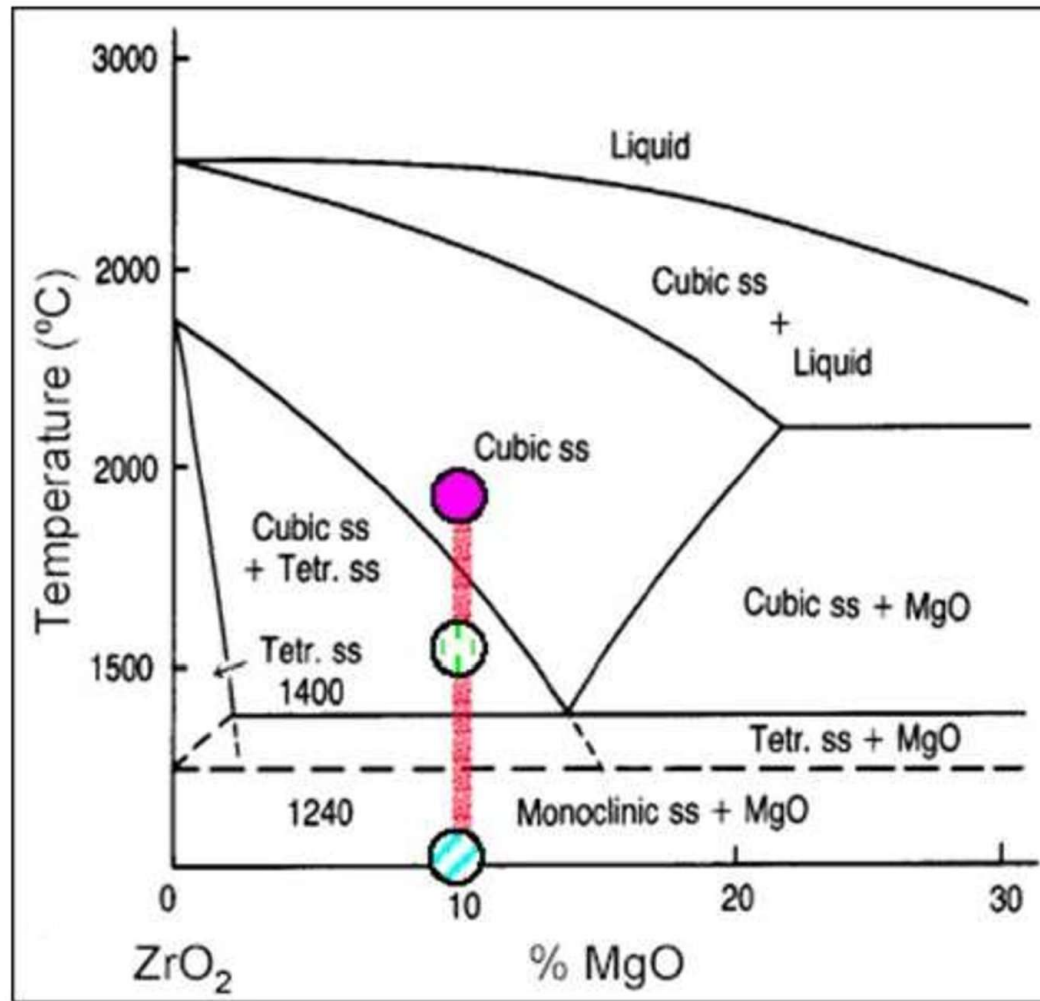


- Almost **no solubility** in m-ZrO₂
- ~1.7 mol% MgO solubility in t-Z at 1400 C.
- PSZ: 10-12 Mol% , sintered at 1800 C, rapid cooling., Reheating at 1400 C.: **Coarsening of t-particle** by rejection of MgO into c-matrix,
- Number of intermediate phases formed: Mg₂Zr₅O₁₂, around 1100 C: Associate with large improvement of Toughness;
- Most Rapid transformation kinetics: around 1200 C. To m-Z,



PSZ:

- (1) Require solution treatment to form supersaturated SS. ; prior to Aging: Sintering Temp/Step: is SS formation step.: Cubic Field: 2-4h,
 - Below 8 mol%: Very high Temp (> 1800) require;
 - However, with increase in Mol%: Vol. fraction t-phase decrease; However, increase in MgO; tow temp economic production: for 9.5%: ~1750 C.
 - Cooling should be fast (~500 C/h) : some t-Z ~ 5-10 nm precipitate.
 - Ageing:



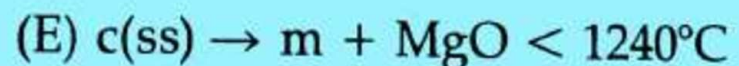
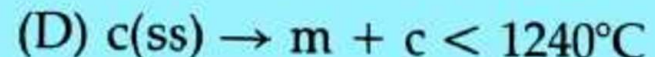
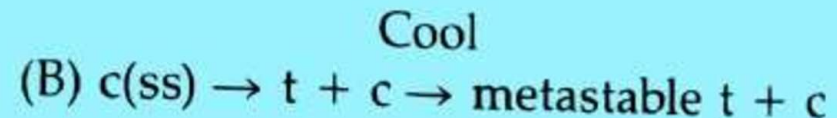
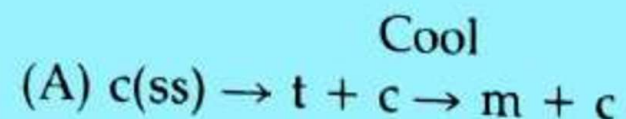
ZrO₂-MgO phase diagram

PSZ: Ageing:

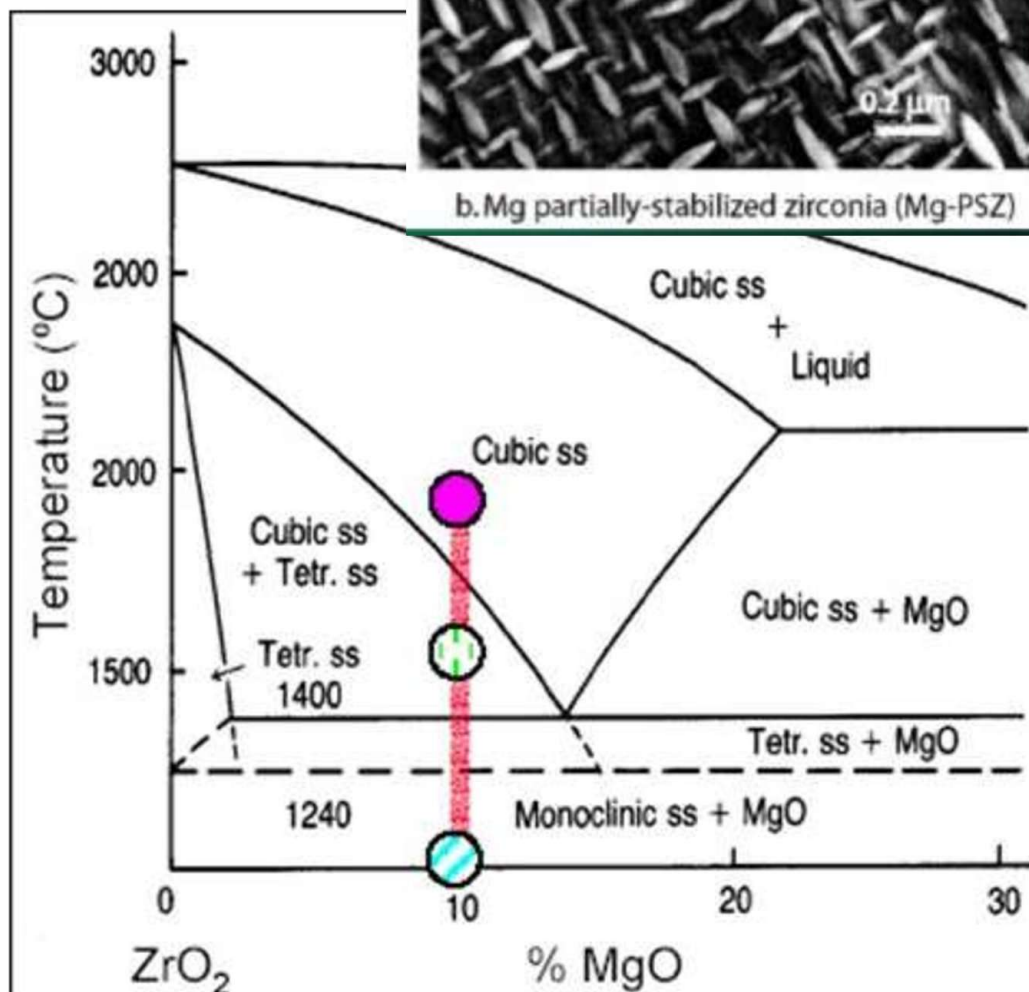
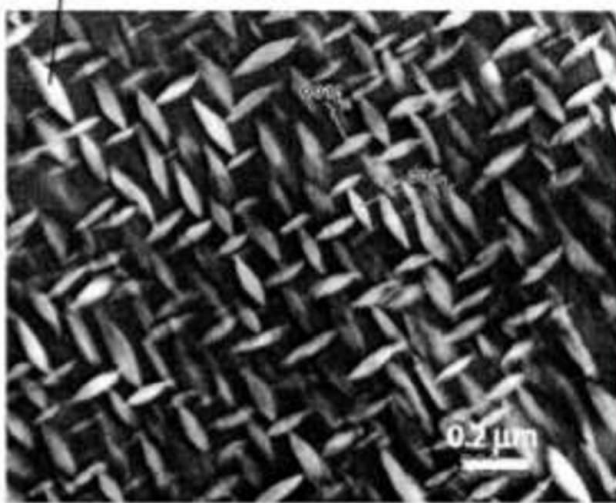
(A): 1600 oC: Heterogeneous t-Z at GB, Transform to m-Z: Degradation of Mechanical Property

(B) 1400-1500: 4-5 h metastable t-Z + c-Z (below 200 nm critical size) ~0.3 vol fraction t-Z, is optimum

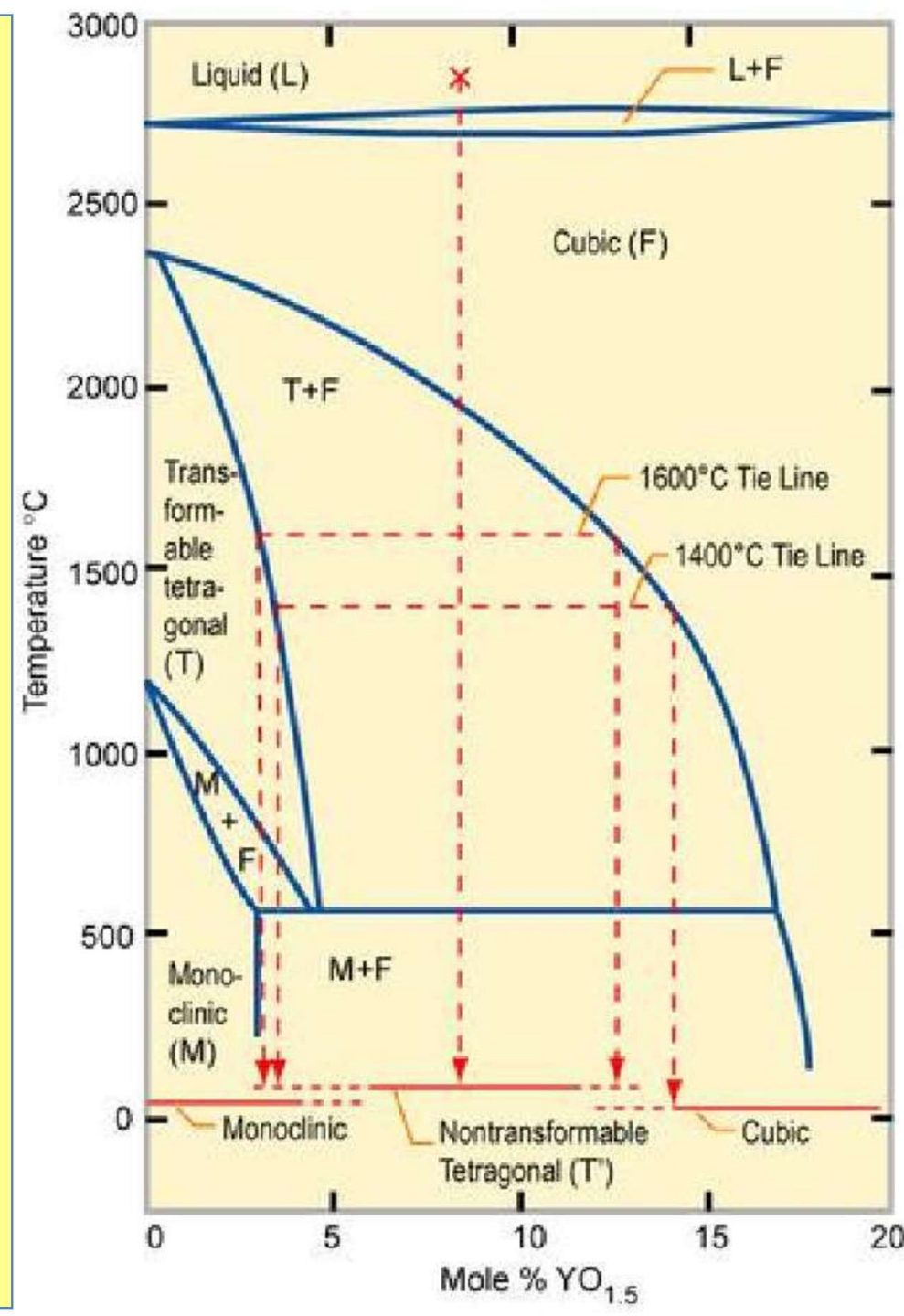
(C) 1200-1300: m-Z+MgO



lenticular $t\text{-ZrO}_2$ precipitates on cubic faces



ZrO₂-Y₂O₃ Phase Diagram:
Euctectoid Reaction of very little interest: as the temp is so low:
Not found in normal cooling; Size of t-phase area: 2.5 mol% Y₂O₃ can be taken in SS ~ 500 oC. -> So Low Eutd.T. -> Fully t-phase can be obtain; called TZP. Provided grain size is very small, : Fine grain is obtained by using ultra-fine powder. And sintering at low (1400-1550) Temp where grain growth can be controlled.
 • A large c+t field: PSD formation easy; However: A slow cooling require to gel transformable t-phase rather than t'-phase formed on rapid cooling.



There are two type of t-Z phase: t ($c/a=1.01$) and t' ($c/a=1.003$). t' : phase is often referred as **non-transformable**; since it cannot undergo t to m martensitic T. However: $t' \rightarrow$ transform to t+c, after extended ageing

Y-TZP: Advantages: Low temp sintering (1400-1550 oC.) compared to **1800** for Mg-TZP.

- Very fine grain; increased strength.
- Secondly: **Eutectoid Temp (~ 500 oC) so low**; no diffusional decomposition.
- Commercial TZP: 2-3 mol% Y₂O₃; 0.2-2 micron equiaxed t-grain: Many TZP contain small c-Z phase.

